EFFECTS OF POROSITY AND CLAY CONTENT ON ACOUSTIC PROPERTIES OF SANDSTONES AND UNCOSOLIDATED SEDIMENTS

A DISSERTATION

SUBMITTED TO THE DEPARTMENT OF GEOPHYSICS

AND THE COMMITTEE ON GRADUATE STUDIES

OF STANFORD UNIVERSITY

IN PARTIAL FULFILLMENT OF THE REQUIREMENTS

FOR THE DEGREE OF

DOCTOR OF PHILOSOPHY

By

De-hua Han

October, 1986.

TABLE OF CONTENTS

ABSTRACT

Ultrasonic compressional and shear velocities V_p and V_s were measured as functions of confining pressure up to 50 MPa and pore pressure 1 MPa at vacuum dried and water saturated states for 80 sandstone samples with porosity ranged from 2 - 30 percent and clay content from zero to 50 percent. Ten samples were clean sandstones, the other were shaly ones, which came from either quarries or well cores.

For shaly sandstones, both V_p and V_s were found to correlate linearly with porosity and approximatedly linearly with clay content. At confining pressure 40 MPa and pore pressure 1 MPa, fits of data by least squares regressions are:

$$V_p\ (km/s) = 5.59 - 6.93\ \phi - 2.18\ C \tag{1}$$

and

$$V_p\ (km/s) = 3.52 - 4.91\ \phi - 1.89\ C. \tag{2}$$

where ϕ is the volume fraction of pores and C is volume fraction of clay. The correlation coefficients are 0.985 for V_p and 0.959 for V_s, and the relative deviations from these equations are less than 3 percent for V_p and 5 percent for V_s. The linear relations can be hold fairly at differential pressure higher than 10 MPa. The fits get worse somewhat at the low pressure. The effects of clay content on velocities are 0.3 of the porosity effect for V_p and about 0.4 for V_s.

This study suggests that except for porosity, the effect of clay content on velocities is the next important parameter whatever the porosity evaluation is needed from velocity data. Other parameters such as the other mineral components, cementation, compaction, pore geometry, grain size and clay types show much less influences on velocities. These minor influences display in the scatters of data from the fits. Based on analyzing of petrophysical data, it is suggested that these scatters are mainly caused by different consolidations of samples.

At confining pressure 40 MPa and pore pressure 1 MPa, the velocities of clean sandstones show linear correlations to porosity:

$$V_p\ (km/s) = 6.08 - 8.06\ \phi \tag{3}$$

and

$$V_s\ (km/s) = 4.06 - 6.28\ \phi \qquad (4)$$

with correlation coefficient 0.99 for both V_p and V_s. The velocities of clean sandstones are significantly higher than the corresponding ones of shaly sandstones.

The velocity differences between clean and shaly sandstones indicate that a small amount of clay (1 or a few percent volume fraction), placed among grain boundaries, can significantly soften sandstone matrix. The clay effect shown in the Equations (1) and (2) is called the matrix clay effect because this effect is not sensitive to locations of clay particles in sandstone matrix. Both bound clay and matrix clay show large effects on shear modulus rather than bulk one. Therefore, the clay effect on shear velocity is greater than that of compressional velocity. Consequently, the velocity ratio increases with increasing clay content. The bound clay effect can be simulated by the Reuss bound. The matrix clay effect can be well limited by the Hashin-Shtrinkman bounds. The moduli of clay minerals in sandstones limited by the bound method are:

$$Bulk\ K = 23.0—24.5\ GPa \quad ; \quad Shear\ \mu = 8.0—10.0\ GPa.$$

Velocity data also reveal that the porosity effect on the V_s is greater than that on the V_p. The theoretical simulations show that the porosity effect on velocities can be delineated by Kuster-Toksöz porous model (1974) with a simple pore aspect ratio spectrum. For simulating the porosity effects on both V_p and V_s at high differential pressure, very thin pores (aspect ratio less than 0.01) in pore aspect ratio spectrum are an intrinsic requisite from the theory. This result is a challenge to the thought suggested by all the pore geometry models that thin pores must be closed at the high differential pressure. The self-consistent model predicts a threshold for shear velocity. This is consistent with the linear empirical equations (1). The combination of different pore shapes for self-consis ent model is required for simulating the velocity data.

The dry velocity data, especially compressional velocity, show not only correlating to porosity and clay content, also correlating crucially to degree of consolidation of sandstones, effect of which, however, is almost overwhelmed by water saturation. For consolidated sandstones, the ratio of $V_{p(sat.)}/V_{p(dry)}$ increase slightly with increasing porosity. The water saturation effect on

V_p is enhanced by increasing clay content, especially in poorly consolidated sandstones. For consolidated sandstones, the ratio of $V_{s\,(sat.)}/V_{s\,(dry)}$ decreases with increasing clay content. However, the water saturation effect on V_s of poorly consolidated sandstones with high clay content is much small or even eliminated. This is because the water saturation effect on elasticity of rocks is not only correlated to porosity but also clay content and consolidation. For consolidated sandstones, the ratio of $\mu_{(sat.)}/\mu_{(dry)}$ decreases with increasing clay content, as well as the amplitude A_p, Thus, the rock matrix is softened with the water saturation. As opposite as those for poorly consolidated sandstones, the rock matrix becomes hardened with the water saturation. The ratio of $K_{(sat.)}/K_{(dry)}$ shows a large increase with increasing clay content. The saturation effect on increase of bulk modulus is enhanced in poorly consolidated shaly sandstones.

Velocity dispersions of water saturated sandstones for frequency from 1 MHz to 1 Hz were calculated from dry and saturated velocities using the Gassmann-Biot theory. The apparent dispersions of V_p at confining pressure 40 MPa and pore pressure 1 MPa are about 1 to 10 percent referenced to measured saturated velocity at ultrasonic frequency. The Biot dispersions, usually less than 1 percent, increase with increasing porosity, and decreasing clay content. The apparent velocity dispersions of clean sandstones are dominated by the Biot dispersion, which is similar to properties of fused glass bead (Winkler, 1985). The apparent velocity dispersions of shaly sandstones is dominated by the non-Biot dispersion. In contrast to the Biot dispersion, the non-Biot dispersion increases with decreasing porosity and increasing clay content. However, the effects of porosity and clay content on the non-Biot dispersion are suppressed by increasing degree of consolidation. The apparent velocity dispersions usually increase with decreasing the differential pressure. The results suggest that local flow is most likely mechanism for the non-Biot dispersion. The local flow does not only relate to pore geometry, also relate to grain contact, cementation, and compaction. The calculated P-wave velocities for saturated sandstones at 1 Hz can be correlated to porosity and clay content with slight higher clay effect on velocities than that at ultrasonic frequency.

Porosities and velocities V_p and V_s of saturated sand-clay mixtures were measured at

confining pressure up to 50 MPa and pore pressure 1 MPa with clay content by weight fraction ranged from zero to 30 percent. Clay effects on velocities of sand-clay mixture differ from that for sandstones. The bound clay (first 1 or a few percent volume fraction) causes a slight increase of V_p by its lubricant effect on leading better grain contact, but this effect has much weak influence to shear velocity. The porous clay (few percent to 10 percent) causes increasing bulk density leading to decrease velocity V_p, V_s and porosity ϕ. As the clay content above 10 percent, both V_p and V_s increase while porosity decreases correlating with increasing clay content. The increase of velocity is mainly resulted from the clay effect on decreasing porosity of the mixtures. If taking off the effect of porosity on velocities, the velocities decrease with increasing clay content, which is called the matrix clay effect. The study also suggests that clay particles can be deformed plastically. Shear velocity of saturated clay show much low value than pure sand. This is consistent with velocity data for both sandstones and sand-clay mixtures. The velocities for clean sandstones and pure sand give a insight into limits of consolidation effects on velocities.

REFERENCES

Kuster, G. T., and Toksöz, M. N., 1974, Velocity and attenuation of seismic waves in two-phase media: Part 1 Theoretical formulations: Geophysics, 39, 587-608.

Winkler, K. W., 1985, Dispersion analysis of velocity and attenuation in Berea sandstone: J. Geophys. Res., 90, 6793-6800.

CHAPTER I

INTRODUCTION

Introduction

The elastic waves with strain of less than 10^{-6} is the most powerful tool to probe properties of subsurface formations in geophysical exploration. It has been widely used by seismologists, well logging engineers and laboratory geophysicists. With development of sophisticated tools and methods, many new parameters such as the shear wave, velocity ratio, and wave amplitude can be measured. The accuracy of measurements is also improved. A great deal more information about subsurface formation has never before been gathered. As in other sciences, the new developments have resulted in more complex data due to more accurate measurements of rock properties. This increase in complex information has create a need for more accurate knowledge of how rock properties and of how the physical environment correlate to the measurements we make. Therefore, the effects of porosity, lithology, fluid saturation, cemetation, pore geometry, grain packing, confining and pore pressure on propagation of elastic waves with different frequencies through rocks must be understood.

Though extensive work has been down experimentally or theoretically in this area, most of it has been based on only a few measurements or rock parameters, which are oversimplified as compared to real rocks. Rocks, especially sedimentary rocks, are extremely complicated, - perhaps the most complicated porous substance in the material world. Many parameters of rocks still remain in qualitatively rather than quantitatively understood. Therefore, tremendous fundamental problems still remain to be solved. Clean sandstones composed of pure quartz grains have the simplest configuration among sedimentary rocks. Bourbie and Zinszner (1985) found that the velocities of clean sandstones may not necessarily correlate to their porosities. They also found that velocities relate to cemetation of rocks. It is still difficult to make accurate estimation of many of the properties of these rocks.

The increasing difficulty and expense of finding new petroleum reservoirs, more geophysicists realize how important is to understand the accurate properties of rocks rather than be satisfied with having a smattering of knowledge. Rock physics research, therefore, has been widely and quickly promoted forward during the last decade.

For thirty years, the evaluation of shaly clastic reservoir rocks has been recognized as a problem. Shaly sandstone and shales which compose most sedimentary basin are the most relevant rocks to petroleum reservoirs. The main components of the shaly sandstones and shales are quartz grains and clay minerals. The effects of clay have posed numerous problems to geologists, geophysicists and petroleum engineers. Since the clay effects, to some degree, affect all well logging measurements available today, such effects must be taken into account in any accurate evaluation of net pay, porosity, fluid saturation and permeability. Though many efforts have been made as reported, for example, in The SPWLA Shaly Sand Reprint Volume (1982), many aspects of the effects of clay on properties of shaly sand still remain poorly understood. Except for the difficulties of the problem itself, lack of complete and reliable data is an important reason. This is because even under laboratory conditions, the measurements made of shaly sandstones with high clay content are difficult to handle and time consuming. Therefore, measuring a great deal of data for shaly sand and drawing reliable conclusions from it presents a real challenge for geophysicists. With support from Stanford Rock Physics Project and guidance from Professor Amos Nur, I have decided to undertake this challenge.

Subjects

In this study I focus on the clay effects as well as the effects of porosity and other parameters on wave propagation through clean and shaly sandstones. Of course, not only velocities, but other rock properties as well, such as resistivity, permeability and dielectric constant are also affected crucially by the clay content. In other words, the clay content plays a key role for many geophysical measurements. A "global approach" (Quirein et al., 1981) has been proposed to determine lithology of rocks in terms of synthetic measurements, in which the velocities are one of the main input. Therefore, the study of wave propagation in sandstones is still fundamental subject in rock physics.

Though many models (Gassmann, 1951; Biot, 1956 a and b; Walsh, 1965; Wu, 1966; Kuster and Toksöz, 1974; O'Connell and Buidiansky, 1974; Garbin and Knopoff, 1975; Korringa et al., 1979; Mavko and Nur, 1979; Walsh and Grosenbaugh, 1979; Mehta, 1983; Crampin, 1984;) have

proposed to estimate elastic properties of porous media in terms of moduli of matrix materials and pore fluid, and pore geometry, almost no theory has been developed to describ the effects of clay on elastic properties of rocks. The results of only a few measurement results related to velocities of shaly sandstones and shales at controlled laboratory conditions has been published.

The clay in sandstones is not only product of the depositional process, it is also product of diagenesis. The structure of the shaly sandstones, such as cementation and specific pore surface area differ greatly from clean ones. Elastic properties of shaly sandstones, consequently, are affected by the clay minerals. The P-wave velocity of shaly sandstones is over-estimated by the time average equation (Wyllie, et al., 1956, 1958), as well as Raymer's equation (1980). Though each of their studies were limited to a few samples, De Martini, et al., (1976), Tosaya and Nur (1982); Kowallis, et al., (1984) show experimental results that the velocities decrease systematically with increasing the clay content in sandstones Castagna et al., (1985) have obtained linear dependencies of V_p and V_s on the porosity and clay content for sonic logging data from Frio Formation. However, they have not emphasized the effects of clay on velocities.

S-wave velocity recently can be measured from well logs and seismic exploration. Dominico (1984) has obtained an empirical relation between shear velocity and porosity by modifying the time average equation. No clay effects on the shear velocity have been considered. In addition, as previously mentioned, even the porosity effects on velocities of clean sandstones are questionable (Bourbie and Zinszner, 1985). The effects of porosity and other parameters on both V_p and V_s of sandstones in addition to the clay effects, remain poorly understood.

Given this situations, we dicided to carry out a laboratory study at carefully controlled conditions on a wide sellectionof samples. 80 sandstone samples have been measured. Ten of them are clean sandstones, the others are shaly sandstones. They come from either quarry or well cores. Their porosity and clay content diffwer widely. This volume, the result of this study, focuses on the following subjects:

In Chapter 2:

1. What are the effects of porosity, clay content, and other rock parameters on wave velocities in

clean and shaly sandstones?

How can the effects of these parameters can be correlated to compressional and shear velocities?

2. If clay content is an important parameters, what are its effects on elastic (dynamic) properties of sandstones?

How can we explain the effect that clay minerals have on elastic properties of shaly sandstones?

In Chapter 3:

3. What kind of theory can be used to simulate the porosity effects and clay content effects on velocity of sandstones?

What kind of information can be drawn from these simulations?

Correlations between water saturation effect and clay are another interesting problem. King (1966) and Chang and Toksös, (1979) have suggested that interaction between clay and pore fluid (water) may decrease rigidity of the saturated sandstones. However, almost no data or theories show how effects of water saturation on velocities are related to the clay content. During analysis of our velocity data, it has been found that the saturated velocities are quite well correlated to porosity and clay content, while the dry velocities show much worse correlations. What does happen due to the water saturation? I have investigated this phenomenon.

In Chapter 4:

4. How do the porosity and clay content correlate to the dry velocities?

How does clay influence the water saturation effects on velocities?

Accurate studies of rock properties at controlled physical conditions to simulate an underground environment must be made in the lab. Velocity measurement at seismic and sonic frequency and controlled pressure is still too difficult to be carried out in the lab. The ultrasonic technique (Birch, 1960) is the most widely available and reliable method to measure velocities under geophysical conditions. However, the velocity dispersion must be estimated inorder to extrapolate the measured results to the low frequencies. Only few data (Winkler, 1985) show that the velocity dispersion for water saturated sandstones is quite small (a few percent). Actually, no

data shows how the apparent velocity dispersion quantitatively relates to the Biot and non-Biot dispersion for sandstones. In addition, no data or theoretical model shows how the Biot and the non-Biot dispersion relates to the porosity, clay content, cement, compaction and other properties of sandstones. Therefore, I study this subject.

In Chapter 5: 5. What is the estimate of the apparent velocity dispersions for 69 samples using Gassmann-Biot theory and measured dry and saturated velocity V_p and V_s at ultrasonic frequency.

What is the estimate of the Biot dispersion and the non-Biot dispersion.

Study how the Biot dispertion and the non-Biot dispersion correlate to properties of sandstones such as porosity, pore geometry, consolidation, compaction, and clay content.

Our study indicates that clay in shaly sandstones plays a crucial role in affecting wave velocities. The question has then arisen: Are the clay influences in unconsolidated sediments similar to that in shaly sandstone or not? To complete the project above, we designed an experiment to measure velocity V_p and V_s and porosity of sand-clay mixtures in which the clay content is accurately controlled. These subjects have been focus on

In Chapter 6:

6. What are pure clay velocities?

How does the clay affect the compaction and velocities of sand-clay mixtures?

What are the differences of velocities between unconsolidated sediments and consolidated sandstones?

REFERENCES

Biot, M. A., 1956 a, Theory of propagation of elastic waves in fluid saturated porous solid I. Low frequency range: Jour. Acoust. Soc. America, 28, 168-178.

Biot, M. A., 1956 b, Theory of propagation of elastic waves in fluid saturated porous solid II. Higher frequency range: Jour. Acoust. Soc. America, 28, 179-191.

Birch, F., 1960, The velocity of compressional waves in rocks to 10 kilobars, 1: J. Geophys. Res., 65, 1083-1102.

Bourbie, T., and Zinszner, B., 1985, Hydraulic and acoustic properties as a function of porosity in Fontainebleau sandstone: J. Geophys. Res., 90, 11524-11535.

Costagna, J. P., Batzle, M. L., and Eastwood, R. L., 1985, Relationship between compressional wave and shear wave velocities in clastic silicate rocks: Geophysics, 50, 551-570.

Crimpin, S., 1984, Effective anisotropic elastic constants for wave propagation through cracked solids: Geophys. J. Roy. Astr. Soc., 76, 135-145.

De Martini, D. C., Beard, D. C., Danburg, J. S., and Robinson, J. H., 1976, Variation of seismic velocities in sandstones and limestones with lithology and pore fluid at simulated in situ conditions: Proc. EGPC Exploration seminar, Nov. 15-17, 1976.

Domenico, S. N., 1984, Rock lithology and porosity determination from shear and compressional wave velocity: Geophysics, 49, 1188-1195.

Garbin, H. D., and Knopoff, L., 1975, Elastic moduli of a medium with liquid-filled cracks: Quart. Appl. Math., 301-303.

Gassmann, F., 1951, Elastic waves through a packing of spheres: Geophysics, 16, 673-685.

King, M. S., 1966, Wave velocities in rocks as a function of changes in overburden pressure and pore fluid saturations: Geophysics, 31, 50-73.

Korringa, J., Brown, R. J. S., Thompson, D. D., and Runge, R. J., 1979, Self-consistent imbedding and ellipsoidal model for porous rocks: J. Geophys. Res., 84, 5591-5598.

Kowallis, B., Jones, L. E. A., and Wang, H. F., 1984, Velocity-porosity-clay content; systematics of poorly consolidated sandstones: J. Geophys. Res., 89, 10355-10364.

Kuster, G. T., and Toksöz, M. N., 1974, Velocity and attenuation of seismic waves in two-phase media, I: Theoretical formulation: Geophysics, 39, 587-606.

Mavko, G. M., and Nur, A. M., 1978, The effect of nonelliptical cracks on the compressibility of rocks: J. Geophys. Res., 83, 4459-4468.

Mehta, C. H., 1983, Scattering theory of wave propagation in a two-phase medium: Geophysics, 48, 1359-1370.

O'Connell, R. J., and Budiansky, B., 1974, Seismic velocities in dry and saturated cracked solids: J. Geophys. Res., **79**, 5412-5426.

Quirein, J.A., Baldwin, J.L., Terry, L., and Hendricks, M., 1981, Estimation of clay types and volumes from well log data—an extension of the global method: SPWLA, 22, Paper Q.

Tosaya, C., and Nur, A., 1982a, Effects of diagenesis and clays on compressional velocities in rocks: Geophys. Res. Lett., **9**, 5-8.

Walsh, J. B., 1965, The effect of cracks on the uniaxial elastic compression of rocks: J. Geophys. Res., 70, 399-411.

Walsh, J.B., and Grosenbaugh, M.A., 1979, A new model for analyzing the effect of fractures on compressibility: J. Geophys. Res., **84**, 3532-3536. Wu, T. T., 1966, The effect of inclusion shape on the elastic moduli of two-phase material, Int. J. Solids Struct., 2, 1-8.

Winkler, K.W., 1985, Dispersion analysis of velocity and attenuation in Berea sandstone: J. Geophys. Res., **90**, 6793-6800.

Wyllie, M. R. J., Gregory, A. R., and Gardner, L. W., 1956, Elastic wave velocities in hetrogeneous and porous media: Geophysics, 21, 41-70.

Wyllie, M. R. J., Gregory, A. R., and Gardner, G. H. F., 1958, A experimental investigation of factors affecting elastic wave velocities in porous media: Geophysics, 23, 459-493.

CHAPTER II

EFFECTS OF POROSITY AND CLAY CONTENT ON WAVE VELOCITIES OF CLEAN AND SHALY SANDSTONES

ABSTRACT

The ultrasonic compressional V_p and shear V_s velocities, and first arrival peak amplitude, A_p were measured as functions of differential pressure to 50 MPa on 80 different saturated sandstone samples, with porosities ϕ ranging from 2 to 30 percent and volume clay content C ranging from 0 to 50 percent. Four different empirical models including a term involving the clay content were used to fit velocity data. Both V_p and V_s were found to correlate linearly with porosity and approximately linearly with clay content in shaly sandstones. At confining pressure of 40 MPa and pore pressure of 1.0 MPa, the best least square fits to the velocity data are:

$$V_p\ (km/s) = 5.59 - 6.93\ \phi - 2.18\ C$$

and

$$V_s\ (km/s) = 3.52 - 4.91\ \phi - 1.89\ C$$

where ϕ is the volume fraction of pores, and C is volume fraction of clay. Deviations from these equations are less than 3 percent and 5 percent, for V_p and V_s respectively.

The best fits to velocities of clean sandstones are

$$V_p\ (km/s) = 6.08 - 8.06\ \phi$$

and

$$V_s\ (km/s) = 4.06 - 6.28\ \phi$$

The velocities of clean sandstones are significantly higher than those of shaly sandstones. This indicates that a very small amount of clay (1 or a few percent of volume fraction) significantly reduces the elastic moduli of sandstones.

For shaly sandstones with water saturation, V_s is more sensitive to porosity and clay content than is V_p. Consequently, velocity ratios V_p/V_s also show clear correlations with clay content and porosity.

For shaly sandstones we conclude that next porosity, clay content is the most important parameter in reducing velocities, with an effect which is about 0.30 of the porosity for the V_p and 0.40 for the V_s.

Introduction

Shaly sandstones and shales comprise a major component of sedimentary basins and are of foremost relevance to hydrocarbon reservoirs. The acoustic properties of these rocks are thus of great interest in seismic and well log interpretation.

For years, the time average equation of Wyllie et al. (1956, 1958) has commonly been used to transform acoustic reciprocal velocity to porosities. The equation for P wave velocity V_p in water saturated rock is

$$\frac{1}{V_p} = \frac{(1-\phi)}{V_m} + \frac{\phi}{V_f} \tag{1}$$

where V_m is the P wave velocity of the rock matrix, and V_f is the velocity of the pore fluid. When both V_m and V_f are fixed, the only variable in the equation is porosity. To a first order this simple equation appears adequate for clean sandstones in the middle range of porosity ($10\% < \phi < 25\%$). Many parameters such as mineralogy, pore geometry, degree of consolidation, cementation, compaction and related physical conditions such as confining pressure, pore fluid, pore pressure, frequency, and temperature are neglected in the time average equation. Consequently, the shortcomings of this equation have been extensively discussed (for example Geertsma, 1961; Geertsma and Smit, 1961; Raymer et al., 1980; Kevin, 1981). A newer empirical equation based on well log data was obtained by Raymer et al. (1980)as follows

$$V_p = (1-\phi)^2 V_m + \phi V_f \tag{2}$$

which was proposed as an alternative to the time average equation for acoustic log interpretation.

Both equations (1) and (2) cannot be directly applied to shaly sandstones. The results of this study and those presented by Tosaya and Nur (1982 a) demonstrate that both the time average equation and Raymer's model significantly overestimate velocities in shaly sandstones and shales. It is therefore a challenge to determine which additional parameter is most significant and how it can be represented in the velocity equation for sandstones.

Although there are many theoretical models for the effects of porosity, pore shape, fluid and matrix moduli on the elastic properties of rocks (for example Gassmann, 1951; Biot, 1956 a and b,

Geertsma, 1961; Kuster and Toksöz, 1974; O'Connell and Budiansky, 1974; Mavko and Nur, 1978; Walsh and Grosenbaugh, 1979), almost none directly include the effect of clays on velocities in sandstones. King (1966) and Toksöz and Cheng (1979) have suggested that interaction between pore fluid and clay mineral in sandstones may respond to a decrease of shear modulus. Minear (1982) applied the Kuster and Toksöz model (1974) to simulate the effects of clays on velocities of sandstones. His results suggest that clay minerals do significantly reduce elastic moduli and velocities of sandstones. However, the magnitude of these effects of clays remain far from clear and no data were presented to support his results. The effect of clay on velocities remains poorly understood. Furthermore, limited experimental and petrographic work has been published on the effects of clay minerals on velocities (De Martini et al., 1976; Tosaya and Nur, 1982a; Kowallis et al., 1984). Although each of the above studies was limited to a few samples, all results have alluded to a general trend that increasing clay content in both well and poorly consolidated sandstones decreases acoustic velocities in a systematic manner. Costagna et al. (1985) have obtained a linear dependence of velocity V_p and V_s on porosity and clay content for sonic log data from the Frio Formation. However, effects of clay on velocities were not emphasized in their study.

Because shear wave velocities are now available from well logs and seismic reflection measurements, it is of particular interest to better understand the relation between shear velocity and porosity. An empirical relation between shear velocity and porosity has been proposed in the past by modifying the time average equation (e.g. Domenico, 1984). However, as shown in below this equation is not appropriate for shaly sandstone. A systematic investigation of the effects of clay content and porosity on shear velocity V_s is consequently in order.

We carried out an experimental study of the effects of porosity and clay content on both compressional velocity V_p and shear velocity V_s as functions of pressure in 80 sandstone samples. Several empirical equations were used to formulate velocity data. We have also investigated the relations among changes in relative attenuation with varying rock porosity and clay content. In addition, the relations among the velocity ratio V_p/V_s, elastic moduli, porosity and clay content

are also examined. The results may significantly improve porosity estimates in shaly sandstones and provide correction factors for log interpretation.

Experimental Procedures

1. Sample description

The 80 sandstone samples used in this study came from either well cores or quarries. The porosity of the samples ranged from 2 to 30 percent, and the clay content by volume fraction ranged between 0 to 50 percent (fig. 1). Ten samples were tight gas sandstones (T) with very low porosities. Twenty-four samples (G) came from a few offshore wells in the Gulf of Mexico. Some of these were poorly consolidated. Eleven samples (P) were also borehole cores which are well-consolidated. Thirty five well-consolidated samples were from quarries. Ten of these (X) were clean sandstones with less than 1 percent clay content; the rest were indicated by (S). Figure 1 shows clay content versus porosity for all samples. It is noteworthy that samples with more than 20 percent clay content tend to have lower porosities, in the range from 5 to 15 percent.

2. Acoustic measurement

Wave velocities V_p and V_s and the associated compressional first arrival peak amplitude, A_p, were measured as functions of pressure and the state of water saturation. Confining pressure P_c and pore pressure P_p were controlled separately. With differential pressure P_d limited to 50 MPa and pore pressure to 1.0 MPa, the test system can simulate pressure conditions at depths of over 2000 m.

The velocities were measured at ultrasonic frequencies using the pulse transmission technique (Birch, 1960). The central frequency of the transducers used for P and S waves were 1.0 MHz and 0.6 MHz respectively. The wave lengths for P and S waves were at least five times greater than a mean grain size of samples. All samples were unflashed and kept at room dried condition for at least a month. Before measuring, samples were vacuum oven-dried. Then, the measurements were first performed at a vacuum dry state (vacuum pressure less than 0.01 Torr), then at full saturation with deionized and deaerated water. For some samples with high clay

content, brine was used as the pore fluid. No velocity differences were found for brine or plain water saturation.

Samples were 5.0 cm in diameter and 2.0 to 5.0 cm in length, or more than 100 times the average grain size. Both sample dimensions were measured to within 0.05 mm. The two end surfaces of each sample were ground parallel to within 0.05 mm.

P-wave arrival times were picked to within 0.03 μsec, which leads to less than 1 percent absolute error in V_p measurement. The error in the V_s measurement is less than 2 percent, except for poorly consolidated sandstones at low differential pressure ($P_d < 10$ MPa), where errors may be up to 3 percent due to poor signals.

Samples were prepressured to 50 MPa for reducing hysteresis effect. Data were measured at unloading process. Generally, hysteresis was observed, but its magnitude was typically small. After the preloading, velocities measured at unloading process were very repeatable, with hysteresis less than 1 percent in well-consolidated samples, and less than 2 percent in poorly consolidated samples. The first peak amplitudes, A_p, were measured using the method proposed by Tosaya (1982 b).

Throughout this paper, unless otherwise mentioned, data shown in the figures are for confining pressure equal to 40 MPa and pore pressure equal to 1 MPa.

3. Density and porosity measurements

Samples were vacuum oven-dried at less than 50^o C for 2 to 8 weeks, and weighed to within 0.01 g so that the density of a dry sample ρ_d can be determined to within 0.3 percent. The density of the wet sample ρ_w was then calculated by the relation

$$\rho_w = \rho_d + \phi \rho_f \tag{3}$$

where ρ_f is the pore fluid density and ϕ is the porosity of the sample.

The porosity at room pressure was measured with a helium porosimeter, repeatably within 1 percent of total bulk volume. This is considered equal to the porosity at differential pressure P_d of 1 MPa. The measured porosity is considered as total porosity. This is supported by the fact

that converted matrix densities for the samples from measured dry bulk density and porosity were around 2.65 gm/cc. This is a typical value for quartz, a major component in sandstone matrix.

Bulk volume of a sample decreases with increasing differential pressure. However, at the pressure we used, the grain volume change was very small. The variation of bulk volume with pressure can, therefore, be considered equal to the change of the pore volume only. The variations of the pore volume were monitored with a pore pressure intensifier while the pore pressure was kept constant. The ambient temperature was $22^{o}\ C$ with 1 deg. uncertainty.

4. Petrographic measurement

The clay content of each sample was obtained by point counting on thin sections. The clay content was obtained by 300 point countings on thin section. Minerals with flakelike textures, such as hematite and other iron oxides were counted as a part of the clays. Usually two thin sections, from the top and bottom of a sample respectively, were taken. At times the clay contents from these two thin sections differed by as much as 20 percent, due mainly to the sample heterogeneity.

Experimental Results

Based on the combination of acoustic and petrographic data, the effects of confining pressure P_c, pore pressure P_p, and fluid saturation on acoustic P and S wave velocities and amplitude are studied. The measured data were tabulated in the appendix.

Compressional velocity V_p and shear velocity V_s versus porosity ϕ of 80 sandstone samples are shown in Figures 2a and 2b. Despite the significant scatter, there is a clear trend indicating that both V_p and V_s decrease with increasing porosity. As a first trial, the modified time average equation $1/V_p = B_{p0} + B_{p1}\,\phi$ was fitted to the data. By least square regression, the fitted results (Table 1) are presented as relative deviations versus porosities (Figure 3a). The matrix P wave velocity computed from the fit is $V_m = 1/B_{p0} = 5.15$ km/s, This result is much lower than the value $V_p = 6.05$ km/s for quartz aggregate (Robert, 1982). The relative deviations of the data from the values predicted by the equation versus porosity are quite large

(Figure 3a). However, the clear trends in the data (as seen in Figure 3b) leave no doubt that clay content in these samples has a systematic effect on the compressional velocity. Similar results with larger scatters for shear velocity data fitted by the equation $1/V_s = B_{s0} + B_{s1}\,\phi$ (Domenico, 1984) are shown in Figure 3c and 3d and listed in Table 1.

We also used the empirical linear model $V = A_0 - A_1\,\phi$ to fit both V_p and V_s data. Again the relative deviations of the data from the values predicted by the equation were quite large (Figures 4a, 4c). The deviations clearly depended upon the clay content (Figures 4b, 4d).

As shown in Figures 3a, 3c, 4a and 4c, velocities of clean sandstones were systematically higher than predicted by the fit. In order to emphasize the effects of clay content and avoid the fit biased by the velocities of clean sandstones, velocity data are grouped as 10 of clean sandstones and 70 of shaly ones. On the basis of results reported above, we can conclude that any model used to fit velocity data of shaly sandstones should include a term with clay content.

Velocity-Porosity Relation for Clean Sandstones

Using least squares regression, different empirical equations are obtained to delineate velocities as a function of porosity and clay content.

The velocities of clean sandstones can be linearly related to porosities. The best fits are

$$V_p\ (km/s) = 6.08 - 8.06\,\phi \tag{4}$$

and

$$V_s\ (km/s) = 4.06 - 6.28\,\phi \tag{5}$$

with correlation coefficients 0.99 for both V_p and V_s as list in Table 1. The relations are shown in Figures 2 a and b. When setting porosity to zero we obtain matrix velocities 6.08 km/s for V_p and 4.06 km/s for V_s, which closely coincide with velocities of the quartz aggregate (Robert, 1982). In using the time average equation to fit data, the correlation coefficients are similar to the linear fits above, with the exception that both P and S wave velocities of matrix are about 5 percent higher than those of the quartz aggregate. Equations (4) and (5) indicate that porosity has a larger effect on the shear V_s than on the compressional V_p,

$$1.55 = \frac{6.08}{4.06} > \frac{8.09}{6.08}.$$

Different Models Used to Fit Velocity Data of Shaly Sandstones

For shaly sandstones four simple equations including a clay content term are used to fit the data by the least squares regression method.

(1) The linear equation

The velocities linearly correlated to porosity and clay content produce the simpliest empirical equation.

$$V = A_0 - A_1 \phi - A_2 C \tag{6}$$

The fitting results listed in Table 1 for both V_p and V_s are

$$V_p \ (km/s) = 5.59 - 6.93 \phi - 2.18 C \tag{7}$$

and

$$V_s \ (km/s) = 3.52 - 4.91 \phi - 1.89 C \tag{8}$$

The correlation coefficient is 0.985 and the relative rms deviation is 0.021 for V_p, and correspondingly 0.959 and 0.043 for V_s. These values show great improvement in comparison with the results using porosity alone.

(2) The time average equation

We modified the time average equation to include a linear term of clay content. The equation can also be used to model shear velocity.

$$1/V \ (s/km) = B_0 + B_1 \phi + B_2 C \tag{9}$$

For compressional velocity the coefficients B_0, B_1, and B_2 can be interpreted as follows

$$B_0 = 1/V_m; \ B_1 = (1/V_f - 1/V_m); \ B_2 = (1/V_c - 1/V_m) \tag{10}$$

where V_m is matrix velocity, V_f is fluid velocity and V_c is clay velocity.

(3) The logarithmic equation

we assume

$$V = V_m^{(1-\phi-C)} \ V_f^{\phi} \ V_c^{C}. \tag{11}$$

Taking the logarithm of both sides of the equation we obtain

$$\log_{10} V = L_0 + L_1 \phi + L_2 C \tag{12}$$

where L_0 is equal to $\log_{10} V_m$, L_1 to $\log_{10}(V_f / V_m)$, and L_2 to $\log_{10}(V_c / V_m)$.

(4) The linear power equation

We also used the following equation to fit the velocity data.

$$V = P_0 - P_1 \phi^{\alpha} - P_2 C^{\beta}. \tag{13}$$

The coefficients and power α and β are found by the least squares regression.

Comparison of Models

Table 1 shows that for shaly sandstones, correlation coefficients of all empirical fits are similar (less than 1 percent difference); as are the relative rms deviations. These results indicate that a model with a clay content term can significantly improve the fitting results. The question arises, however: which equation is the best fit ?

The time average equation with the clay term has some physical meaning for V_p, however, the fluid velocity is too high. This physical meaning is especially inappropriate for shear velocity because pore fluid, like water, cannot bear any shear stress.

of the above models, the linear equation (Table 1) is the best fit. The relative residuals of V_p and V_s data from the fits versus porosity and clay content are shown in Figures 5 a, b, c, and d, respectively. A tremendous improvement over the equation without a clay term (Figure 3 and 4) is obtained by the fitting with a clay content term. Deviations of data from the linear fits are uniformly and randomly distributed; no relation has found between the residuals with either the porosity or clay content. In contrast, deviations for the time average model, show a definite pattern (Figure 6). At porosities either lower than 0.07 or higher than 0.25, velocities appear systematically lower than predicted by the time average model, as opposed to the velocities at middle porosities. Moreover, the linear models show an exceptional feature that they will break down at high porosity. This may be a correct prediction for velocities of sand grains without contact at porosity above 60 percent. The above features are explored in Figures 7 a and b, showing the fitting results of V_p and V_s versus porosities for the four models. These models diverge in the manner of porosity lower than 0.07 with a low clay content and porosity higher

than 0.25 with a high clay content. The time average model shows velocity higher than the others at these ranges. The logarithmic model falls in the middle, while the linear and power models closely coincide except at low clay content. Our data best fit the linear model. For clean sandstones, velocity data also fit the linear model better than they do the time average one. From the above analyses, it can be concluded that the time average model with the clay term is not adequate to describe velocities as functions of porosity and clay content. The logarithmic model involves scale transformation which is not shown to be necessary in our case.

As concerns the linear and linear power models, the latter confirms that the linear fit for porosity is perfect. Significant differences between the linear and the linear power fits appear at low clay content, especially for the V_s. This result could indicate that at low clay content, velocities may not be linearly related to clay content. However, this conclusion is tentative because of uncertainty in estimating the clay content and insufficiency of data. Moreover, the fitting results of the linear power model (Table 1) do not show significant improvement over the simple linear fits. At this stage, then the linear model is the best choice to fit velocity data of sandstones to the first order. The equations are similar to those proposed by Tosaya and Nur (1982a), Kowalis et al. (1984), and Costagna et al. (1985). However, quantifying a small amount of clay effect remains problematic.

Bound Clay Effects on Velocities

The velocities of clean sandstones are obviously higher than those of shaly ones. Setting clay content to zero and dividing Equations (4) and (5) by (7) and (8) respectively. we can obtain

$$\frac{(V_p)_{cl.}}{(V_p)_{sh.}} = 1.088 - \frac{0.52\ \phi}{5.59 - 6.93\ \phi} \tag{14}$$

$$\frac{(V_s)_{cl.}}{(V_s)_{sh.}} = 1.15 - \frac{0.61\ \phi}{3.52 - 4.91\ \phi} \tag{15}$$

This result is encouraging for the analysis of clean sandstones and how they differ from shaly sandstones. The velocity ratios of clean and shaly sandstones are significantly greater than one, and decrease with increasing porosity. The above relations suggest that small amounts of clay (1 or a few percent of bulk volume fraction) can strongly reduce velocities. Most likely such

softening is related to clay particles situated between grain boundaries. Because grain size of clay particles is so small, and their surface area is so large, even a small volume fraction of clay can spread throughout the rock matrix, including grain boundaries. We believe that this bound clay is responsible for drastically softening grain contacts and cements for shaly sandstones. This explanation is supported by MES photos (SPR Rock Catalog, 1985) of shaly sandstones. Contrasts of elastic moduli between the boundary clay and rock matrix decrease with increasing porosities. Thus, as shown in Equations (14) and (15), the bound clay effects on velocities decrease with increasing porosity.

The velocities of shaly sandstones are reduced by the bound clay effect. Becuase of this, when setting porosity and clay content to zero, matrix velocities shown in Equations (7) and (8) are much lower than those of quartz aggregate. In addition, when setting clay content to zero, the velocity ratios of clean sandstones to shaly ones are significantly greater than one as shown in Equations (14) and (15). The ratio for shear velocity is significantly higher than that for the compressional velocity. This indicates that the bound clay effect on the shear velocity is larger than on the compressional velocity. This is because the bound clay mainly reduces shear moduli rather than bulk moduli, which will be shown in following section.

The Matrix Clay Effect on Velocities

This bound clay effect should be differentiated from the clay content effect presented in Equations (7) and (8). The clay content C shown in Equations (7) and (8) should exclude the bound clay. However, the volume fraction of the bound clay is very limited by its specified location. Therefore, the volume fraction of the bound clay can be neglected and we can assume the matrix clay content equal to the total clay content without bringing significant errors.

The results of the linear model indicate that within a few percent deviations, velocity measurements are not sensitive enough to identify clay types or clay locations in matrix, and are only related to the clay volume fraction. Minear (1982) has investigated models of sandstone with (1) laminated, (2) structural, and (3) porous clay suspended in pore fluid. His model results show that the porous clay has only a slight effect on reducing velocities of sandstones, whereas both

laminated and structural clays have significant and similar effects on velocities. Both arrangements predict a nearly linear relation between velocities and clay content for clay content below 50 percent. Because the exact arrangement of clays within sandstones is not known, we can only suggest that something like Minear's (1982) laminated or structural arrangement is typical. This clay effect is, therefore, known as matrix clay effect.

Similar to the bound clay, the matrix clay effects on the shear velocity are also greater than on the compressional velocity as shown in Equations (7) and (8).

$$0.54 = \frac{1.89}{3.52} > \frac{2.18}{5.59} = 0.39.$$

This is because the matrix clay mainly acts to decrease shear moduli rather than bulk moduli. This will be shown in the following section.

Microporosity was proposed as a physical ground for the effects of clay content on the P-wave velocities of unconsolidated sandstones (Kowallis et al., 1984). Our study shows this assumption may be not adequate to delineate clay effects on sandstones. First, it is not clear how one can directly quantify the microporosity in sandstones. Second, on the basis of this assumption, clay effect on velocities relative to the porosity effect must be consistent for both V_p and V_s. Actually, as shown in Equations (7) and (8), the clay effects on the V_s are larger than on the V_p. Moreover, from the measured density-porosity relation, the converted density for sandstone matrix is around 2.65 gm/cc. This value is typical for sandstones. If extra 30 percent of clay volume adds to the measured porosity as proposed by Kowallis et al. (1984) this should result in much higher density than 2.65 gm /cc for high clay content sandstones. This is not consistent with our data. Therefore, it is reasonable to assume that the pores in shaly sandstones are connected with each other so that porosity measured by the helium-porosimeter is total porosity including microporosity of clay. The microporosity effect is taken account as part of the porosity effect.

We consider the matrix clay effect to be caused simply by that clay with low elastic moduli as a component of matrix mixed with quartz grains can soften sandstone matrix. It will be discussed in Chapter III (Han, 1986).

Effects of Porosity and Other Parameters on Velocities

The petrographic data and SEM photos for the samples exhibit wide differences of pore geometry, cementation, packing of grains, type of clays, distribution of clays and mineral composition. One surprising result of this study is that in addition to porosity, in the statistical sense, only the volume fraction clay content emerged as an important parameter. All other parameters, without separating their effects, have only small effects on velocities.

As shown by Bourbie et al. (1985), velocities of sandstones may not dominated by porosity. Grain contact, pore geometry, and cementation also play an important role in influencing velocities. Therefore, the velocities of sandstones show wide responses to differential pressure. However, at high differential pressure, different effects on velocities caused by these parameters are suppressed. Our experimental results indicate that at high pressure, only the porosity remains as a dominant parameter in reducing velocities of clean sandstones as shown in Equations (4) and (5). It is also true for shaly sandstones. The porosity is the strongest influence on both V_p and V_s. In comparison with the porosity content effect, the influence of clay content (by volume) is about $\frac{2.19}{6.93} = 0.315$ that of porosity for V_p and $\frac{1.89}{4.91} = 0.385$ for V_s. Again, as seen for clean sandstones, the porosity effect on reducing V_p is larger than V_s,

$$1.40 = \frac{4.91}{3.52} > \frac{6.93}{5.59} = 1.23.$$

As previously mentioned, the effects of pore geometry, grain contact and packing, and cement are suppressed by increasing differential pressure. Our data show that with uncertainty of 3 percent for V_p and 6 percent for V_s, only the porosity and the clay content emerge as dominant parameters in the velocity-sandstone property relations at differential pressure above 10 MPa. Our data also show that the coefficients of the linear fits in Equations (7) and (8) are slightly changed with differential pressure over 10 MPa (Table 2). This suggests that the effects of porosity and clay content are fairly independent of differential pressure. Therefore, Equations (7) and (8) can be extrapolated to a higher pressure range. For data with P_d below 10 MPa the fits are somewhat worse. In addition, the ratio of the effects of clay content to that of porosity

increases slightly with increasing pressure (Table 2). This means the clay effect is enhanced by suppressing the pore geometry effect at high pressure.

The linear fit for shear velocity V_p displaies larger deviations than that for V_p. This indicates that other parameters have larger effects on the shear velocity than on the compressional velocity. One of them is the effect of different composition. In additon to clay minerals, some of the samples contain carbonates, feldspars, iron oxide and other minerals. The P-wave velocities of these minerals do not differ much (about 5 percent high) from $V_p = 6.05$ km/s for quartz aggregate (Robert, 1982). However, S-wave velocities of them are around 20 percent less than the $V_s = 4.09$ km/s for quartz aggregate. Because these minerals are not main components in our samples, their effects on velocities can be neglected as shown in the data, but their influence can still be traced. Boise sandstone contains 44 percent feldspar. The residual of its shear velocity is about 5 percent less than that predicted by Equation (8). We conclude that the different composition is a reason for larger deviations of the fit from the shear velocity data.

The consolidation (e.g. cement, grain contact and packing) effects are suppressed not only by the differential pressure but also by interaction between clay and pore fluid. Differences in consolidation among dry sandstones are nearly overwhelmed by the water saturation effect which will be discussed in the next Chapter.

In summary, it appears that at high differential pressure, after the porosity, the volume clay content in consolidated shaly sandstones is the next most important parameter when accurate porosity evaluations from seismic or acoustic data (e.g. well logs) are required. Other parameters, including pore geometry, grain size, grain contacts, cementation, type of clay, distribution of clays and mineralogy, have much smaller influence on velocities at high differential pressure for shaly, water saturated sandstones.

Effects on Wave Amplitudes

We also studied the dependence of wave amplitude on porosity and clay content, using a comparative method as described by Tosaya (1982 b). For P waves we find that the amplitude

A_p of a wave transmitted through a unit length of rock sample increases in relation to an aluminum sample with decreasing porosity (Figure 8), although the scatter is quite substantial. For 46 water saturated samples, the best fit by linear regression of the amplitudes as functions of the porosity and clay content is

$$A_p = 0.58 - 1.57\ \phi + 0.23\ C \tag{16}$$

with a correlation coefficient of 0.68. The results show that the amplitude depends heavily on the porosity and only slightly on clay content. We conclude that parameters other than clay content are probably important. No clear relations were observed between shear amplitude A_s and porosity. This is probably due to the fact that the shear signal is often distorted in a sample with high clay content; thus accurate measurement of A_s cannot be obtained.

The Effect of Clay Content on the Elastic Moduli

The effective elastic moduli for our samples are computed from the velocities by the expressions:

$$K = \rho\,(V_p^2 - \frac{4}{3}\,V_s^2) \tag{17}$$

and

$$\mu = \rho\,V_s^2$$

where ρ is the sample's density. Clearly, elastic moduli relate to porosity and clay content in a manner similar to the velocities as shown for bulk and shear moduli versus porosity in Figures 9 a and 9 b. However, for shaly sandstones, clay content effects on the shear modulus rather than on the bulk modulus are more emphasized.

As seen in Figure 9 b, clean sandstones have much higher shear moduli than do shaly sandstones with the same porosities. This reveals that the bound clay effects on velocities are also mainly due to its effects on reducing shear modulus rather than bulk moduli. The matrix velocities biased by the bound clay are equal to the constants in Equations (7) and (8). The matrix moduli with the bound clay effect can be calculated from the matrix velocities and density using Equation (17).

$$Bulk\ K_s = 39.0\ GPa \quad ; \quad Shear\ \mu_s = 32.8\ GPa.$$

The shear modulus for the matrix with the bound clay is much less than $\mu_q = 43.7$ GPa for pure quartz, while the bulk modulus for the shaly matrix is slightly less than $K_q = 40.0$ GPa for pure quartz. These data confirm that the bound clays can significantly reduce the shear modulus but have only little influence on the bulk modulus.

As shown in Figures 9 a and b, the clay content (the matrix clay) effects on the shear modulus are much larger than on the bulk modulus. Similar to the bound clay effects, the matrix clay effects on V_p and V_s (Equations (7), (8)) are mainly due to its effects on reducing the shear modulus rather than the bulk modulus of sandstones. The large effects of the bound and matrix clays on the shear modulus of sandstone matrix may caused by larger contrasts of shear moduli between clay mineral and quartz grain in sandstones.

Moreover, larger porosity effects on the shear velocity than on the compressional velocity are due to its larger effects on the shear modulus rather than on the bulk modulus as shown in Figures 9 a and b. This reveals that porosity has different responses to the bulk and shear moduli.

The Effects of Clay Content on velocity Ratio

As shear velocity data are becoming more available in seismic exploration and well logging, the velocity ratio V_p/V_s is becoming a useful parameter in the determination of rock properties. Laboratory and well-logging studies in the past suggested correlations between lithology, porosity, and V_p/V_s values (Pickett, 1963; Gregory, 1977; Benzing, 1978; Johnson, 1978; Tatham, 1982; Eastwood, 1983; Domenico, 1984; Rafavich et al., 1984; Costagna et al., 1985). Our data show that the velocity ratio for water saturated shaly sandstones depends on both porosity and clay content. By least square regression, this dependence is found to be

$$V_p/V_s = 1.55 + 0.56\ \phi + 0.43\ C \qquad (18)$$

with a correlation coefficient of 0.70. The results show that V_p/V_s increases with increasing porosity or clay content. The velocity ratio is more sensitive to porosity changes, in agreement with the results of Costagna et al. (1985). Figure 10 a reveals that clean sandstones have the

lowest velocity ratios (1 5 to 1.6) which increase slightly with increasing porosity. For shaly sandstones, the velocity ratios with more scatters and higher values than those of clean sandstones show a trend to increase with increasing porosity. Figure 10 b shows that at least some of the large scatters in Figure 10 a are caused by clay content effects on the velocity ratios. The clear separation of the data of Gulf sandstone with high clay content from those of P-sandstone suggests that the degree of consolidation may also have an important affect on the velocity ratios, because the Gulf sandstones are much less consolidated than are the P-sandstones.

Sandstones with high clay content have velocity ratios and Poisson's ratios similar to carbonate rocks. The resulting ambiguity in the interpretation of velocity data may be resolved by the combined use of the velocity as well as the velocity ratio, providing a useful tool for reliable lithology discrimination.

Costagna et al. (1985) found that shear velocity is nearly linearly related to compressional velocity for water saturated clastic silicate sedimentary rocks by the equation

$$V_p\ (km/s) = 1.16\ V_s + 1.36 \tag{19}$$

Our data also show V_s to be nearly linearly related to V_p with somewhat different coefficients than in Equation (19). For our samples, the best linear least square fit yields

$$V_p\ (km/s) = 1.26\ V_s + 1.07 \tag{20}$$

with a correlation coefficient of 0.97.

Conclusion

On the basis of our experimental results, we conclude the following:

1. Any model used to fit both V_p and V_s data of shaly sandstones should contain a term with a clay content. Models with a clay term greatly improve fit results for both V_p and V_s.

2. Of the above mentioned models, the linear relation is the best fit for the velocity-porosity-clay content relation in water-saturated shaly sandstones. The compressional velocity V_p and shear velocity V_s are linearly related to porosity over the range from 2 to 30 percent and to clay content over the range from 1 to 50 percent. The effect of clay content in reducing velocity is

about 0.3 as great as the effect of porosity for V_p and 0.4 as great for V_s.

Other parameters, such as pore geometry, grain size, grain cement, grain packing, clay types, and other lithology do not show important effects on to the saturated velocities of shaly sandstones at higher differential pressure. However, though degree of consolidation (i.e. grain cement, packing) is not so important for modeling the saturated velocities, in comparison with the other parameters, it may be the most important factor causing the scatters related to velocity systematics.

3. Generally, the effects of porosity and clay content on shear velocity V_s are larger than on compressional velocity V_p. Thus a sample with high porosity and clay content tends to have a high V_p/V_s ratio.

4. Compressional and shear wave velocities V_p and V_s of clean sandstones can be linearly correlated to the porosity. They are significantly higher than for shaly sandstones with the same porosity. The differences of corresponding velocities of clean and shaly sandstones decrease with increasing porosity.

The matrix velocities 5.59 km/s for V_p and 3.52 km/s for V_s obtained from Equations (7) and (8) with porosity and clay content set to zero, are significantly lower than the corresponding velocities for quartz aggregates of 6.05 km/s for V_p and 4.09 km/s for V_s (Robert, 1982). This difference implies that a small amount of clay (1 or a few percent volume fraction) can significantly soften the sandstone matrix leading to reduced velocities.

5. The clay effects on the velocities can be classified as the bound clay effect and matrix clay effect. Small amounts of clay particles (1 or few percent volume fraction) can cover all grain surfaces including the grain boundaries. This bound clay with very low elasticity can significantly reduce the rigidity of sandstone matrix.

The effects of all clays other than the first 1 percent or so (called the matrix clay) on velocities is described by Equations (7) and (8). The effect depends on the volume clay fraction, and is not sensitive to clay location in sandstone matrix. A simple model by Minear (1982) shows

that clays are mainly arranged as laminated in the rocks, or as grains between the sand grains. The clay minerals with low elasticity, especially low rigidity, as part of rock matrix can significantly soften the matrix, depending on its volume fraction.

6. The effects of both bound and matrix clays on velocities V_p and V_s are caused mainly by the reduction of the shear modulus rather than the bulk modulus.

APPENDIX: DATA TABLE

Velocity V_p and V_s, density, porosity, and clay content at confining pressure 40, 30, 20, 10, 5 MPa and pore pressure 1 MPa for 80 sandstone samples.

REFERENCES

Benzing, W. M., 1978, V_p/V_s relationships in carbonates and sandstones: laboratory data: presented at the 48th Ann. Internat. Mtg., Soc. Expl. Geophys., San Francisco.

Biot, M. A., 1956 a, Theory of propagation of elastic waves in fluid saturated porous solid I, Low-frequency range: J. Acoust. Soc. America, 28, 168-178.

Biot, M. A., 1956 b, Theory of propagation of elastic waves in fluid saturated porous solid II, Higher frequency range: J. Acoust. Soc. America, 28, 168-178.

Birch, F., 1960, The velocity of compressional waves in rocks to 10 kilobars, 1: J. Geophys. Res., 65, 1083-1102.

Bourbie, T., 1985, Hydraulic and acoustic properties as a function of porosity in Fontainebleau sandstone: J. Geophys. Res., 90, 11524-11535.

Costagna, J. P., Batzle, M.L., and Eastwood, R.L., 1985, Relationship between compressional wave and shear wave velocities in clastic silicate rocks: Geophysics, 50, 551-570.

De Martini, D.C ., Beard, D. C., Danburg, J. S., and Robinson, J. H., 1976, Variation of seismic velocities in sandstones and limestones with lithology and pore fluid at simulated in situ conditions: Proc. EGPC Exploration seminar, Nov. 15-17, 1976.

Domenico, S. N., 1984, Rock lithology and porosity determination from shear and compressional wave velocity: Geophysics, 49, 1188-1195.

Eastwood, L. R., 1983, Basis for interpretation of V_p/V_s ratios in complex lithologies: Soc. Prof. Well Log Anal., 24, paper G.

Gassmann, F., 1951, Elastic waves through a packing of spheres: Geophysics, 16, 673-685.

Geertsma, J., 1961, Velocity log interpretation: the effect of rock bulk compressibility: Soc. Petr. Eng. J., 1, 235-248.

Geertsma, J., and Smit, D. C., 1961, Some aspects of acoustic wave propagation in fluid saturated porous solids: Geophysics, 26, 169-181.

Gregory, A. R., 1977, Aspects of rock physics from laboratory and log data that are important to seismic interpretation: Am. Assoc. Pet. Geol. Memoir 26, 15-46.

Han, D., 1986, Effects of porosity and clay content on wave velocities of sandstones -- a theoretical consideration: in this volume Chapter III.

Johnson, W. E., 1978, Relationship between shear-wave velocity and geotechnical parameters: Presented at the 48th Ann. Internat. Mtg., Soc. Expl. Geophys., San Francisco.

Kevin, B. H., 1981, Factors affecting acoustic compressional velocities and an examination of empirical correlations between velocities and porosities: Soc. Prof. Well Log Anal., 22, Paper PP.

King, M. S., 1966, Wave velocities in rocks as a function of changes in overburden pressure and pore fluid saturations: Geophysics, 31, 50-73.

Kowallis, B., Jones, L. E. A., and Wang, H. F., 1984, Velocity-porosity-clay content; systematics of poorly consolidated sandstones: J. Geophys. Res., 89, 10355-10364.

Kuster, G. T., and Toksöz, M. N., 1974, Velocity and attenuation of seismic waves in two-phase media, I: Theoretical formulation: Geophysics, 39, 587-606.

Mavko, G. M., and Nur, A., 1978, The effect of nonelliptical cracks on the compressibility of rocks: J. Geophys. Res., 83, 4459-4468.

Minear, M. J., 1982, Clay models and acoustic velocities: Presented at the 57th Ann. Mtg. of Am. Inst. Min. Eng., New Orleans.

O'Connell, R. J., and Budiansky, B., 1974, Seismic velocities in dry and saturated cracked solids: J. Geophys. Res., 79, 5412-5426.

Nur, A., and Simmons, G., 1969, The effect of saturation on velocity in low porosity rocks: Earth Planet. Sci. Lett., 7, 183-193.

Pickett, G. R., 1963, Acoustic character logs and their application in formation evaluation: J. Petr. Tech., 15, 659-667.

Quirein, J. A., Baldwin, J. L., Terry, L., and Hendricks, M., 1981, Estimation of clay types and volumes from well log data--an extension of the global method: SPWLA, 22, Paper Q.

Rafavich, F., Kendall, C. H. St. C., and Todd, T. P., 1984, The relationship between acoustic properties and the petrographic character of carbonate rocks: Geophysics, 49, 1622-1636.

Raymer, D. S., Hunt, E. R., and Gardner, J. S., 1980, An improved sonic transit time-to-porosity transform: Soc. Prof. Well Log Anal., 21, Paper P.

Robert, C. W., 1975, CRC handbook of chemistry and physics: F-18.

Robert, S. C., 1982, 1982 CRC handbook of physical properties of rocks: 2, 213.

Tatham, R. H., 1982, V_p/V_s and lithology: Geophysics, 47, 336-344.

Toksöz, M. N., Cheng, C. H., and Timer, A., 1976, Velocities of seismic waves in porous rocks: Geophysics, 41, 621-645.

Tosaya, C., and Nur, A., 1982a, Effects of diagenesis and clays on compressional velocities in rocks: Geophys. Res. Lett., 9, 5-8.

Tosaya, C., 1982b, Acoustical properties of clay-bearing rocks: Ph.D. dissertation, Stanford University.

Walsh, J. B., and Grosenbaugh, M. A., 1979, A new model for analyzing the effect of fractures on compressibility: J. Geophys. Res., 84, 3532-3536.

Wyllie, M. R. J., Gregory, A. R., and Gardner, L. W., 1956, Elastic wave velocities in heterogeneous and porous media: Geophysics, 21, 41-70.

Wyllie, M. R. J., Gregory, A. R., and Gardner, G. H. F., 1958, An experimental investigation of factors affecting elastic wave velocities in porous media: Geophysics, 23, 459-493.

TABLE CAPTIONS

Table 1. Model fitting to the experimental velocity data.

Table 2. The pressure dependence of the coefficients in the linear velocity-porosity-clay model.

FIGURE CAPTIONS

Figure 1. The range of clay content and porosity for the 80 shaly sandstones of this study. Ten samples are clean sandstones, the others (70) are shaly sandstones. Porosities range from 2 to 30 percent and clay content from 0 to about 50 percent. The data indicate that sandstones with high clay content tend to have low porosities.

Figure 2. Measured (a) compressional and (b) shear velocities vs. porosity for 80 sandstone samples at $P_c = 40$ MPa and $P_p = 1.0$ MPa.

Figure 3. Compressional and shear velocity V_p data (80 samples) at $P_c = 40$ MPa and $P_p = 1.0$ MPa fitted by the modified time average equation.

(a) Relative deviations of V_p vs. porosity showing fairly random scatter.

(b) Relative deviations of V_p showing a clear correlation with clay contents.

(c) Relative deviations of V_s vs. porosity showing fairly random scatter.

(d) Relative deviations of V_s showing a clear correlation with clay contents.

Figure 4. Compressional V_p and shear V_s velocities (80 samples) at confining pressure 40 MPa and pore pressure 1 MPa fitted by the linear model $V = A_0 - A_1 \phi$.

(a) Relative deviations of V_p vs. porosity showing large scatter.

(b) Relative deviations of V_p vs. clay content showing clear correlation.

(c) Relative deviations of V_s vs. porosity showing large scatter.

(d) Relative deviations of V_s vs. clay content showing clear correlation.

Figure 5. Compressional V_p and shear V_s velocities (80 samples) at confining pressure 40 MPa and pore pressure 1 MPa fitted by the model $V = A_0 - A_1 \phi - A_2 C$.

(a) Relative deviations of V_p vs. porosity showing randomly distribution

(b) Relative deviations of V_p vs. clay content showing no clear correlation.

(c) Relative deviations of V_s vs. porosity.

(d) Relative deviations of V_s vs. clay content.

Figure 6. Compressional velocity data (80 samples) fitted by the modified time average equation with a clay content term. Relative deviations vs. porosities indicate that the model overestimated V_p at porosity lower than 7 percent or higher than 25 percent, and underestimated V_p at intermediate porosity.

Figure 7. Fitting results of four models for (a) compressional velocity, (b) shear velocity versus porosity and clay content.

Figure 8. Normalized amplitude A_p vs. porosity for 51 sandstone samples at $P_c = 40$ MPa and $P_p = 1.0$ MPa. The results indicate that A_p tends to decrease with porosity.

Figure 9. (a) Bulk modulus K and (b) shear modulus μ vs. porosity (80 samples) at $P_c = 40$ MPa and $P_p = 1$ MPa. Porosity has more influence on reducing the shear modulus than the bulk modulus. Scatter of the shear modulus values, caused by the clays, are larger than scatter of bulk modulus data.

Figure 10. Velocity ratios V_p/V_s (80 samples) at $P_c = 40$ MPa and $P_p = 1$ MPa vs. (a) porosity and (b) clay content.

SAMP. #	Dw	CLAY	40 MPa			30 MPa			20 MPa			10 MPa			5 MPa		
			Vp	Vs	Φ	Vp	Vs	Φ	Vp	Vs	Φ	Vp	Vs	Φ	Vp	Vs	Φ
1	2.33	0.00	4.66	2.91	.1821	4.64	2.89	.1825	4.58	2.84	.1831	4.44	2.69	.1838	4.26	2.53	.1846
2	2.31	0.00	4.42	2.72	.1989	4.40	2.70	.1992	4.34	2.66	.1998	4.27	2.54	.2001	4.08	2.39	.2006
3	2.59	0.00	5.52	3.60	.0636	5.47	3.56	.0644	5.42	3.49	.0652	5.27	3.39	.0661	5.15	3.17	.0670
4	2.39	0.00	4.81	3.10	.1539	4.78	3.08	.1542	4.76	3.06	.1544	4.71	3.01	.1547	4.61	2.91	.1550
5	2.32	0.00	4.46	2.85	.1973	4.43	2.82	.1976	4.40	2.81	.1980	4.32	2.73	.1984	4.16	2.59	.1988
6	2.25	.10	3.68	2.22	.2355	3.64	2.20	.2361	3.58	2.16	.2368	3.49	2.10	.2377	3.43	2.02	.2382
7	2.24	.16	3.36	1.99	.2597	3.29	1.97	.2605	3.22	1.91	.2615	3.15	1.81	.2625	3.02	1.72	.2635
8	2.24	.10	3.69	2.17	.2403	3.64	2.15	.2409	3.58	2.10	.2416	3.47	2.03	.2425	3.35	1.92	.2432
9	2.38	.28	3.82	2.07	.1589	3.77	2.05	.1599	3.71	2.02	.1611	3.59	1.96	.1629	3.51	1.88	.1640
10	2.45	.06	4.73	3.00	.1056	4.70	2.96	.1063	4.66	2.93	.1072	4.62	2.89	.1082	4.57	2.85	.1091
11	2.23	.04	3.92	2.35	.2297	3.89	2.33	.2305	3.84	2.29	.2314	3.74	2.17	.2324	3.58	2.01	.2334
12	2.38	.03	4.60	2.81	.1546	4.55	2.78	.1559	4.51	2.74	.1562	4.45	2.68	.1572	4.40	2.62	.1580
13	2.47	.05	4.73	2.89	.1056	4.68	2.85	.1062	4.61	2.80	.1071	4.50	2.68	.1081	4.37	2.56	.1090
14	2.18	.06	3.74	2.08	.2536	3.72	2.07	.2546	3.69	2.05	.2556	3.63	2.01	.2568	3.56	1.98	.2575
15	2.53	.07	5.20	3.17	.0412	5.16	3.14	.0419	5.09	3.09	.0427	4.99	3.02	.0439	4.90	2.94	.0447
16	2.41	.27	4.06	2.24	.1256	4.01	2.20	.1262	3.93	2.15	.1270	3.79	2.03	.1280	3.67	1.94	.1289
17	2.36	.06	4.30	2.57	.1807	4.26	2.54	.1811	4.22	2.52	.1817	4.13	2.44	.1823	4.02	2.33	.1829
18	2.25	.16	3.54	2.05	.2557	3.49	2.02	.2564	3.43	1.98	.2573	3.34	1.91	.2583	3.24	1.81	.2590
19	2.50	.06	4.94	3.12	.0569	4.91	3.10	.0572	4.88	3.08	.0575	4.83	3.04	.0579	4.81	3.00	.0582
20	2.47	.14	4.23	2.41	.1309	4.17	2.37	.1315	4.07	2.31	.1322	3.98	2.21	.1332	3.85	2.14	.1339

App. 1

SAMP. #	Dw	CLAY	40 MPa			30 MPa			20 MPa			10 MPa			5 MPa		
			Vp	Vs	Φ	Vp	Vs	Φ	Vp	Vs	Φ	Vp	Vs	Φ	Vp	Vs	Φ
21	2.35	.06	4.32	2.62	.1761	4.28	2.59	.1765	4.23	2.55	.1771	4.14	2.46	.1777	4.03	2.35	.1785
22	2.28	.04	4.03	2.40	.2072	3.98	2.36	.2078	3.91	2.30	.2084	3.73	2.18	.2092	3.58	2.06	.2100
23	2.34	.05	4.18	2.50	.1880	4.14	2.47	.1885	4.08	2.41	.1891	3.94	2.28	.1900	3.79	2.16	.1908
24	2.57	.08	4.69	2.94	.0912	4.65	2.90	.0916	4.60	2.86	.0920	4.51	2.77	.0928	4.41	2.68	.0935
25	2.57	.08	4.88	3.05	.0920	4.85	3.02	.0924	4.80	2.98	.0928	4.72	2.91	.0934	4.65	2.82	.0940
26	2.27	.03	3.89	2.37	.2369	3.84	2.34	.2374	3.79	2.30	.2380	3.69	2.24	.2389	3.58	2.15	.2397
27	2.34	.06	4.15	2.51	.1903	4.11	2.48	.1907	4.04	2.43	.1913	3.92	2.33	.1920	3.71	2.15	.1928
28	2.30	.03	3.95	2.39	.2165	3.91	2.37	.2170	3.86	2.32	.2176	3.77	2.23	.2184	3.66	2.13	.2194
29	2.28	.06	4.03	2.40	.2213	4.00	2.37	.2219	3.94	2.33	.2226	3.85	2.28	.2236	3.70	2.11	.2246
30	2.31	.09	4.08	2.54	.1887	4.04	2.50	.1895	3.98	2.45	.1905	3.86	2.35	.1917	3.73	2.23	.1927
31	2.51	.13	4.62	2.80	.0835	4.58	2.75	.0848	4.48	2.65	.0857	4.34	2.53	.0876	4.18	2.40	.0902
32	2.57	.13	4.77	2.80	.0612	4.76	2.75	.0624	4.57	2.66	.0636	4.52	2.52	.0660	4.30	2.42	.0682
33	2.55	.12	4.78	3.23	.0690	4.77	3.19	.0700	4.72	3.03	.0712	4.57	2.87	.0735	4.32	2.38	.0755
34	2.54	.13	4.79	2.67	.0624	4.72	2.60	.0638	4.67	2.49	.0653	4.54	2.41	.0671	4.45	2.29	.0689
35	2.56	.12	5.00	3.13	.0313	4.99	3.02	.0320	4.95	2.90	.0330	4.80	2.77	.0348	4.63	2.59	.0370
36	2.61	.15	5.23	3.26	.0264	5.22	3.23	.0268	5.18	3.18	.0273	5.11	3.14	.0284	4.92	3.06	.0314
37	2.57	.07	5.23	3.09	.0312	5.09	3.07	.0315	4.97	2.97	.0324	4.88	2.75	.0345	4.73	2.61	.0365
38	2.54	.18	5.13	3.13	.0390	5.06	3.09	.0395	4.99	2.99	.0404	4.82	2.84	.0425	4.66	2.73	.0450
39	2.62	.15	5.11	3.10	.0225	5.10	3.09	.0229	5.08	3.06	.0235	5.00	2.95	.0245	4.87	2.90	.0260
40	2.61	.15	4.68	2.73	.0612	4.67	2.72	.0617	4.61	2.70	.0627	4.53	2.60	.0642	4.44	2.51	.0672

SAMP. #	Dw	CLAY	40 MPa			30 MPa			20 MPa			10 MPa			5 MPa		
			Vp	Vs	Φ	Vp	Vs	Φ	Vp	Vs	Φ	Vp	Vs	Φ	Vp	Vs	Φ
41	2.55	.38	4.37	2.62	.0634	4.33	2.59	.0641	4.30	2.56	.0651	4.23	2.49	.0665	4.11	2.41	.0683
42	2.56	.40	4.24	2.49	.0719	4.21	2.46	.0725	4.16	2.41	.0735	4.10	2.36	.0747	4.04	2.30	.0762
43	2.49	.37	4.08	2.34	.1118	4.04	2.30	.1127	3.99	2.28	.1139	3.91	2.22	.1153	3.81	2.13	.1170
44	2.53	.40	4.24	2.52	.0885	4.21	2.50	.0892	4.16	2.45	.0903	4.06	2.38	.0916	3.97	2.29	.0932
45	2.55	.35	4.17	2.43	.0927	4.12	2.40	.0935	4.05	2.35	.0947	3.97	2.28	.0964	3.89	2.20	.0983
46	2.57	.45	4.32	2.57	.0677	4.28	2.53	.0685	4.22	2.48	.0697	4.12	2.39	.0713	4.03	2.30	.0738
47	2.41	.13	4.47	2.64	.1402	4.40	2.60	.1407	4.31	2.54	.1419	4.10	2.39	.1425	3.92	2.23	.1437
48	2.42	.14	4.32	2.55	.1632	4.28	2.53	.1637	4.21	2.47	.1646	4.10	2.39	.1656	3.98	2.28	.1668
49	2.38	.10	4.24	2.51	.1560	4.18	2.45	.1565	4.10	2.39	.1571	3.96	2.26	.1582	3.81	2.13	.1593
50	2.38	.11	4.22	2.43	.1735	4.17	2.38	.1741	4.11	2.31	.1747	3.95	2.18	.1760	3.78	2.04	.1772
51	2.38	.16	4.19	2.42	.1696	4.13	2.38	.1701	4.03	2.32	.1716	3.91	2.21	.1726	3.76	2.06	.1739
52	2.40	.44	3.71	1.97	.1278	3.66	1.94	.1288	3.62	1.90	.1302	3.52	1.81	.1322	3.42	1.74	.1360
53	2.38	.46	3.64	1.99	.1310	3.59	1.97	.1323	3.53	1.93	.1338	3.44	1.87	.1360	3.37	1.81	.1380
54	2.35	.51	3.68	2.01	.1146	3.63	1.98	.1160	3.54	1.94	.1178	3.43	1.86	.1205	3.33	1.75	.1246
55	2.09	.11	3.20	1.75	.2993	3.16	1.73	.3005	3.11	1.69	.3019	3.01	1.60	.3039	2.86	1.51	.3061
56	2.12	.12	3.17	1.77	.2945	3.13	1.75	.2956	3.08	1.72	.2970	2.99	1.65	.2987	2.94	1.57	.3004
57	2.35	.27	3.99	2.13	.1500	3.90	2.08	.1512	3.78	2.01	.1525	3.60	1.86	.1551	3.44	1.72	.1575
58	2.35	.27	4.00	2.16	.1454	3.93	2.11	.1467	3.83	2.03	.1479	3.70	1.94	.1505	3.55	1.76	.1535
59	2.20	.22	3.36	1.89	.2435	3.31	1.86	.2446	3.24	1.79	.2458	3.08	1.64	.2475	2.93	1.47	.2492
60	2.19	.12	3.55	1.94	.2531	3.49	1.90	.2541	3.41	1.84	.2554	3.22	1.71	.2574	3.05	1.53	.2590

App. 3

SAMP. #	Dw	CLAY	40 MPa			30 MPa			20 MPa			10 MPa			5 MPa		
			Vp	Vs	Φ	Vp	Vs	Φ	Vp	Vs	Φ	Vp	Vs	Φ	Vp	Vs	Φ
61	2.41	.37	3.76	2.11	.1430	3.73	2.08	.1440	3.65	2.00	.1458	3.54	1.90	.1480	3.41	1.79	.1504
62	2.48	.44	3.84	2.15	.1089	3.80	2.13	.1095	3.74	2.08	.1113	3.64	2.00	.1129	3.58	1.92	.1146
63	2.47	.41	3.97	2.19	.0937	3.92	2.16	.0947	3.85	2.12	.0965	3.76	2.03	.0991	3.63	1.91	.1035
64	2.37	.27	3.98	2.19	.1434	3.95	2.15	.1445	3.88	2.09	.1461	3.74	2.00	.1493	3.65	1.88	.1506
66	2.17	.08	3.67	2.20	.2625	3.62	2.17	.2632	3.57	2.13	.2641	3.42	2.00	.2656	3.27	1.85	.2675
66	2.25	.06	3.61	2.09	.2679	3.56	2.06	.2686	3.50	2.00	.2696	3.33	1.84	.2710	3.15	1.73	.2724
67	2.12	.11	3.56	2.07	.2785	3.52	2.03	.2793	3.46	1.98	.2803	3.28	1.84	.2818	3.12	1.66	.2835
68	2.17	.07	3.50	1.99	.2655	3.43	1.95	.2664	3.33	1.89	.2674	3.13	1.75	.2692	2.98	1.50	.2705
69	2.14	.07	3.58	2.09	.2742	3.53	2.05	.2750	3.43	1.96	.2760	3.23	1.81	.2774	3.04	1.60	.2789
70	2.29	.11	3.88	2.23	.2021	3.81	2.17	.2028	3.69	2.08	.2037	3.48	1.91	.2052	3.32	1.76	.2065
71	2.47	.21	4.25	2.48	.1089	4.19	2.42	.1100	4.08	2.32	.1118	3.90	2.18	.1146	3.71	2.08	.1177
72	2.39	.06	4.61	2.73	.1508	4.54	2.66	.1516	4.42	2.53	.1529	4.17	2.36	.1548	3.96	2.16	.1567
73	2.47	.23	4.42	2.61	.1021	4.35	2.55	.1031	4.27	2.46	.1047	4.09	2.30	.1071	3.91	2.14	.1100
74	2.64	.24	4.60	2.77	.0586	4.56	2.72	.0594	4.44	2.64	.0605	4.31	2.54	.0631	4.10	2.28	.0651
75	2.38	.18	4.07	2.37	.1442	4.01	2.32	.1452	3.93	2.27	.1466	3.85	2.17	.1490	3.67	2.02	.1514
76	2.52	0.00	5.42	3.55	.0746	5.41	3.54	.0748	5.38	3.51	.0749	5.30	3.42	.0752	5.24	3.36	.0755
77	2.55	0.00	5.73	3.77	.0550	5.72	3.76	.0550	5.71	3.74	.0551	5.65	3.70	.0552	5.60	3.63	.0553
78	2.49	0.00	5.34	3.51	.0973	5.34	3.51	.0974	5.33	3.51	.0975	5.32	3.50	.0976	5.31	3.48	.0977
79	2.35	0.00	4.68	2.96	.1769	4.66	2.95	.1772	4.63	2.93	.1774	4.60	2.88	.1777	4.53	2.82	.1779
80	2.28	0.00	4.34	2.70	.2235	4.32	2.69	.2238	4.29	2.67	.2242	4.25	2.63	.2247	4.19	2.57	.2249

FOR CLEAN SANDSTONES (10 samples)

$V_p = 6.08 - 8.06 \times \phi$	**R: 0.994**	**RMS: 1.0%**
$V_s = 4.06 - 6.28 \times \phi$	**R: 0.992**	**RMS: 1.6%**

FOR SHALY SANDSTONES (70 samples)

WITHOUT CLAY TERM

$\frac{1}{V_p} = 0.194 + 0.328 \times \phi$	**R: 0.844**	**RMS: 6.6%**
$\frac{1}{V_s} = 0.322 + 0.628 \times \phi$	**R: 0.750**	**RMS: 10.3%**

WITH A CLAY CONTENT TERM

1. LINEAR EQUATION

$V_p = 5.59 - 6.93 \times \phi - 2.18 \times C$	**R: 0.985**	**RMS: 2.1%**
$V_s = 3.52 - 4.91 \times \phi - 1.89 \times C$	**R: 0.959**	**RMS: 4.3%**

2. TIME AVERAGE EQUATION

$\frac{1}{V_p} = 0.163 + 0.399 \times \phi + 0.119 \times C$	**R: 0.972**	**RMS: 2.8%**
$\frac{1}{V_s} = 0.242 + 0.812 \times \phi + 0.307 \times C$	**R: 0.945**	**RMS: 5.1%**

3. LOGARITHMIC EQUATION

$\log_{10} V_p = 0.763 - 0.718 \times \phi - 0.220 \times C$	**R: 0.981**	**RMS: 2.4%**
$\log_{10} V_s = 0.571 - 0.859 \times \phi - 0.329 \times C$	**R: 0.956**	**RMS: 4.6%**

4. LINEAR POWER EQUATION

$V_p = 5.68 - 6.93 \times \phi^{0.995} - 2.00 \times C^{0.810}$		**RMS: 2.1%**
$V_s = 3.82 - 4.43 \times \phi^{0.876} - 1.64 \times C^{0.598}$		**RMS: 4.2%**

R: correlation coefficient. RMS: relative root mean square deviation with 68.3 % confidence.

TABLE 1

VELOCITY EQUATION

$$V = A_0 - A_1 \times \phi - A_2 \times C$$

FOR V_p

P_e bars	A_0 km/s	A_1 km/s	A_2 km/s	R	S_d km/s	RMS %
400	5.59	6.93	2.18	0.985	0.09	2.1
300	5.55	6.96	2.18	0.985	0.09	2.1
200	5.49	6.94	2.17	0.981	0.10	2.4
100	5.39	7.08	2.13	0.978	0.11	2.8
50	5.26	7.08	2.02	0.969	0.14	3.4

FOR V_s

400	3.52	4.91	1.89	0.959	0.11	4.3
300	3.47	4.84	1.87	0.957	0.11	4.5
200	3.39	4.73	1.81	0.951	0.12	4.9
100	3.29	4.73	1.74	0.937	0.14	5.8
50	3.16	4.77	1.64	0.916	0.16	7.2

R: CORRELATION COEFFICIENT

Sd: STANDARD DEVIATION

RMS: RELATIVE ROOT MEAN SQUARE DEVIATION WITH 68.3 % CONFIDENCE.

TABLE 2

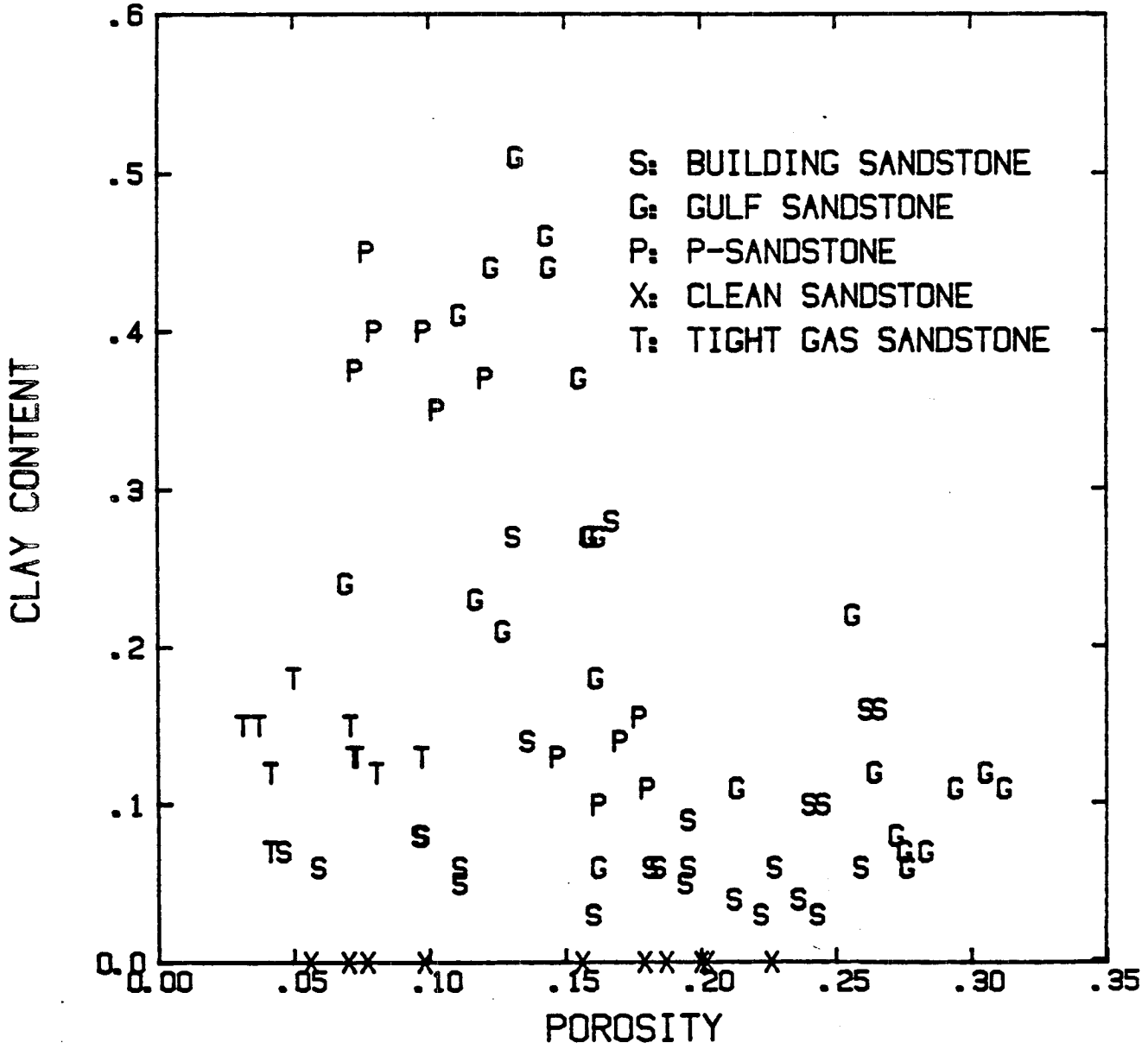
S: BUILDING SANDSTONE
G: GULF SANDSTONE
P: P-SANDSTONE
X: CLEAN SANDSTONE
T: TIGHT GAS SANDSTONE
CLAY CONTENT
POROSITY
.6
.5
.4
.3
.2
.1
0.0
0.00
.05
.10
.15
.20
.25
.30
.35

Fig. 1

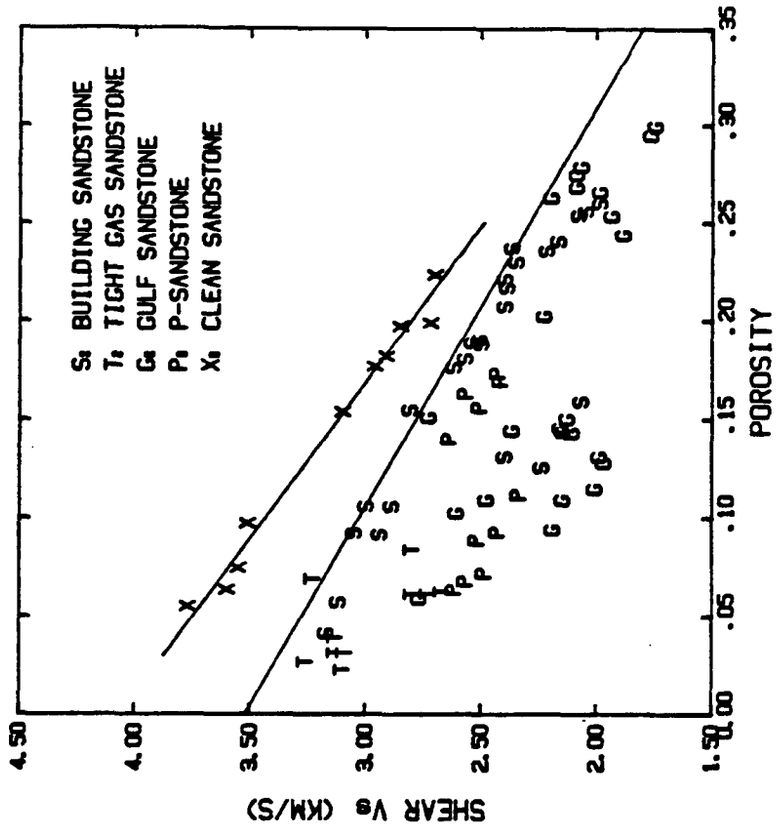
Sa BUILDING SANDSTONE
Ti TIGHT GAS SANDSTONE
Ga GULF SANDSTONE
Pa P-SANDSTONE
Xa CLEAN SANDSTONE
SHEAR Vs (KM/S)
POROSITY

Fig. 2b

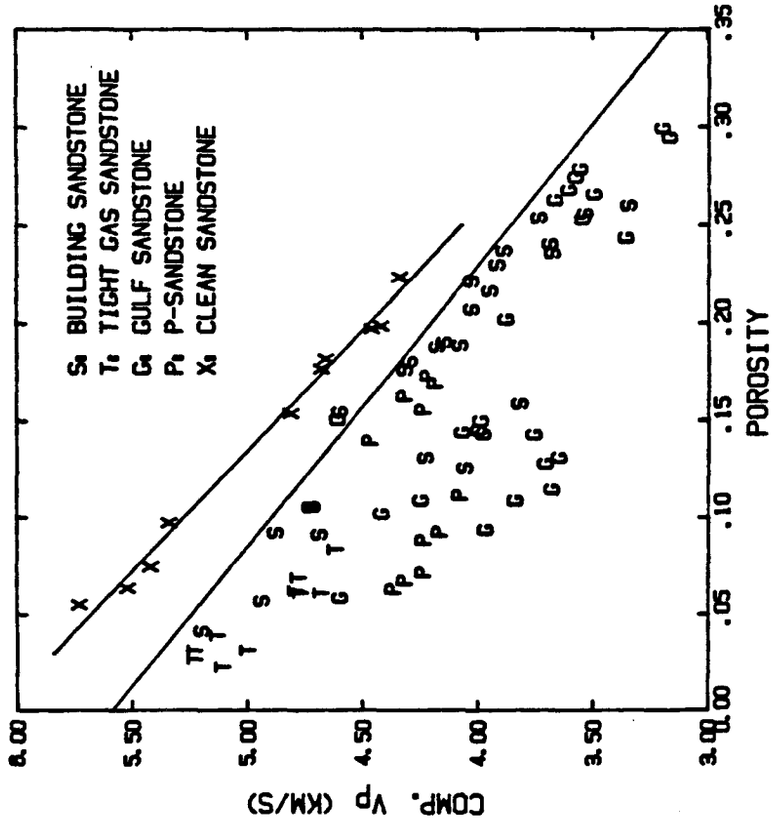
Sa BUILDING SANDSTONE
Ti TIGHT GAS SANDSTONE
Ga GULF SANDSTONE
Pa P-SANDSTONE
Xa CLEAN SANDSTONE
COMP. Vp (KM/S)
POROSITY

Fig. 2a

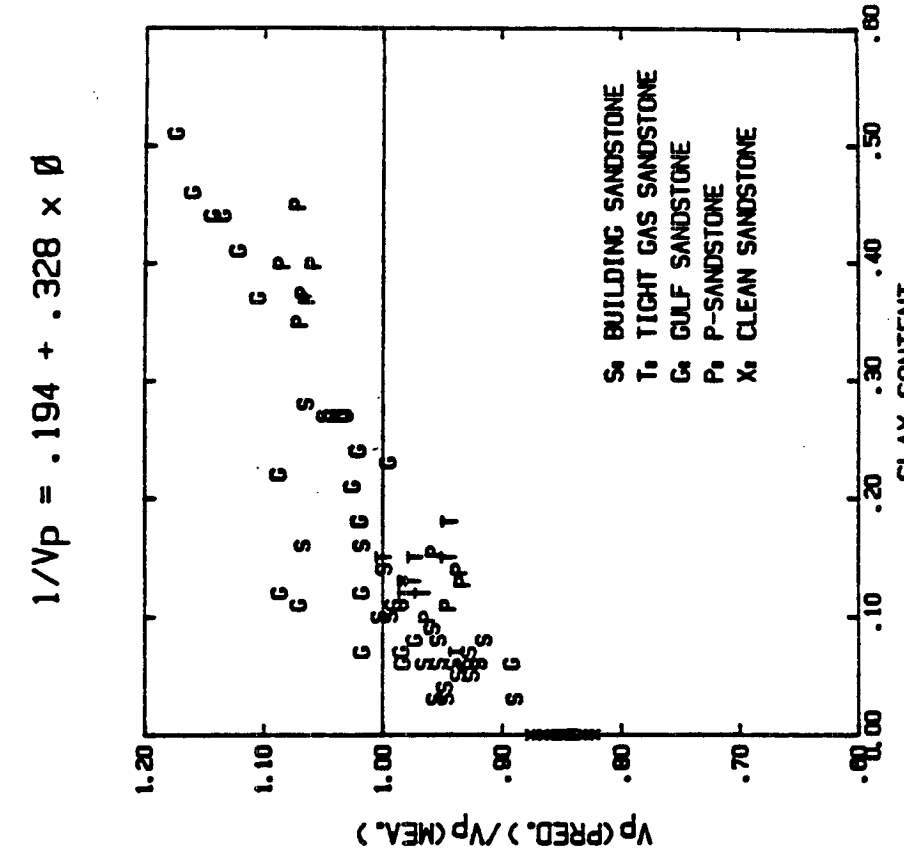
1/Vp = .194 + .328 x Ø
Vp (PRED.) /Vp (MEA.)
1.20
1.10
1.00
.90
.80
.70
.60
.00
.05
.10
.15
.20
.25
.30
.35
POROSITY
Sa BUILDING SANDSTONE
Ti TIGHT GAS SANDSTONE
Ga GULF SANDSTONE
Pa P-SANDSTONE
Xa CLEAN SANDSTONE

Fig. 3a

1/Vp = .194 + .328 x Ø
Vp (PRED.) /Vp (MEA.)
1.20
1.10
1.00
.90
.80
.70
.60
.00
.10
.20
.30
.40
.50
.60
CLAY CONTENT
Sa BUILDING SANDSTONE
Ti TIGHT GAS SANDSTONE
Ga GULF SANDSTONE
Pa P-SANDSTONE
Xa CLEAN SANDSTONE

Fig. 3b

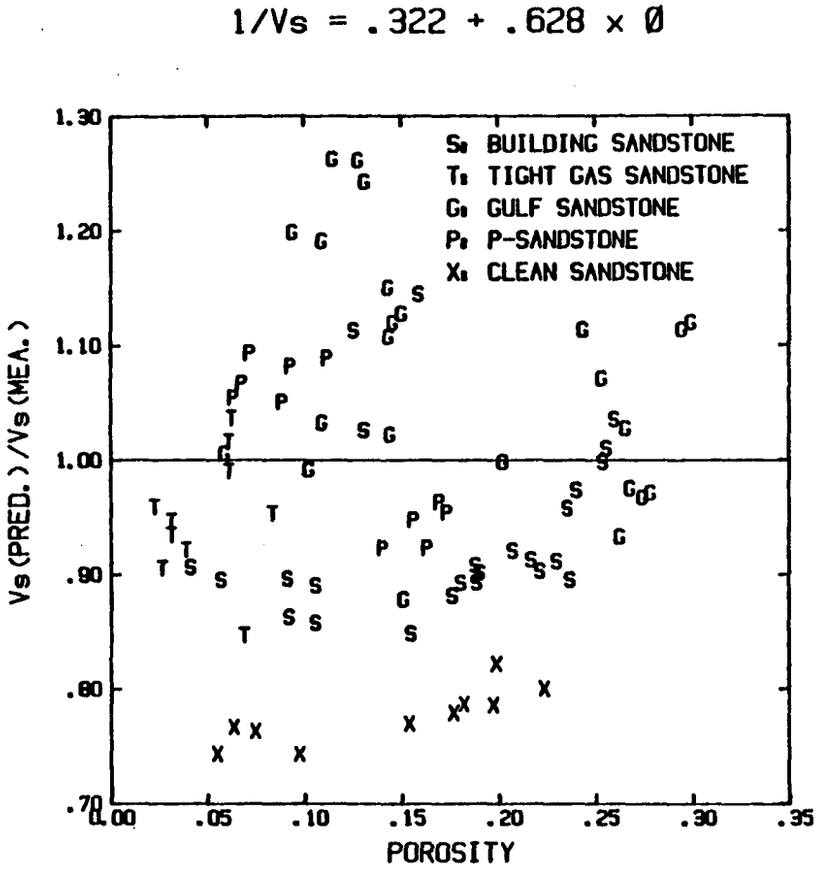
1/Vs = .322 + .628 x Ø
S= BUILDING SANDSTONE
T= TIGHT GAS SANDSTONE
G= GULF SANDSTONE
P= P-SANDSTONE
X= CLEAN SANDSTONE
Vs (PRED.) /Vs (MEA.)
POROSITY
1.30
1.20
1.10
1.00
.90
.80
.70
0.00
.05
.10
.15
.20
.25
.30
.35

Fig. 3c

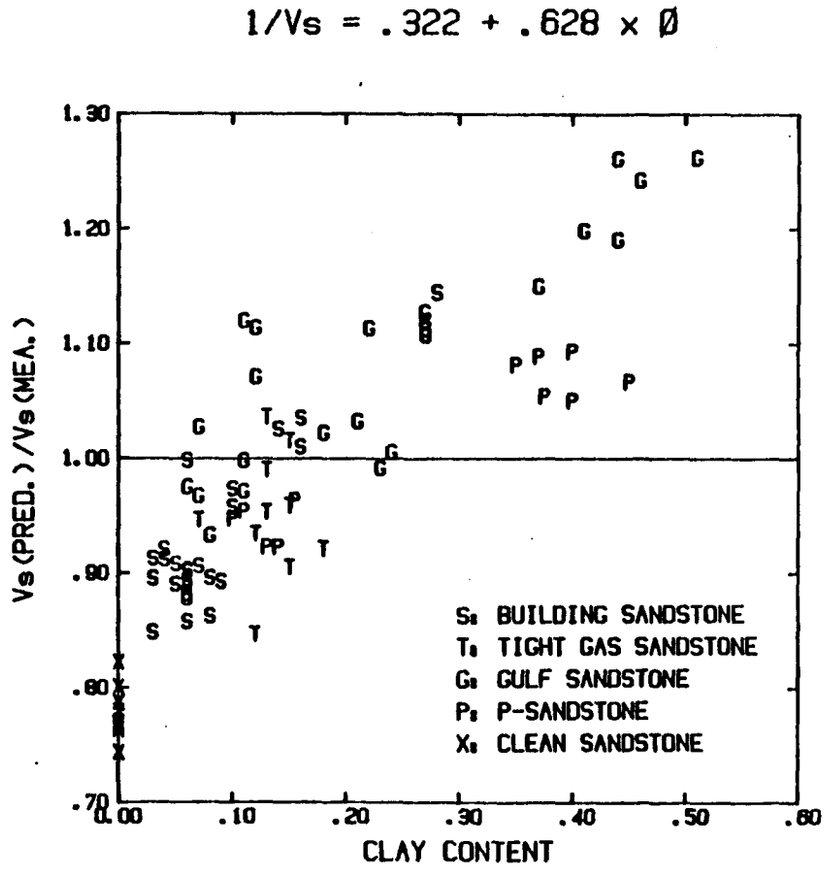
1/Vs = .322 + .628 x Ø
S= BUILDING SANDSTONE
T= TIGHT GAS SANDSTONE
G= GULF SANDSTONE
P= P-SANDSTONE
X= CLEAN SANDSTONE
Vs (PRED.) /Vs (MEA.)
CLAY CONTENT
1.30
1.20
1.10
1.00
.90
.80
.70
0.00
.10
.20
.30
.40
.50
.60

Fig. 3d

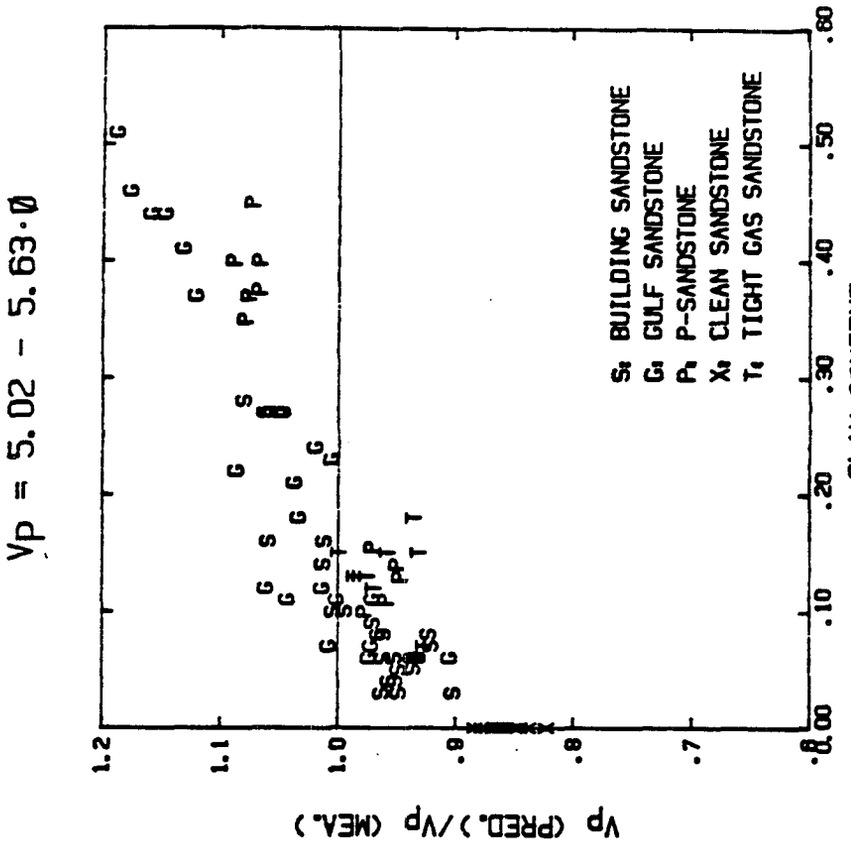
Vp = 5.02 - 5.63·Ø
Vp (PRED.)/Vp (MEA.)
CLAY CONTENT
Sa BUILDING SANDSTONE
Ga GULF SANDSTONE
Pa P-SANDSTONE
Xa CLEAN SANDSTONE
Ta TIGHT GAS SANDSTONE

Fig. 4b

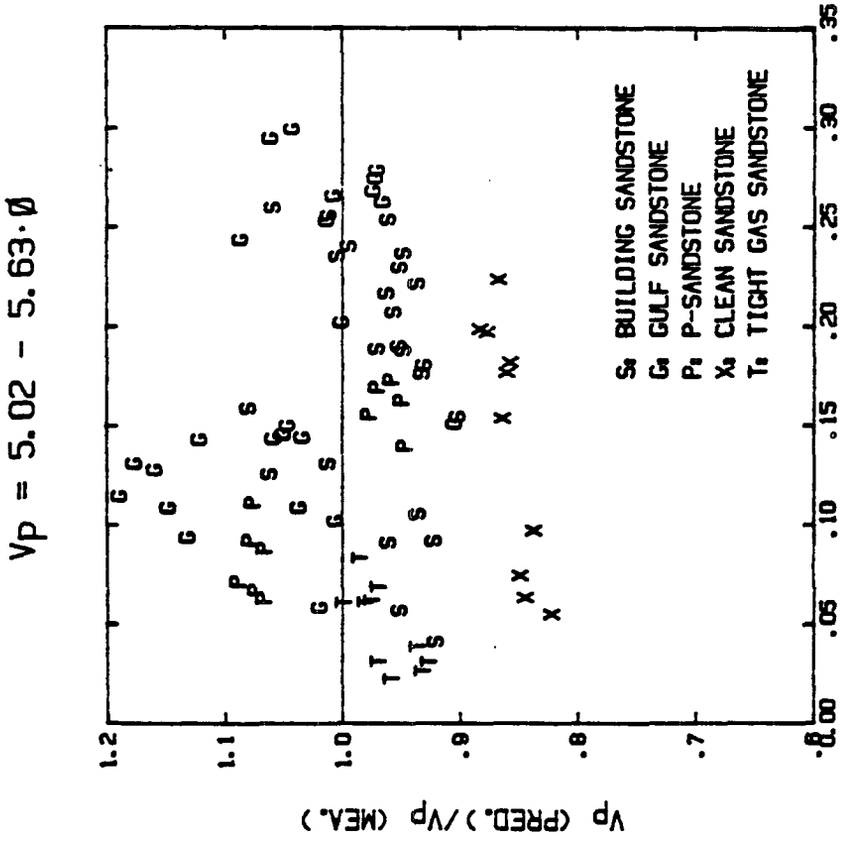
Vp = 5.02 - 5.63·Ø
Vp (PRED.)/Vp (MEA.)
POROSITY
Sa BUILDING SANDSTONE
Ga GULF SANDSTONE
Pa P-SANDSTONE
Xa CLEAN SANDSTONE
Ta TIGHT GAS SANDSTONE

Fig. 4a

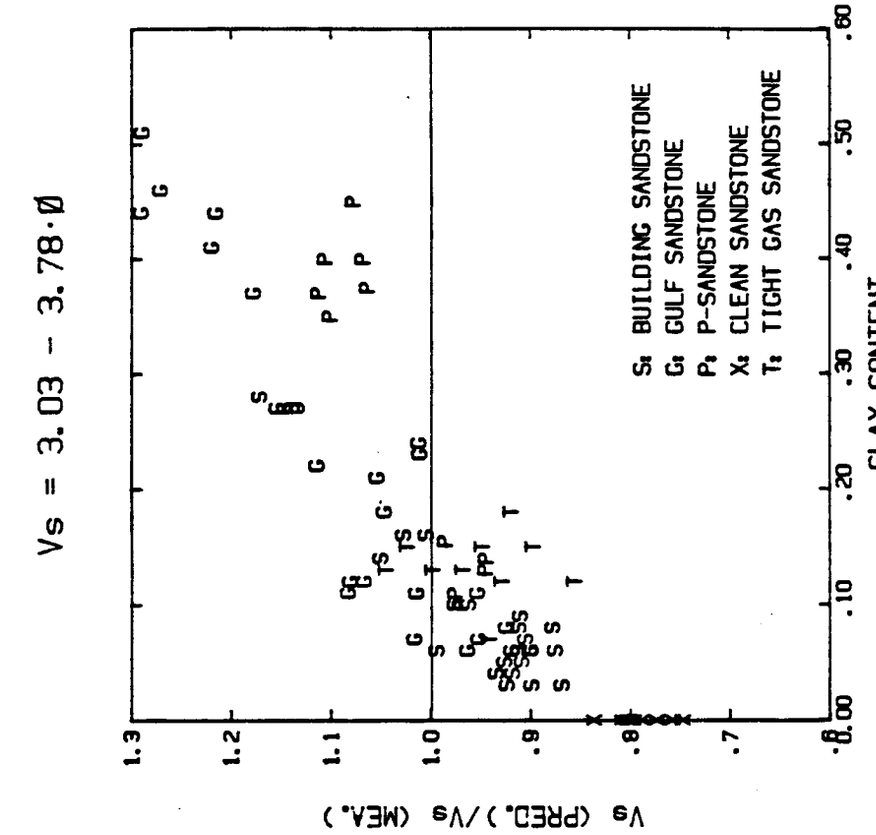
Vs = 3.03 - 3.78·Ø
Vs (PRED.)/Vs (MEA.)
CLAY CONTENT
S: BUILDING SANDSTONE
G: GULF SANDSTONE
P: P-SANDSTONE
X: CLEAN SANDSTONE
T: TIGHT GAS SANDSTONE

Fig. 4d

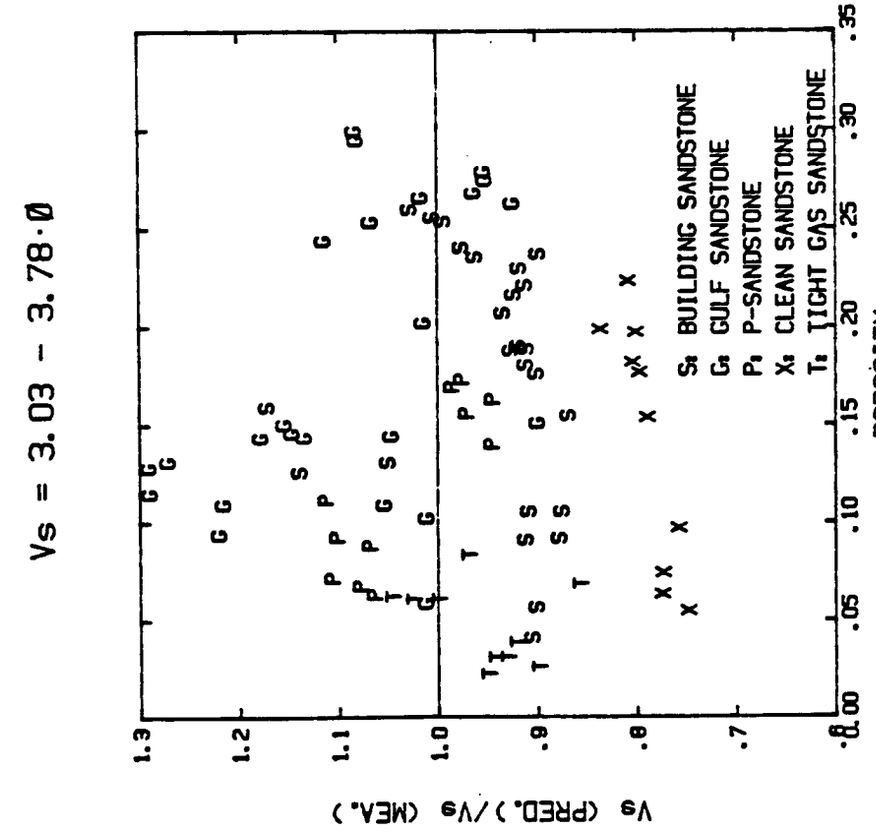
Vs = 3.03 - 3.78·Ø
Vs (PRED.)/Vs (MEA.)
POROSITY
S: BUILDING SANDSTONE
G: GULF SANDSTONE
P: P-SANDSTONE
X: CLEAN SANDSTONE
T: TIGHT GAS SANDSTONE

Fig. 4c

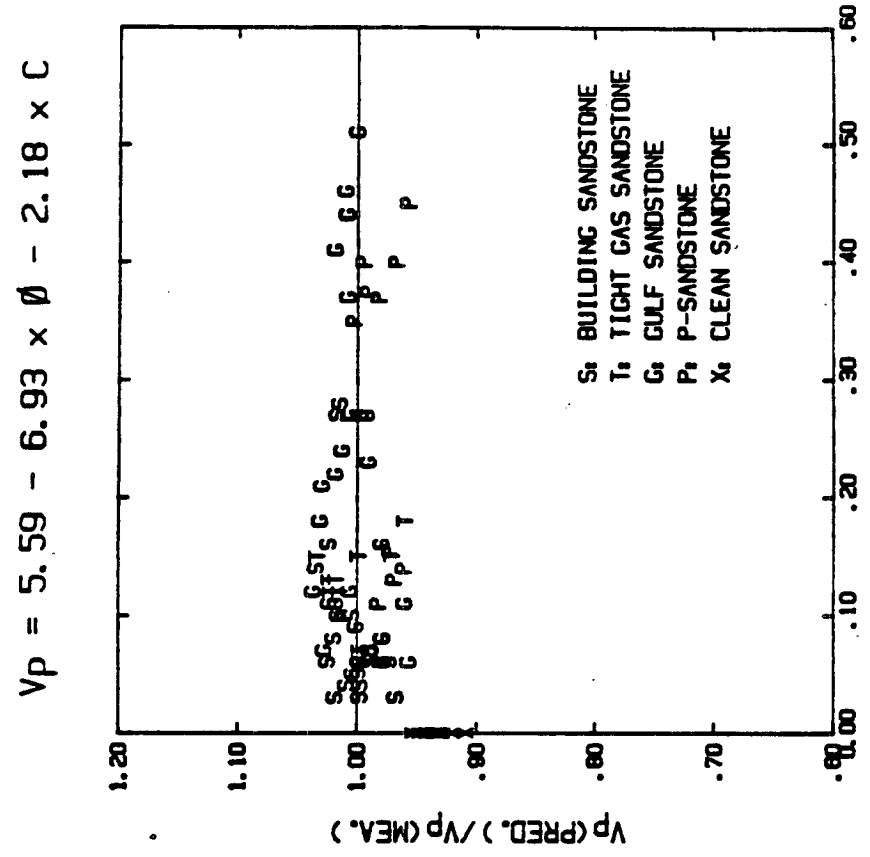
Vp = 5.59 - 6.93 x Ø - 2.18 x C
Vp (PRED.) /Vp (MEA.)
POROSITY
S: BUILDING SANDSTONE
T: TIGHT GAS SANDSTONE
G: GULF SANDSTONE
P: P-SANDSTONE
X: CLEAN SANDSTONE

Fig. 5a

Vp = 5.59 - 6.93 x Ø - 2.18 x C
Vp (PRED.) /Vp (MEA.)
CLAY CONTENT
S: BUILDING SANDSTONE
T: TIGHT GAS SANDSTONE
G: GULF SANDSTONE
P: P-SANDSTONE
X: CLEAN SANDSTONE

Fig. 5b

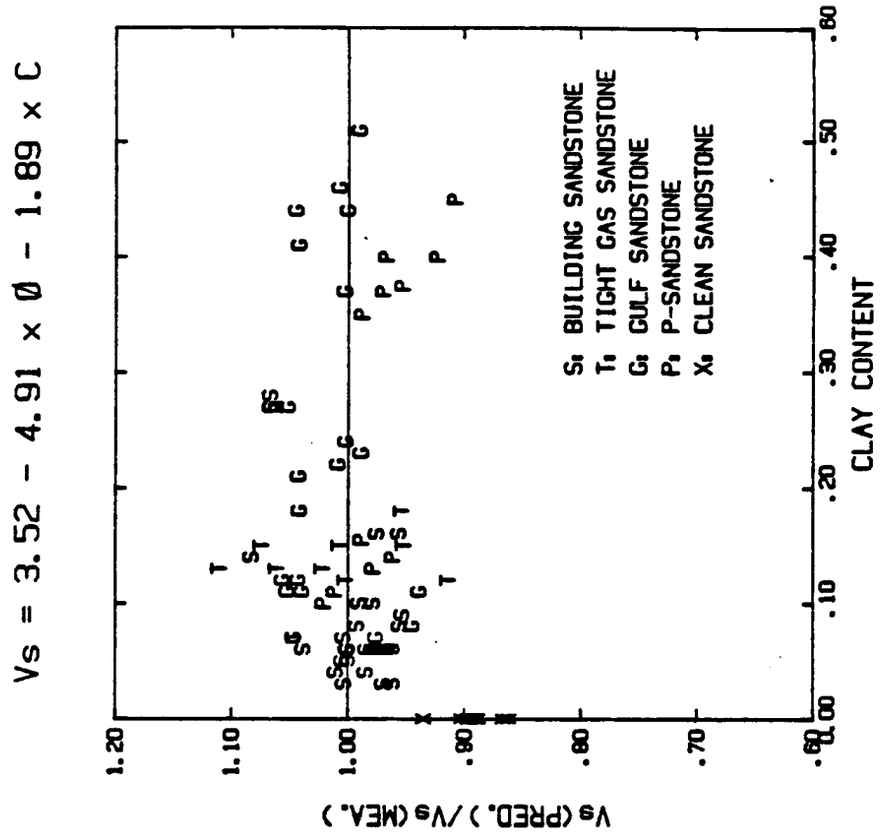
Vs = 3.52 - 4.91 x Ø - 1.89 x C
Vs (PRED.) /Vs (MEA.)
1.20
1.10
1.00
.90
.80
.70
.60
.00
.05
.10
.15
.20
.25
.30
.35
POROSITY
S: BUILDING SANDSTONE
T: TIGHT GAS SANDSTONE
G: GULF SANDSTONE
P: P-SANDSTONE
X: CLEAN SANDSTONE

Fig. 5c

Vs = 3.52 - 4.91 x Ø - 1.89 x C
Vs (PRED.) /Vs (MEA.)
1.20
1.10
1.00
.90
.80
.70
.60
.00
.10
.20
.30
.40
.50
.60
CLAY CONTENT
S: BUILDING SANDSTONE
T: TIGHT GAS SANDSTONE
G: GULF SANDSTONE
P: P-SANDSTONE
X: CLEAN SANDSTONE

Fig. 5d

$$1/V_p = .163 + .399 \times \emptyset + .119 \times C$$

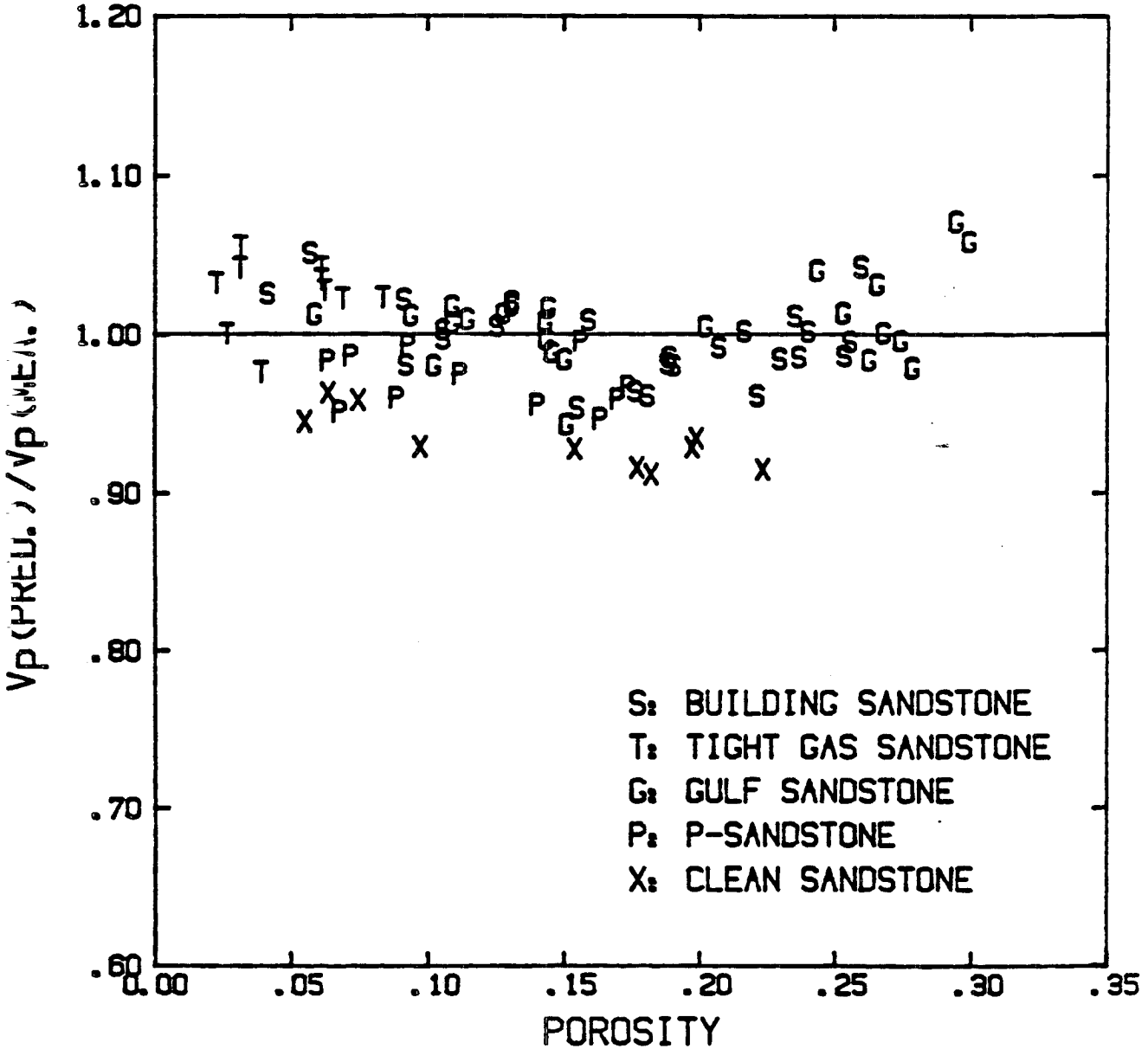

Fig. 6

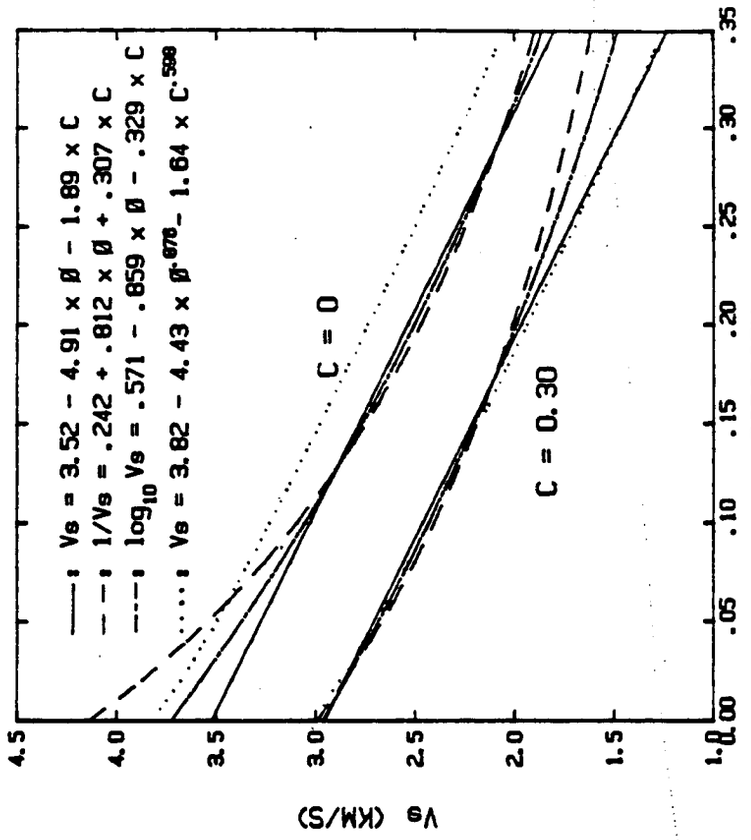
Vs = 3.52 − 4.91 × Ø − 1.89 × C
1/Vs = .242 + .812 × Ø + .307 × C
log10 Vs = .571 − .859 × Ø − .329 × C
Vs = 3.82 − 4.43 × Ø^.676 − 1.64 × C^.508
C = 0
C = 0.30
Vs (KM/S)
POROSITY

Fig. 7b

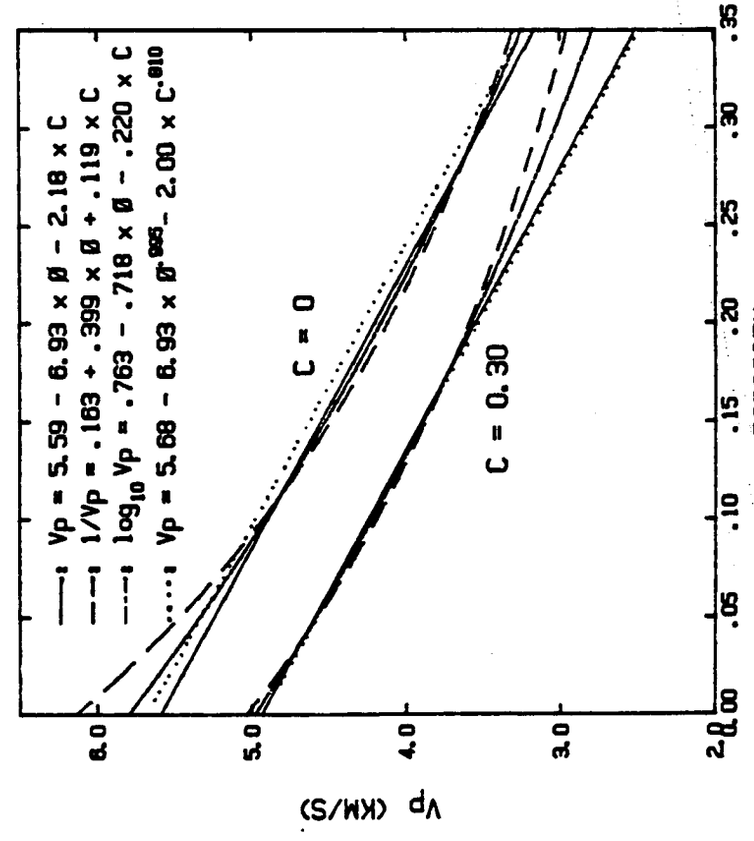
Vp = 5.59 − 6.93 × Ø − 2.18 × C
1/Vp = .183 + .399 × Ø + .119 × C
log10 Vp = .763 − .718 × Ø − .220 × C
Vp = 5.68 − 6.93 × Ø^.905 − 2.00 × C^.810
C = 0
C = 0.30
Vp (KM/S)
POROSITY

Fig. 7a

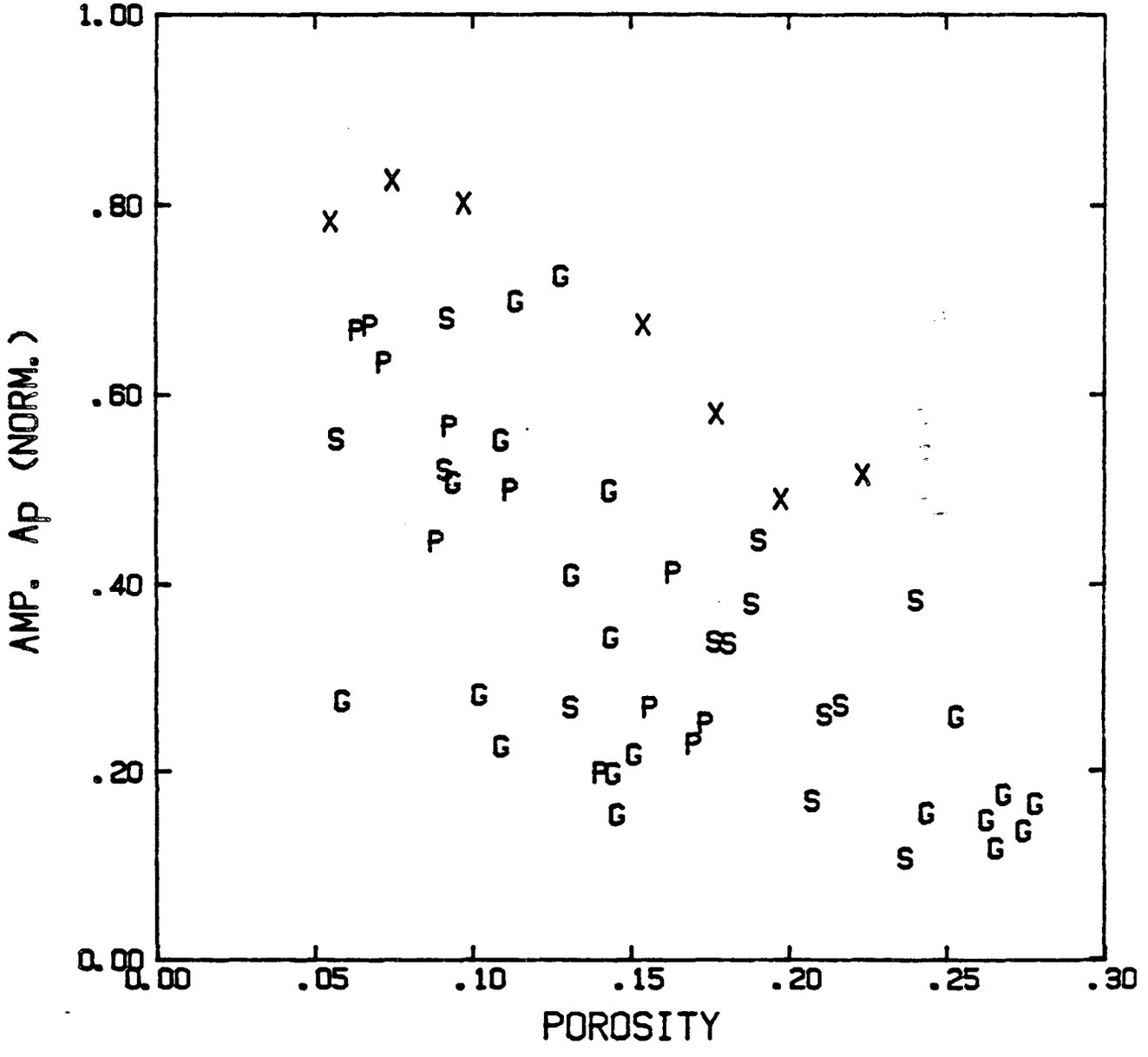

Fig. 8

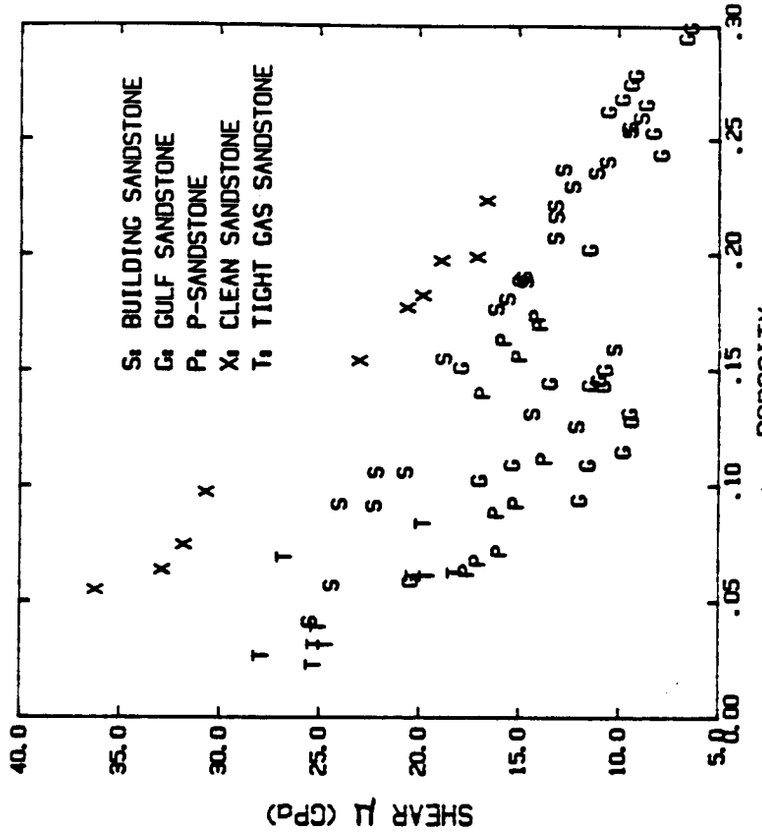
SHEAR μ (GPa)
POROSITY
S: BUILDING SANDSTONE
G: GULF SANDSTONE
P: P-SANDSTONE
X: CLEAN SANDSTONE
T: TIGHT GAS SANDSTONE

Fig. 9b

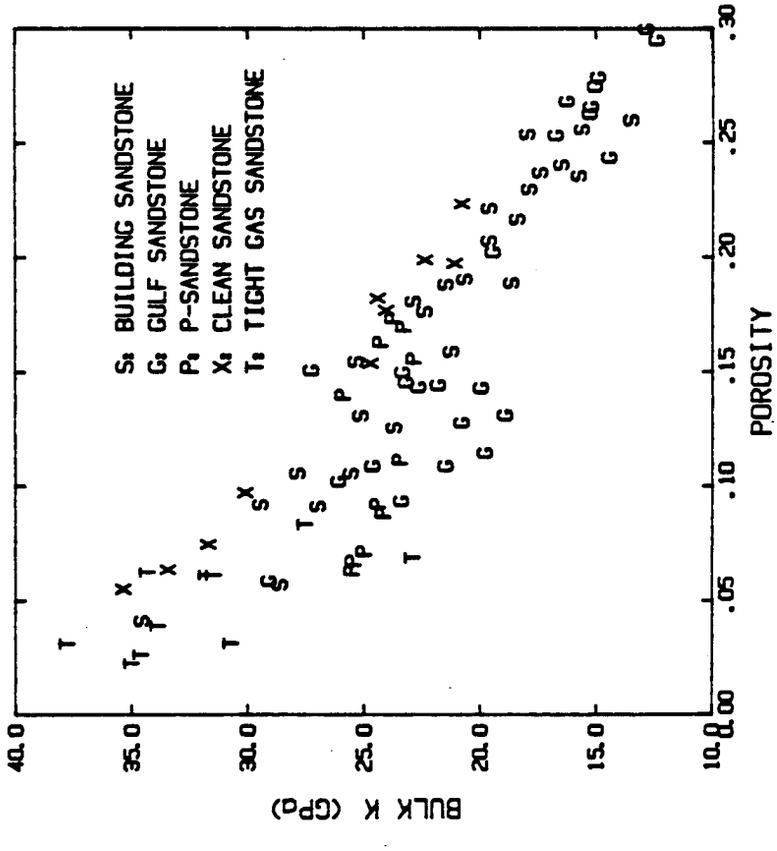
BULK κ (GPa)
POROSITY
S: BUILDING SANDSTONE
G: GULF SANDSTONE
P: P-SANDSTONE
X: CLEAN SANDSTONE
T: TIGHT GAS SANDSTONE

Fig. 9a

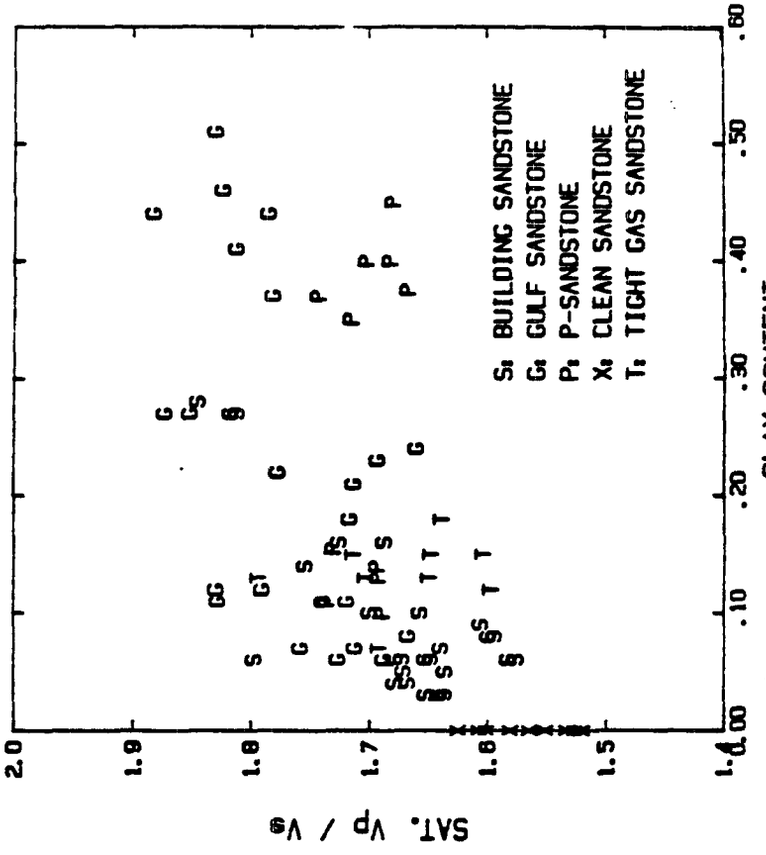

Fig. 10a

Fig. 10b

CHAPTER III

EFFECTS OF POROSITY AND CLAY CONTENT ON WAVE VELOCITIES OF SANDSTONES: --A THEORETICAL CONSIDERATION

ABSTRACT

The effects of porosity and clay content on velocities of sandstones were empirically formulated on the ultrasonic measurements for 80 saturated sandstone samples (Han, 1986 a). The results give a chance to test different theoretical models using the measured parameters. For simplification, only the relations at confining pressure 40 MPa and pore pressure 1 MPa were modeled, and the effect of variations in pressure was not studied.

The porosity effects on velocities can be fairly estimated by the pore geometry models, but not by the bound theory. The self-consistent needle model (O'Connell and Budiansky, 1974) fits better with empirical data. but still significantly underestimates the porosity effects. The triangular pores model (Mavko, 1980) fits well with empirical data at porosity of less than 10 percent. The pore aspect-ratio spectrum model (Kuster and Toksöz, 1974; Chang and Toksöz, 1979) can model well the porosity effects using the simplest spectrum. The K-T model reveals that very thin pores (aspect-ratio less than 0.01) are an intrinsic requirement for fitting both compressional and shear velocities. This requirement is enhanced with increasing clay content. This implies that at high differential pressure, the thin pores remain open in sandstones.

The bound clay effect (Han, 1986 a) is hardly reflected using a porous model. It can be modeled using the Reuss bound. The calculated moduli of the bound clay using the Reuss bound are in reasonable agreement with velocity data measured for clay powders mixed with water. Significant clay effects on velocities are caused by clay's lower moduli (especially the shear modulus) and by it's being located between grain boundaries.

The matrix clay effects (Han, 1986 a) can be well estimated using the Hashin-Shtrikman bounds. The results show that the "clay point" extrapolated from empirical relations (Castangna et al., 1985; Zimmerman and King, 1986) is underestimated. The bulk modulus of matrix clay is bounded from 23 GPa to 24.5 GPa and shear modulus is from 8 GPa to 10 GPa. The K-T model with clay filled into sphere inclusions coincides with the high H-S bound. The clay moduli, therefore, are underestimated by the K-T model.

The model results reveal that even a simple relation between velocities and porosity for clean sandstones cannot be accurately modeled using present theories. Many uncertainties indicate there is still a long way to go to understand and describe the properties of sandstones.

Introduction

In our experimental study, we measured compressional velocity V_p and shear velocity V_s as functions of pressure in 80 sandstone samples with porosity ranging from 2 to 30 percent and clay content ranging from zero to 50 percent. Figures 1 a and b show V_p and V_s versus porosity at confining pressure 40 MPa and pore pressure 1 MPa for 80 different sandstone samples. In principle, the velocities and elastic moduli (dynamic) of sandstones correlate with the following parameters: porosity, mineral compositions, grain cement, grain contact, grain packing, pore geometry, and pore fluid. These parameters are influenced by conditions such as confining pressure, pore fluid, saturation, pore fluid pressure, temperature, and wave frequency. Unfortunately, some of these parameters, such as grain cement and contact, have hardly even been measured or defined. Therefore, the data is often complicated.

It is well known that all elastic models of porous media predict that velocities decrease with increasing porosities in sandstones. Bourbie and Zinsezner (1985) shown an opposite behavior in Fontainbleau sandstones. Our data show a result similar to those of them. Font. E and C have 9.8 and 7.7 percent porosity respectively. At differential pressure lower than 10 MPa, velocities of Font. E are higher than those of Font. C (Figure 2 a and b). This suggests that even for similar rocks, the velocity may not have a simple relation to the porosity because the velocities also relate to pore geometry, grain cement, grain packing and other parameters. However, at high pressure, P_d above 20 MPa, the effects of these parameters are suppressed. Velocities of sandstones approach to terminal values, thus, only porosity remains as a dominate parameter to the velocities. A sample with higher porosity usually shows a low velocity at the high pressure. This result tell us that under certain conditions, the complicated relations of velocities and moduli to properties of rocks can be simplified.

We found that at high differential pressure, sandstones with water saturation exhibit simple relations of velocities to rock properties (Han, 1986 a). For clean sandstones, the velocities can simply be related to porosity. For shaly sandstones, the velocities can be correlated linearly to the porosity and clay content. Consolidations of rocks show some effects on velocities. However, their effects are withheld by the effect of pressure and water saturation, and therefore, they can be neglected (Han, 1986 a). Thus, it turns out that only the clay content is as important as porosity in influencing velocities.

The velocities are measured at ultrasonic frequency. The dispersion of velocity can not simply be neglected (Han, 1986 b). It's influence will be discussed later.

These systematic relationships give us a chance to compare experimental results to theoretical models. From these empirical relations, we can obtain moduli for pure quartz aggregate, the bound clay effects, and the porosity and clay content (matrix clay) effects on velocities. Though there are deviations of data from the empirical fits, they can be neglected as we deal with the first order problems.

Many models have been presented to delineate effective moduli of porous media. Different bounding methods can be used to find high- and low-bounds for a composite. Voigt-Reuss bounds and Hashin-Shtrikman bounds will be used in our study. The specific pore geometry models (Walsh, 1965, 1968; Kuster and Toksöz, 1974; O'Connell and Budiansky, 1974; Garbin and Knopoff, 1975; Korringa et al., 1979; Mavko and Nur, 1979; Mavko, 1980; Berryman, 1980; Toksöz and Chang, 1980; Hudson, 1981; Gaunard and Uberall, 1982; Mehta, 1983; Crampin, 1984) consider the rock as a solid with isolated pores or cracks in it. Yet, rock structures are over simplified by these models. The isolated pores in models are not realistic, though some models use a self-consistent approach to estimate interactions between neighboring pores. All these models are geometric ones; they do not take into account any effects of grain cement, contact and packing. Thus, theoretical models, even for clean sandstones, are far from perfect completion. However, to some extent, these porous models have advantages and flexibility in estimating velocities and moduli in sandstones.

None of the above models was developed to estimate the effects of clay content on velocities and elastic moduli of shaly sandstones. Toksöz and Chang (1979) have only alluded to the fact that a decrease of shear modulus in sandstone might be caused by clay minerals. Minear (1982) applied the Kuster and Toksöz porous model (1974) to simulate the clay effects on velocities. His results show that clay with low moduli than quartz do significantly reduce velocities of sandstones. However, no data were presented to support his results and the effects of clay on velocities remain poorly understood. Our study, based on widely collected data (Han, 1986 a) is first time that clay content and porosity effects on velocities of sandstones have been explored in detail. Therefore, we also need to carry out a theoretical analysis of our data. This is not only to help understand the physical mechanism of the clay content and porosity effects; it is also a good chance to test different theoretical models.

In our study, the following models were compared with our experimental results: Mavko's triangular tube model (1980), the self-consistent model (O'Connell and Budiansky, 1974) and the single scattering porous model (Kuster and Toksöz, 1974; Chang and Toksöz, 1979).

Bound Theory

The bounding method is frequently used to estimate elastic moduli of isotropic composites. Here we only discuss the simplest bounds involved.

Voigt and *Reuss bounds*

For a composite of two isotropic phases the average strain and stress are computed based on the volume fraction. The Voigt average is yielded by considering the strain to be uniform through out the composite. The Reuss average assumes equal stress throughout the aggregate. The result for an isotropic mixture of isotropic phases (Hill, 1963 a) is

$$M_r^* = (\upsilon_1/M_1 + \upsilon_2/M_2)^{-1} < M^* < (\upsilon_1 M_1 + \upsilon_2 M_2) = M_v^* \qquad (1)$$

and

$$\upsilon_1 + \upsilon_2 = 1$$

where M and υ are moduli (either bulk K or shear μ) and the volume fraction of each component referenced to subscripts, M^* is the actual modulus of the composite, and subscripts r

and v denote the Reuss and Voigt averages, respectively. Equation (1) represents a generalized V-R bound (Voigt, 1928; Reuss, 1929), which is verified by Hill (1952).

Hashin –Shtrikman bounds

Hashin and Shtrikman (1961, 1962) and Hill (1963 b) derived new variational principles which led to tighter bounds for isotropic composites than Voigt and Reuss averages. For the common case of a two-phase aggregate, one of the bounds can be computed from the expressions:

$$K^* = K_1 + \frac{\upsilon_2}{(K_2 - K_1)^{-1} + \upsilon_1(K_1 + \frac{4}{3}\mu)^{-1}} \tag{2}$$

and

$$\mu_1^* = \mu_1 + \upsilon_2/[(\mu_2 - \mu_1)^{-1} + [2(K_1 + 2\mu_1)\upsilon_1]\ [5\mu_1(K_1 + 4/3\mu_1)]^{-1}\ ]. \tag{3}$$

The other bounds are obtained by interchanging subscripts 1 and 2 in (2) and (3). The physical meaning of the H-S bounds is clear from the work of Hashin (1962). The bounds on K^* are exact results for a

so-called 'composite spheres assemblage,' a composite in which the volume of the aggregate is filled with composite sphere, each consisting of a spherical particle of radius a_n of phase 1 and a concentric spherical shell of phase 2 between a_n and b_n. The H-S bounds are much tighter than the V-R bounds. The arithmetic mean of the H-S bounds is a reasonable approximation of modulus for a composite of two phases with similar elasticities.

If the constituent phases of an aggregate have widely differing moduli, then in general the bounds on the aggregate moduli are widely separated. A special case occurs when a phase is fluid or consists of voids (shear $\mu = 0$), as is the case of sandstones. In this case, the low bounds are both zero. Therefore, the porosity effects on velocities of sandstones are hardly estimated using the bound methods.

Pore Geometry Models

In order to describe the porosity effects on the velocities of sandstones it is necessary to specify the geometrical structure of the pores in sandstones. In this section, the triangular pore model (Mavko, 1980), self-consistent sphere, needle and disc model (O'Connell and Budiansky,

1974), and pore aspect-ratio spectrum model (Kuster and Toksöz, 1974) are briefly mentioned.

Triangular model

A tube model with the triangular cross section was proposed to estimate seismic velocity and attenuation in rocks with partial melt phase (Mavko, 1980). In the tube model suggested by Smith (1964), the tube, in cross section, is roughly triangular with sharp edges. As the geometric constant $\epsilon = 0$, the softening effect is about twice that for tubes with $\epsilon = \infty$, which corresponds to needle-shaped cavities given by Wu (1966). The interesting thing is that the model gives intermediate moduli between moduli of rigid spherical inclusion and those of complaint films (Mavko, 1980). It may be useful for modeling the porosity effects of sandstones.

Accouding to the triangular model, the saturated bulk modulus is given by

$$\frac{1}{K^*} = \frac{1}{K} + \phi\left[\frac{K\ K_f}{K - K_f} + \frac{3(1-2\nu)\phi K}{2(1+\nu)[(13-4\nu-8\nu^2)/4(1+\nu)]}\right]^{-1}, \tag{4}$$

where K is the bulk modulus of solid materials, ν is Poisson's ratio of the solid materials, which can be calculated from K and ν.

$$\nu = \frac{3K - 2\nu}{2(3K + \nu)}$$

The saturated shear modulus is given by

$$\frac{1}{\mu^*} = \frac{1}{\mu'} - \frac{\phi}{15\mu}\frac{5-4\nu}{[\mu/K_f\ (5-4\nu)] + 1} \tag{5}$$

where $\frac{1}{\mu'}$ is equal to

$$\frac{1}{\mu'} = \frac{1}{\mu} + \frac{2\phi}{\mu}\left[\frac{40-26\nu}{15}\right].$$

Self -consistent approach

The self-consistent scheme (SCS) (Hershey, 1954; Kroner, 1958; Hill, 1965; Budiansky, 1965; Wu, 1966; Walpole, 1969; O'Cnnoll and Budiansky, 1974) provides one way of approximating the interactions between neighboring pores. Gubernatis et al., (1975) and Berryman (1980) have derived the SCS results as an approximate solution to the scattering problem. In the SCS approach, instead of being embedded in the matrix material, the crack or inclusion 'sees' the

effective rock matrix material around it. The SCS theory can give a reasonable estimate for a composite with high porosities. It is also the only one to predict that threshold of rigidity must exist at some finite concentration when solid material is added to a fluid. Here, only the simpliest pore geometry was used to model the porosity effects on velocities of sandstones.

Based on the single ellipsoidal inclusion results of Eshelby (1957), the SCS result for spherical inclusion was derived out by Hill (1965); Budiansky (1965); Wu, 1966; Walpole, 1966). Hill (1965) has shown that the SCS-sphere results lie within the H-S bound for all volume fractions. Wu (1966) has carried out self-consistent analyses for disc and needle-shaped inclusions, as did Walpole (1969). Boucher (1974) gives the SCS results for discs and demonstrates that this case corresponds to the one of the H-S bound. Watt, et al., (1976) have analytically verified the equivalence of the various formulae for both needles and discs. Explicit formulae for the SCS results for spheres, discs, and needles (Watt, et al., 1976) are given in Appendix 1.

All the SCS results yield the correct limiting behavior for small concentrations of inclusions; they reduce to the corresponding dilute suspension results (Dewey, 1947; Mackenzie, 1950; Hashin; 1955, 1959; Eshelby, 1957) as the volume fraction of one component approaches zero. They also yield the correct limit for equal shear moduli (Hill, 1963 a).

Finally, it has been pointed out by Chang and Toksöz (1979) and others that the SCS models may break down at high porosity because the experimental evidence (Walsh et al., 1965) shows a nonzero bulk modulus for porous glass at porosities about 70 percent which is higher than the predicted by the SCS-sphere model in which the bulk modulus vanishes at porosity about 50 percent. However, as Berryman commented (1980 a), the comparison between theory and experiment is questionable. The SCS approach may not be complete. More work will be required to improve the theory in different applications. Yet, the theory has many good and important features and no other contemporary theory has been conclusively demonstrated to be better.

Pore aspect-ratio spectrum model

Using single scattering theory, Kuster and Toksöz (1974) have obtained effective moduli as a

function of pressure for porous media with oblate spheroidal pores. Toksöz et al. (1976) have modeled the increase in moduli of sandstones by calculating the change in the pore aspect-ratio spectrum. Chang and Toksöz (1979) have presented the inverse method to determine the pore aspect-ratio spectra using dry and saturated velocities measured at different pressure for several sandstones. As pointed out by Mavko and Nur (1978), the pore aspect-ratio spectrum model is extremely ununique. In addition, the model predicts the thinner pore close with increasing pressure leading to minimal porosity decrease. This is contradicts observed behavior of the porosity as a function of pressure. Yet, in this study, we adopt the model to simulate the porosity effects on velocities of sandstones but the effect of variation in pressure on velocities was not studied.

For sandstones with matrix moduli K, μ, pore fluid moduli K', μ' and concentrations of pores with different aspect-ratio $c(\alpha_m)$, the effective moduli of K^* and μ^* are:

$$\frac{K^* - K}{3K^* + 4\mu} = \frac{K' - K}{25\mu(3K + 4\mu)} \sum_{m=1}^{m=n} c(\alpha_m) T_1(\alpha_m) \tag{6}$$

$$\frac{\mu^* - \mu}{6\mu^*(K + 2\mu) + \mu(9K + 8\mu)} = \frac{\mu' - \mu}{25\mu(3K + 4\mu)} \sum_{m=1}^{m=n} c(\alpha_m) [T_2(\alpha_m) - \frac{1}{3} T_1(\alpha_m)]. \tag{7}$$

T_1 and T_2 are scalars, function of K, μ, K', and μ'. The expression for T_1 and T_2 is given in appendix 2. $c(\alpha_m)$ is the fractional porosity of the m th inclusion with aspect-ratio α_m. The assumptions involved in the derivation of the above equations are macrohomogeneity and isotropy and dilute concentration of inclusions. For sandstones, the dilute concentration condition is not always satisfied. The limitation is that the concentration for each type inclusion must be less than its aspect-ratio.

$$c(\alpha_m) < \alpha_m . \tag{8}$$

A self-consistent approach has been discussed by Chang and Toksöz (1979). If effective moduli K^* and μ^* do not change rapidly with c, then the equations (6) and (7) can be simplified.

$$\frac{K^* - K_0}{K' - K_0} = \frac{T_1}{3} \sum_{m=1}^{m=n} \Delta c(\alpha_m) \tag{9}$$

$$\frac{\mu^* - \mu_0}{\mu' - \mu_0} = \frac{1}{5}[T_2 - \frac{1}{3} T_1] \sum_{m=1}^{m=n} \Delta c(\alpha_m). \tag{10}$$

As pointed out in Chang (1978), the two formulas give the same results. We can use the simpler

expression without getting significantly different results.

In our study, we give a trial aspect-ratio α_m, then inverse fraction R_m corresponding to the m th inclusion. The concentration $c(\alpha_m)$ is calculated from

$$c(\alpha_m) = R_m \phi \quad ; \quad \sum_{m=1}^{m=n} R_m = 1.$$

For modeling the porosity effects on velocities, seven date sets of the V_p and V_s at different porosities are given for forming fifteen equations (including $\Sigma R_m = 1$). The fraction R_m for m th inclusion can be obtained by the least squares method. The better spectrum is judged by its validity for maximum porosity.

Effects of Porosity on Velocities of Clean Saturated Sandstones.

We had 10 sandstone samples that are clay free. Porosity of the samples ranged from 5 percent to 22 percent. Seven of them were Fontainbleau sandstones, two were St. Peter sandstones, and one was Beaver sandstone. Clean sandstones have the simpliest configuration among sandstones. Though we can trace cemetation effects on velocities for different samples, they are not important at high pressure. At confining pressure 40 MPa and pore pressure 1 MPa, their compressional velocity V_p and shear velocity V_s can be linearly correlated to their porosities (Han, 1986 a).

$$V_p\ (km/s) = 6.08 - 8.06\ \phi, \tag{11}$$

and

$$V_s\ (km/s) = 4.06 - 6.28\ \phi. \tag{12}$$

with correlation coefficients 0.99 respectively. The shear velocity shows a stronger dependence on the porosity than does the compressional velocity.

$$1.55 = \frac{6.28}{4.06} > \frac{8.06}{6.08} = 1.33.$$

This is because the shear modulus declines more faster than the bulk modulus as the porosity increases. Setting ϕ to zero, the empirical equations (11) and (12) give velocities for pure quartz aggregate at ultrasonic frequency.

$$V_{pq} = 6.08\ (km/s) \quad ; \quad V_{sq} = 4.06\ (km/s).$$

Elastic moduli (dynamic) computed from the velocities of pure quartz are:

$$Bulk\ K_q = 40.0\ GPa \quad ; \quad Shear\ \mu_q = 43.7\ GPa.$$

These values almost coincide with those given by Robert (1982). The moduli of water are:

$$Bulk\ K_f = 2.2\ GPa \quad ; \quad Shear\ \mu_f = 0\ GPa.$$

The data give us a chance to input measured moduli of quartz and water into theoretical models, and to compare model results with the empirical data.

The model results are shown in Figure 3 a and b. For the R-V bound and H-S bound, there is no adjustable parameter. The velocity data locate in middle of the bounds. However, as we pointed out in the last section, when elastic moduli for two composites are far different each other the bound method gives a poor estimate for composite moduli. The H-S (+) gives a linear relation of velocities V_p and V_s at porosity less than 60 percent. However, the porosity effect on the velocities is underestimated. In contrast, the porosity effects are much overestimated by the Reuss and H-S (-) bounds. The latter coincides with the Reuss bound. The Reuss and H-S (-) shear velocity bounds are equal to zero because the one of component, water, has zero shear modulus. As the porosity goes above 60 percent, eg. for sand suspension, the Reuss and H-S (-) bounds may give a reasonable estimation. Therefore, the Bound method is very poor for delineating the porosity effects on velocities of sandstones. We need a model with specified pore geometry to simulate the porosity effects.

For pore geometry models, porosity of sandstone is usually too high for the dilute limitation. The self-consistent models were used to compare with the empirical equations. Three pore shapes were computed: sphere, needle and disc shapes. The SCS-disc model coincides with Reuss and H-S (-) bound, in which the porosity effects on velocities are overestimated. Therefore, the disc is not a typical pore shape for sandstones. The SCS-sphere and needle models are close to empirical data, specially in their prediction of thresholds of the shear velocity at porosity about 60 percent. This coincides with the tendencies of our empirical equation extrapolated to higher porosity. Similar situation is shown for compressional velocity, except that empirical equation breaks down, while the SCS model predicts an unvanished the V_p (near water velocity) at porosity above 60

percent. It is true because sand grains may be suspended in fluid and are not contact each other at porosity above 60 percent. The agreements between the empirical equations and the SCS model suggest that the linear empirical relation is a right choice to present correlation of velocity to porosity. The time average equation (Wyllie et al., 1956, and 1958) does not show such agreement.

When porosity is below 30 percent, the porosity effects on velocities are still significantly underestimated by the SCS-sphere and needle models. The needle shape can give better estimate. Yet, for sandstones with high porosity, most pores have round shapes rather than needle shapes. This implies that the model with single pore shape is not good enough to simulate the porosity effects on velocities. The more realistic geometry model should be a combination of the different pore shapes. For example, a simple combination of sphere and disc pores may give better fits of model to data. This result indicates that even at confining pressure 40 MPa and pore pressure 1 MPa, there are a number of thin pores (disc shape) remained opening in sandstones.

The model (Mavko, 1980) of triangular pores was also used to fit our data. The triangular pore is much more compliant than the sphere or needle pore. At low porosity (below 10 percent) the model can fit both V_p and V_s very well (Figure 3 a and b). But at the high porosity, the porosity effects shown in the model are much less than shown by our data. The discrepancy is caused by violating the dilute assumption in the model. Therefore, the model is not adequate for sandstones with high porosities.

The model using pore aspect-ratio spectrum (Kuster and Toksöz, 1974; Cheng and Toksöz, 1979) gives more flexibility to describe the porosity effects on velocities of sandstones. The spectrum of the model is strongly nonunique (Mavko and Nur, 1978). We took the simpliest spectrum. For fitting both V_p and V_s data with porosity ranging from zero to 30 percent, the combination of three pore aspect-ratios are required. One restriction of the model is that the concentration of each component pore shape must be less than its aspect-ratio. Therefore, choice of pore aspect-ratio spectrum was restricted by its validity for a high porosity limit. Using this restriction, we can search different combinations of pore aspect-ratios for the highest porosity

limit. Figure 4 shows a very good fit of the model to both V_p and V_s. The spectrum is also shown in Figure 4. The α is the aspect-ratio and R is the relative concentration. The data indicate that in order to fit both V_p and V_s to porosity over 30 percent, very low aspect-ratio (0.004) pores are required. If there are no such thin pores, the fits of model to data are much worse (Figure 4). The same spectrum can also be used well to simulate the porosity effects for shaly sandstones without matrix clay (C = 0). This will be discussed in following sections.

This result reveals a interesting problem. The Kuster and Toksöz model (1974) proposed originally to describe how the pore geometry responds to the pressure dependence of elasticity of porous media. Thus, a logical result is that the closing thin pores respond to an increase in the stiffness of porous media as differential pressure increases (Toksöz et al., 1976). Numerical calculations have shown that almost no thin pores (aspect-ratio α less than 0.01) should remain opening for sandstones at differential pressure above 30 MPa. On other hand, if using the model to delineate the porosity effects on the both V_p and V_s (the bulk and shear moduli) at P_d equal to 39 MPa, very thin pores ($\alpha = 0.004$) are required. This is caused by the intrinsic relation of the model. The data show that the shear modulus is more dependent on the porosity than the bulk modulus. In the model shown in Figure 5 for the pore with aspect-ratio greater than 0.01, both bulk and shear moduli have similar responses to the porosity. As the pore aspect-ratio becomes less than 0.01, the shear modulus declines faster and faster (T_{ijij} goes to infinity) while the bulk modulus is not sensitive to thinner pores (T_{iijj} closes to the terminal value as α becomes less than 0.01) with increasing porosity. This is because intrinsicly thinner pores are required to fit both V_p and V_s data. Therefore, at high pressures, what thinner pores in sandstones is whether closed or still opening is an important criterion in justification of the pore geometry model. This need to be tested in a designed experiment. At least this result indicates that the porous model may phenomenologically explain some properties of rocks but is still too simple to model real rocks.

We believe that at high pressures the thinner pores ($\alpha < 0.01$) remain opening. This is consistent with the report by Yale (1985): "Recent work by Abdel-Gawad (pers. comm.) has

shown that direct observation of the pore space under different pressure yields aspect-ratio spectrum where the number of thin pores increases with pressure. In other words, the thin pores do not close with pressure; they just become thinner." The pore geometry model may miss important parameters such as degree of cementation and compaction of sandstones, therefore, the model should be rethought in a more proper manner.

The Bound Clay Effects on Velocities.

The velocities of clean sandstones are significantly higher than corresponding velocities of shaly sandstones (Figure 1 a and b). Therefore, they should be dealt with separately (Han, 1986 a). For shaly sandstones (70 samples), using least squares regression, velocities V_p and V_s can be linearly correlated to the porosity and clay content respectively (Han, 1986 a):

$$V_p\,(km/s) = 5.59 - 6.93\phi - 2.18C. \tag{13}$$

and

$$V_s\,(km/s) = 3.52 - 4.91\phi - 1.89C. \tag{14}$$

with correlation coefficient 0.985 and 0.959 and relative rms error 2.1 and 4.3 percent for V_p and V_s respectively. The clay content C in the equation (13) and (14) is the matrix clay which does not include the bound clay (Han, 1986 a). The matrix velocities (the constants in equations (13) and (14)) for shaly sandstones are significantly lower than velocity for quartz aggregate (the constants in equations (11) and (12)). This is because velocities of shaly sandstones are biased by the effects of the bound clay. Clay mineral in sandstones has much higher surface area (about 2 orders higher) and lower moduli than quartz grain. Therefore, small amount of clay (1 or few percent of volume fraction) can cover all grain surfaces including grain boundaries, and can greatly reduce moduli and velocities of sandstones. The moduli for shaly matrix are:

$$Bulk\ K_s = 39.0\ GPa \quad ; \quad Shear\ \mu_s = 32.8\ GPa.$$

which are computed from velocities for shaly matrix:

$$V_{ps} = 5.59\ km/s \quad ; \quad V_{ss} = 3.52\ km/s\,,$$

and density of matrix $\rho = 2.65$ g/cc. In comparison with moduli of quartz aggregate:

$$Bulk\ K_q = 40.0\ GPa \quad ; \quad Shear\ \mu_q = 43.7\ GPa\,,$$

effects of the bound clay are mainly to reduce the shear modulus.

The analysis using different models indicates that the bound clay effects on reducing shear modulus cannot be explained by the porous models. The Reuss bound (parallel structure) can fairly delineate the bound clay effects. If we assume that 1 percent bulk volume fraction is the bound clay, then from equations

$$\frac{1}{K_s} = \frac{0.99}{K_q} + \frac{0.01}{K_{bc}} \tag{15}$$

$$\frac{1}{\mu_s} = \frac{0.99}{\mu_q} + \frac{0.01}{\mu_{bc}} \tag{16}$$

we obtain the bulk and shear modulus of the bound clay

$$Bulk\ K_{bc} = 11.2\ GPa \quad ; \quad Shear\ \mu_{bc} = 1.3\ GPa.$$

We know only small amounts of clay are bound clay but we do not know its exact quantity. Actually, the volume of bound clay may vary in different sandstones. Therefore, we cannot determine the moduli for bound clay. However, we still can conclude that the moduli of bound clay are less than those of pure clay, which will be shown in the following sections. The moduli calculated from velocities measured for montmorillonite mixed with water (Han, 1986 c) are

$$Bulk\ K_c = 4.0\ GPa \quad ; \quad Shear\ \mu_c = 0.4\ GPa.$$

This indicates that clay with plenty pores saturated with water can have very low moduli. This is the case for the moduli of bound clay.

The bulk modulus for shaly matrix is slightly lower than that for quartz. This indicates that the effects of the bound clay on the bulk modulus can be ignored.

The Matrix Clay Effects on Velocities

Analysis of clay locations in sandstone shows that clay can be classified as bound, laminated, structural, and porous clay (Minnear, 1982). The calculation has shown that laminated and structural clay have similar effects on reducing elastic moduli, while porous clay has only slight effects on the moduli (Figure 6). However, the measurements indicate that velocities correlate to clay content only. They appear not to be sensitive to clay locations (Han, 1986 a). This reveals that clay distributions for different sandstones may be essentially the same. They are

mainly not porous clay suspended in pore fluid, thus, effects of clay locations cannot be shown. The probable reason is that the matrix clay is accumulated around grain boundaries, where it can significantly reduce velocities and moduli of matrix. We assume the clay is part of a solid matrix and do not care about their locations.

Setting the porosity in the equations (13) and (14) equal to zero, velocities of a shaly matrix can be computed by following equations:

$$V_{p_0} \mid_{\phi=0}(km/s) = 5.59 - 2.18C, \tag{17}$$

and

$$V_{s_0} \mid_{\phi=0}(km/s) = 3.52 - 1.89C, \tag{18}$$

where C is clay volume fraction which does not include microporosity in it (Han 1986 a). The equations indicate that as clay content increases the velocities V_p and V_s decrease as well as moduli. The "clay point" can be obtained by setting clay content equal to 100 percent.

$$V_{pc} = 3.41\ km/s \quad ; \quad V_{sc} = 1.63\ km/s. \tag{19}$$

These values almost coincide with $V_{pc} = 3.4$ km/s and $V_{sc} = 1.6$ km/s obtained from Tosaya's equations (Tosaya and Nur, 1982) by Costagna et al. (1985) and Zimmerman and King (1986). The moduli of clay can be computed from "clay point" and clay density $\rho_c = 2.60$ g/cc,

$$Bulk\ K_c = 20.8\ GPa \quad ; \quad Shear\ \mu_c = 6.9\ GPa.$$

The effects of clay content on moduli of a shaly matrix can be modeled using the elastic moduli of quartz and clay. The H-S bounds show in Figure 7. The data actually locate above the H-S (+) bound. The H-S bound was proved to be a rigorous bound for a composite (Hashin, 1962, 1970). Therefore, the moduli of quartz-clay aggregate should be fit into the bounds. The data, however, fall out of the bounds. This indicates that the "clay point" extrapolated from equation (6) and (7) is wrong. A empirical relation is only valid for its data range. Beyond this range, the empirical relation will break down. What we can do is to estimate the "clay point" using H-S bounds. From fitting the empirical equation (6) and (7), the moduli of pure clay can be obtained: For the H-S (-) bound,

$$Bulk\ K_c = 24.5\ GPa \quad ; \quad Shear\ \mu_c = 10.0\ GPa. \tag{20}$$

For the H-S (+) bound,

$$Bulk\ K_c = 23.0\ GPa \quad ; \quad Shear\ \mu_c = 8.0\ GPa. \tag{21}$$

These values are much higher than the "clay point" obtained before. The Figure 7 shows the data located in the middle of the H-S bounds for the clay moduli equal to:

$$Bulk\ K_c = 24.5\ GPa \quad ; \quad Shear\ \mu_c = 9.5\ GPa. \tag{22}$$

The H-S (+) bound show a better fit to the data than the H-S (-) bound. The deviations are less than the residuals for the empirical relations (6) and (7).

Empirical data is also tested against the porous model. The quartz-clay matrix is assumed as quartz matrix with spherical inclusions fully filled clay. The calculations indicate that the K-T spherical model coincides with the H-S (+) bound, which is in agreement with the conclusion by Berryman (1980 a). Therefore, the model underestimates the clay effects. Again, we use the model to search clay moduli in order to obtain the best fit. The results coincide with the H-S (+) bound.

$$Bulk\ K_c = 23.0\ GPa \quad ; \quad Shear\ \mu_c = 8.0\ GPa. \tag{23}$$

It gives a lower estimation for the clay moduli. The above estimations give a reasonable bound for matrix clay in sandstones.

Clay minerals in sandstones contain plenty of micropores. The microporosity was proposed to explain the clay effects on dry velocities in poorly consolidated sandstones (Kowallis et al., 1984). In our study, the microporosity was measured as part of total porosity. Our data suggest that the microporosity cannot be used to delineate the clay content effects on velocities as discussed by (Han, 1986 a).

The experimental results (Han, 1986 c) show that clay minerals can be permanently deformed, and shear moduli of clays can be drastically reduced by saturated water. They are substantially different from elastic crystal. The lower bulk modulus and specially lower shear modulus of clay minerals as opposed to crystal may be related to layered structures in clay aggregate and interactions between water and clays.

Effects of Porosity on Velocities of Saturated Shaly Sandstones

The equations (3) and (4) give correlations of velocities to the porosity and the clay content. In last two sections, we dealt with the bound and matrix clay effects. In this section we assume the moduli of the shaly matrix (including bound clay) are:

$$Bulk\ K_s = 39.0\ GPa \quad ; \quad Shear\ \mu_s = 32.8\ GPa\,,$$

and the effects of the matrix clay can be computed from

$$V_{ps}\ (km/s) = 5.59 - 2.18C\,,$$

and

$$V_{ss}\ (km/s) = 3.52 - 1.89C.$$

Then we use a different model to simulate porosity effects on velocities.

$$V_{ps}\ (km/s) = (5.59 - 2.18C) - 6.93\phi, \tag{24}$$

and

$$V_{ss}\ (km/s) = (3.52 - 1.89C) - 4.91\phi. \tag{25}$$

The results are similar to those for clean sandstones (Figures 8 a and b). The Reuss-Voigt bound and H-S bound are too disperse to model the porosity effects. The triangular model (Mavko, 1980) can fit data excellently at the porosity less than 10 percent but far underestimates the porosity effects at porosity more than 10 percent. The SCS-sphere and -needle model can predict the threshold of the shear velocity and limited compressional velocity to near water velocity at porosity about 60 percent. These are in agreement with the tendency of empirical relations to be extrapolated to higher porosity. This increases our confidence in the belief that the linear relation, rather than the time average equation, is the right choice to delineate velocities as a function of porosity for shaly sandstones. For porosity less than 30 percent, the SCS-needle model gives a close fit to data but there are still large deviations over the range of the data. The SCS-sphere model underestimates while the SCS-disc model overestimates the effects of porosity on velocities. The combination of different pore shapes is more realistic for simulating pores in sandstones, and may be a better choice for modeling porosity effects on velocities.

The K-T model was used to delineate data. Again, the simplest spectrum, a combination of

three pore aspect-ratio, is used to model the porosity effects. First, the spectrum for clean sandstones was inputed into the model. The only difference is that the moduli used are for shaly matrix instead of for pure quartz. The model can fit very well to the equation (23) and (24) as the matrix clay content is below 10 percent (Figure 4 and Figures 9 a and b). This indicates that the bound clay or only a few percent of the matrix clay do not significantly change the pore structures. When the matrix clay is above 10 percent, the fits get worse, especially for the porosity higher than 10 percent (Figures 9 a and b). Data show that the simple pore aspect-ratio spectrum can fit quite well to the porosity effects when the porosity is less than 5 percent and regardless of the clay content.

Changing the pore aspect-ratio spectrum with clay content can improve the fit. The results show that the pore aspect-ratio decreases with increasing clay content (Table 1). The maximum porosity validated for the spectrum also decreases with increasing the clay content. This seems to be consistent with the data that when clay content is above 20 percent, the porosity of shaly sandstones tends to fall between 5 and 15 percent (Han, 1986 a). The lowerest aspect-ratio decreases drastically with increasing clay content (from 0.004 to 0.00007). On one hand, this is to be expected because of the fact that differences of the porosity effects on V_p and V_s are enhanced as clay content increases. On the other hand, this may be caused by the fact that the matrix clay contains micro-porosity with low pore aspect-ratios to influence the moduli for shaly sandstones with high clay content.

Another possible explanation is that the measured porosity is less than effective porosity because part of clays may be porous clay. Thus, if data is compared to the effective porosity, the data will be close to the model. The estimation of porous clay, however, is difficult task. If such correction is profitable, the porosity effects on velocity of sandstones can be explained by a simple pore aspect-ratio spectrum. This is consistent with the thought that at high differential pressure, the pore aspect-ratio spectra of sandstones are more convergent than at low pressure.

The porosity effects on the velocities of sandstones can be fairly well simulated by the K-T model with a simple pore aspect-ratio spectrum. The porosity effects on shear velocity are larger

than on compressional velocity. The model reveals that pores with very low aspect-ratios (about 10^{-3} to 10^{-5}) are requisite for modeling the porosity effects on the both V_p and V_s even at high differential pressure. This requirement is enhanced as clay content increases. Though the SCS-needle and the SCS-sphere models cannot fit well with the data, they give a good prediction of the threshold of rigidity at a limited concentration of pores (e.g. $\phi = 0.6$) in porous media transformed from consolidated sandstone to suspension (Figure 9). On the basis of the single-scattering theory and self-consistent approach, the porosity effects on velocity at low frequency were modeled using sphere, prolate spheroid with aspect-ratio $\alpha = 0.1$, and oblate spheroid with aspect-ratio $\alpha = 0.1$ respectively (Berryman, 1980 b). The model results show similar characteristics to our empirical relation (Equation 1 and 2) though there are slight differences of input data. The better fits of models to data may be reached by adjusting the aspect-ratio, or by combining different pore shapes.

Our velocities are measured for water saturated sandstones at ultrasonic frequency. In the above modeling, for simplicity, no water saturation effects and no velocity dispersion are taken into account. Therefore, the model results are valid for saturated velocities at ultrasonic frequencies. Though the velocity dispersion of sandstones cannot be neglected, it is still less than 10 percent (Han, 1986 b) Thus, effects of the porosity and clay content on velocities are slightly influenced by the dispersion. The features of models for low frequency data are basically the same as from that for ultrasonic data except for minimal changes of parameters. For example, the moduli of clay may decrease corresponding to enhanced clay effects on velocities at low frequency.

Summary

Complete velocity data and obtained empirical relations give a chance to examine different theoretical models for porous media. During the model process, the limits of the models can be revealed. Insight into the physical basis of the effects of porosity and clay content on velocities and moduli of sandstones can also be gained.

The porosity effects cannot be well estimated using the bound methods, although these are mathematically rigorous. The main reason is because the elastic properties of fluid are far different from those of solid matrixes. The bulk modulus of fluid is usually one order of magnitude less than that for solid grains while the shear modulus of fluid is zero, completely different from solid grains. The bound methods cannot handle a composite composed of solid grains and fluid.

The pore geometry model can be used to simulate the porosity effects on velocity of sandstones. Interactions between pores are the most difficult problem to handle in the models but it cannot be avoided in modeling high porosity rocks such as sandstones. The triangular model (Mavko, 1980) is excellent to delineate velocity data at porosities less than 10 percent, but not higher than that this is because the dilute assumption was made in the triangular model. Inaccurate effective medium theories (including the self-consistent approach) was criticized by Hashin (1970). However, as the rigorous bounds are far from each other in our case, the self-consistent approach is still valuable to estimate the effective moduli and velocities (Berryman, 1980 a).

For clean and shaly sandstones, the SCS models locate in between H-S bounds. The SCS-needle model matches fairly closely with the empirical relations. The SCS-prolate or oblate spheroid models (Berryman, 1980 b) with selected aspect-ratio may fit the data better. Yet, the combination of different pore shapes is more realistic, and should reach the best fit of the data. The important feature of the SCS model is its ability to predict the threshold of rigidity for water saturated porous media at porosity about 60 percent. This coincides with our empirical relations which also break down at similar porosity. The time average equation (Wyllie et al., 1956, 1958) does not predict such features. This is one reason that we have chosen the linear equation rather than the time average one (Han, 1986 a).

The K-T model with a simple pore aspect-ratio spectrum can delineate the empirical relations very well for the data range. The spectrum is not unique (Mavko and Nur, 1978), especially at low porosity. At high porosity, the spectrum is restricted by the dilute assumption.

The K-T model shows that different responses between bulk and shear moduli as well as V_p and V_s to the porosity occur only for pores with aspect-ratios of less than 0.01. Therefore, thinner pores (α less than 0.01) are required to make the model fit both V_p and V_s. This requirement is enhanced with increasing clay content. It is reveals that there are thinner pores in sandstones even at differential pressure 39 MPa. This disagrees with the thought that pores with low aspect-ratios will be close at high differential pressure (Toksöz et al., 1976). However, this is in agreement with the observation that with increasing differential pressure, thin pores become thinner rather than close (Yale, 1985).

The effects of bound clay on moduli are mainly in reducing shear modulus of a sandstone matrix. The model process suggests that the Reuss bound can be used to explain the bound clay effects. The calculation indicates that the bound clay has lower moduli than the "clay point", especially lower shear modulus. The measured results for clay mixed with water (Han, 1986 c) show that the bound clay is the clay with plenty thinner pores rather than pure solid clay.

The effects of matrix clay can be well estimated by the H-S bounds. The results show that the "clay point" which is obtained from empirical equations and used by Castagna et al. (1985) and Zimmerman and King (1986), was underestimated. This "clay point" has led the empirical relations to fall out of the H-S bounds. A new estimate from the H-S bound for moduli of the matrix clay is:

$$Bulk\ K_c = 23.0 - 24.5\ GPa \quad ; \quad shear\ \mu_c = 8.0 - 10.0\ GPa.$$

The K-T model with spherical pores coincides with the H-S (+) bound. Therefore it gives low bound for moduli of the matrix clay. For the matrix clay (excluding the bound clay), laminal clay and clay as individual grain in sand matrix show similar effects on reducing velocities, while porous clay has much less effect except for pores fully filled by the clay. We do not know how clays distributes in sandstone matrixes. However, large clay effects on velocities indicate that the matrix clays are mainly not suspended porous clay. Finally, it needs to be pointed out that the clay moduli obtained are based on empirical relations. It assumes that moduli of pure clay with a history of water saturation can be obtained by limiting porosity to zero. Therefore, obtained

moduli may not be good for a block pure clay (if it exists) but good for a clay aggregate with a history of water saturation in sandstones.

APPENDIX 1

General form of H-S bounds and SCS effective moduli

For two phase aggregates, the Hashin-Shtrikman bounds and self-consistent results can be written in the form

$$\frac{M^* - M_1}{M_2 - M_1} = v_2[\, 1 + \frac{v_1(M_2 - M_1)}{M_1 + F}\,]^{-1} \tag{1-1}$$

where M denotes K *or* μ and F equal $F(K_1, \mu_1, K_2, \mu_2, K^*, \mu^*)$. The particular forms of F are given below.

Hanshin –Shtrinkman Bounds and *SCS discs*

For bulk modulus of a composite K^*:

$$H\text{-}S(+)\text{: } F = 4/3\mu_2 \quad ; \quad H\text{-}S(-)\text{: } F = 4/3\mu_1\,, \tag{1-2}$$
$$\text{if } (\mu_2 - \mu_1)(K_2 - K_1) > 0.$$

$$H\text{-}S(+)\text{: } F = 4/3\mu_1 \quad ; \quad H\text{-}S(-)\text{: } F = 4/3\mu_2\,,$$
$$\text{if } (\mu_2 - \mu_1)(K_2 - K_1) < 0.$$

For shear modulus of a composite μ^*:

H-S (+):

$$F = \frac{\mu_2(9K_2 + 8\mu_2)}{6}(K_2 + 2\mu_2) \tag{1-3}$$

H-S (-):

$$F = \frac{\mu_1(9K_1 + 8\mu_1)}{6}(K_1 + 2\mu_1),$$
$$\text{if } (\mu_2 - \mu_1)(K_2 - K_1) > 0$$

H-S (+):

$$F = \frac{\mu_2(9K_1 + 8\mu_2)}{6}(K_1 + 2\mu_2) \tag{1-4}$$

H-S (-):

$$F = \frac{\mu_1(9K_2 + 8\mu_1)}{6}(K_2 + 2\mu_1),$$

if $(\mu_2 - \mu_1)(K_2 - K_1) < 0$

SCS Spheres

For bulk modulus of a composite K^*

$$F = 4/3\mu^* \tag{1-5}$$

For shear modulus of a composite μ^*

$$F = \mu^*(9K^* = 8\mu^*)/6(K^* + 2\mu^*) \tag{1-6}$$

SCS Needles

For bulk modulus of a composite K^*

$$F = 1/3\mu_1 + \mu^* \tag{1-7}$$

For shear modulus of a composite μ^*

$$F = 5[\ (3(K_1 + 1/3\mu_1 + \mu^*))^{-1} + \frac{2(2\mu_1 + \mu^* + g\ )}{(\mu_1 + \mu^*)(\mu_1 + g\ )}\ ]^{-1} - \mu_1 \tag{1-8}$$

where

$$g = \mu^*(K^* + 1/3\mu^*)/(K^* + 7/3\mu^*)$$

For self-consistent spheres and needles the expressions for K_* and μ^* are coupled and must be solved by iteration. Equation (A1) has been found to give rapid convergence if successive approximations to K^* and μ^* are substituted into F.

APPENDIX 2

Scalar T for Kuster and Toksöz model

The two scalars T_1 and T_2 are given by the following expression:

$$T_1 = \frac{3F_1}{F_2} \tag{2-1}$$

$$T_2 - \frac{1}{3}\ T_1 = \frac{2}{F_3} + \frac{1}{F_4} + \frac{F_4F_5 + F_6F_7 - F_8F_9}{F_2F_4} \tag{2-2}$$

$$F_1 = 1 + A\left[\frac{3}{2}(g + \phi) - R\left(\frac{3}{2}g + \frac{5}{2}\phi - \frac{4}{3}\right)\right] \tag{2-3}$$

$$F_2 = 1 + A\left[1 + \frac{3}{2}(g + \phi) - \frac{R}{2}(3g + 5\phi)\right] + B(3 - 4R) + F_{21} \tag{2-4}$$

$$F_{21} = \frac{A}{2}(A + B)(3 - 4R)[g + \phi - R(g - \phi + 2\phi^2)]$$

$$F_3 = 1 + \frac{A}{2}\left[R(2 - \phi) + \frac{(1 + \alpha^2)}{2\alpha}g(R - 1)\right] \tag{2-5}$$

$$F_4 = 1 + \frac{A}{4}[3\phi + g - R(g - \phi)] \tag{2-6}$$

$$F_5 = A\left[R\left(g + \phi - \frac{4}{3}\right) - g\right] + B\phi(3 - 4R) \tag{2-7}$$

$$F_6 = 1 + A[1 + g - R(g + \phi)] + B(1 - \phi)(3 - 4R) \tag{2-8}$$

$$F_7 = 2 + \frac{A}{4}[9\phi + 3g - R(5\phi + 3g)] + B\phi(3 - 4R) \tag{2-9}$$

$$F_8 = A\left[1 - 2R + \frac{g}{2}(R - 1) + \frac{\phi}{2}(5R - 3)\right] + B(1 - \phi)(3 - 4R) \tag{2-10}$$

$$F_9 = A[g(R - 1) - R\phi] + B\phi(3 - 4R) \tag{2-11}$$

$$A = \frac{\mu'}{\mu} - 1 \tag{2-12}$$

$$B = \frac{1}{3}\left(\frac{K'}{K} - \frac{\mu'}{\mu}\right) \tag{2-13}$$

$$R = \frac{3\mu}{3K + 4\mu} \tag{2-14}$$

Here, $\alpha = c/a$ is aspect ratio.

REFERENCES

Berryman, J. G., 1980 a, Long-wavelength propagation in composite elastic media I. spherical inclusions: J. Acoust. Soc. Am., 68, 1809-1819.

Berryman, J. G., 1980 b, Long-wavelength propagation in composite elastic media I. ellipsoidal inclusions: J. Acoust. Soc. Am., 68, 1820-1831.

Boucher, S., 1974, On the effective moduli of isotropic two-phase elastic composites: J. Compos. Mater., 8, 82-89.

Buduansky, B., 1965, On the elastic moduli of some heterogeneous materials: J. Mech. Phys. Solids struct., 13, 223-227.

Bourbie, T., and B. Zinsezner, 1985, Hydraulic and acoustic properties as a function of porosity in Fontainbleau sandstone: J. Geophys. Res., 90, 11524-11532.

Castagna, J. P., M. L. Batzle, and R. L. Eastwood, 1985, Relationships between compressional-wave and shear wave velocities in clastic silicate rocks: Geophysics, 50, 571-581.

Chang, C. H., and M. N. Toksöz, 1979, Inversion of seismic velocities for the pore aspect ratio spectrum of a rock: J. Geophys. Res., 84, 7534-7543.

Chang, C. H., 1978, Seismic velocities in porous rock-direct and inverse problems: Sc. D. thesis, Mass. Inst. of Technol., Cambridge.

Crampin, S., 1984, Effective anisotropic elastic constants for wave propagation through cracked solids: Geophys. J. Roy. Astr. Soc., 76, 135-145.

Dewey, J. W., 1947, The elastic constants of materials loaded with no-rigid fillers: J. Appl. Phys., 18, 578-581.

Eshelby, J. D., 1957, the determination of elastic field of an ellipsoidal inclusion, and related problems: Proc. Roy. Soc. London, Ser. A, 241, 376-396.

Garbin, H. D., and L. Knopoff, 1975, Elastic moduli of a medium with liquid-filled cracks: Quant. Appl. Math., 301-303.

Gaunard, G. C., and H. Uberall, 1982, Resonance theory of the effective properties of perforated solids: J. Acoust. Soc. Am., 71, 282-295.

Gubernatis, J. E., And J. A. Krumhansl, 1975, Macroscopic engineering properties of polycrystalline materials: elastic properties: J. Appl. Phys., 46 1875-1883.

Han, D., 1986 a, Effects of porosity an clay content on wave velocities of sandstones. in this volume Chapter II. Main body of this Chapter was published with coauthor, Nur. A., and Morgan, F. D., in name, Effect of porosity and clay content on wave velocities of sandstones: Geophysics, 51, Nor, and in name, Velocity measurement and empirical modeling in sandstones: the Log Analyst.

Han D., 1986 b, Velocity dispersions in sandstones: in this volume Chapter V.

Han D., 1986 c, Study of compaction and velocities of sand-clay mixture: in this volume Chapter VI.

Hashin, Z., 1955, The moduli of elastic solid reinforced by rigid particles: Bull. Res. Counc. Israel. 5C. 46-59.

Hashin, Z., 1959, The moduli of an elastic solid containing spherical particles of another elastic material: in Proc. Intern. U. Theor. and Appl. Mech. Symp. on non-homogeneity in elasticity and plasticity. edited by W. Olszak, Pergamon, New York, p. 463.

Hashin, Z., 1962, The elastic moduli of heterogeneous materials: J. Appl. Mech., 29, 143-150.

Hashin, Z., 1970, Theory of composite materials: in Mechanics of Composite Materials, 5th Sump. on Naval Structural Mechanics, edited by F. W. Wendt, H. Liebowitz, and N. Perrone, Pergamon, New York, 201-242.

Hashin, Z., and S. Shtrikman, 1961, Note on a variational approach to the theory of composite elastic materials: J. Franklin Inst., 271, 336-341.

Hashin, Z., and S. Shtrikman, 1962, On some variational principles in anisotropic and nonhomogeneous elasticity: J. Mech. Phys. Solids, 10, 335-342.

Hashin, Z., and S. Shtrikman, 1962, A variational approach to the theory of the elastic behavior of polycrystals: J. Mech. Phys. Solids: 10, 343-352.

Hershey, A. V., 1954, The elasticity of an isotropic aggregate of anisotropic cubic crystals: J. Appl. Mech., 21, 236-240.

Hill, R., 1952, The elastic behavior of a crystalline aggregate. Proc. Phys. Soc. London, Sect. A, 65, 349-354.

Hill, R., 1963 a, Elastic properties of reinforced solids: some theoretical principles: J. Mech. Phys. Solids, 11, 357-372.

Hill, R., 1963 b, New derivations of some elastic extremum principles: in Progress in Applied Mechanics, The Prager Anniversary Volume, MacMillan, New York, 99-106.

Hill, R., 1965, A self-consistent mechanics of composite materials: J. Mech. Phys. Solids, 13, 213-222.

Hudson, J. A., 1981, Wave speeds and attenuation of elastic wave in material containing cracks: Geophys. J. Roy. Astr. Soc., 64, 133-150.

Korringa, J., R. J. S. Brown, D. D. Thompson, and R. J. Runge, 1979, Self-consistent imbedding and ellipsoidal model for porous rocks: J. Geophy. Res., 84, 5591-5598.

Kowallis, B., Jones, L.E.A., and Wang, H.F., 1984, Velocity-porosity-clay content; systematics of poorly consolidated sandstones: J. Geophys. Res., 89, 10355-10364.

Kroner, E., 1958, Berechnung der elastischen K onstanten des vielkristalle aus dem K onstanten des einkristalls: Z. Phys., 151, 504-508.

Kuster, G. T., and M. N., Toksöz, 1974, Velocity and attenuation of seismic waves in two-phase media: Part 1 theoretical formulations: Geophysics, 39, 587-608.

Mackenzie, J. K., 1950, the elastic constants of a solid containing spherical holes: Proc. Phys. Soc. London, Sect. B, 63, 2-11. Mavko, G. M., and A. Nur, 1978, The effect of non-elliptical cracks on the compressibility of rocks: J. Geophys. Res., 83, 4459-4468.

Mavko, G. M., and A. Nur, 1979, Wave attenuation in partial saturated rocks: geophysics, 44, 161-178.

Mavko, G. M., 1980, Velocity and attenuation in partially molten rocks: J. Geophy. Res., 85, 5173-5189.

Mehta, C. H., 1983, Scattering theory of wave propagation in two phase media: Geophysics, 48, 1659-1370.

Minear, M. J., 1982, Clay Models and Acoustic Velocities: presented at the 57th Ann SPE of AIME. New Orleans.

O'Connell, R.J., and B.Budanisky, 1974, Seismic velocities in dry and saturated cracked solids: J. Geophy. Res., 79, 5412-5426.

Robert, S.C., 1982, Handbook of physics properties of rocks.

Reuss, A., 1929, Berechnung der fliessgrenze von mischkristallen auf grund der plastizitatsbedingung fur einkristalle: Z. Angew. Math. Mech., 9, 49-58.

Smith, C. S., 1964, Some elementary principles of polycrystalline micro-structure, Met. Rev., 9, 1-48.

Toksöz, M. N., C. H. Chang, and A. Timur, 1976, Velocities of seismic waves in porous rocks: Geophysics, 41, 621-645.

Toksöz, M. N., and C. H. Chang, 1980, velocities of seismic waves in composite, multi-phase media: J. Acoust. Soc. Am., 67, S43(A).

Voigt, W., 1928, Lehrbuch der Kristallphysik: Teubner, Leipzig.

Walpole, L. J., 1969, On the overall elastic moduli of composite materials: J. Mech. Phys. Solids, 17, 235-251.

Walsh, J. B., 1965, The effect of cracks on the compressibility of rock: J. Geophys. Res., 70, 381-389.

Walsh, J. B., W. F. Brace, and A. W. Englend, 1965, Effect of porosity on compressibility of glass: J. Amer. Ceramic Soc., 48, 605-608.

Walsh, J. B., 1968, Attenuation in partially melted material: J. Geophys. Res., 73, 2209

Walsh, J. B., 1969, New analysis of attenuation in partially melted rock: J. Geophys. Res., 74, 4333-4337.

Watt, J. P., G. F. Davies, and R. J. O'Connell, 1976, The elastic properties of composite materials: Rev. Geophys. and Space Phys., 14, 541-563.

Wallie, M. R. J., A. R. Gregory, and L. W. Gardner., 1956, Elastic wave velocities in heterogenerous and porous media: Geophysics, 21, 41-70.

Wallie, M. R. J., A. R. Gregory, and G. H. F. Gardner., 1958, An experimental investigation of factors affecting elastic wave velocities in porous media: Geophysics, 23, 459-493.

Wu, T. T., 1965, The effect of inclusion shape on the elastic moduli of two-phase material: Int. J. solids Struct., 2, 1-8.

Wuenschel, P.C., 1965, Dispertive body wave - an experimental study: Geophysics, 30, 539-551.

Yale, D.P., 1985, Recent advances in rock physics: Geophysics, 50, 2480-2491.

Zimmerman, R. W., and M. S. King, 1986, The effect of extent of freezing on seismic velocities in unconsolidated permafrost. Geophysics, 51, 1285-1290.

TABEL CAPTION

Table. Spectrum for fitting velocity-porosity relations with different clay content. The Table shows that the pore aspect ratio decreases with increasing clay content.

FIGURE CAPTIONS

Figure 1. (a) Compressional velocity and (b) shear velocity at confining pressure 40 MPa and pore pressure 1 MPa versus porosity for 80 different sandstone samples. Velocities of clean sandstones data are clearly separated from those of shaly sandstones.

Figure 2. Velocity versus confining pressure for (a) Font. E, and (b) Font. C.

Figure 3. Different bounds and porous model to fit the porosity effects on (a) compressional velocity V_p and (b) shear velocity V_s of clean sandstones.

Figure 4. Pore aspect ratio spectra model (K-T model) used to fit porosity effects on (a) compressional velocity V_p and (b) shear velocity V_s of clean sandstones.

Figure 5. For oblate sphere, as a pore aspect ratio is larger than 0.01, both V_p and V_s as function of porosity show a similar behavior (after Kuster and Toksöz, 1974).

Figure 6. Laminated clay and structure clay show a similar influence on velocities, especially on compressional V_p. The porous clay (dispersed clay) shows much less effect on reducing velocities except pores fully filled by clay (after Minear, 1982).

Figure 7. The bound clay (1 or a few percent) effect can be explained by the Reuss model. However, quantifing the bound clay effect is quite difficult (see text). The matrix clay effect on velocities can be fairly described by the H-S bounds. Moduli of clay should be higher than those obtained from empirical equations.

Figure 8. Different bounds and porous model to fit the porosity effects on (a) compressional velocity V_p and (b) shear velocity V_s of shaly sandstones.

Figure 9. The porosity effect on velocities for shaly sandstones can be modeled using simple pore aspect ratio spectrum. In order to obtain better fits, the pore aspect ratio decreases with increasing clay content.

PORE ASPECT RATIO SPECTRA FOR SIMULATE POROSITY EFFECTS ON VELOCITIES AT DIFFERENT CLAY CONTENT

C	α_1	R_1	α_2	R_2	α_3	R_3	$\phi_{max.}$
0.0	0.32	0.8965	0.032	0.0921	0.0040	0.0114	0.35
0.1	0.30	0.9162	0.025	0.0783	0.0030	0.0055	0.33
0.2	0.30	0.9052	0.025	0.0897	0.0015	0.0051	0.28
0.3	0.25	0.9326	0.019	0.0654	0.0005	0.0020	0.24
0.4	0.25	0.9175	0.019	0.0815	0.0002	0.0010	0.20
0.5	0.22	0.9326	0.015	0.0670	0.00007	0.00038	0.18

C : matrix clay content excluding small amounts of the bound clay.

α : pore aspect ratio.

R : fraction of porosity for the pore refered by the subscript.

$\phi_{max.}$: valided maximum porosity for the pore spectrum.

Table

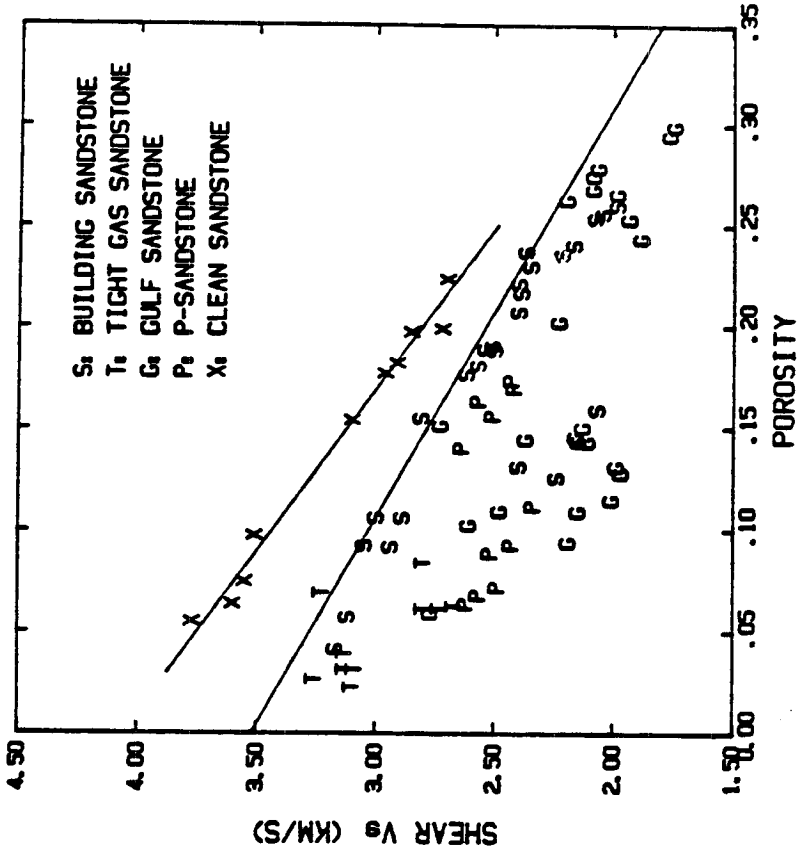
S BUILDING SANDSTONE
T TIGHT GAS SANDSTONE
G GULF SANDSTONE
P P-SANDSTONE
X CLEAN SANDSTONE
SHEAR Vs (KM/S)
POROSITY

Fig. 1b

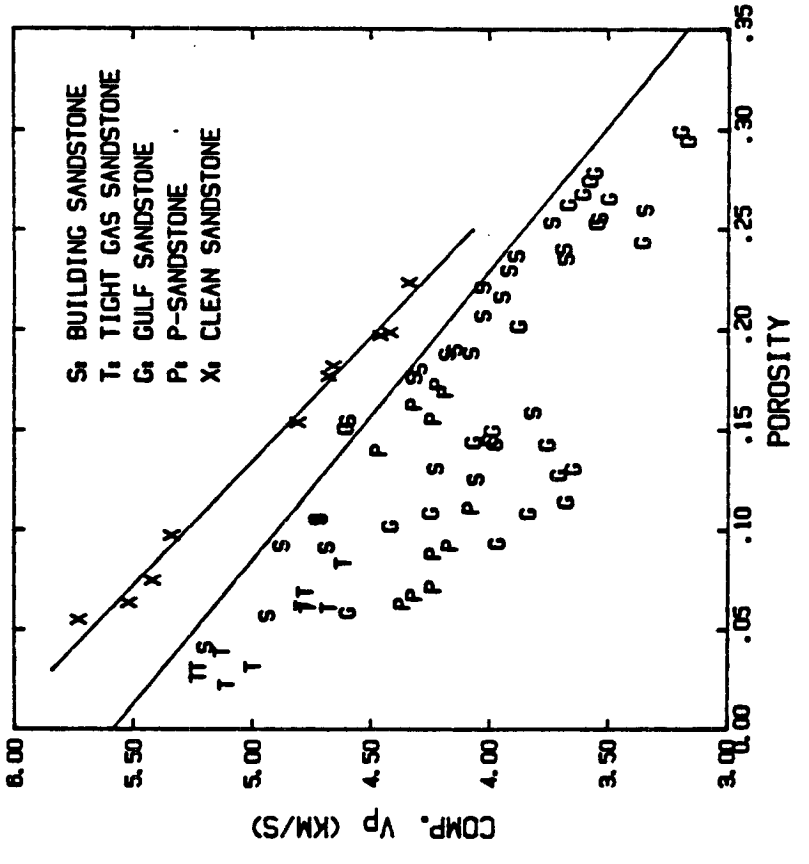
S BUILDING SANDSTONE
T TIGHT GAS SANDSTONE
G GULF SANDSTONE
P P-SANDSTONE
X CLEAN SANDSTONE
COMP. Vp (KM/S)
POROSITY

Fig. 1a

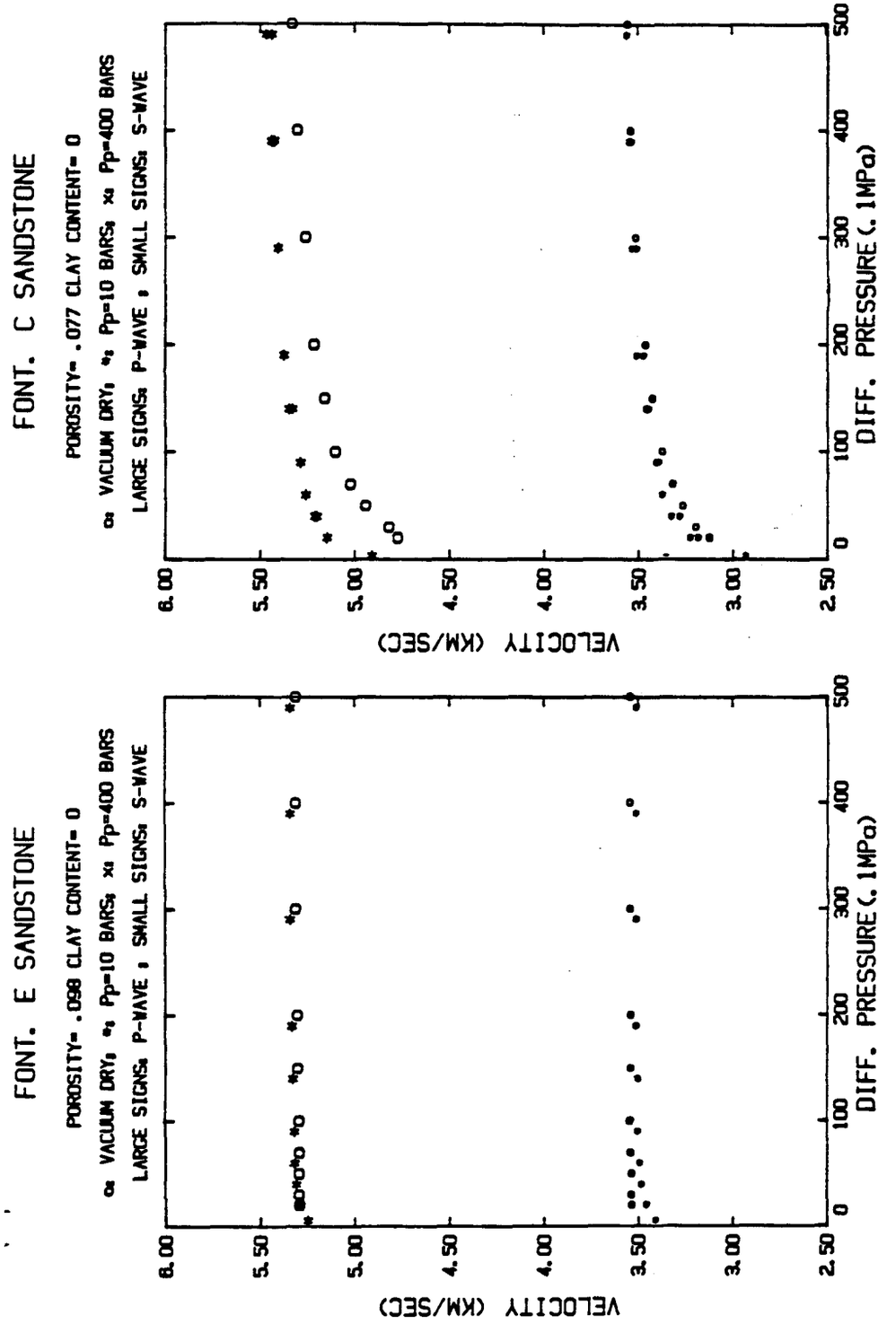
FONT. C SANDSTONE
POROSITY= .077 CLAY CONTENT= 0
o= VACUUM DRY; *= Pp=10 BARS; x= Pp=400 BARS
LARGE SIGNS= P-WAVE ; SMALL SIGNS= S-WAVE
VELOCITY (KM/SEC)
DIFF. PRESSURE(.1MPa)
FONT. E SANDSTONE
POROSITY= .098 CLAY CONTENT= 0
o= VACUUM DRY; *= Pp=10 BARS; x= Pp=400 BARS
LARGE SIGNS= P-WAVE ; SMALL SIGNS= S-WAVE
VELOCITY (KM/SEC)
DIFF. PRESSURE(.1MPa)

Fig. 2b

Fig. 2a

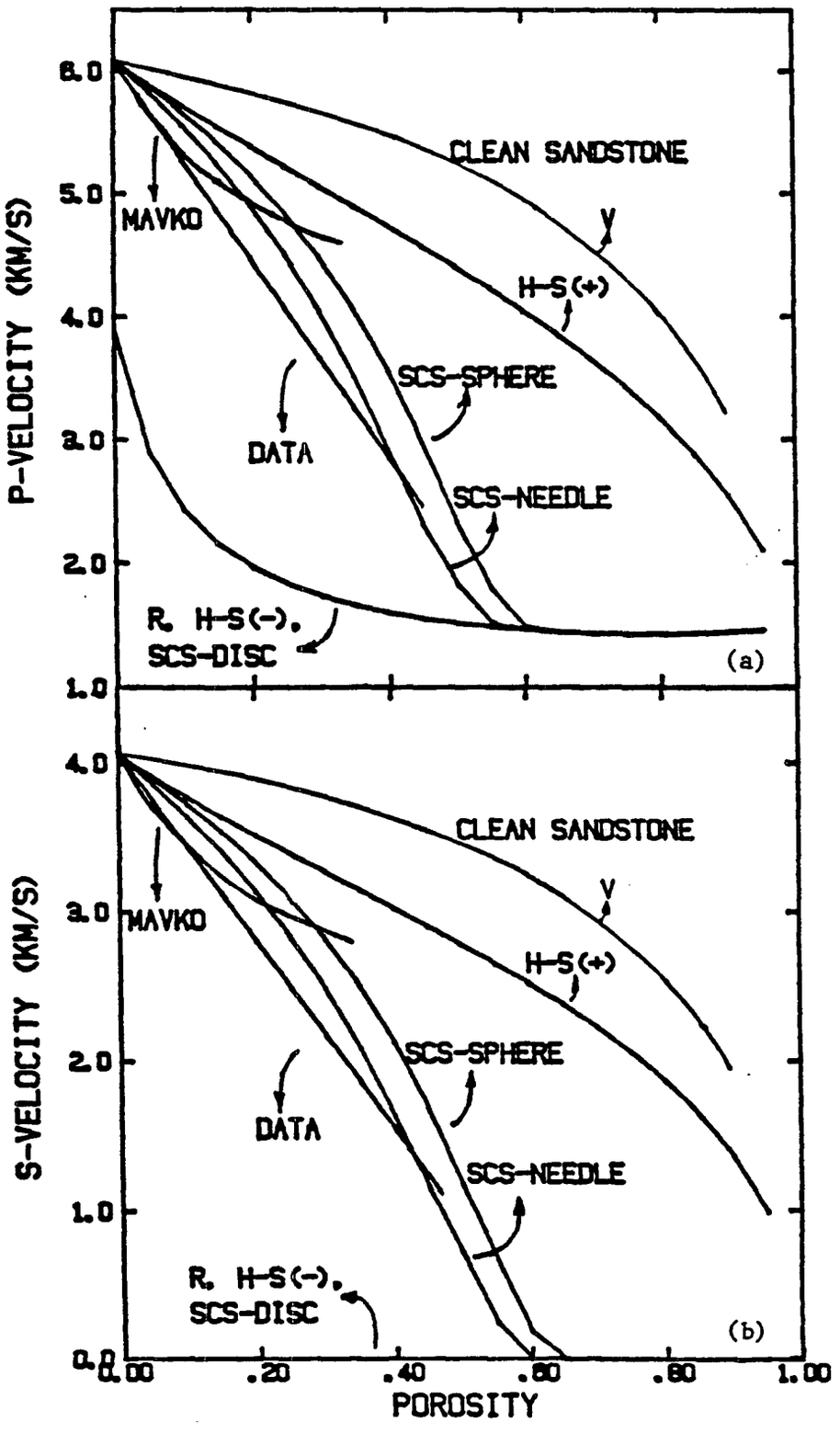
P-VELOCITY (KM/S)
6.0
5.0
4.0
3.0
2.0
1.0
CLEAN SANDSTONE
MAVKO
H-S(+)
SCS-SPHERE
DATA
SCS-NEEDLE
R. H-S(-), SCS-DISC
(a)
S-VELOCITY (KM/S)
4.0
3.0
2.0
1.0
0.0
CLEAN SANDSTONE
MAVKO
H-S(+)
SCS-SPHERE
DATA
SCS-NEEDLE
R. H-S(-), SCS-DISC
(b)
0.00
.20
.40
.60
.80
1.00
POROSITY

Fig. 3

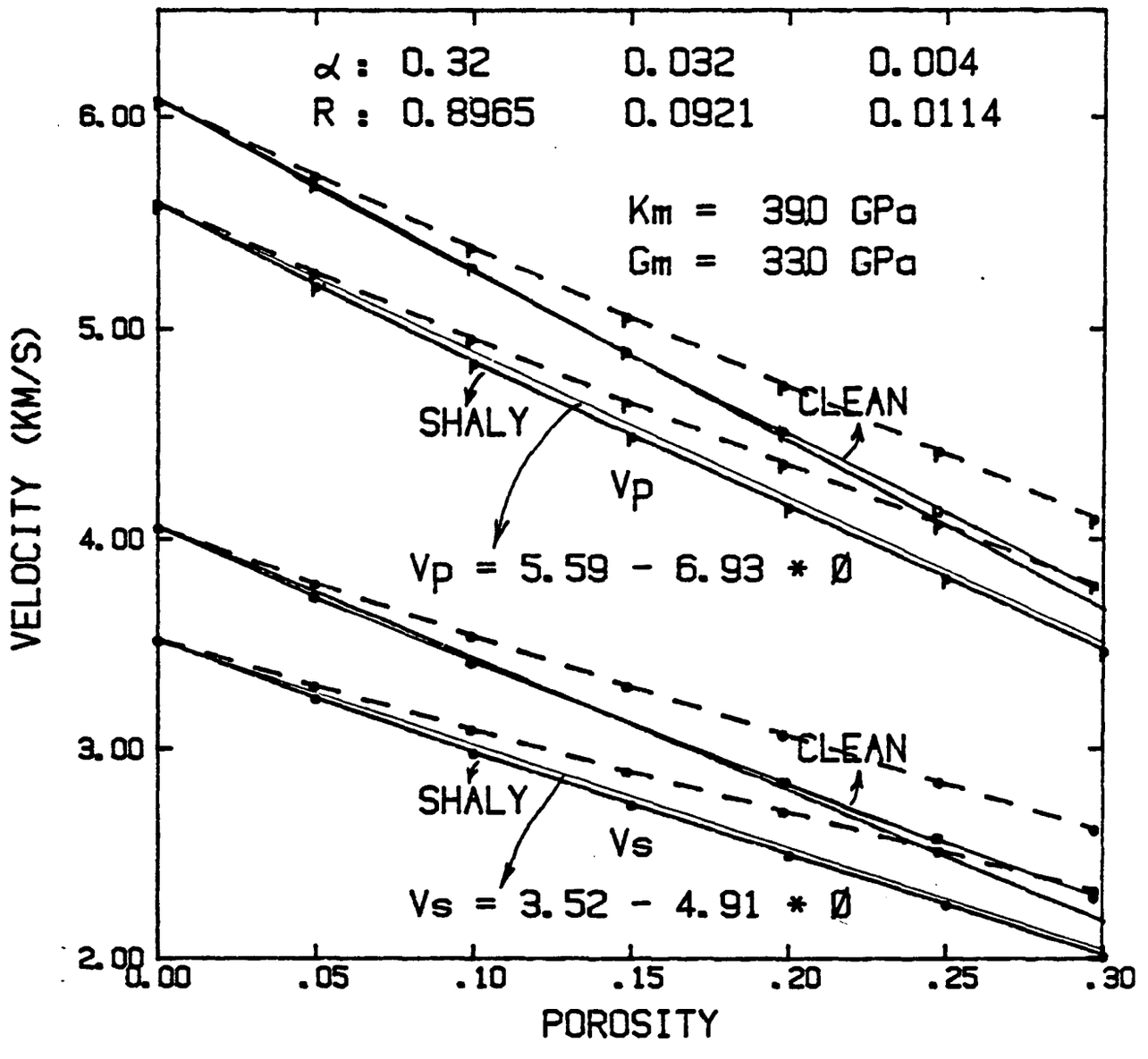

— — : RESULT OF EXCLUDING THINNER PORES

Fig. 4

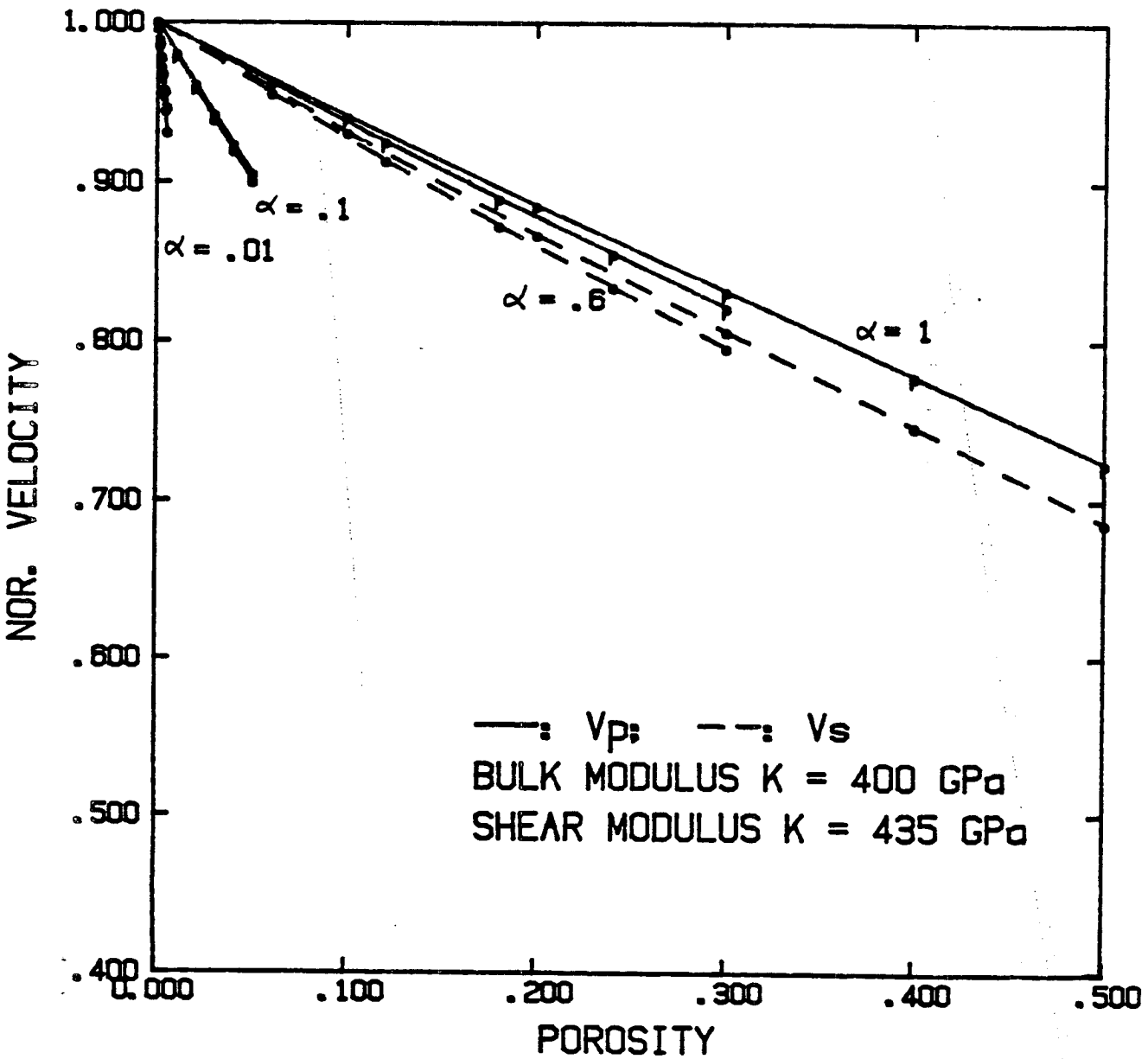
1.000
.900
.800
.700
.600
.500
.400
NOR. VELOCITY
0.000
.100
.200
.300
.400
.500
POROSITY
α = .01
α = .1
α = .6
α = 1
——: Vp; — —: Vs
BULK MODULUS K = 400 GPa
SHEAR MODULUS K = 435 GPa

Fig. 5

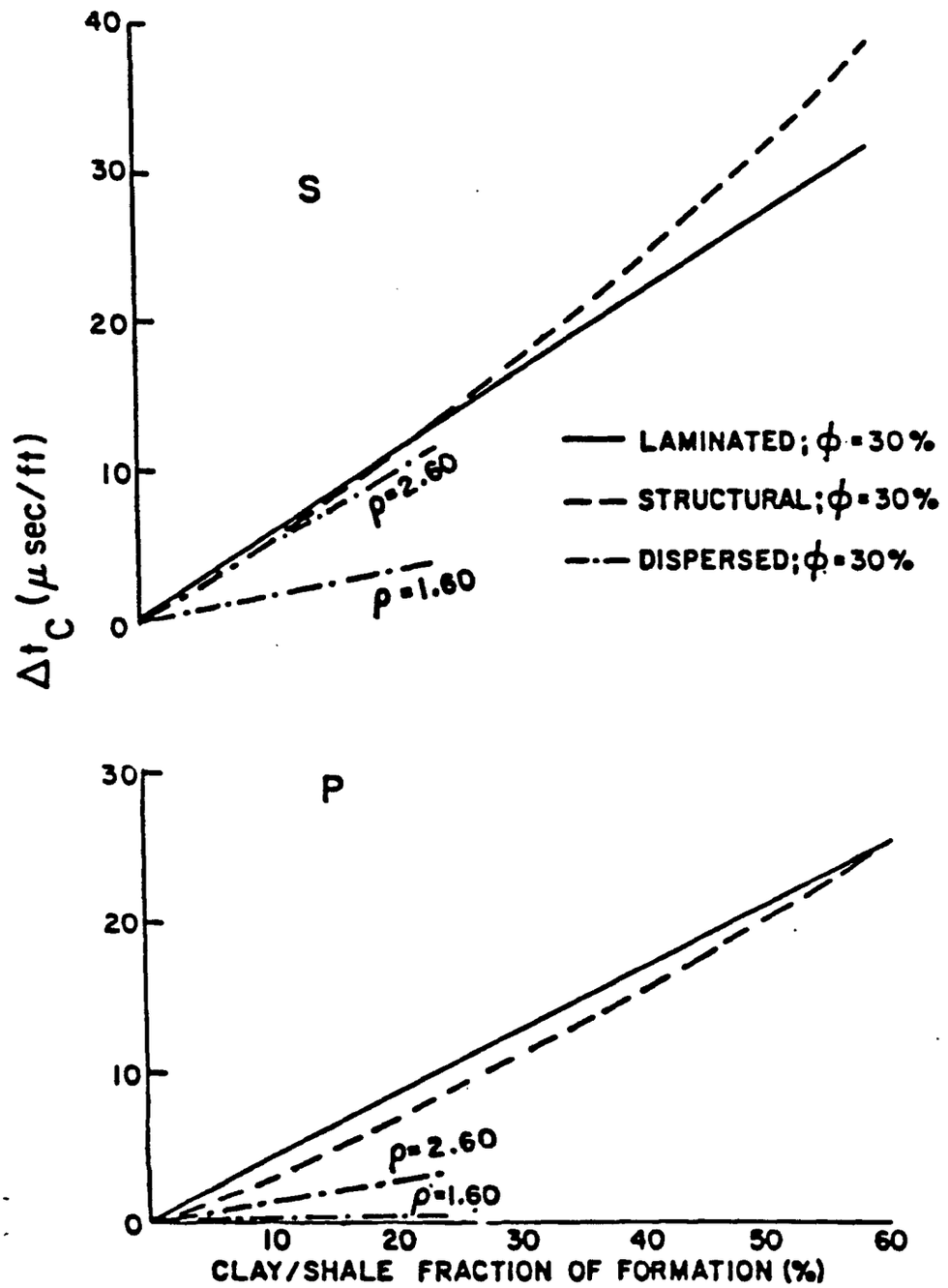
40
30
20
10
0
S
Δt_c (μsec/ft)
LAMINATED; ϕ = 30%
STRUCTURAL; ϕ = 30%
DISPERSED; ϕ = 30%
ρ = 2.60
ρ = 1.60
30
20
10
0
P
ρ = 2.60
ρ = 1.60
10
20
30
40
50
60
CLAY/SHALE FRACTION OF FORMATION (%)

Fig. 6

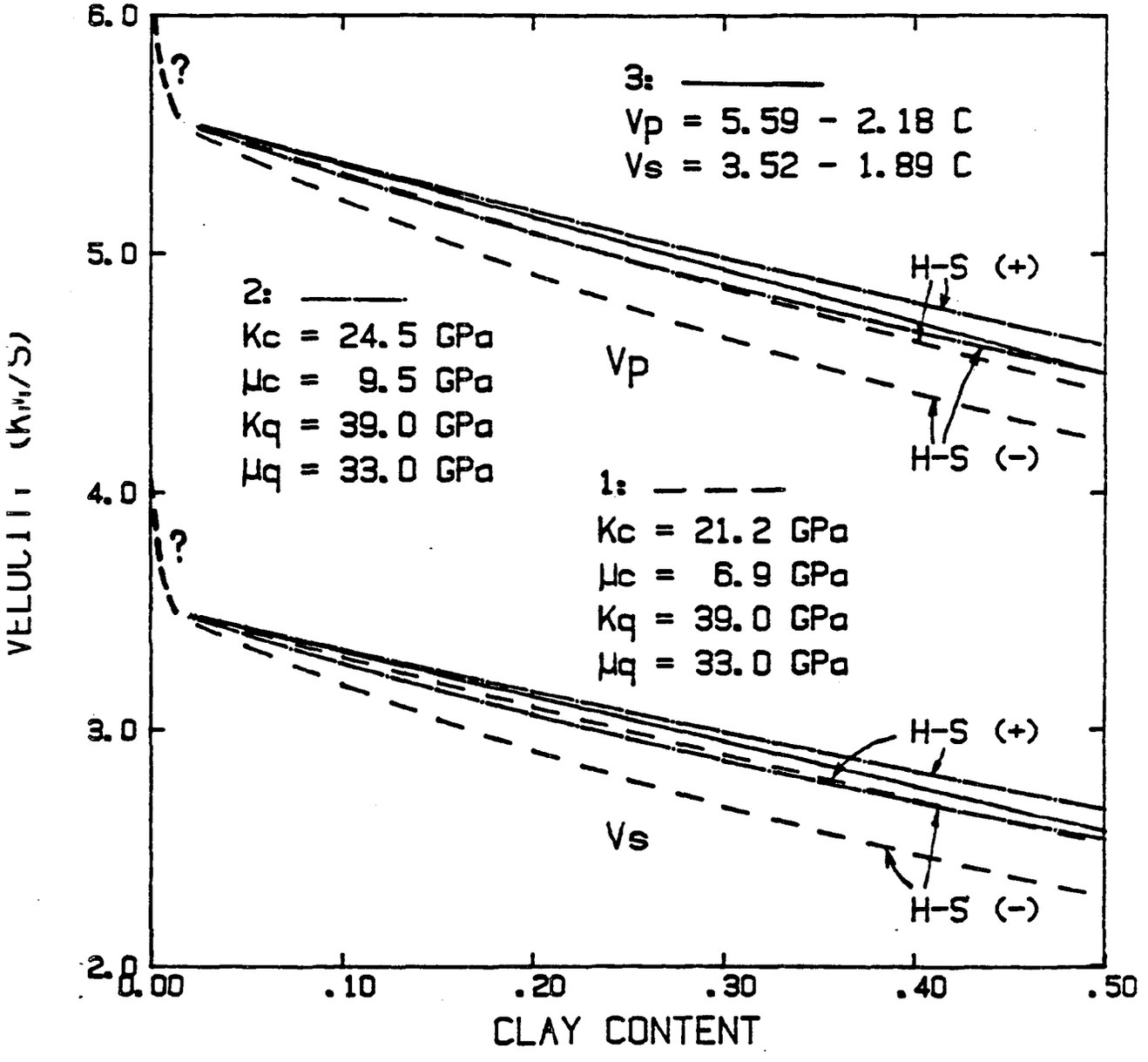
6.0
5.0
4.0
3.0
2.0
0.00
.10
.20
.30
.40
.50
CLAY CONTENT
VELOCITY (KM/S)
3: ———
Vp = 5.59 - 2.18 C
Vs = 3.52 - 1.89 C
2: ———
Kc = 24.5 GPa
μc = 9.5 GPa
Kq = 39.0 GPa
μq = 33.0 GPa
1: — — —
Kc = 21.2 GPa
μc = 6.9 GPa
Kq = 39.0 GPa
μq = 33.0 GPa
Vp
Vs
H-S (+)
H-S (-)
H-S (+)
H-S (-)
?
?

Fig. 7

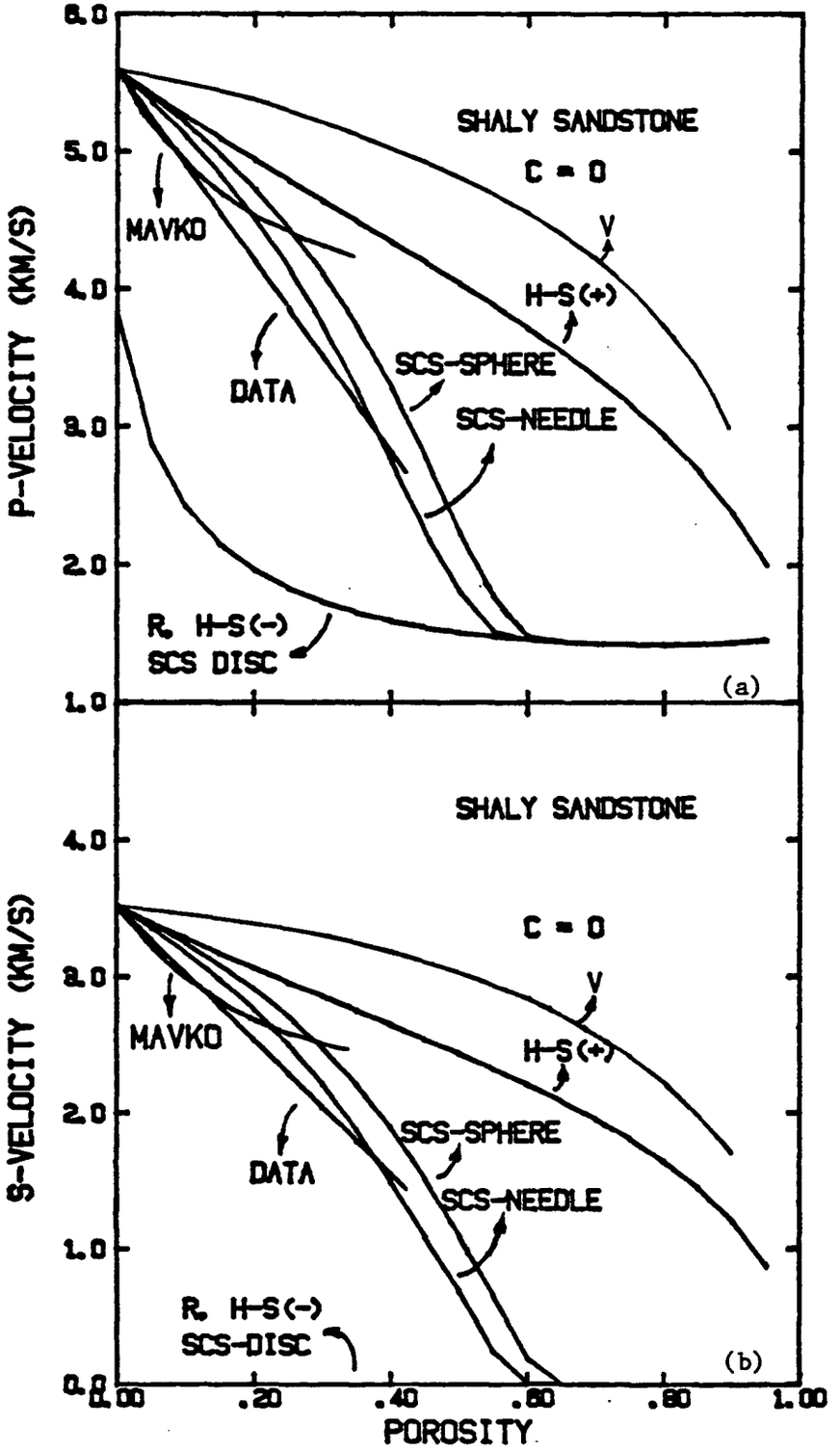
P-VELOCITY (KM/S)
6.0
5.0
4.0
3.0
2.0
1.0
SHALY SANDSTONE
C = 0
V
MAVKO
H-S(+)
DATA
SCS-SPHERE
SCS-NEEDLE
R. H-S(-)
SCS DISC
(a)
S-VELOCITY (KM/S)
4.0
3.0
2.0
1.0
0.0
SHALY SANDSTONE
C = 0
V
MAVKO
H-S(+)
DATA
SCS-SPHERE
SCS-NEEDLE
R. H-S(-)
SCS-DISC
(b)
0.00
.20
.40
.60
.80
1.00
POROSITY

Fig. 8

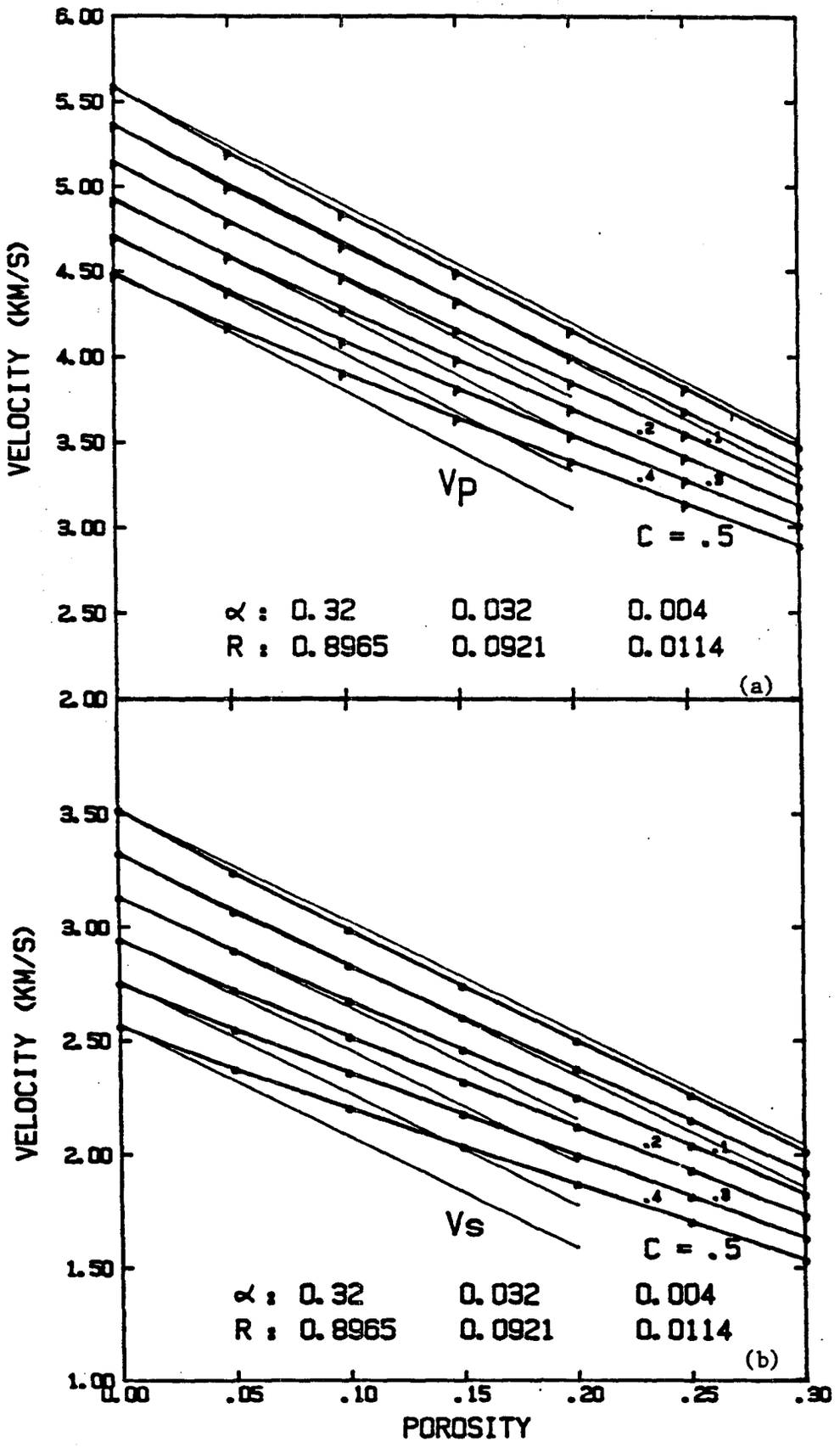
VELOCITY (KM/S)
6.00
5.50
5.00
4.50
4.00
3.50
3.00
2.50
2.00
Vp
C = .5
.2
.1
.4
.3
α : 0.32 0.032 0.004
R : 0.8965 0.0921 0.0114
(a)
VELOCITY (KM/S)
3.50
3.00
2.50
2.00
1.50
1.00
Vs
C = .5
.2
.1
.4
.3
α : 0.32 0.032 0.004
R : 0.8965 0.0921 0.0114
(b)
0.00
.05
.10
.15
.20
.25
.30
POROSITY

Fig. 9

CHAPTER IV

EFFECTS OF WATER SATURATION ON WAVE VELOCITIES OF SANDSTONES

ABSTRACT

The ultrasonic compressional V_p and shear V_s velocities were measured as functions of differential pressure to 50 MPa on 69 different sandstone samples, with porosity ranging from 5 to 30 percent and volume clay content ranging from 0 to 50 percent. The samples were first vacuum-dried, then fully water-saturated. Data indicate that the velocities of dry sandstones are not only correlated to porosity and clay content as shown for the saturated velocities (Han, 1986 a), but also related to degree of consolidation. However, effects of the consolidation on velocities are suppressed by effects of water saturation. The study shows the effects of water saturation on velocities correlated to clay content and degree of consolidation of sandstones. For well consolidated sandstones, the ratios of saturated to dry shear moduli decrease, while the ratios of saturated and dry bulk moduli increase with increasing clay content. The rigidities of these rocks are softened by the water saturation. After water saturation, poorly consolidated sandstones with high clay content become harden. This is supported by the tendency to increase shear moduli, and to increase bulk moduli more, as well as to increase the P-wave amplitudes A_p. The effects of the consolidation on velocities, therefore, are nearly overwhelmed so that velocities can be linearly correlated to porosity and clay content.

Introduction

Gassmann (1951) and Biot (1956 a, b) put forth theories on the effect of fluid on wave propagation through porous media. Since then extensive theoretical and experimental studies of this effect have been made (Wyllie, et al., 1958; King, 1966; Gregory, 1976; Murphy, 1982; Dominico, 1976; Ogushwizt, 1985; Geertsma and Smit, 1961; O'Connell and Budiansky, 1974; Toksöz et al., 1976). The Gassmann-Biot theory predicts that after fluid saturation, the bulk modulus of a granular matrix increases while the shear modulus is not affected by the pore fluid saturation. For ultrasonic velocities, the low- and high-frequency limit of the Biot theory predicts that there is velocity dispersion on water saturated rocks. However, no theory or experimental study which focuses on interactions between fluid saturation and shaly matrix of sandstones has

been published. Only a few investigators (King, 1966; Gregory, 1976; Change and Toksöz, 1979) have suggested that interaction between pore fluid (water) and clay may decrease shear moduli of sandstones.

The saturated velocities show a simple linear relation to the porosity and clay content (Han, 1986 a). However, the dry velocities have shown much worse correlation to the porosity and clay content. The question has then arisen what happens during the fluid saturation ?

Gregory (1976) has suggested that many factors, such as fluid compressibility, also porosity comprised of cracks, fluid wettability characteristics of rocks, chemical and physical interactions between water and clays, and differential pressure have significant influences on elastic properties of saturated rocks. However, many effects of these factors and their interrelationships still remain unclear. We carried out an experimental study of the water saturation effects on ultrasonic velocities and elastic moduli of clean and shaly sandstones. In our study, effects of water saturation on velocities include effects of water wetting and saturation on velocities at low frequency and velocity dispersions in saturated sandstones. However, we did not try to separate them; this question has been dealt within the Chapter V (Han, 1986 b). Our study indicates that for shaly sandstones, water saturation is a complex process which is related not only to clay mineral in sandstones, but also to the degree of consolidation of sandstones.

Experimental Procedures

The experimental technique and samples were described in detail by Han (1986 a). The difference is that Tight gas sandstone samples and few other samples were not included in this study because we did not measure dry velocity data for them. The 69 sandstone samples used in this study came from either well cores or quarries. The porosity of the samples ranged from 5 to 30 percent, and the clay content by volume fraction ranged from 0 to 50 percent (fig. 1). Twenty-three samples (G) came from a few offshore wells in the Gulf of Mexico. Some of these were poorly consolidated. Eleven samples (P) were also borehole cores which were well consolidated. Thirty five well-consolidated samples were from quarries, of which Ten (X) were clean sandstones with less than 1 percent clay content and the rest of them are indicated by (S). Figure 1 shows

clay content versus porosity for all samples. It is noteworthy that samples with more than 20 percent clay content tend to have lower porosities, in the range from 5 to 15 percent.

The measurements were first performed at a sample that was vacuum dryed (vacuum pressure less than 0.01 Torr), then at the sample fully saturated with water. In some samples with high clay content, brine was used as the pore fluid. No velocity differences were found for brine or plain water saturation. P-wave arrival times were picked to within 0.03 μ sec, which leads the total error of less than 1 percent in V_p measurement. The error in the V_s measurement was less than 2 percent, except for poorly consolidated sandstones at low differential pressure (P_d $<$ 10 MPa), where errors may be up to 3 percent due to poor signals. The velocities were measured during loading and unloading pressure cycles. Generally, hysteresis was observed, but its magnitude was typically small. After the first up-loading pressure, measured velocities were very repeatable. In the well-consolidated samples, the hysteresis was less than 1 percent, and in the poorly consolidated samples it was less than 2 percent. The first peak amplitudes, A_p, were measured using the method of Tosaya (1982).

Samples were vacuum oven-dried at temperature of less than 50° C for 2 to 8 weeks, and weighed to within 0.01 g so that the density of a dry sample ρ_d could be determined to within 0.3 percent. The density of the wet sample ρ_w was then calculated by the relation

$$\rho_w = \rho_d + \phi \times \rho_f \tag{1}$$

where ρ_f is the pore fluid density and ϕ is the porosity of the sample. The porosity at room pressure was measured with a helium porosimeter, repeatably within 1 percent of total bulk volume. It was considered equal to the porosity at differential pressure P_d of 1.0 MPa. The variations of the pore volume were monitored with a pore pressure intensifier while the pore pressure was kept constant.

The clay content of each sample was obtained by 300 point countings on thin sections. Minerals with flakelike textures, such as hematite and other iron oxides were counted as a part of the clays.

Velocity in Dry Sandstones

Under vacuum dried conditions, compressional velocity V_{pd} and shear velocity V_{sd} were measured as function of confining pressure up to 50 MPa. For comparison, dry velocities at confining pressure 40 MPa and saturated velocities at confining pressure 40 MPa and pore pressure 1 MPa are shown in Figures 2 a and b, and 3 a and b, respectively. We assume that 1 MPa difference of the high differential pressure for data of the above two group does not bring a significant influence to the comparison.

For clean sandstones with water saturation, the velocities are significantly higher than corresponding velocities of shaly sandstones (Han, 1986 a). Similar to the saturated data, the dry velocities of clean sandstones are distinctly higher than corresponding velocities for shaly sandstones. The data indicate that the dry velocities decrease with increasing porosity. However, this effect is distinct to the saturated velocities; dry velocities of clean sandstones show more scatters from the trend than the saturated ones. For shaly sandstone, the dry P-wave velocity V_{pd} shows much larger scatters. The dry S-wave velocity V_{sd} shows few differences from the saturated ones. Questions have then arisen: what is the reason for the larger scatters of the dry P-wave velocity V_{pd} ? What is the effect of water saturation on P-wave and S-wave velocities ?

Data indicate that Beaver sandstone has the largest deviation of both V_p and V_s from velocity-porosity trends of clean sandstones. This sandstone shows less consolidation and compaction than other samples. Analysis reveals that less consolidated samples which can be indicated by larger pressure dependence of velocities, show low velocities from the velocity-porosity trend. This suggests that dry velocities of clean sandstones not only correlate to porosity, but also to the degree of consolidation and compaction.

For shaly sandstones with water saturation, the velocities can be linearly correlated to the porosity and clay content (Han, 1986 a).

$$V_p = 5.59 - 6.93\ \phi - 2.18\ C \tag{2}$$

and

$$V_s = 3.52 - 4.91\ \phi - 1.89\ C \tag{3}$$

with correlation coefficient 0.985 and relative rms deviation 0.021 for V_p and correlation coefficient 0.959 and relative rms deviation 0.043 for V_s. Similarly, if we assume that the scatters shown in Figures 2 a and b are mainly caused by the effect of clay content, the dry velocities of shaly sandstones also can be correlated to the porosity and clay content only. The correlation results for confining pressure 40 MPa by the least squares regression are

$$V_{pd} = 5.41 - 6.35\ \phi - 2.87\ C \tag{4}$$

and

$$V_{sd} = 3.57 - 4.57\ \phi - 1.83\ C. \tag{5}$$

The correlation coefficients are 0.925 for the V_{pd} and 0.909 for the V_{sd}. The relative rms deviations are 0.045 for the V_{pd} and 0.054 for V_{sd}. The fitting results are much worse than those of the saturated velocities, especially P-wave velocities (Han, 1986 a). Equation (4) shows a larger clay effect on the dry velocity than on the saturated one. This may correspond to data showing that most Gulf sandstones with high clay content have very low dry velocities, especially low P-wave velocities as shown in Figures 2 a and b. Very different responses of dry velocity between Gulf sandstones and P-sandstones to the clay content cause a decrease in the correlation coefficients. This was supported by the relative deviation distribution of data from predicted by Equations (4) and (5) vs. the clay content as shown in Figure 4 a and b. The velocities of Gulf sandstones are less than predicted but the velocities of P-sandstones are greater than predicted. It is not very surprising because most Gulf sandstones with high clay content (mainly montmorillonite) are poorly consolidated, while P-sandstones show that the degree of consolidation increases with increasing clay content (mainly kaolinite). This consolidation effect is also shown in the velocity trend for clean sandstones. Beaver sandstone is less cemented than Fontainbleau sandstone, thus its velocity is distinctly lower than the velocity trend for clean sandstones. This implies that the dry velocities of sandstones not only correlate to the porosity and clay content, but also to the degree of consolidation.

The consolidation is an important parameter in the relation of velocities to the properties of dry sandstones, even at high differential pressure. Its influence on the velocity dispersion was

studied in detail (Han, 1986 b). We have also tried to give a limit to this effect (Han, 1986 c). However, quantifying the effect of consolidation on dry velocity of sandstones still needs to be done. Here we are only studying how this consolidation effect is overwhelmed by the water saturation effects for saturated velocities of sandstones.

The Effect of Water Saturation on Velocities of Clean Sandstones

Clean sandstone has the simplest matrix structure which is composed of pure quartz grains with quartz cement. Therefore, the water saturation effect on velocities of clean sandstones is fundamental for understanding its effect on velocities of porous media. Figure 5 a and b show relative changes of bulk and shear moduli by water saturation versus porosity for clean sandstones. The water saturation effect shows a trend to increase with increasing porosity for both bulk and shear moduli except for a large effect off the trend for Beaver sandstone which is less consolidated than Fontainbleau sandstone. Analysis indicated that scatters of data from the trend depended on the degree of consolidation. St. Peter sandstone is poorly consolidated, but, it shows a similar behavior to Fontainbleau sandstones because it is well compacted at the high differential pressure.

The conclusion can be drawn that for consolidated clean sandstones at high differential pressure, both bulk and shear moduli at ultrasonic frequency increase with water saturation. The water saturation effect increases with increasing porosity. This is consistent with prediction of the Biot theory, which we will discussed in Chapter 5. Therefore, though the dry velocities show a large influence by the degree of consolidation as previously mentioned, its effect is almost overwhelmed by the water saturation effect. Of basis on a expiremental study, Gregary (1976) has concluded that fluid saturation effects on compressional-wave velocity are much larger in low-porosity than in high-porosity rocks. Our data reveal a opposite trend for well-consolidated sandstones. It suggests that Gregory's conclusion is only valid for low-porosity rocks with poorly consolidation or crack-like pores.

Effect of Water Saturation on Velocities of Shaly Sandstones

For shaly sandstones, the relative change of velocity V_p and V_s by the water saturation versus porosity and clay content show in Figure 6 a, b, c, and d, respectively. The V_p increases with water saturation. These water saturation effect on V_p are affected by porosity and clay content. Figure 6 a shows a trend that the ratio V_p (sat.)/V_p (dry) increases slightly with increasing porosity. The large deviations of data from the above trend correlate to clay content shown in Figure 6 b. The ratio V_p (sat.)/V_p (dry) increases with increasing clay content. Figure 6 b indicates that data of P-sandstones are much less than those of Gulf sandstones with a similar clay content. This may be caused by poor consolidations of the Gulf sandstones than the P-sandstones. The ratios V_s (sat.)/V_s (dry) in Figures 6 c and d do not appear a clear pattern. Most of data are less than one. They decrease with increasing porosity, which is partially caused by increasing density. Scatters of data from this trend suggest that other parameters are also important. Figure 6 d shows that the ratio V_s (sat.)/V_s (dry) decreases with increasing clay content except for some data from Gulf sandstones with high clay contents which show high ratios close or even greater than one. This indicates again that these Gulf sandstones differ from other sandstones. The complicated patterns of data suggest that effects of different parameters on velocities related to water saturation are hardly separated. For simplicity, we taken off influence of an increase of density with water saturation on velocities and focus on effects of water saturation on shear and bulk moduli of shaly sandstones.

In following sections, we present data to show how these relations affect shear and bulk moduli and the amplitude A_p.

The Effects of Water Saturation on Shear modulus

In the comparison of dry and saturated velocity data at high pressure, strong correlations among the effect of water saturation on elasticity of matrix and clay content and consolidation were found.

The shear and bulk moduli for our dry samples were computed from velocities and density

by expressions:

$$Shear\ \mu = \rho\ V_s^2 \quad ; \quad Bulk\ K = \rho\ (V_p^2 - \frac{4}{3} V_s^2). \tag{6}$$

It is commonly expected that the shear modulus should remain constant or increase slightly when rock is saturated from its dry state (Gassmann, 1951; Biot, 1956; Kuster and Toksöz, 1974: O'Connell and Budiansky, 1974). This agrees with our data for clean sandstones (Figure 5 a and b). The data for shaly sandstones, however, displays a more complex situation. Figures 6 a and b show that the ratios μ (sat.)/μ (dry) deviates significantly from the expected value of 1. King (1966) and Toksöz et al. (1976) have alluded to possible interactions between pore fluid and clay minerals as processes to soften rock matrix and decrease the shear modulus. Our data suggest that some of sample do show such decrease of shear moduli but others do not; their shear moduli increase with the water saturation. The deviations have no clear correlation with porosity as shown in Figure 7 a except for clean sandstones the ratios μ (sat.)/μ (dry) of which increase slightly with increasing porosity as previously shown in Figure 5 b. Figure 7 b shows that these deviations correlate to interaction between water and clay minerals. The ratios μ (sat.)/μ (dry) show (excluding the poorly consolidated Gulf sandstones) a decreasing trend with increasing clay content. It suggests that shear moduli of clays can be significantly reduced by water saturation. Much data, and Gulf sandstones in particular, deviate from this trend with their ratios μ (sat.)/μ (dry) being greater than 1 even though they have high clay contents. This may indicate that the Gulf sandstones have exceptional structures relative to the other samples.

Effects of Water Saturation on Bulk Modulus

The effects of water saturation on the bulk moduli of rock were studied by several researchers (Gassmann, 1951; Biot, 1956; Nur and Simmons, 1969; Kuster and Toksöz, 1974; O'Connell and Budiansky, 1974) who showed that water saturation can significantly increase bulk moduli of rocks. This agrees with data for clean sandstones (Figure 5 a and 8 a). However, effects of clay content during water saturation on the bulk moduli have not been mentioned in the literature. Figure 8 a shows a trend that the ratio K (sat.)/K (dry) increases with increasing

porosity as shown for the clean sandstones. Yet, many data, mainly for samples with high clay content, exhibit much higher water saturation effects on bulk moduli than the trend. This reveals that the water saturation effect on bulk moduli also relates to clay content. Figure 8 b indicates that the ratios of K (sat.)/K (dry) are from 1.20 for the clean sandstones to over 2.0 for some samples with a high clay content. This large effect of increasing K (sat.) suggests that bulk moduli of saturated clays may be much greater than those of dry clays. In comparison, the effects of water saturation on bulk moduli are much greater than those on shear moduli. The effects of water saturation on bulk modulus K may be the consequence of water saturated clays being more structurally rigid than vacuum dry ones. Though the data are scattered, it is easy to note that for most sandstones, K (sat.)/K (dry) increases slightly with increasing clay content, whereas, Gulf sandstones with high clay content show exceptional larger K (sat.)/K (dry) than do other samples. Again, this indicates that the Gulf sandstones are structurely different from other samples.

Effect of Water Saturation on Amplitude

Moreover, the first arrived peak amplitude is another important index to relate the degree of consolidation. For consolidated sandstones, the amplitude decreases with water saturation, the opposite of poorly consolidated shaly sandstones. Thus, for most Gulf sandstones, the P-wave amplitude ratios A_p (sat)/A_p (dry) are greater than 1, while for other sandstones, these ratios are less than 1 (Figure 9). This result again suggests that most Gulf sandstones are systematically different from the other sandstones in our study.

Effect of Water Saturation on Consolidation

Indeed, most Gulf sandstones are poorly consolidated and show larger porosity reductions than do other sandstones with increasing differential pressure. Moreover, clays of Gulf sandstone are mainly composed of illite and montmorillonite, which differ from the other sandstones, such as P sandstones which contain clays mainly composed of kaolinite with carbonate cement. With increasing clay content, Gulf sandstones show a general trend of decreasing consolidation but P-

sandstones show increases of consolidation. It appears that in the Gulf sandstones, one of the effects of water saturation is to stiffen the contacts between the quartz grains. This effect is particularly pronounced in poorly consolidated sandstones, possibly because grain contacts are loose to begin with.

The combined effects of water saturation and matrix hardening on the moduli of shaly sandstones may account for much of the scatter in Gulf sandstone data presented in Figures 6, 7 and 8. More accurate petrographic description of these rocks may be required in the future.

Finally, we need to summarize the effects of water saturation on the velocities. The features of $V_{p(sat.)}/V_{p(dry)}$ data (Figures 6 a and b) show it being dominated by the characters of bulk modulus (Figures 8 a and b). It is not a surprise because of relatively smaller effect of water saturation on the shear moduli than on the bulk moduli. The density increase by the water saturation does not bring a significant influence to the data distribution, except that the porosity effect on the V_p are suppressed by the density effects. Therefore, the velocity data only show a slight increase with increasing the porosity. The shear velocity data (Figures 6 a and b) show features similar to the shear modulus (Figures 7 c and d), except for the density effect on $V_{s(sat.)}$. Data indicate that water saturation has the smallest influence on velocities of clean sandstones. The clay content and degree of consolidation of shaly sandstones play important roles to influence the water saturation effects on velocities.

Effect of Water Saturation on Velocity Ratio

Owing to differing responses of bulk modulus K and shear modulus μ to the water saturation versus the clay content for shaly sandstones, the differences between velocity ratios V_p/V_s of fully saturated (s) and dry (d) samples can more clearly be related to the clay content and porosity as follows:

$$D = (V_p/V_s)_s - (V_p/V_s)_d = 0.018 + 0.36 \times \phi + 0.47 \times C \qquad (7)$$

with a correlation coefficient of 0.89. The effect of the clay content on the D is shown in Figure 10. This effect is greater than that of the porosity in equation (7). This relation suggests that the velocity ratio may favorably be used as an index of saturated states in shaly sandstones.

Conclusion

For clean sandstones, both bulk and shear moduli at ultrasonic frequency and at high differential pressure show increases with water saturation from a dry state, which is enhanced by increasing porosity. The water saturation effect is also enhanced by less consolidation. However, this effect shows a similar influence to St. Peter sandstone with consolidated ones, because former is well compacted at the high differential pressure. Therefore, though the dry velocities are affected by degree of consolidation, their effect is suppressed by the water saturation.

For shaly sandstones, the dry velocity data show poor correlation to porosity and clay content, especially for the V_p data. This is because the clay effects on V_p and V_s for poorly consolidated Gulf sandstones are much larger than on well consolidated sandstones with similar clay content. This indicates that the degree of consolidation somehow should be involved in the relations between velocities and properties of sandstones.

The interactions between clay minerals and pore fluid (water) does influence elastic moduli and velocities. The water saturation appears to decrease shear moduli while increasing bulk moduli with increasing clay content. This is consistent with observations of the effect of water saturation on clays (Han, 1986 c).

In poorly consolidated sandstones, however, water saturated clays actually tend to stiffen grain contacts. Consequently, bulk and shear moduli increase as a result of better grain contacts and water saturated clays. Differences in consolidation among dry sandstones are nearly overwhelmed by the water saturation effects.

The differing responses of shear and bulk moduli μ and K in relation to water saturation versus clay content indicate that the differences between V_p/V_s ratios for saturated and dry samples increase with increasing clay content.

REFERENCES

Biot, M.A., 1956 a, Theory of propagation of elastic waves in fluid saturated porous solid I. low-frequency range: Jour. Acoust. Soc. America, 28, 168-178.

Biot, M.A., 1956 a, Theory of propagation of elastic waves in fluid saturated porous solid II. Higher frequency range: Jour. Acoust. Soc. America, 28, 179-191.

Chang, C. H., and M. N., Toksöz, 1979, Inversion of seismic velocities for the pore aspect ratio spectrum of a rock: J. Geophys. Res., 84, 7534-7543.

Domenico, S. N., 1976, Effect of brine-gas mixture on velocity in an unconsolidated sand reservoir: Geophysics, 41, 882-894.

Gassmann, F., 1951, Elastic waves through a packing of spheres: Geophysics, 16, 673-685.

Geertsma, J., and Smit, D. C., 1961, Some aspects of acoustic wave propagation in fluid saturated porous solids: Geophysics, 26, 169-181.

Gregory, A. R., 1977, Aspects of rock physics from laboratory and log data that are important to seismic interpretation: Am. Assoc. Pet. Geol. Memoir 26, 15-46.

Gregory, A. R., 1976, Fluid saturation effects on dynamic elastic properties of sedimentary rocks: Geophysics, 41, 895-921.

Han, D., 1986 a, Effects of porosity and clay content on wave velocities of sandstones: in this volume Chapter II. Main body of this Chapter was published with coauthor Nur, A., and Morgan, F. D., in name, Effects of porosity and clay content on wave velocities of sandstones: Geophysics, 51, Nov., and in name, Velocity measurement and empirical modeling in sandstones: the Log Analyst.

Han, D., 1986 b, Velocity dispersions in sandstones: in this volume Chapter V.

Han, D., 1986 c, Study of compaction and velocities of sand-clay mixtures: in this volume Chapter VI.

King, M.S., 1966, Wave velocities in rocks as a function of changes in overburden pressure and pore fluid saturations: Geophysics, 31, 50-73.

Kuster, G.T., and Toksöz, M.N., 1974, Velocity and attenuation of seismic waves in two-phase

media, I: Theoretical formulation: Geophysics, 39, 587-606.

Murphy, W. F. III, 1982, Effects of microstructure and pore fluid on the acoustic propertied of granular sedimentary materials: Ph.D thesis, Stanford University.

Nur, A., and Simmons, G., 1969, The effect of saturation on velocity in low porosity rocks: Earth planet. Sci. Lett. 7, 183-193.

Ogushwizt, P. R., 1985, Applicability of the Biot theory I. low-porosity material: J. Acoust. Soc. Am., 77, 429-440.

O'Connell, R.J., and Budiansky, B., 1974, Seismic velocities in dry and saturated cracked solids: J. Geophys. Res., 79, 5412-5426.

Toksöz, M. N., Cheng, C. H., and Timer, A., 1976, Velocities of seismic waves in porous rocks: Geophysics, 41, 621-645.

Tosaya, C., 1982, Acoustical properties of clay-bearing rocks: Ph.D. dissertation, Stanford University.

Wyllie, M. R. J., Gregory, A. R., and Gardner, L. W., 1956, Elastic wave velocities in heterogeneous and porous media: Geophysics, 21, 41-70.

Wyllie, M. R. J., Gregory, A. R., and Gardner, G. H. F., 1958, An experimental investigation of factors affecting elastic wave velocities in porous media: Geophysics, 23, 459-493.

FIGURE CAPTIONS

Figure 1. The range of clay content and porosity for the 69 shaly sandstones of this study. Porosity ranges from 5 to 30 percent and clay content from 0 to about 50 percent. The data indicate that sandstones with a high clay content tend to have a low porosity, from 5 to 15 percent.

Figure 2. Measured (a) compressional and (b) shear velocities vs. porosity for 69 vacuum dried sandstone samples at $P_c = 40$ MPa.

Figure 3. Measured (a) compressional and (b) shear velocities vs. porosity for 69 saturated sandstone samples at $P_c = 40$ MPa.

Figure 4. Deviation of (a) dry compressional velocities V_p and (b) dry shear velocities V_s data from the linear correlations to porosity and clay content at $P_c = 40$ MPa versus clay content. The data show a clear separation of deviations of Gulf sandstones from P-sandstones.

Figure 5. The relative changes of (a) bulk moduli and (b) shear moduli from saturated to the dry state referenced to saturated moduli at differential pressure 40 MPa versus to porosity for clean sandstones.

Figure 6. The velocity ratios of saturated to dry velocity at differential pressure near 40 MPa for 69 samples.

(a) V_p (sat.)/V_p (dry) versus porosity.

(b) V_p (sat.)/V_p (dry) versus clay content.

(c) V_s (sat.)/V_s (dry) versus porosity.

(d) V_s (sat.)/V_s (dry) versus clay content.

Figure 7. The ratio of shear modulus at saturated state to that at dry state versus (a) porosity and (b) clay content. Data show that the ratio decreases with increasing clay content for well consolidated sandstones. For poorly consolidated sandstones with high clay content, the ratio shows more or less an increase from the above tendency of consolidated sandstones.

Figure 8. The ratio of bulk moduli at saturated state to dry state versus (a) porosity and (b) clay content. Data show that an increase of bulk moduli by water saturation correlates to an increase of clay content for well consolidated sandstones. For poorly consolidated sandstones with high clay content, the bulk moduli shows more or less an extra increase relative to the consolidated ones.

Figure 9. The amplitude ratio A_p (sat)/A_p (dry) vs. porosity at differential pressure near 40 MPa. The data show that for saturated poorly consolidated Gulf sandstones, the amplitude A_p increases over that of dry ones, the opposite of that for consolidated sandstones.

Figure 10. Differences of velocity ratios V_p / V_s between saturated (s) and dry (d) samples vs. clay content at differential pressure near 40 MPa.

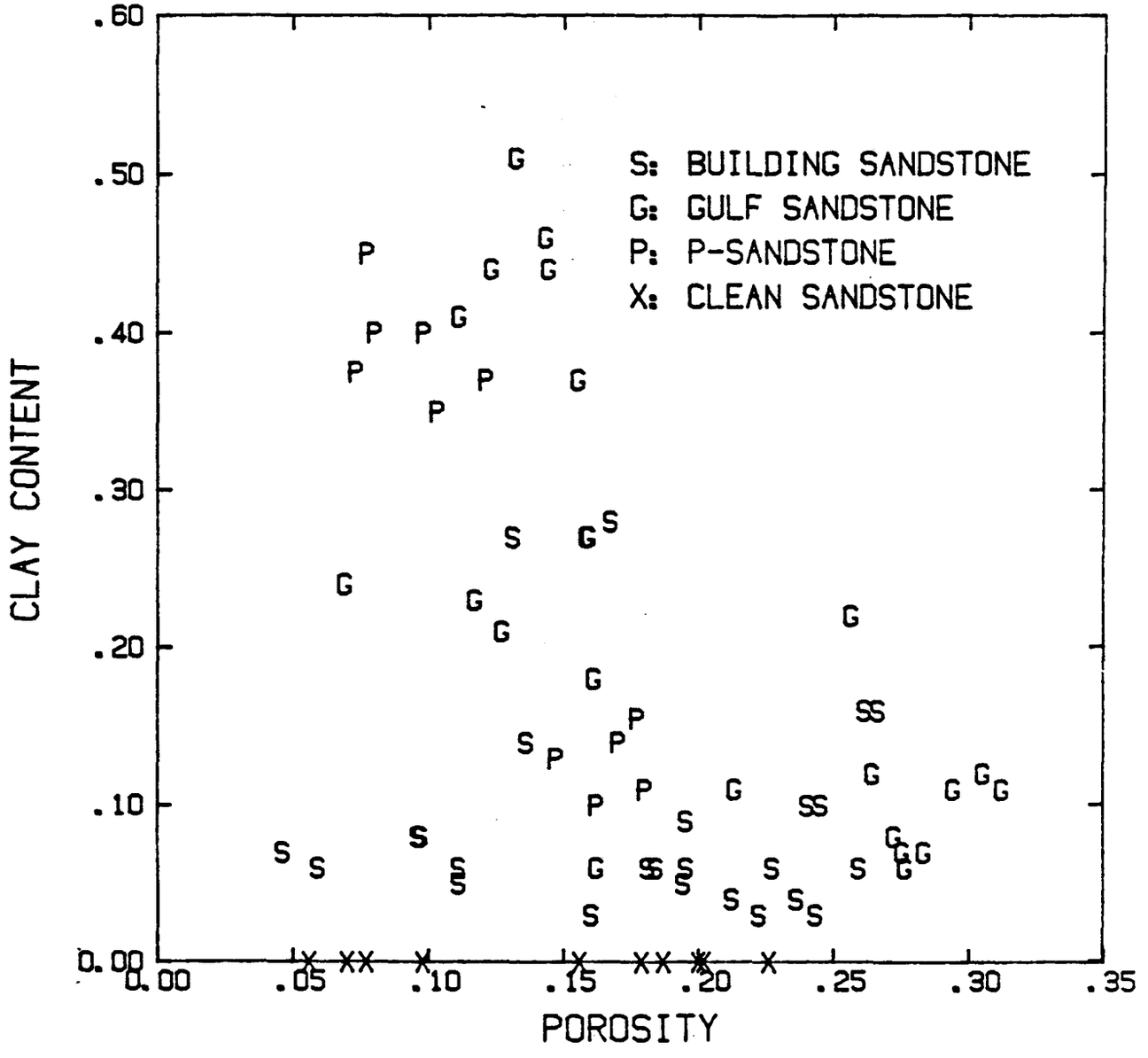
S: BUILDING SANDSTONE
G: GULF SANDSTONE
P: P-SANDSTONE
X: CLEAN SANDSTONE
CLAY CONTENT
POROSITY
.60
.50
.40
.30
.20
.10
0.00
0.00
.05
.10
.15
.20
.25
.30
.35

Fig. 1

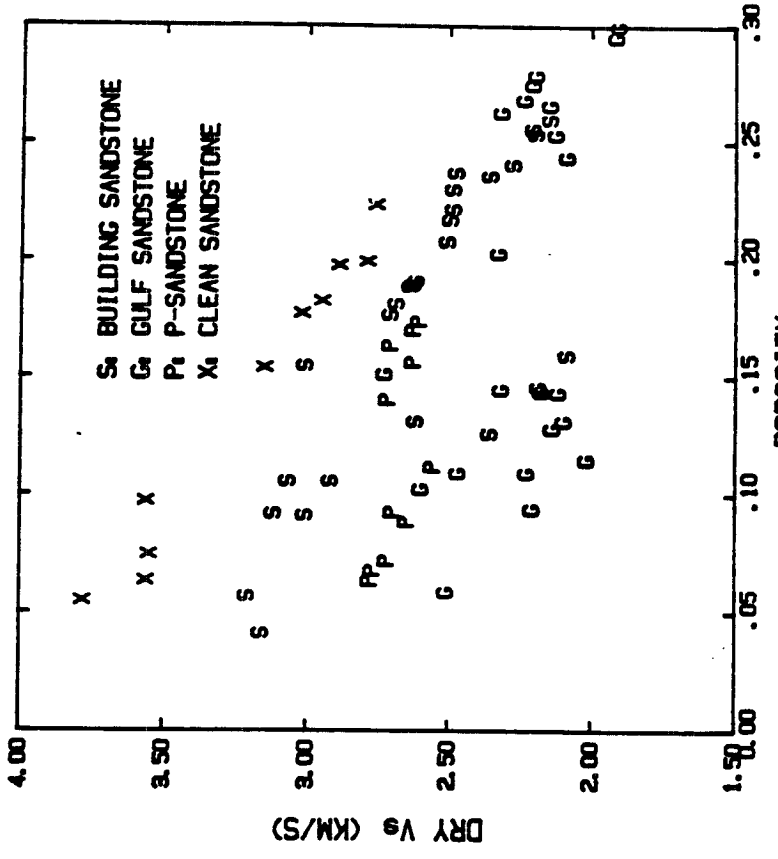
S BUILDING SANDSTONE
G GULF SANDSTONE
P P-SANDSTONE
X CLEAN SANDSTONE
DRY Vs (KM/S)
POROSITY
4.00
3.50
3.00
2.50
2.00
1.50
1.00
.05
.10
.15
.20
.25
.30

Fig. 2b

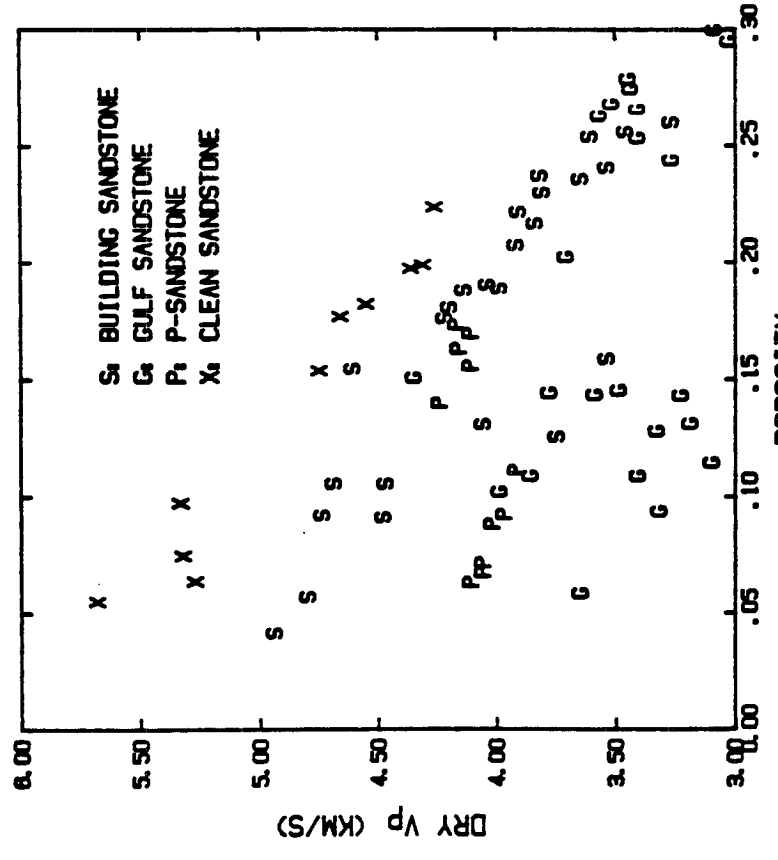
S BUILDING SANDSTONE
G GULF SANDSTONE
P P-SANDSTONE
X CLEAN SANDSTONE
DRY Vp (KM/S)
POROSITY
6.00
5.50
5.00
4.50
4.00
3.50
3.00
.05
.10
.15
.20
.25
.30

Fig. 2a

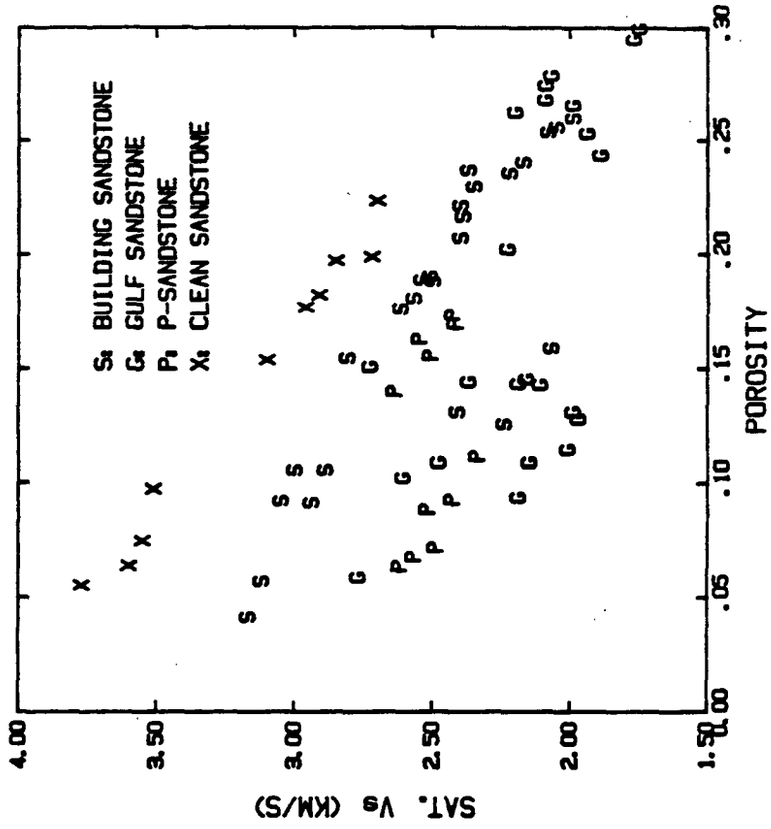
S BUILDING SANDSTONE
G GULF SANDSTONE
P P-SANDSTONE
X CLEAN SANDSTONE
SAT. V_S (KM/S)
POROSITY
4.00
3.50
3.00
2.50
2.00
1.50
.00
.05
.10
.15
.20
.25
.30

Fig. 3b

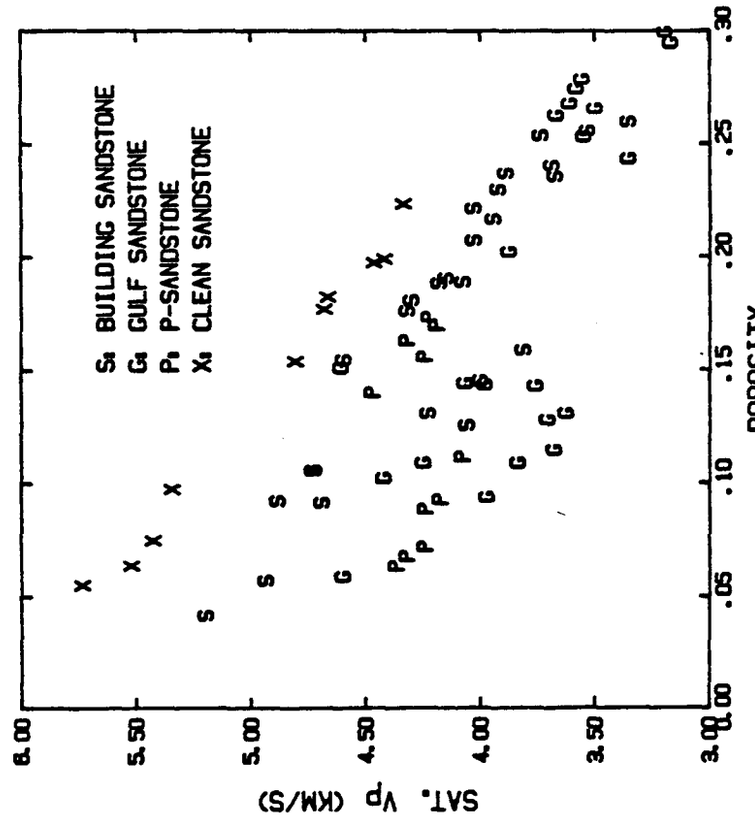
S BUILDING SANDSTONE
G GULF SANDSTONE
P P-SANDSTONE
X CLEAN SANDSTONE
SAT. V_P (KM/S)
POROSITY
6.00
5.50
5.00
4.50
4.00
3.50
3.00
.00
.05
.10
.15
.20
.25
.30

Fig. 3a

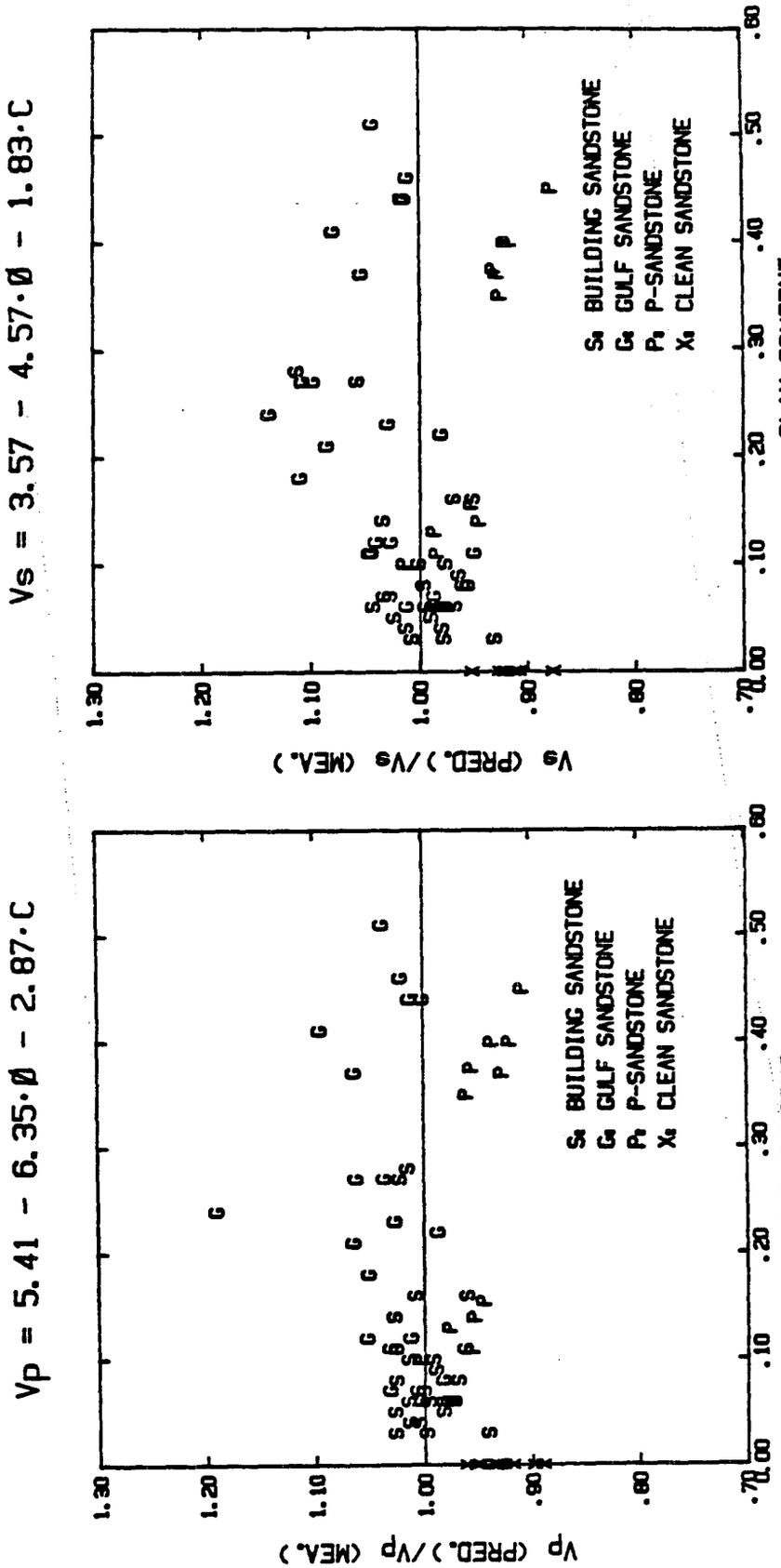
Vp = 5.41 - 6.35·Ø - 2.87·C
Vp (PRED.)/Vp (MEA.)
CLAY CONTENT
Sa BUILDING SANDSTONE
Ga GULF SANDSTONE
Pa P-SANDSTONE
Xa CLEAN SANDSTONE
Vs = 3.57 - 4.57·Ø - 1.83·C
Vs (PRED.)/Vs (MEA.)
CLAY CONTENT
Sa BUILDING SANDSTONE
Ga GULF SANDSTONE
Pa P-SANDSTONE
Xa CLEAN SANDSTONE

Fig. 4a

Fig. 4b

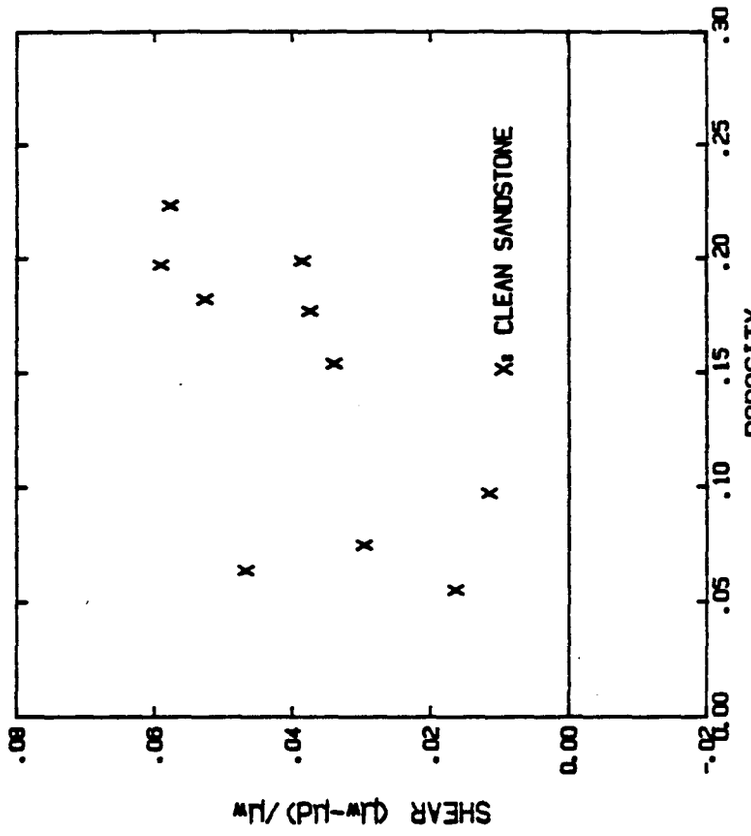
SHEAR (μw-μd)/μw
.08
.06
.04
.02
0.00
-.02
Xs CLEAN SANDSTONE
0.00
.05
.10
.15
.20
.25
.30
POROSITY

Fig. 5b

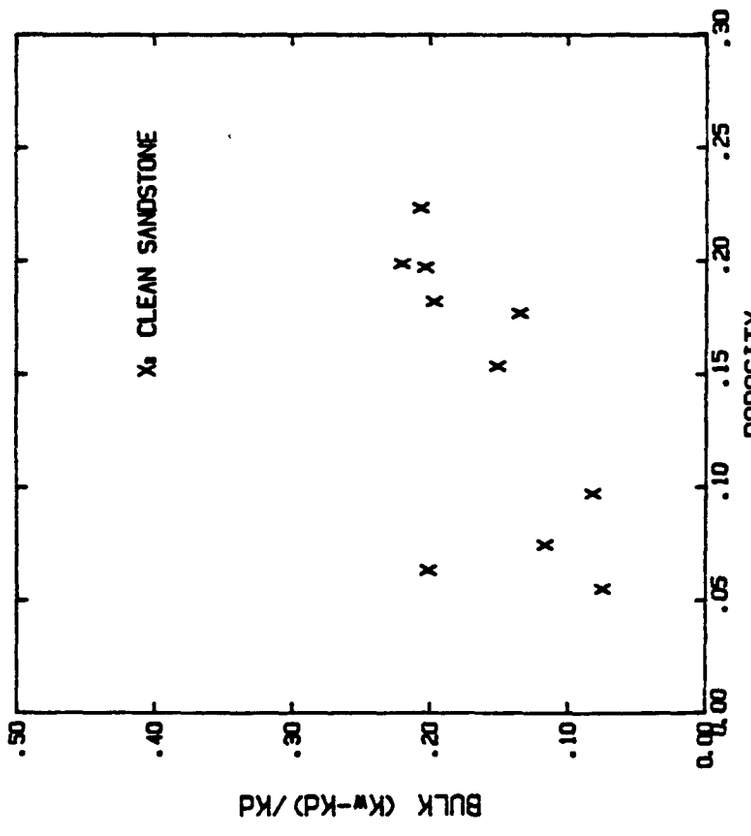
BULK (Kw-Kd)/Kd
.50
.40
.30
.20
.10
0.00
Xs CLEAN SANDSTONE
0.00
.05
.10
.15
.20
.25
.30
POROSITY

Fig. 5a

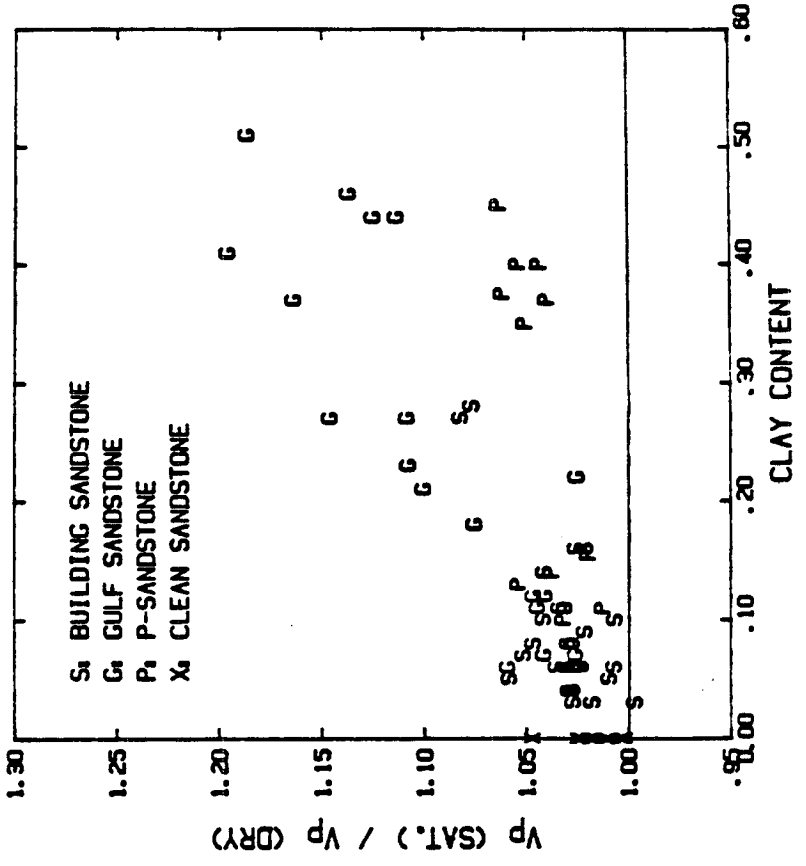
S BUILDING SANDSTONE
G GULF SANDSTONE
P P-SANDSTONE
X CLEAN SANDSTONE
Vp (SAT.) / Vp (DRY)
CLAY CONTENT

Fig. 6b

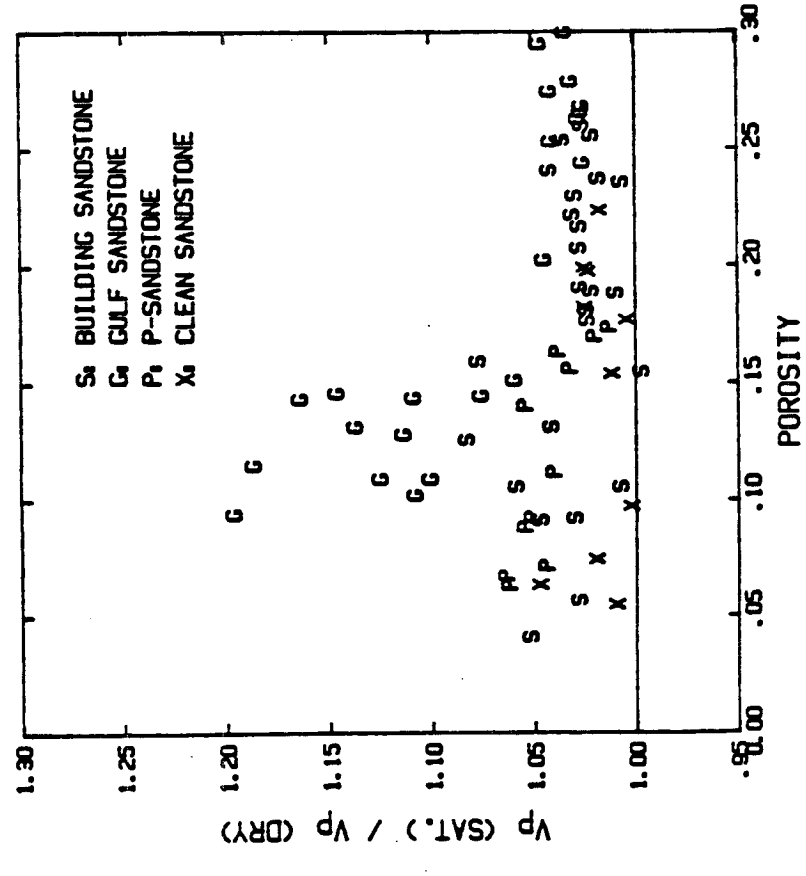
S BUILDING SANDSTONE
G GULF SANDSTONE
P P-SANDSTONE
X CLEAN SANDSTONE
Vp (SAT.) / Vp (DRY)
POROSITY

Fig. 6a

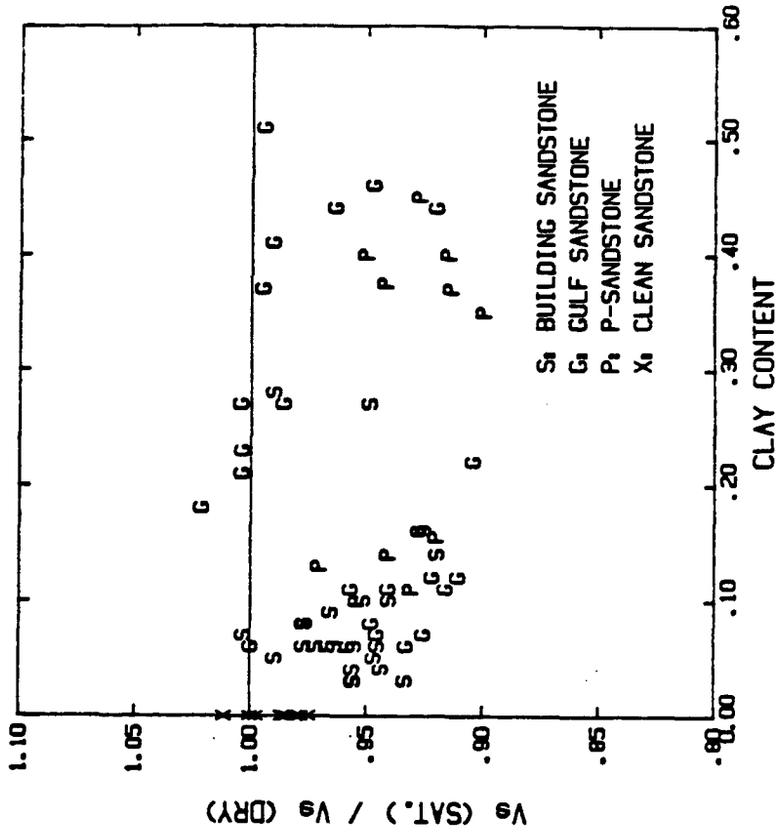
Vs (SAT.) / Vs (DRY)
1.10
1.05
1.00
.95
.90
.85
.80
.00
.10
.20
.30
.40
.50
.60
CLAY CONTENT
S BUILDING SANDSTONE
G GULF SANDSTONE
P P-SANDSTONE
X CLEAN SANDSTONE

Fig. 6d

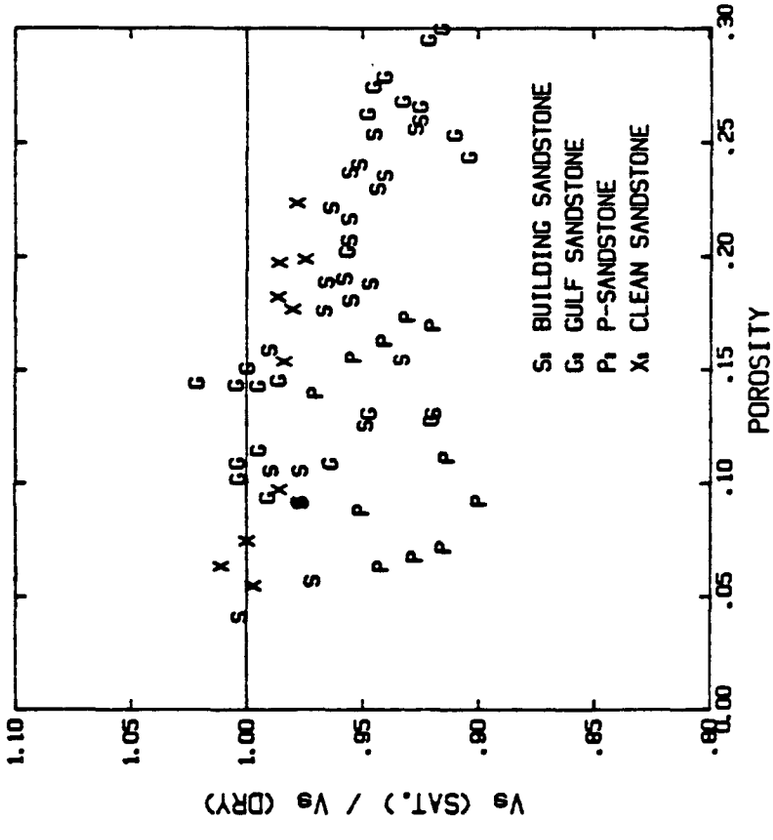
Vs (SAT.) / Vs (DRY)
1.10
1.05
1.00
.95
.90
.85
.80
.00
.05
.10
.15
.20
.25
.30
POROSITY
S BUILDING SANDSTONE
G GULF SANDSTONE
P P-SANDSTONE
X CLEAN SANDSTONE

Fig. 6c

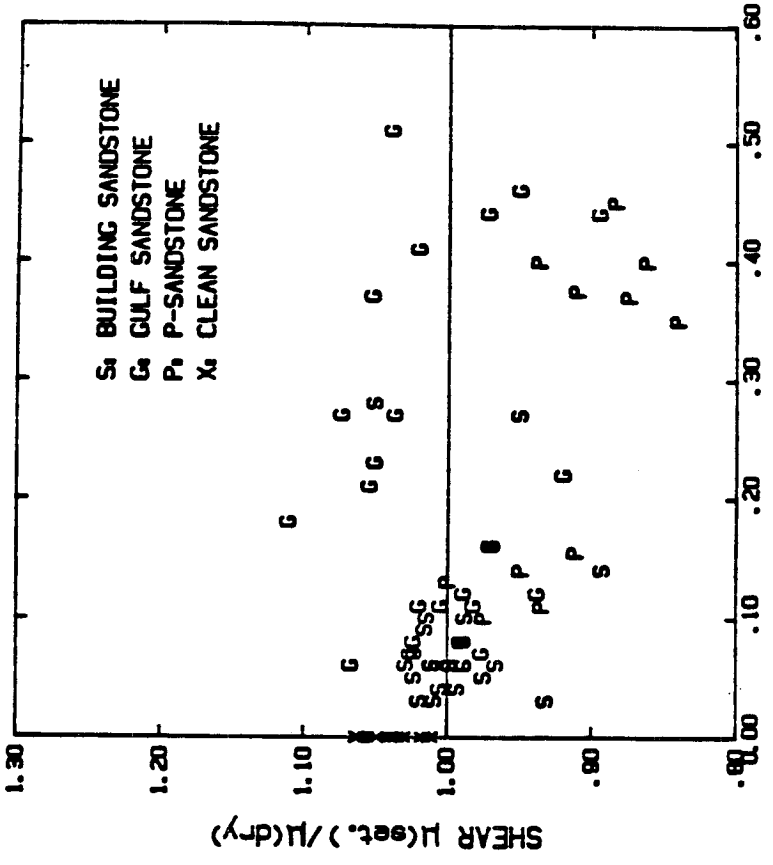
S BUILDING SANDSTONE
G GULF SANDSTONE
P P-SANDSTONE
X CLEAN SANDSTONE
SHEAR μ(wet.)/μ(dry)
CLAY CONTENT
1.30
1.20
1.10
1.00
.90
.00
.10
.20
.30
.40
.50
.60

Fig. 7b

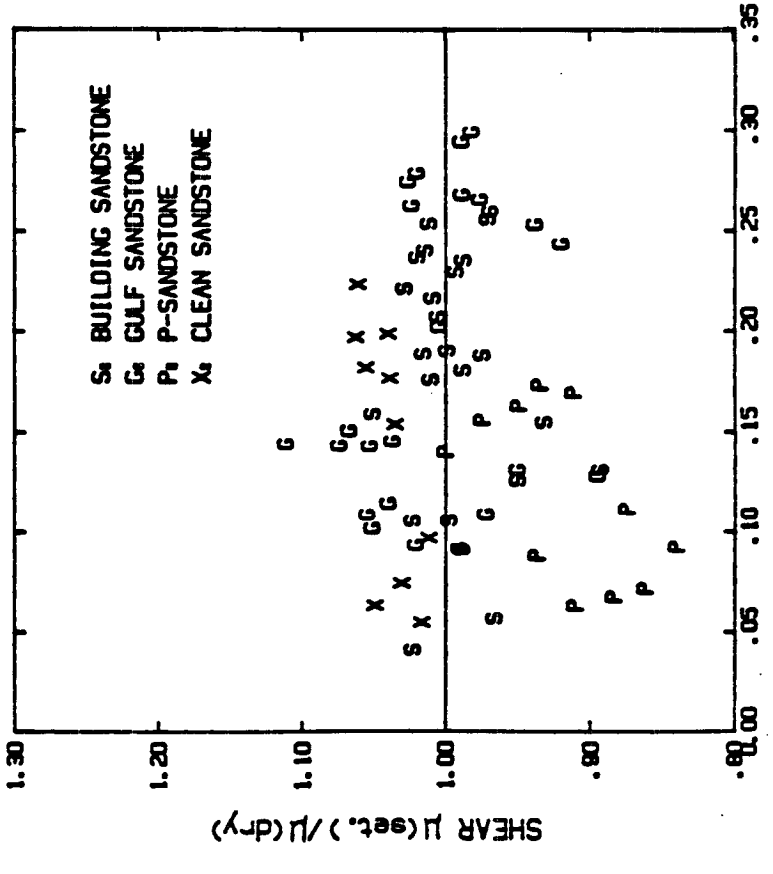
S BUILDING SANDSTONE
G GULF SANDSTONE
P P-SANDSTONE
X CLEAN SANDSTONE
SHEAR μ(wet.)/μ(dry)
POROSITY
1.30
1.20
1.10
1.00
.90
.00
.05
.10
.15
.20
.25
.30
.35

Fig. 7a

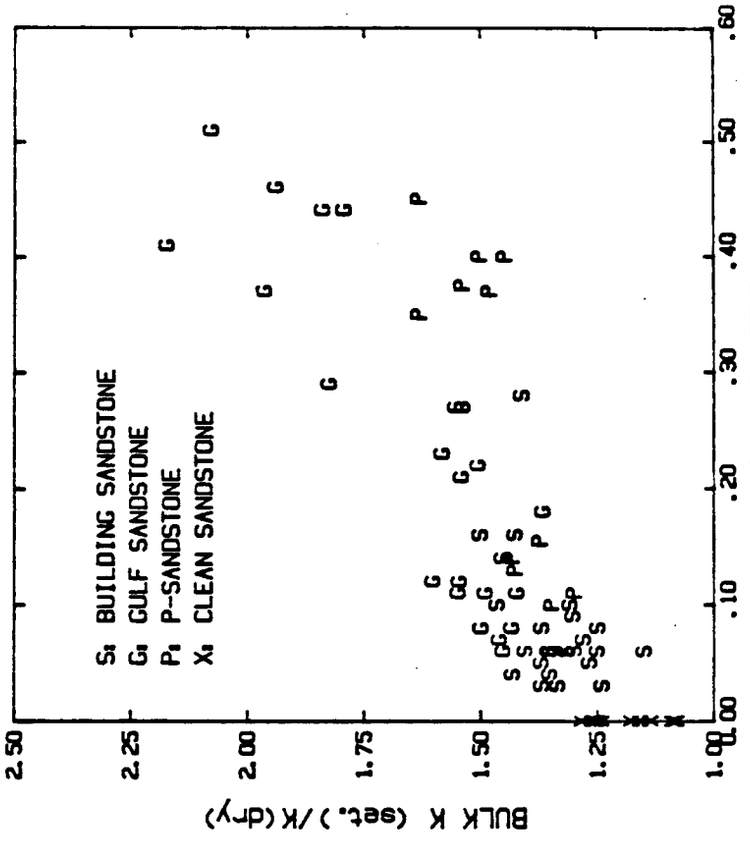
S BUILDING SANDSTONE
G GULF SANDSTONE
P P-SANDSTONE
X CLEAN SANDSTONE
BULK K (sat.)/K(dry)
CLAY CONTENT
2.50
2.25
2.00
1.75
1.50
1.25
1.00
.00
.10
.20
.30
.40
.50
.60

Fig. 8b

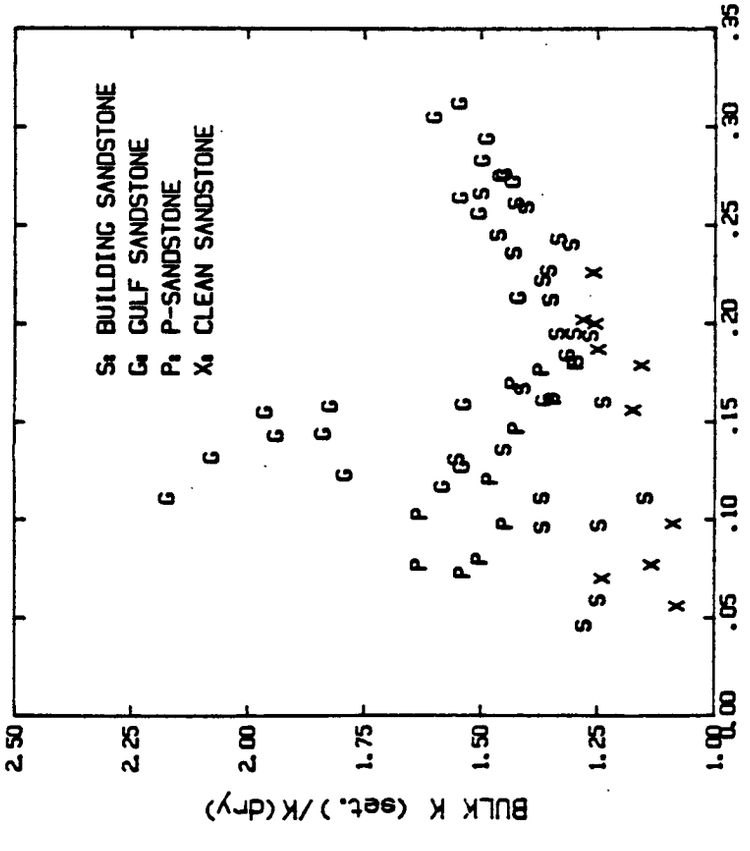
S BUILDING SANDSTONE
G GULF SANDSTONE
P P-SANDSTONE
X CLEAN SANDSTONE
BULK K (sat.)/K(dry)
POROSITY
2.50
2.25
2.00
1.75
1.50
1.25
1.00
.00
.05
.10
.15
.20
.25
.30
.35

Fig. 8a

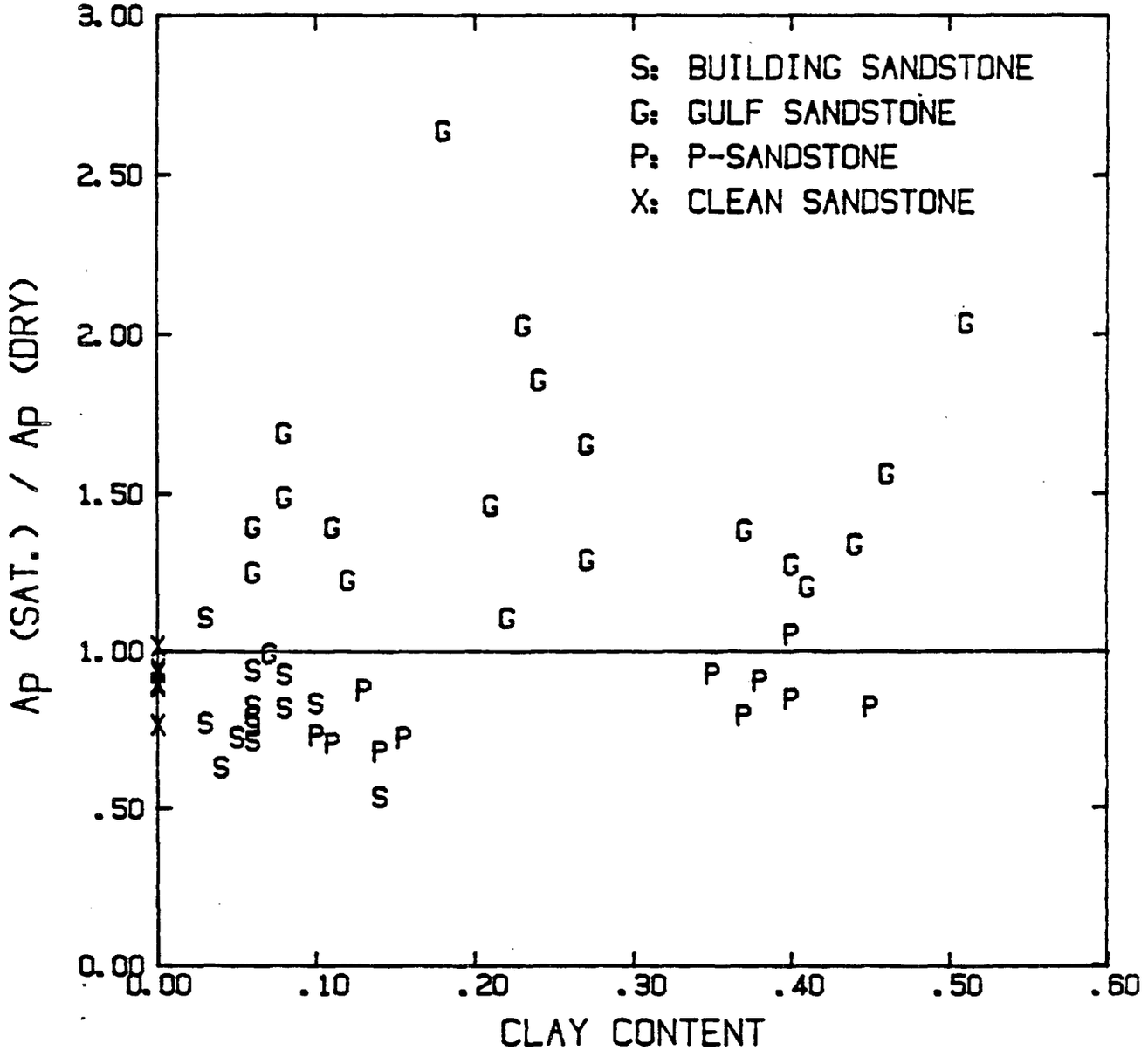
S: BUILDING SANDSTONE
G: GULF SANDSTONE
P: P-SANDSTONE
X: CLEAN SANDSTONE
Ap (SAT.) / Ap (DRY)
CLAY CONTENT
3.00
2.50
2.00
1.50
1.00
.50
0.00
0.00
.10
.20
.30
.40
.50
.60

Fig. 9

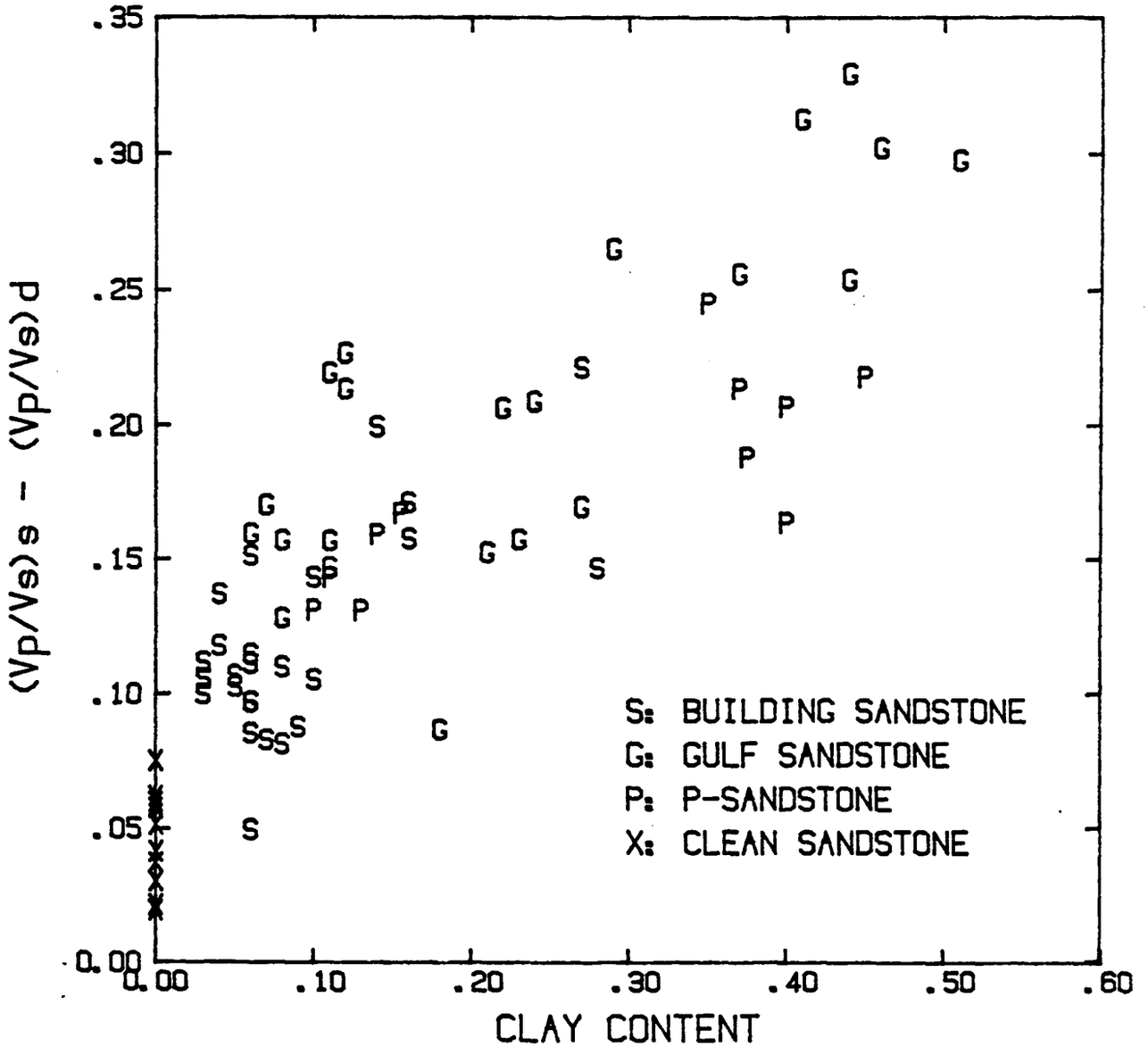
(Vp/Vs)s - (Vp/Vs)d
CLAY CONTENT
.35
.30
.25
.20
.15
.10
.05
0.00
0.00
.10
.20
.30
.40
.50
.60
S: BUILDING SANDSTONE
G: GULF SANDSTONE
P: P-SANDSTONE
X: CLEAN SANDSTONE

Fig. 10

CHAPTER V

VELOCITY DISPERSIONS IN SANDSTONES

ABSTRACT

The ultrasonic compressional (V_p) and shear (V_s) velocities were measured on 69 different sandstone samples, at dried and saturated states under external confining pressure up to 50 MPa and internal pore pressure 1 MPa. Porosities of the samples range from 5 to 30 percent and volume clay content of the samples range from 0 to 50 percent. These velocity data were treated to estimate velocity dispersion on saturated sandstones with frequencies from 1 MHz to 1 Hz using the Biot theory proposed by Winkler (1985). "Biot dispersion" is the percent difference between the high- and the low-frequency limits calculated from the Biot theory. Calculations indicated that for our samples, the Biot dispersions are about 1 or less than 1 percent, which increase with increasing porosities and decrease with increasing clay content. "Apparent dispersion" is the percent difference between the measured ultrasonic velocity and the low-frequency Biot limit. Calculated results indicated that for sandstones, the apparent dispersions at frequency 1 MHz relative to 1 Hz are greater than the Biot dispersions even at differential pressure equal to 39 MPa. This suggest that the non-Biot absorption/dispersion mechanism is present. For well consolidated sandstones, especially clean sandstones, the non-Biot dispersions are minimal so that they can be neglected. Therefore, their behavior is like that of fused glass beads in that apparent dispersions agree well with the predictions of the Biot theory. For less consolidated sandstones, especially shaly sandstones, the apparent dispersions (2 to 9 percent) are much greater than the predictions of the Biot theory, dominated by the non-Biot dispersions. These velocity dispersions appear to increase with decreasing porosity, increasing clay content, and decreasing differential pressure. The effects of porosity, clay content and pressure are suppressed by increasing consolidation. The non-Biot dispersions of sandstones are most likely dominated by the local flow mechanism. It can happen at a wide range of frequency from hundreds of Hz to above MHz depending scales in which the flow could be driven by created pore pressure gradient when waves propagate through there.

Introduction

Velocities of a formation can be obtained by three methods: seismic reflection; sonic logging; and core measurement at ultrasonic frequency. Measured velocity data using different approaches show various features. The frequency ranges for seismic, sonic, and ultrasonic velocities are swept from 10-100 Hz, around 10,000 Hz, to MHz (Figure 1). The resolutions of these velocities are swept from several decade meters, to a meter, to a centimeter. The seismic data can give information of geologic structure with a large scale, while core measurement made under controlled conditions can give data with the best resolution and repetition. Naturally the following questions are raised: What are the effects of the frequencies on velocities ? How are these velocities related to each other ?

The acoustic velocities in fluid-saturated rocks are known to vary with frequency. On basis of the laboratory measurements, some investigators believe that the ultrasonic velocity is higher than the seismic velocity, which is associated with an attenuation peak in kelo Hz range (Spencer, 1981; Murphy, 1982; Jones, 1986). However, the measurements at low frequencies are frequently affected by boundary conditions of the sample (Dunn, 1986). As a results, erroneous conclusions on acoustic attenuation are often reached.

Geophysicists also try to measure directly the velocity dispersion. Velocities measured at logging frequencies (about 10,000 Hz) are slightly higher than those measured at seismic frequencies (10-100 Hz) (Goetz et al., 1979). The ultrasonic velocities measured on shale samples are 10-15 percent higher than data obtained by the sonic logging (Jones et al., 1984). However, the core velocities of carbonate rocks coincide perfectly with the sonic logging data reported by Rafavich, et al., (1984). Contradictory results can even be obtained from the same type of measurement, or even from the same data by different authors (McDonal et al., 1958; Wuenschel, (1965); Ricker, 1953; Kjartansson, 1979). Moreover, the core velocities are much higher (more than 20 percent) than the velocities measured in situ of the San dress fault (Stirman and Kovach, 1979). It suggests that velocity differences may mainly be caused by scale heterogeneity such as macrocracks or faults in seismic or sonic measurement and microcracks in ultrasonic

measurement. A similar conclusion based on analysis of seismic and sonic logging (Moos and Zoback, 1983), and ultrasonic data (Murphy, 1984) was reached. We need to distinguish the intrinsic velocity dispersions from the pseudo-dispersion caused by the scale heterogeneity. These results bring more confusions: Does the velocity dispersion does exist? If yes, how large an influence does it have at the above frequency range? What parameters do dominate it's effect?

Murphy (1984) calculated the intrinsic dispersion of Sierra White granite from dry and water saturated ultrasonic data using the Biot-Gassmann-Domenico relation. Winkler (1985) systematically developed this technique that can give an insight into the intrinsic velocity dispersion at frequencies from seismic to ultrasonic. The only assumption involved in this technique is that velocities in dry rock are independent of frequency, and this assumption is supported by the experiments (Peselnick and Outerbridge, 1961; Spencer, 1981). Using this technique, from dry and saturated velocities of cores measured at ultrasonic frequencies, one can compute the Biot low-frequency limit of velocity (Biot, 1956a, b) for fluid-saturated rocks. Any discrepancy between the velocity measured at ultrasonic frequency and calculated velocity at low frequency, say 1 Hz, may be assumed to be caused by the inherent dispersion.

The velocity dispersion analysis in Berea sandstones reveals that beyond the Biot dispersion, there is a non-Biot dispersion. This extra dispersion is interpreted as being caused by local flow relaxation located somewhere below the measurement frequency (Winkler, 1985). In this study, we present velocity dispersions on 69 sandstone samples. Following the previous work (Han, 1986), we present a new empirical equation for V_p correlated with porosity and clay content at low frequency. The velocity dispersions and the calculated Biot dispersions in sandstones correlated to the porosity, the clay content, the consolidation degree and the external pressure are discussed.

Experimental Procedure

Velocity data used in this study are from 69 sandstone samples. Ten of these samples are clean sandstones (X) including well consolidated Fontainebleau sandstone and poorly consolidated St. Peter sandstone and Beaver sandstone. Fifty-nine samples are shaly sandstones with porosities

ranging from 5 to 30 percent and volume clay content from 2 to 50 percent. Twenty five of them from quarry (S) are well consolidated. Twenty three of them are cores (G) from the Gulf of Mexico; some of them are poorly consolidated. Eleven cores are P-sandstones (P) which are well consolidated.

The experiment technique was described in detail by Han (1986). Compressional (V_p) and shear (V_s) velocities were measured at dry and saturated states. External confining pressure and internal pore fluid (water) pressure are controlled independently. The central frequency of transducers are 1 MHz for V_p and 0.6 MHz for V_s. Error is less than 1 percent for V_p and 2 or 3 percent for V_s.

Each sample was initially dried in a vacuum oven with heat about 50 C for 2-8 weeks. Before making any measurement, each sample was compacted to 50 MPa to minimize hysteresis effects. Measurements were taken during down-loading pressure. Each sample was first measured at a vacuum dried state (lower than 0.01 Torr) then fully saturated with water (some samples with high clay contents were saturated with brine). The pore pressure was kept at 1 MPa. The velocity dispersions were calculated using data from vacuum dried samples and from saturated samples.

Porosities of samples were measured by the porosimeter within 1 percent of bulk volume uncertainty. Porosity of a sample varies with differential pressure. The porosity change can be measured by monitoring volume change of the pore fluid when the internal pore pressure is kept constant. For a dry sample the porosity change with pressure was assumed to be equal to the change measured for the sample saturated with water.

The sample is a core about 5 cm in diameter. Its length and diameter were measured within 0.05 mm. Density of a dry sample ρ_d was calculated from measured weight and volume. Density of matrix material, ρ_m, was calculated by the expression:

$$\rho_m = \frac{\rho_d}{(1-\phi)}.$$

Density of a saturated sample ρ_s was calculated from the ρ_m using the expression:

$$\rho_s = \rho_m (1 - \phi) + \rho_f \phi,$$

where ρ_f is density of the fluid.

Dispersion Calculation

The expressions for the low- and high-frequency limits of the Biot theory can be found in the work by Biot (1956a, b) and related works such as Gassmann (1951), Geertsman and Smit (1961), Stoll (1974), Johnson and Plona (1982), and Winkler (1985). We shall use the nomenclature as follows:

ϕ porosity;

V_{pd} measured P-wave velocity of the dry frame at ultrasonic frequency;

V_p measured P-wave velocity of the saturated frame at ultrasonic frequency;

V_{sd} measured S-wave velocity of the dry frame at ultrasonic frequency;

V_s measured S-wave velocity of the saturated frame at ultrasonic frequency;

V_{pl} P-wave velocity of the saturated frame at 1 Hz;

V_{ph} high-frequency limit of P-wave velocity of the saturated frame;

V_{sl} S-wave velocity of the saturated frame at 1 Hz;

V_{sh} high-frequency limit of S-wave velocity of the saturated frame;

K_m bulk modulus of the matrix material;

K_f bulk modulus of the fluid;

K_d bulk modulus of the dry (or drained) frame at ultrasonic frequency;

K_{dl} bulk modulus of the dry (or drained) frame at 1 Hz;

K bulk modulus of the saturated frame at ultrasonic frequency;

K_{sl} calculated bulk modulus of the saturated frame at 1 Hz;

K_{sh} calculated high frequency limit of bulk modulus of the saturated frame;

μ_d shear modulus of the dry (or drained) frame at ultrasonic frequency;

μ_{dl} shear modulus of the dry (or drained) frame at 1 Hz;

μ shear modulus of the saturated frame;

μ_{sl} calculated shear modulus of the saturated frame at 1 Hz;

μ_{sh} calculated high frequency limit of shear modulus of the saturated frame;

α tortuosity parameter (Johnson et al., 1982).

We assume that dry velocities V_{pd} and V_{sd} measured at ultrasonic frequency are equal to those at 1 Hz. The bulk (K_{dl}) and shear (μ_{dl}) moduli at 1 Hz can be calculated from dry velocity V_{pd} and V_{sd} using the following expressions:

$$K_{dl} = \rho_d (V_{pd}^2 - \frac{4}{3} V_{sd}^2) \tag{1}$$

and

$$\mu_{dl} = \rho_d V_{sd}^2. \tag{2}$$

Therefore,

$$K_{dl} = K_d \quad ; \quad \mu_{dl} = \mu_d .$$

The low-frequency limit of the Biot theory (1956a,b) agrees exactly with Gassmann's relation (Gassmann, 1951) which can be expressed as follows:

$$\frac{K_{sl}}{K_{sl} - K_m} = \frac{K_{dl}}{K_{dl} - K_m} + \frac{K_f}{\phi (K_f - K_m)} \tag{3}$$

and

$$\mu_{sl} = \mu_{dl}. \tag{4}$$

If we know bulk moduli of matrix material (K_m) and saturated fluid (K_f) and bulk (K_{dl}) and shear (μ_{dl}) moduli of a dry frame at low frequency, the bulk (K_{sl}) and shear (μ_{sl}) moduli of the saturated frame can be calculated from Equations (3) and (4). The low-frequency limit of the saturated shear velocity V_{sl} is given by

$$V_{sl}^2 = \mu_{sl}/\rho_s = \mu_{dl}/\rho_s , \tag{5}$$

where

$$\rho_s = (1 - \phi)\rho_m + \phi\rho_f .$$

The low-frequency limit of the saturated compressional velocity V_{pl} is given by

$$V_{pl}^2 = (K_{sl} + \frac{4}{3}\mu_{sl})/\rho_s = (K_{sl} + \frac{4}{3}\mu_d)/\rho_s . \tag{6}$$

The high-frequency limit of the saturated shear velocity V_{sh} is given by

$$V_{sh}^2 = \frac{\mu_d}{(1-\phi)\,\rho_m + (1-(1/\alpha))\,\phi\,\rho_f}. \tag{7}$$

The high-frequency limit of the saturated compressional velocity V_{psh} is given by

$$V_{ph}^2 = \frac{A + (A^2 - 4B\,(PR - Q^2))^{1/2}}{2B} \tag{8}$$

where

$$A = P\,\rho_{22} + R\,\rho_{11} - 2Q\,\rho_{12}$$

$$B = \rho_{11}\rho_{22} - \rho_{12}$$

$$P = \frac{(1-\phi)(1-\phi-(K_d/K_m))K_m + \phi\,(K_m/K_f)K_d}{D} + \frac{4}{3}\mu_d$$

$$R = \phi^2\,K_m/D$$

$$Q = \frac{(1-\phi-(K_d/K_m))\,\phi K_m}{D}$$

$$D = 1-\phi-\frac{K_d}{K_m} + \phi\,\frac{K_m}{K_f}$$

$$\rho_{11} + \rho_{12} = (1-\phi)\,\rho_s$$

$$\rho_{22} + \rho_{12} = \phi\,\rho_f$$

$$\rho_{12} = (1-\alpha)\,\phi\,\rho_f$$

The moduli in the above equations are dynamic moduli. As Winkler (1985) emphasized the moduli at low frequency such as 1 Hz are not relevant to "static moduli" because the former are dominated by the effect of frequency while the latter are affected by strain amplitudes (Cook and Hodgson, 1965; Brennan and Stacey, 1977; Winkler et al., 1979).

The low-frequency limit of Gassmann-Biot relations can be used to calculate effects of pore fluid saturation on elastic moduli, as well as on velocities. The discrepancy between the measured velocity at ultrasonic frequency and the calculated velocity at 1 Hz is the apparent dispersion. The difference between high- and low-frequency limits of the Biot theory is the Biot dispersion. In

this study, the Biot dispersions were first calculated, then the apparent dispersions of bulk moduli and velocities were calculated.

In the calculations of the Biot low-frequency limit, the bulk modulus of a dry sandstone K_d is computed from measured dry velocities and density using equation (3). The bulk modulus of water is equal to 2.2 GPa. The next problem is how to find out the bulk modulus K_m for rock matrixes with different clay contents. They should be reasonably estimated as required by accurate calculation of the velocity dispersion.

For clean sandstones, the empirical relations of porosity and velocity at differential pressure 40 MPa and pore pressure 1 MPa were obtained by previous work (Han, 1986).

$$V_p\,(km/s) = 6.08 - 8.06\phi, \tag{9}$$

and

$$V_s\,(km/s) = 4.06 - 6.28\phi. \tag{10}$$

The velocities for quartz aggregate are obtained by setting ϕ equal to zero.

$$V_{pq} = 6.08\ km/s\ ; \qquad V_{sq} = 4.06\ km/s.$$

These values coincide perfectly with the values $V_p = 6.05$ km/s and $V_s = 4.09$ km/s for quartz grain aggregate given in the CRC book (Robert, 1982). The density of quartz grains is equal to 2.65 gm/cc. The moduli of the quartz grain aggregate calculated from the velocities and the density are:

$$K_m = 40.0\ GPa\ ; \qquad \mu_m = 43.7\ GPa.$$

We assumed these values are correct estimates for the clean sandstones.

For shaly sandstones, the moduli relate to the clay content. Effects of clay content on elastic moduli were hardly estimated. The grain bulk moduli for different sandstones chosen by different investigators often vary abiguously from 32 GPa to above 40 GPa. Here, we give a method to count the clay content effects on the moduli. For shaly sandstones, at differential pressure 40 MPa, and pore pressure 1 MPa velocities can be correlated to porosity and clay content (Han, 1986) as follows:

$$V_p\,(km/s) = 5.59 - 6.93\,\phi - 2.18\,C\,, \tag{11}$$

and

$$V_s\,(km/s) = 3.52 - 4.91\ \phi - 1.89\ C. \tag{12}$$

As setting ϕ and C equal to zero at Equations (11) and (12), the velocities of grain matrix for shaly sandstones are less than that for quartz aggregates. This is because the velocities for shaly sandstones are biased by the bound-clay effects (Han, 1986). Yet, the clay effects shown in Equations (11) and (12) are the matrix clay effects. Therefore, Equations (11) and (12) include both bound and matrix clay effects. The matrix velocity for shaly sandstones can be estimated by empirical equations:

$$V_p\,(km/s) = 5.59 - 2.19\ C, \tag{13}$$

and

$$V_s\,(km/s) = 3.52 - 1.89\ C. \tag{14}$$

The density of a shaly matrix is computed from measured dry density and porosity.

$$\rho_m = \frac{\rho_d}{(1-\phi)}.$$

Thus the bulk modulus of a shaly matrix can be calculated by the expression:

$$K_m = \rho_m\ (V_p^2 - \frac{4}{3}\ V_s^2). \tag{15}$$

Through equations (11) and (12) are empirical ones with 2.1 percent rms error for V_p and 4.3 percent rms error for V_s, they are still valuable to be used to estimate the clay effects (both bound- and matrix-clay effects) on velocities and elastic moduli.

Substituting the bulk moduli of matrix materials K_m, the drained bulk modulus K_d, and the fluid (water) bulk modulus K_f, and porosity into the low-frequency limit of Gassmann-Biot equation (2), the bulk modulus for the saturated sample at 1 Hz can be calculated. Here, the dry bulk modulus was assumed to be equal to "drained" bulk modulus with few percent water saturation used in the Biot theory.

In order to compute saturated velocity V_{pl} at low frequency, effects of water wetting on the shear modulus must be estimated. These effects not only affect study of the dispersion of the shear velocity but of the compressional velocity as well. The Biot theory (equation (2)) assumes that the

shear modulus remains a constant as a sample saturated from dry state. Thus, the shear modulus involved in the expressions of the Biot theory is the dry modulus μ_d. Winkler (1985) calculated the apparent and the Biot dispersions using the dry modulus μ_d without considering effects of water wetting. Under this assumption, the Biot dispersion would be negligibly affected. However, the apparent dispersion may be affected significantly by the above approach because for shaly sandstones, the shear moduli are strongly affected by water wetting. The ratios of the saturated shear moduli to dry ones for 69 samples are shown in Figure 2. This gives an insight into the effects of the water wetting because for the shear modulus, the water saturation effects are similar to the wetting effects (Murphy, 1982). Deviations of data from the Gassmann-Biot equation were assumed to be caused by chemical weakening (Winkler, 1985). This is typically true for consolidated sandstones with clay bearing. The ratios decrease with increasing clay content. However, for poorly consolidated sandstones with high clay content, the frame might be hardened by squeezing clay out of grain boundaries leading to better grain contacts which can suppress the weakening effect and increase shear moduli. These hardening effects are emerged in data for some Gulf sandstones (Figure 2). The matrix configuration of shaly sandstones can be substantially changed by the wetting effects. This occurs in a static process and nothing relates to the dispersion process. Specially, these effects are quite large so that they cannot be neglected as one needs to estimate the "drained" shear modulus. This was discussed in detail in an earlier work (Han, 1986).

The "drained" moduli used in the Biot theory must be chosen to include these "weakening" and "hardening" effects on the moduli. If we choice the dry modulus μ_d as the "drained" shear modulus, these interactions would be ignored. In this case, there is no way can be used to make valuable estimation of the apparent dispersions for these rocks. An alternative way is to estimate "drained" modulus from the water saturated shear velocity. Assuming the shear velocity dispersion is equal to the Biot dispersion calculated from high- and low-frequency limits of the Biot theory, we derived the "drained" shear modulus from measured V_s at the saturated sample

$$\mu_d' = ((1-\phi)\,\rho_m + (1-1/\alpha)\,\phi\,\rho_f\,)\,V_s^2. \tag{16}$$

Therefore, the calculated μ_d' on that the wetting effect is included. Given this assumption, the low- and high-frequency limit of the compressional velocities as well as the apparent dispersion can be estimated though there are still some ambiguities. Here, the real Biot dispersion may be less than the limit of the Biot dispersion. The non-Biot dispersion, which perhaps existed in the dispersion of the shear velocity, is totally ignored. Again, there is no way can be used to judge the apparent dispersion of the shear velocity. For the purpose of comparison, both "drained" shear modulus μ_d' and dried shear modulus μ_d were used to calculate dispersions.

The Biot dispersion can be calculated from the high- and low-frequency limits of the Biot theory (equations 1-8). The only parameter that has not been measured for our samples is the tortuosity α used in the calculation of the Biot high-frequency limit. This is a dimensionless parameter and depends on the pore geometry. For the parallel tube, the tortuosity α is equal to 1. For our samples, we assume the tortuosity α equal to 2, which is larger than 1.8 for a fused glass bead as measured by Johnson et al. (1982). This value may be too small for low permeability samples. However, it did not bring any significant influence to the calculations that will be discussed later.

Results

Measured porosities, clay contents, and velocities at ultrasonic frequencies, and computed velocities at 1 Hz under conditions of confining pressure 40 MPa (high) and 10 MPa (low) with pore pressure 1 MPa for 69 sandstone samples are tabulated in Table. The Biot velocity dispersions in the Table are percent differences between the Biot high- and low-frequency limits referenced to the measured V_p at ultrasonic frequency. The apparent velocity dispersions are percent differences between the measured V_p at ultrasonic frequency and the Biot low-frequency limit referenced to the measured V_p. Comparison of the apparent dispersions with the Biot dispersions would reveal whether there is non-Biot dispersion in sandstones and how it correlates to properties of sandstones.

Biot Dispersions

The calculated the Biot dispersion of V_p in percent versus porosity for 69 sandstones at confining pressure 40 MPa and pore pressure 1 MPa are presented in Figure 3a and Table 1. The calculated results show interesting features. For most samples, the Biot dispersions are quite small, less than 1 percent. Clean sandstones have the highest Biot dispersion compared to shaly samples with the same porosities. The Biot dispersions of the clean sandstones exhibit a linear increase with increasing porosity. When porosity increases from 5 percent to 22 percent, the dispersion increases from 0.3 percent to 1.3 percent. These values are maximum for the Biot dispersion of the sandstones at the given pressure conditions.

For shaly sandstones, the Biot dispersions also tend to decrease with increasing porosity. Scatters of the dispersions show that other parameters may play a moderate role. The plot of the Biot dispersions versus clay content reveals that clays in sandstones can significantly suppress the Biot dispersion (Figure 3b). When the clay content is above 20 percent, the Biot dispersion is less than 0.3 percent, and there is no Biot dispersion as the clay content goes above 40 percent.

Our calculations also show that at low differential pressure (9 MPa) the Biot dispersions are slightly less than those at high pressure (39 MPa), which is consistent with Winkler's results. It would be expected that the pressure effects are emphasized at a low pressure and in a less consolidated sample.

The Biot absorption/dispersion mechanism involves relative movement between viscous fluid and solid. If fluid is locked to the frame whatever the frequencies are, the Biot loss and dispersion will be eliminated. The above correlations suggest that the Biot dispersion may be dominated by the permeability. This is because a decrease in porosity and an increase in clay content in sandstones as well as an increase of the external pressure can significantly decrease the Biot dispersion, as well as the permeability.

Apparent Dispersions

Calculated apparent dispersions of bulk modulus versus the porosity and clay content for 69

water saturated samples at differential pressure 39 MPa are shown in Figure 4 a and b. The data exhibit a wide range from 1 percent to above 20 percent. Corresponding dispersions of velocities V_p (shown in Figure 5 a and b) are less than the modulus dispersions but still ranging from 1 to about 10 percent. The apparent dispersions have a much larger range than that of the Biot dispersions. The data strongly suggest the non-Biot absorption/dispersion mechanism in the sandstones corresponding to the apparent dispersions beyond the predicted by the Biot theory (Winkler, 1985). Moreover, the dispersions with a wide range of distribution should correlate to the different properties of the sandstones. Close investigation of data for each group of samples is required to find the correlations of the dispersion to properties of sandstones.

Dispersion of Clean Sandstones

The matrix of a clean sandstone is composed of pure quartz aggregate which is the simplest configuration for a sandstone frame. To study the dispersion of clean sandstones it is convenient to reveal the correlations to intrinsic properties of sandstones.

The dispersions of bulk moduli of clean sandstones are shown in Figure 6a. At confining pressure 40 MPa and pore pressure 1 MPa, the bulk moduli at 1 Hz computed from the Gassmann-Biot equations are less than the bulk moduli at the ultrasonic frequency. For most of them, the dispersions are quite small (less than 5 percent). As the differential pressure decreases, for example, at P_c equal to 10 MPa and P_p 1 MPa, the dispersions of bulk moduli usually increase.

The Fontainbleau E has a minimum dispersion (about 1.7 percent), and no pressure dependence of dispersion. This can be explained by the best consolidation of this sample. The velocity of this sample is almost independent of pressure shown in Figure 7a. Water saturation has a minimum effect on the V_p leading to the minimum dispersion. The slopes of velocity V_p as functions of pressure for the sample at dry and saturated states are similar, resulting in the dispersion of no pressure dependence.

For the Fontainbleau C sample, water saturation has a larger effect on increasing velocity

than that of the Font. E, and the slope of dry velocity and its change with pressure is also higher than that of the Font. E (Figure 7b). These suggest that the Font. C may be less consolidated and may have more pores with low aspect ratios. Thus, its dispersion (4.8 percent) is higher than that of the Font. E, and depends heavily on the differential pressure. For other Fontainbleau sandstones, the dispersions of bulk moduli are around 2-5 percent at the high pressure and 6-13 percent at the low pressure.

The St. Peter sandstone is poorly consolidated. Two samples of this sandstone show about 8 percent dispersions at the high pressure, 13 and 17 percent dispersion at the low pressure. For the Beaver sandstone, the dispersions of the bulk moduli are about 10 percent at the high pressure and 17 percent at the low pressure. The velocities as functions of pressure for St. Peter A and Beaver show in Figures 7c and 7d. Both figures display large water saturation effects on increasing velocities V_p. For St. Peter A, the slope of dry velocity V_p decreases rapidly as pressure increases, showing an easy compaction at low pressure for poor cement sandstones. Visually, the Beaver sandstone has better consolidation than the St. Peter sandstone. The slope of dry velocity V_p of the Beaver decreases slowly as differential pressure increases. The higher resistant of compaction for the Beaver sandstone may be caused by its better cement. The higher dispersion might be caused by the low porosity with more pores having smaller sizes and sharp corners.

SEM photomicrographes reveal different features of these sandstones. The Font. C and E (Figures 8a and 8b) show well developed quartz overgrowth cements. However, it is hard to tell how the strengthes of cements and pore shapes differ between these two samples. The St. Peter A has poor cements and strong quarts dissolution (Figure 8c). Thus, St. Peter is easily compacted at low pressure. The Beaver shows fair quartz overgrowth, as well as dissolution surfaces of quartz grains (Figure 8d). The small grains tend to fill in pore spaces between much larger grains, making more pores with smaller sizes and sharp corners.

The apparent dispersions of velocity V_p are shown in Figure 6b. As previously mentioned, in order to include the wetting effect, the shear modulus is calculated from the water saturated

shear velocity (equation (16)) which is assumed to be equal to the high-frequency limit of the Biot theory. For clean sandstones, the calculated shear moduli almost coincide (less than 1 percent difference) with the shear moduli calculated from dry shear velocities. Therefore, the apparent dispersions (shown in Table 1) and the Biot dispersions calculated upon these two shear moduli also coincide perfectly. These results strongly suggest that for clean sandstones, there are no water wetting effects on the shear modulus and only the Biot dispersion exists for the shear velocity dispersion. The measured saturated shear velocity at high frequency (0.6 MHz) is equal to the prediction of the Biot high-frequency limit. The only exception is the Beaver sandstone that has a deviation of about 2 percent between these two shear moduli.

The apparent dispersions of the compressional velocity (V_p) calculated for clean sandstones are from 1 to 3 percent, much smaller than the bulk modulus dispersions. This is not surprising because V_p is a square root of moduli, and the dispersion of the V_p is mainly caused by the dispersion of the bulk modulus. For Fontainbleau sandstones, discrepancies between the apparent and Biot dispersions are about 1 or less than 1 percent. At least, one can say that for these sandstones, the non-Biot dispersions are very small, and for well consolidated ones, they can be neglected. For poorly consolidated clean sandstones, such as the St. Peter sandstone, the apparent dispersions are larger than the Biot dispersions. The non-Biot dispersions in these rocks with water saturation may not be neglected, however; in comparison with shaly sandstones (shown later), the dispersions are still small.

Finally, it can be concluded that the well consolidated sandstones are pretty much like Fused glass beads, the apparent dispersions of which are quite consistent with the predicted Biot dispersions (Winkler, 1985). Because the Biot dispersion is very small (about 1 or less than 1 percent), therefore, for clean sandstones, velocity (V_p) dispersions at confining pressure 40 MPa and pore pressure 1 MPa can be neglected at frequency ranging from 1 Hz to 1 MHz. For less consolidated clean sandstones, apparent dispersions increase and depend on the degree of consolidation or compaction and pore geometry.

Dispersion of Shaly Sandstones with Poor Consolidation

Gulf sandstone samples are well-cores most of which are poorly consolidated with higher clay content (above 10 percent). The dispersions of the bulk moduli vs. porosity at confining pressure 40 MPa and pore pressure 1 MPa are shown in Figure 9a. The results suggest that the porosity is an important parameter correlated to the dispersion. The sandstones with high porosity –above 0.20– have a small dispersion. The Gulf 10431 and 10432 have porosities of 0.299 and 0.295 respectively and are poorly consolidated. They have the lowest dispersions of bulk moduli–0.04. These results imply that at differential pressure 39 MPa, the poorly cemented sandstones can be well compacted. For samples with porosity of less than 0.15, the dispersion of bulk moduli are greater than 0.15. However, it is hard to say whether the dispersion is caused by the porosity alone. The dispersions for most Gulf sandstones are much higher than those for clean sandstones. It is reasonable to correlate clay content with these dispersions (Figure 9b). Though there are scatters of data, it is easy to recognize that the dispersions increase roughly with increasing clay content. The clay effects on the dispersion of bulk moduli may relate to weaken the cement, soften the sandstone frame and form pores with low aspect ratios.

The apparent dispersions of compressional velocity V_p are much less than the dispersions of bulk moduli (Figures 9 c and d). They distribute from 0.03 for samples with high porosities and up to about 0.08 for samples with low porosities and high clay contents. These values are much higher than those of clean sandstones and cannot be neglected. The results roughly agree with the observation by Jones et al. (1984). They found that for shale formation, velocity measured on core at ultrasonic frequency is 10-15 percent higher than the velocity obtained from logging data. In our case, the Gulf samples are not shales. The matrix of Gulf sandstones is formed by sand grains much larger than clay particles. Maybe, this is one reason for the clay effects of sandstones on the dispersion being smaller than that of shales.

Finally, for Gulf sandstones, the dispersions increase with decreasing pressure, shown in the Table. This suggests that the pressure dependences in dispersions are dominated by their poor cementation.

In comparison with the Biot dispersions, the apparent dispersions are much greater. This implies that the non-Biot absorption/dispersion mechanism dominates the apparent dispersions of Gulf sandstones. The most interest thing is that porosity and clay content have opposite effects on the Biot and on the apparent dispersions. This implies that effects of porosity and clay content on the non-Biot dispersion are even greater than those on the apparent dispersions. A similar feature was shown by Winkler (1985): the peaks of the Biot and non-Biot dissipations move in opposite directions with increasing viscousity of pore fluid. These results indicate that properties of the non-Biot mechanism are entirely different from those of the Biot mechanism.

For Gulf sandstones, the dispersions are correlated with the porosity and the clay content. For high porosity samples, the dispersions are small. For low porosity samples, high dispersions of bulk moduli are clearly caused by the clay effects.

Dispersions of Shaly Sandstones with Good Consolidation

Sandstones from quarries are fairly well consolidated. Samples with high porosities (above 18 percent) usually show low dispersions (Figure 10a). A sample with high clay contents such as Santa Barbara (27 percent clay content) shows higher dispersions (Figure 10 b). Dispersions for these sandstones usually increase with decreasing differential pressure (Table 1). However, the increases are not as large as those for the Gulf sandstones, because these sandstones are well consolidated.

The Boise sandstone with porosity 0.254 has 10 percent dispersion of bulk modulus. This dispersion is fairly independent of differential pressure (Table 1). The Boise sandstone is a well cemented rock. Under pressure, the pore shapes do not change much, thus the pressure dependence of the dispersion is small. The dispersion for the Boise is fairly high (10 percent). This may be caused by the fact that the Boise has more pores with low aspect ratio, keeping open at high pressure.

The Indiana light, Coconino and Berea 500 sandstones show very small dispersions. The calculated dispersion for the Indiana light even shows a negative value but it is very small, only 1

percent. Perhaps, it is caused by errors of estimating parameters used in the calculation. The small dispersions may be explained by the good consolidation and the fact that only stiff pores remain open in these rocks at high pressure.

The P-sandstones are consolidated well-cores. Clay in these samples is mainly kaolinite that are well consolidated with carbonate and sand grains. The more clay it has, the stronger the frame is. This is a contradiction to the clay effect on Gulf sandstones. Thus, for the P-sandstones with high clay content the dispersions are about 12 to 17 percent at the high pressure (Figure 10 b), but they have no pressure dependences. For the P-samples with less clay content, the dispersions are similar to the former but have much high pressure dependences because they are less consolidated. Dispersions of bulk moduli do not show a clear correlation with porosity or clay content.

The apparent dispersions of velocities V_p for these sandstones range from 1 to 6 percent (Figure 10 c and d). These values are higher or much higher than the Biot dispersions. The decrease in disperson is roughly correlated to increased consolidation. For most samples, including all the P-samples, the dispersions are higher than those for the clean sandstones but less than those for the Gulf sandstones with high clay contents. A sandstone with a high clay content shows a higher dispersion (above 4 percent). For sandstones with clay content of less than 15 percent, the dispersions are less than 4 percent and do not show clear correlation to the porosity and clay content. A reasonable explanation is that consolidation of these samples suppresses the effects of the porosity and clay content. Again, this result confirms that the porosity and clay content are only phenomenologically related to the dispersion but not parameters which directly dominate dispersions of sandstones. However, the consolidation and compaction show strong effects on the dispersion, especially on the pressure dependence of dispersion.

In summary, the non-Biot velocity dispersions for a total of 69 saturated samples at differential pressure 39 MPa versus porosity and clay content are shown in Figures 11 a and 11 b, respectively. The calculated bulk modulus at 1 Hz versus the bulk modulus at ultrasonic frequency are shown in Figure 12 a. Similarly, calculated V_{p1} at 1 Hz versus the measured

velocity V_p at ultrasonic frequency are shown in Figure 12 b.

Correlation of Velocity V_p at 1 Hz to Porosity and Clay Content

For all 69 samples, the calculated velocities V_{p1} at 1 Hz versus porosities are shown in Figure 13. Clean sandstones show much higher velocities than shaly sandstones. This is caused by small amounts of bound clay effects (Han, 1986). With the emphasis on clay effects, we separate velocity data of shaly sandstones from those of clean sandstones. Upon 59 shaly sandstone data, velocity V_p can correlated linearly to porosity and clay content. At confining pressure 40 MPa and pore pressure 1 MPa, by least squares regression the best fit result is:

$$V_{p1}\ (km/s) = 5.45 - 6.78\ \phi - 2.44\ C.$$

The correlation coefficient is 0.976, and relative rms error is 0.023. From earlier work (Han, 1986), upon 70 velocity data (including data from 59 of the above samples) at ultrasonic frequency the correlation of velocity V_p to porosity and clay content is:

$$V_p\ (km/s) = 5.59 - 6.93\phi - 2.18C\,,$$

with correlation coefficient 0.985 and relative rms error 0.021. Comparing of these two equations, one can say that the influences of velocity dispersion are small. However, several features still can be traced. Decrease of the constant is caused by the velocity at low frequency always being less than measured velocity at ultrasonic frequency. The changes of coefficients of the porosity and the clay content correspond roughly to opposite effects of them on the dispersions. Samples with high porosity usually have smaller dispersions, while samples with high clay content usually have large dispersions, therefore, the clay effects are more emphasized at low frequency.

For shear velocity, the dispersion is assumed to be caused by the Biot dispersion only. This is consistent with the observations of well consolidated clean sandstones. The correlation of shear velocity to porosity and clay content obtained at ultrasonic frequency (Han, 1986) is:

$$V_s\ (km/s) = 3.52 - 4.91\ \phi - 1.89\ C.$$

On basis of the above assumption, the correlation at 1 Hz is slightly different.

$$V_{s1}\ (km/s) = 3.54 - 5.24\ \phi - 1.92\ C.$$

Discussion

From analysis of the velocity dispersions of glass bead and Berea sandstone at brine and oil saturated states, Winkler (1985) derived the following conclusions. In brine-saturated Berea sandstone, significantly more dispersion is observed at low pressures than predicted by Biot theory. At higher pressures the observed dispersion is in close agreement with Biot predictions. These results suggest that the "non-Biot" absorption/dispersion mechanism is present that is inhibited by increasing pressure. He also makes an argument to prove this mechanism is most likely the local flow mechanism that has a range of at least five to six decades in frequency (1000 Hz to 100 MHz) in brine saturated Berea sandstone. Our results are not only a approval of Winkler's results, but they also give correlations of the Biot and non-Biot dispersion to properties of sandstones.

The frequencies we used are about 1 MHz for V_p and 0.6 MHz for V_s. The wave lengthes are at least 5 times greater than sand grain size, thus the scattering is assumed to have a minimum effect on the velocity dispersion.

The apparent dispersion is caused by the Biot and non-Biot dispersion. The Biot mechanism involves viscous interaction between pore fluid and frame. At low frequencies the viscous skin depth is much larger than the pore size. The pore fluid locked to the frame is dragged along with it. Maximum attenuation occurs at a resonant frequency when the skin depth is comparable to the pore size. At higher frequencies the viscous skin depth is very small, and inertia of the pore fluid caused it to lag behind the motion of the frame leading to higher velocity. The calculated Biot dispersion is the difference between the high- and low-frequency limits of velocities, that gives a maximum of the Biot dispersion. This value decreases slightly with decreasing differential pressure.

The real Biot dispersion depends on the frequency used in measurements. If the frequency is much higher than that of the peak of the Biot dissipation, the real Biot dispersion is equal to its maximum limit, otherwise the real Biot dispersion is less than the maximum. We do not exactly know where to locate our measurement relative to the Biot critical frequency for the samples with

water saturation. For well consolidated sandstones with water saturations, the shear velocities are consistent with the Biot dispersions. The compressional velocities are slightly higher than the Biot high-frequency limit. The differences are quite small (less than 1 percent), so that they can be neglected. Therefore, for these sandstones, our measurements are at the high-frequency limit of the Biot dissipation region. For shaly sandstones with high clay content, since their permeabilities are much less than those of the clean ones, the peak of the Biot loss shifts to a higher frequency. Thus, our measurement may be below the Biot critical frequency. The calculated Biot dispersions for these samples may overestimate the real Biot dispersions. However, this does not bring any problem to our analysis because the maximum Biot dispersions for these rocks are much smaller than the non-Biot dispersions.

Our results show that for well consolidated sandstones, the apparent dispersions at high pressure (39 MPa) are approximately in agreement with the predicted Biot dispersions, which is consistent with observations by Winkler (1985). However, for less consolidated sandstones, the apparent dispersions are higher or much higher than the Biot dispersions, especially for a sandstone with small porosity or high clay content. This strongly suggests that even at high pressure, the non-Biot absorption/dispersion mechanism is present in water saturated sandstones.

Many other mechanisms such as a thermoelastic mechanism (Kjartansson and Nur, 1979), a surface mechanism (Tittmann et al., 1980; Spencer, 1981) were proposed to explain the non-Biot absorption/dispersion of rocks under different conditions. Many discussions were made of mechanisms of observed attenuations (Murphy, 1982; Jones, 1983). The "local flow" was chosen as a major non-Biot absorption/dispersion mechanism to explain observation in sandstones (Winkler and Nur, 1979, Murphy, 1982, 1984; Jones and Nur, 1983; Winkler, 1985). This mechanism has been discussed in literature using different models (O'Connell and Budiansky, 1977; O'Connell, 1984; Mavko and Nur, 1979; Palmer and Traviolia, 1980; Murphy et al., 1984). These models are extremely dependent upon details of the microstructure of the rock. The essential features of the models are strain heterogeneity leading to pore fluid pressure heterogeneity. For example, for crack-like cylindrical pores (pore aspect ratio c/a - 0), the pore

pressure is similar to externally applied pressure. For circular cylindrical pores ($c/a = 1$), the fluid pressure is much less than the external pressure as shown in Figure 14 (after O'Connell, 1984). At low frequency, there will be sufficient time for the fluid flow to occur and pressure gradient to relax. At high frequency there will not be enough time for the flow to occur and rock will be in an unrelaxed state. Maximum attenuation will occur at intermediate frequency at which viscous interaction between fluid and solid will be a maximum. This model was used to explain data of attenuation and modulus dispersion at frequency in KHz range (O'Connell, 1984).

This model indicates that the dispersion related causally to the dissipation. The maximum dispersion of velocity (difference between "unrelaxed" and "relaxed" velocity) increases with increasing maximum attenuation. In addition, if the frequency used in velocity measurement is in the energy dissipation range the dispersion of velocity (called "partial relaxed" velocity) increases with increasing frequency.

In the above model, only the pore geometry was emphasized. The contact relaxation model (Murphy, et al. 1984) is also a geometry model in which micro-gaps between grain contact can drive the fluid flow. Our dispersion data, however, strongly suggest that the dissipation of local flow are also dominated by consolidation or grain contacts. This is because the magnitude of strain heterogeneity depends not only on pore geometry, but also on the elastic moduli of the matrix.

For well consolidated sandstones, the strong quartz cement and high contact area of grain can significantly reduce the magnitude of strain as well as strain heterogeneity. Thus, only a minimum of local pore pressure gradient can be created. Therefore, the dispersion of local flow can be neglected. In addition, as the elastic moduli are less dependent on external pressure, the dispersions are also less dependent on it. For the above situation, the pore shape is less important. This may be because there are only stiff pores in the well consolidated sandstones.

Poorly consolidated sandstones may be well compacted and reach good contacts between grains at high pressure. Therefore, they could have high elastic moduli and low dissipation/dispersion peaks similar to well consolidated sandstones.

For less consolidated sandstones, which may have less cement, soft cement material or less contact area, the magnitude of strain increases, as does the local pore pressure gradient. In this case, the pore geometry may be emphasized in the effects on the local flow dissipation. Data suggest that for less consolidated sandstones, the non-Biot dispersions exhibit clear correlation with porosity and clay content. As porosity decreases the dispersions increase. This may relate to pore shape change with increasing porosity. For a sample with low porosity, its pore shapes are more like cracks. The cracks usually cause strong local flow. As clay content increases the dispersions also increase. Increased clays often changes elastic moduli and forms flake-shape pores causing more strain heterogeneity.

In addition, as previously mentioned, the magnitude of dispersion is not only dependent upon the magnitude of maximum dissipation, but also dependent on the wave frequency. The local flow relaxation may extend from approximately 1000 Hz to 100 MHz in brine-saturated Berea sandstone (Winkler, 1985). The wave frequency we used may still locate in the dissipation range. For the samples with lower porosity or high clay content, their permeability are lower than Berea sandstone that is used by Winkler (1985), therefore, the frequency range of dissipation for these rocks moves to low frequency. Thus, measurements made on these samples are at relatively high frequency side of the dissipation, which results in high dispersions. Evidence was given by amplitude measurement (Han, 1986) that the peak amplitude of the first arrival increases with decreasing porosity and slightly increases with increasing clay content. Therefore, a sample with low porosity and high clay content show less attenuation. In addition, our measured dispersion for the Berea sandstone is slightly higher than Winkler's result (1985). It may be caused by the fact that our measurements are made at a dissipation region which may extend to much higher frequency and our frequency (1 MHz) is slightly higher than his frequency (400 KHz).

For some samples, such as P-sandstone, an increase in clay content makes the sample more consolidated. Thus the dispersions show a complicated situation. As the clay content increases, the dispersion slightly decreases but the magnitude of the dissipation still higher than other well consolidated sandstones.

Moreover, as differential pressure decreases, in general, the non-Biot dispersions increase. A well consolidated or compacted sample usually shows less pressure dependence. However, the magnitude of the dispersion is not necessarily to be small. This suggests that the behaviors of the dispersion and its pressure dependence may be dominated by different mechanisms. The former is a dynamic process, while the latter is static one. They have different relations to the degree of consolidation and to pore geometries.

Complex results and a wide range of scatters shown in the data indicate the complexity of the relation of the non-Biot dispersions to properties of sandstones. This suggests that elastic properties of sandstones cannot be modeled simply by the pore geometry models or contact models, or even by their combinations suggested by Yale (1985). The model must also take into account the effects of consolidation and compaction. Here, we present a simple sketch (Figure 15) to show how combinations of local cement, contact and pore geometry and their pressure dependence can change the magnitude of strain in sandstones. For real sandstones, every parameter may have a wide contribution to the structure of the frame depending on the history of the diagenesis. Therefore, the dispersions of sandstones present of a complicated picture.

The frequency of relaxation by local flow was extended to a much higher frequency than 1 MHz we used (Winkler, 1985). The frame and pore pressure gradient can be relaxed at frequencies higher than 1 MHz. This may be caused by strain heterogeneity in a pore. At a sharp corner, the strain is higher than that of round corner caused by the stress concentration. Therefore, the fluid at a sharp corner can be squeezed out of and sucked back into it producing a flow or vibration. The mechanism of this hydrodynamic relaxation is similar to the contact model delineated by Murphy et al. (1984). This mechanism can work at frequencies much high than 1 MHz. Because the extent of the flow or the vibration in a pore is dependent on the pore sizes which are usually much smaller than the wave length in water at 1 MHz, the fluid has enough time to relax. Usually, a sandstone has a wide range of pore structures. The local flow may occur at different scales even less than 0.1 mm, depending very much on the pore structures. Therefore, the relaxation of the local flow can occur at a broad band of frequencies.

It is interesting that, in comparison with the non-Biot dispersion, the Biot dispersions have an opposite relation to properties of sandstones. The Biot dispersion increases with increasing porosity, consolidation and external pressure, and decreases with increasing clay content. This may be because the maximum Biot dispersion comes from inertial coupling between homogeneous porous media with specified tortuosity and liquid, while the local flow is dominated by the different scale of the heterogeneity of pore structures.

Several points need to be made. First, the tortuosity was assumed equal to 2 for all samples. For a sample with low permeability, this value may be underestimated. However, the effect of increasing the tortuosity is to decrease the predicted velocity in high-frequency limits of the Biot theory. Thus, the Biot dispersion also decreases. Again, the non-Biot dispersions from the calculated Biot dispersions may slightly be underestimated. However, its influence is quite small because the total Biot dispersions are very small.

Second, our data show that the effects of water saturation on the shear modulus for sandstones depend on the clay content and consolidation (Han, 1986). These effects are caused mainly by the water wetting grain cement. The wetting effects including "soften" and "harden" effects are very complicated and much larger than earlier reported in the literature (Born and Owen, 1935; Wyllie et al., 1962; Gregory, 1976; Clark et al., 1980). Therefore, these effects cannot be neglected when using the shear modulus to calculate the low- or high-frequency limit of compressional velocity. In order to estimate the water wetting effect on the shear modulus the shear velocity at ultrasonic frequency was assumed equal to the high-frequency limit of the Biot theory. The non-Biot dispersion of shear velocity was assumed to be neglected, because the shear strain is not crucial to the flow relaxation. This assumption is in excellent agreement with data for well consolidated clean sandstones. For other sandstones, there are two possible sources of error. First, the measurements may be not made at the Biot high-frequency limit. This may happen for a sample with low porosity or high clay content. However, the maximum Biot dispersion is very small thus its influence can be neglected. Second, there is the non-Biot dispersion for shear velocity. If this is true, the calculated shear modulus may be overestimated

leading to an underestimate of the dispersion of compressional velocity. Therefore, the conclusions arrived at earlier will be reinforced.

In the calculation of low-Biot limit, the modulus of matrix materials was estimated from the empirical relation (equations 13 and 14). These values may be overestimated for less consolidated sandstones and underestimated for well consolidated sandstones. The calculation show that this only brings very small uncertainty to the results. The effects of consolidation are suppressed by the uncertainty, therefore, real consolidation effects are enhanced.

Conclusion

From our measurements and calculations for sandstones, several conclusions can be drawn. They are valid for water saturated sandstones at frequencies ranging from 1 Hz to 1 MHz for V_p and to 0.6 MHz for V_s.

1. For well consolidated sandstones, especially clean ones, the velocity dispersions are quite small (1 or 2 percent). Clean sandstones have the highest Biot dispersion (about 1 or less than 1 percent) corresponding to shaly sandstones with the same porosities. Shear velocities of the clean sandstones measured at ultrasonic frequency are consistent with the high-frequency limits V_s of the Biot theory. Though there are non-Biot dispersions of compressional velocities, they can be neglected. At high pressure the observed dispersion can be considered to be in good agreement with the Biot predictions. The non-Biot dispersion will increase as the degree of consolidation decreases. These results imply that for well consolidated clean sandstones the ultrasonic measurements are on the high frequency side of the Biot theory, and no local flow exists, which is consistent with the observation for fused glass bead (Winkler, 1985).

2. Poorly consolidated sandstones may be well compacted leading to solid grain contacts at high differential pressure. Their dispersions are similar to or a little larger than those for well consolidated sandstones. The higher apparent dispersions are caused by increased of the non-Biot dispersions.

3. For less consolidated sandstones, the apparent dispersions show clear correlation with porosity

and clay content. The Biot dispersions increase with increasing porosity, and decrease with increasing clay content. In comparison with the non-Biot dispersions, the Biot dispersions are too small so that the apparent dispersions can be considered as caused by the non-Biot dispersion alone. In contrast, the non-Biot dispersions decrease with increasing porosities, and increase with increasing clay contents. However, effects of porosity and clay content emerged clearly only as they reached higher values. They are suppressed by increasing degree of consolidation. This strongly suggests that the porosity and clay content may be phenomenologically correlated with the dispersions but they are not primary parameters to determine dispersion in sandstones. The dispersions for the less consolidated sandstones range from 2 to 8 percent which cannot be ignored in shaly sandstones.

4. The dispersion also depends on differential pressure. The Biot dispersion decreases slightly as differential pressure P_d drops from 39 MPa to 9 MPa. For well consolidated sandstones, the non-Biot dispersion is independent of or less dependent on differential pressure because good consolidation confers high resistance to change in pore geometry with increasing pressure. For less consolidated or poorly contacted sandstones, the non-Biot dispersion decreases with increasing differential pressure because an increase of the solid contacts and the stiffness of pores will lead to a decrease of local strain and pore pressure heterogeneity.

5. Our results suggest that the non-Biot dispersion is most likely the local flow mechanism. The essential features of all local flow models is to create strain and pore pressure heterogeneity. The strength of the local flow not only depends on pore structures but also depends on elastic moduli of rock matrix. The former relates to pore shape, size and orientation. The latter relates to cement, cement material, type of contact and external pressure. The energy dissipation of local flow is determined by the combinations of these factors and wave frequency.

At low frequency the flow may happen between cracks in different orientations or between cracks and round pores. In addition, the flow may happen in a pore where the fluid can squeezed out of and sucked back into a sharp corner. This is because the sharp corner has higher strain than the other part of the pore. Relaxation by the fluid vibration in pores can extend to high

frequency, which may be helpful in understanding the non-Biot dissipation with broad band of frequency.

6. The dispersions of velocities relate causally to the dissipations. The magnitude of the dispersion depends on the magnitude of the maximum dissipation and the wave frequency used in velocity measurement relative to the frequency range of the dissipation. If the frequency of measurement is in the dissipation range the measured velocity is "partial relaxed" velocity and lower than "unrelaxed" velocity. Therefore, the "partial relaxed" velocity increases with increasing frequency.

Our results show that for well consolidated sandstones, the small dispersions are caused by small energy dissipations. The frequency (1 MHz) we used may be less than "unrelaxed frequency". However, the effect of the wave frequency on dispersion is very small. For less consolidated sandstones, the maximum dissipations as well as the maximum dispersions increase. For sandstones with low porosity or high clay content, the high dispersions may be caused not only by high dissipation but also by the wave frequency. The amplitude measurements show (Han, 1986) that the attenuations decrease with decreasing porosity, and decrease slightly with increasing clay content. The high dispersions accompanying with low dissipations suggest that the frequency of dissipation may move somewhat to low frequency. Thus, the velocities are measured relatively at high frequencies nearly equal to "unrelaxed" velocities.

The local flow mechanism has not been sufficiently developed theoretically so that quantitative comparison can be made to experimental results. Here, we only try to give one possible explanation for our dispersion results.

7. Following an earlier work (Han, 1986), the effects of porosity and clay content on velocities at seismic frequency can be formulated. The velocity V_p can be linearly correlated to porosity and clay content in terms of the least squares regression method.

$$V_{p1}\,(km/s) = 5.45 - 6.78\,\phi - 2.44\,C.$$

and

$$V_{s1}\,(km/s) = 3.54 - 5.24\,\phi - 1.92\,C.$$

A decrease of the coefficient of porosity and an increase of the coefficient of clay content correspond to their effects on the apparent dispersions.

8. Our results suggest that the velocity measurement made at ultrasonic frequency is valuable to estimate seismic velocity and dispersions using the Biot-Gassmann equations.

REFERENCES

Biot, M. A., 1956, Theory of propagation of elastic waves in a fluid-saturated porous solid,

I. Low frequency range: J. Acoust. Soc. Am. 28, 168-178.

II. High frequency range: J. Acoust. Soc. Am. 28, 179-191.

Born, W. T., and J. E. Owen, 1935: Effect of moisture upon velocity of elastic waves in Amherst sandstone: Am. Assoc. Pet. Geol. Bull., 19, 9-18.

Brennan B. J., and F. D. Stacey, 1977, Frequency dependence of elasticity of rock-test of seismic velocity dispersion: Nature, 268, 220-222.

Clark, V. A., B. R. Tittmann and T. W. Spencer, 1980, Effect of volatiles on attenuation (Q^{-1}) and velocity in sedimentary rocks, J. Geophys. Res., 85, 5190-5198. Cook, N. H., and K. Hodgson, 1965, Some detailed stress-strain curves for rock: J geophys. Res., 70, 2883-2888.

Gassmann, F., 1951, Elastic waves through a packing of spheres: Geophysics, 16, 673-685.

Goetz, J. F., L. Dupal and J. Bowler, 1979, An investigation into the discrepancies between sonic logging and seismic check shot velocities: APEAJ., 19, 131-141.

Gregory, A. R., 1976, Fluid saturation effects on dynamic elastic properties of sedimentary rocks: Geophysics, 41, 895-921.

Han D., 1986, Effects of porosity and clay content on wave velocities of sandstones: in this volume Chapter II. Main body of this Chapter was published with coauthor Nur, A., and Morgan, F. D. in name, Effects of porosity and clay content on wave velocities of sandstones: Geophysics, 51, Nov., and in name, Velocity measurement and empirical modeling in sandstones: the Log Analyst.

Jones, T., and A. Nur, 1983, Velocity and attenuation in sandstones at elevated temperature and pressure: Geophys. Res. Lett., 10, 141-143.

Jones, T., 1982, Wave propagation in porous rock and models for crystal structure: Ph.D Dissertation, Stanford University.

Jones, L. E. A. and H. F. Wang, 1982 Ultrasonic velocities in Cretaceous shales from the Williston basin: Geophysics, 46, 288-297.

Johnson, D. L., and T. J. Plona, 1982, Acoustic slow waves and the consolidation transition: J. Acoust. Soc. Am., 72, 556-565.

Johnson, D. L., and T. J. Plona, C. Scala, F. Pasierb, and H. Kojima, 1982, Tortuosity and acoustic slow waves: Phys. Rev, Lett., 49, 1840-1844.

Keh-jim Dunn, 1986, Acoustic attenuation in fluid-saturated porous cylinders at low frequencies: J. Acoust. Soc. Am., 79, 1709-1721.

Kjartansson, E., 1979, Constant Q-wave propagation and attenuation: J. Geophys. Res., 84, 4737-4748.

Kjartansson, E., and A. Nur, 1979, Attenuation due to thermal relaxation in porous rocks: in Ph.D dissertation, 55-88, Stanford university.

McDonal, F. J., F. A. Angona, R.L. Mills, R.L. Sengbush, R.G. Van Nostrand and J.E. White, 1958, Attenuation of shear and compressional waves in pierre shale: Geophysics, 23, 421-439.

Moos, D., and M. D. Zoback, 1983, In situ studies of velocity in fractured crystalline rocks: J. Geophys. Res., 88, 2345-2458.

Murphy, W. F., 1982, Effects of microstructure and pore fluids on the acoustic properties of granular sedimentary materials: Ph.D dissertation, Stanford University.

Murphy, W. F., 1982, Effects of partial water saturation on attenuation in Massilon sandstone and Vycor porous glass: J. Acoust. Soc. Am., 71, 1458-1468.

Murphy, W. F., 1984, Seismic to Ultrasonic velocity drift: Intrinsic absorption and dispersion in crystalline rock: Geophys. Res. Let., 11, 1239-1242.

Murphy, W. F., K.W. Winkler, and R. L. Kleinberg, 1984, Contact microphysics and viscos relaxation in sandstones: in Physics and Chemistry of Porous Media, edited by D.L. Johnson and P.N. Sen, American Institute of Physics, New york, 176-190.

Murphy, W. F., 1984, Acoustic measures of partial gas saturation in tight sandstones: J. Geophys. Res. 89, 11549-11559.

Stierman D. J. and R.L. Kovach, 1979, An in situ velocity study: The stone Canyon well: J.

Geophys. Res., 84, 672-678.

Kowallis, B., Jones, L. E. A., and Wang, H. F., 1984, Velocity-porosity-clay content; systematics of poorly consolidated sandstones: J. Geophys. Res., 89, 10355-10364.

O'Connell, R. J., 1984, A viscoelastic model of anelasticity of fluid saturated porous rocks: in Physics and Chemistry of Porous Media, edited by D.L. Johnson and P.N. Sen, American Institute of Physics, New York, 166-175.

O'Connell, R. J., and B. Budanisky, 1977, Viscoelastic properties of fluid-saturated cracked solids: J. Geophys. Res. 82, 5719-5775.

Peselnick, L., and W. F. Outerbridge, 1961, Internal friction in shear and shear modulus of Solenhofen limestone over frequency range of 10^7 cycle per second: J. geophys. Res., 84, 581-588.

Rafavich, F., C. H. St. C. Kendall, and T. P. Todd, 1984, The relationship between acoustic properties and petrographic character of carbonate rocks: Geophysics, 49, 1622-1636.

Ricker, N., 1953, The form and laws of propagation of seismic wavelets: Geophysics, 18, 10-40.

Robert, S. C., 1982, Handbook of physics properties of rocks.

Spencer, J. W., 1981, Stress relaxations at low frequencies in fluid-saturated rocks: attenuation and modulus dispersion, J. Geophys. Res. 86, 1803-1812.

Tittmann, B. R., Clark, V. A., Richadson, J.M., and Spencer, T.W., 1980, Possible mechanism for seismic attenuation in rocks containing small amounts of volatiles: J. Geophys. Res., 85, 5199-5208.

Winkler, K. W. and A. Nur, 1979, Pore fluid and seismic attenuation in rocks: Geophys. Res. Lett., 6, 1-4.

Winkler, K. W., A. Nur and M. Gladwin, 1979, Friction and seismic attenuation in rocks: Nature, 277, 528-531.

Winkler, K. W., 1985, Dispersion analysis of velocity and attenuation in Berea sandstone: J. Geophys. Res., 90, 6793-6800.

White, J. E., 1983, Q of fluid-saturated rods: Trans. Am. Geophys. Un. 64, 268.

Wuenschel, P. C., 1965, Dispertive body wave - an experimental study: Geophysics, 30, 539-551.

Wyllie, M. R. J., G. H. F. Gardner, and A. R. Gregory, Studies of elastic wave attenuation in porous media: Geophysics, 27, 569-589.

Yale, D. P., 1985, Recent advances in rock physics: Geophysics, 50, 2480-2491.

TABLE CAPTION

Table. Tabulation of velocity data and dispersions for 69 sandstone samples.

ϕ is porosity at given pressure.

C is clay content

V_p is saturated compressional velocity at ultrasonic frequency.

V_s is saturated shear velocity at ultrasonic frequency.

V_{pd} is dry compressional velocity at ultrasonic frequency.

V_{sd} is dry shear velocity at ultrasonic frequency.

V_{pl} is saturated compressional velocity at 1 Hz calculated from water saturated shear modulus with consideration of the water wetting effect (see texture).

V_{pl}' is saturated compressional velocity at 1 Hz calculated from dry shear modulus without correction of the water wetting effect.

K is measured saturated bulk modulus at ultrasonic frequency.

K_{sl} is saturated bulk modulus at 1 Hz.

ΔV_{pb} is the relative Biot dispersion of compressional velocity.

ΔV_{pa} is the relative apparent dispersion of compressional velocity.

ΔK_a is the relative apparent dispertion of bulk modulus.

FIGURE CAPTIONS

Figure 1. Spectrum of geoacoustic waves.

Figure 2. The ratios of water saturated shear moduli to dry ones versus clay content at confining pressure 40 MPa and pore pressure 1 MPa for 69 sandstone samples.

Figure 3. The calculated Biot dispersions of V_p at confining pressure 40 MPa and pore pressure 1 MPa for 69 samples,

(a) relative to porosities. The Biot dispersion of clean sandstones increase with increasing porosity and larger than that of shaly sandstones with the same porosity.

(b) relative to clay content. The Biot dispersions decrease with increasing clay content.

Figure 4. The apparent dispersions of bulk moduli versus (a) porosity (b) clay content at confining pressure 40 MPa and pore pressure 1 MPa for 69 sandstone samples.

Figure 5. The apparent dispersions of compressional velocity V_p versus (a) porosity (b) clay content at confining pressure 40 MPa and pore pressure 1 MPa for 69 sandstone samples.

Figure 6. The dispersion of (a) bulk moduli (b) compressional velocity versus porosity at confining pressure 40 MPa and pore pressure 1 MPa for clean sandstones.

Figure 7. The velocities as functions of pressure for:

(a) Font. E shows independence of velocity V_p confining pressure and small water saturation effects.

(b) Font. C shows pressure dependence of velocity V_p.

(c). St. Peter exhibits rapid increase of V_p at low pressure and stability at high pressure.

(d) Beaver displays a mild changes of slop of velocity as function of pressure.

Figure 8. SEM photomicrographes for:

(a). Font. E and (b) font. C show well quartz cement and consolidation.

(c). St. Peter shows a poor cement and strong quartz dissolution in grain surfaces leading to easy compaction.

(d). Beaver exhibits better cement and tendency of small grains filled into pore spaces.

Figure 9. The dispersions of 23 Gulf sandstones:

The dispersions of (a) bulk moduli and (b) compressional velocities versus porosities showing lower dispersion for sandstones with higher porosities.

The dispersions of (a) bulk moduli and (b) compressional velocity versus clay content showing increases with increasing clay content.

Figure 10. The dispersions of quarry and P-sandstones:

The dispersions of (a) bulk moduli (c) compressional velocity versus porosities showing lower dispersion for sandstones with higher porosities.

The dispersions of (b) bulk moduli (d) compressional velocity versus clay content.

Figure 11. The non-Biot dispersions of velocity V_p versus (a) porosity and (b) clay contents at confining pressure 40 MPa and pore pressure 1 MPa for 69 sandstone samples.

Figure 12.

(a) the calculated bulk moduli at 1 Hz versus bulk moduli computed from measured velocities at ultrasonic frequency at confining pressure 40 MPa and pore pressure 1 MPa.

(b) the calculated velocity V_p at 1 Hz versus velocity measured at ultrasonic frequency at confining pressure 40 MPa and pore pressure 1 MPa.

Figure 13. The calculated velocity V_p at 1 Hz versus porosity at confining pressure 40 MPa and pore pressure 1 MPa for 69 sandstone samples.

Figure 14. Strain and pore pressure change with pore aspect ratios as elastic wave propagates in saturated porous media (after O'Connell, 1984).

Figure 15. Local strain magnitudes are dependent on different combinations of (1) degree of cementing, (2) cement material, (3) angle near contact (pore shapes) (4) porosity, (5) grain contact area, (6) compaction, and their pressure dependences.

SAMPLE NAME	CLAY	40 MPa												10 MPa		
		Vp	Vs	Φ	Vpd	Vsd	Vpl	Vpl'	K	Ksl	ΔVpb%	ΔVpa%	ΔKa%	ΔVpb%	ΔVpa%	ΔKa%
FONT A	0.00	4.81	3.10	.1539	4.75	3.15	4.73	4.72	24.6	23.8	.84	1.6	3.1	.81	2.4	6.5
FONT B	0.00	4.46	2.85	.1973	4.36	2.89	4.36	4.34	21.0	20.1	1.13	2.3	4.2	.85	4.4	13.2
FONT C	0.00	5.42	3.55	.0746	5.32	3.55	5.34	5.32	31.8	30.3	.47	1.5	4.8	.39	1.9	6.4
FONT D	0.00	5.74	3.77	.0550	5.68	3.78	5.66	5.66	35.6	34.0	.40	1.3	4.3	.32	1.7	6.2
FONT E	0.00	5.34	3.51	.0973	5.33	3.56	5.29	5.30	30.0	29.5	.66	1.0	1.7	.61	.9	1.3
FONT G	0.00	4.68	2.96	.1769	4.66	3.02	4.60	4.60	24.0	23.4	1.16	1.7	2.6	1.01	2.4	5.8
FONT H	0.00	4.34	2.70	.2235	4.26	2.76	4.22	4.21	20.7	19.5	1.31	2.7	5.5	1.21	2.9	6.6
PETERA	0.00	4.66	2.91	.1821	4.55	2.95	4.52	4.50	24.3	22.3	1.09	3.1	8.2	.87	2.4	13.3
PETERC	0.00	4.42	2.72	.1989	4.31	2.79	4.28	4.28	22.2	20.5	1.22	3.1	7.4	.83	5.6	16.6
BEAVER	0.00	5.52	3.60	.0636	5.27	3.56	5.37	5.31	33.4	29.9	.30	2.8	10.4	.16	4.4	17.2
IDLIGHT	.10	3.68	2.22	.2355	3.65	2.36	3.64	3.69	15.6	15.8	.93	1.0	-1.2	.73	.7	-2.2
IDDARK	.16	3.36	1.99	.2597	3.27	2.15	3.28	3.36	14.4	14.0	.64	2.1	2.8	.39	1.9	2.0
IDLIGHT1	.10	3.69	2.17	.2403	3.54	2.28	3.58	3.61	16.7	15.4	.94	3.1	8.1	.58	3.7	10.7
REDSTONE	.28	3.82	2.07	.1589	3.54	2.09	3.65	3.64	21.0	18.7	.49	4.3	11.2	.29	3.4	8.5
COCONINO	.06	4.73	3.00	.1056	4.69	3.07	4.68	4.72	25.5	25.2	.49	.9	1.1	.38	2.6	8.2
CONATTON	.04	3.92	2.35	.2297	3.81	2.49	3.78	3.83	17.9	16.3	1.05	3.7	8.7	.77	4.7	12.3
DETANBUF	.03	4.60	2.81	.1546	4.61	3.01	4.46	4.58	25.3	23.2	.82	3.0	8.3	.74	3.5	10.2
DELBROWN	.05	4.73	2.89	.1056	4.47	2.92	4.54	4.54	27.8	24.1	.46	4.1	13.3	.23	5.5	18.0
BOISE	.06	3.74	2.08	.2536	3.61	2.20	3.58	3.62	17.9	16.2	1.16	4.3	9.8	.97	4.6	11.1
DLITGRY	.07	5.20	3.17	.0412	4.94	3.16	5.02	5.00	35.1	30.2	.16	3.4	14.0	.05	4.2	16.8
SANTABAR	.27	4.06	2.24	.1256	3.75	2.36	3.82	3.89	23.7	19.6	.31	6.0	17.3	.10	6.9	19.9
MASDARK1	.06	4.30	2.57	.1807	4.20	2.69	4.15	4.20	22.9	20.6	.88	3.7	10.0	.66	4.8	13.9
INDDARK1	.16	3.54	2.05	.2557	3.46	2.21	3.45	3.52	15.8	14.8	.89	2.4	5.8	.68	2.5	6.0

SAMPLE NAME	CLAY	40 MPa												10 MPa		
		Vp	Vs	φ	Vpd	Vsd	Vpl	Vpl'	K	Ksl	ΔVpb%	ΔVpa%	ΔKa%	ΔVpb%	ΔVpa%	ΔKa%
UTAHBUFF	.06	4.94	3.12	.0569	4.80	3.21	4.86	4.92	28.4	27.1	.16	1.5	4.8	.13	1.8	6.1
TORY-AV	.14	4.23	2.41	.1309	4.06	2.62	4.02	4.15	25.0	21.3	.40	5.0	14.7	.19	5.6	16.4
MASSDARK	.06	4.32	2.62	.1761	4.22	2.71	4.19	4.22	22.4	20.6	.88	3.1	8.3	.60	5.1	15.2
MASSILIA	.04	4.03	2.40	.2072	3.92	2.51	3.90	3.94	19.6	18.1	.98	3.2	7.4	.53	4.9	13.4
UNH1	.05	4.18	2.50	.1880	4.14	2.64	4.07	4.14	21.4	20.2	.97	2.7	5.8	.69	3.3	8.0
NUGGETV	.08	4.69	2.94	.0912	4.48	3.01	4.56	4.60	27.0	24.4	.28	2.9	9.7	.17	4.1	14.0
NUGGETH	.08	4.88	3.05	.0920	4.74	3.12	4.74	4.78	29.6	26.8	.40	2.9	9.5	.31	3.4	11.5
MASSBURG	.03	3.89	2.37	.2369	3.82	2.48	3.80	3.83	17.4	16.7	1.04	2.3	3.7	.84	2.5	4.4
BEREA1	.06	4.15	2.51	.1903	4.04	2.62	4.02	4.07	20.6	19.1	.94	3.2	7.7	.56	4.6	13.2
BEREA4	.03	3.95	2.39	.2165	3.84	2.50	3.84	3.87	18.2	17.2	.95	2.7	5.4	.73	3.1	7.2
BEREA35	.06	4.03	2.40	.2213	3.91	2.49	3.89	3.91	19.6	17.9	.97	3.5	8.7	.83	4.1	10.5
BEREA5	.09	4.08	2.54	.1887	3.99	2.63	4.01	4.04	18.6	18.2	.74	1.7	2.4	.56	2.9	6.8
P61-5561	.38	4.37	2.62	.0634	4.11	2.78	4.21	4.33	25.4	22.3	.07	3.7	12.1	.05	3.7	11.9
P63-6249	.40	4.24	2.49	.0719	4.06	2.72	4.08	4.25	24.9	21.8	.05	3.8	12.2	.06	3.7	11.7
P63-6254	.37	4.08	2.34	.1118	3.92	2.56	3.89	4.04	23.3	20.1	.26	4.6	13.9	.14	5.1	15.5
P64-6256	.40	4.24	2.52	.0885	4.02	2.65	4.08	4.16	24.0	21.1	.10	3.8	12.2	.10	4.1	13.0
P64-6258	.35	4.17	2.43	.0927	3.97	2.70	3.96	4.16	24.3	20.5	.20	5.1	15.9	.07	4.7	14.6
P64-6260	.45	4.32	2.57	.0677	4.06	2.77	4.11	4.27	25.4	21.3	.15	4.9	16.0	.04	4.6	14.8
P64-6264	.13	4.47	2.64	.1402	4.24	2.72	4.25	4.28	26.3	21.8	.61	5.0	17.1	.21	7.6	25.8
P72-7154	.14	4.32	2.55	.1632	4.16	2.71	4.10	4.19	24.2	20.4	.68	5.2	15.5	.37	7.7	23.9
P74-8797	.10	4.24	2.51	.1560	4.11	2.63	4.09	4.16	22.9	20.6	.66	3.6	10.0	.30	6.3	18.8
P82-7377	.11	4.23	2.43	.1735	4.17	2.61	4.06	4.16	23.7	21.2	.78	3.9	10.6	.47	6.5	18.4
P82-7379	.16	4.19	2.42	.1696	4.11	2.63	4.00	4.13	23.3	20.3	.74	4.6	12.9	.41	6.2	17.9

SAMPLE NAME	CLAY	40 MPa												10 MPa		
		Vp	Vs	φ	Vpd	Vsd	Vpl	Vpl'	K	Ksl	ΔVpb%	ΔVpa%	ΔKa%	ΔVpb%	ΔVpa%	ΔKa%
G-10379	.44	3.71	1.97	.1278	3.33	2.14	3.45	3.56	20.6	16.7	.12	7.0	19.2	.02	8.4	22.8
G-10381	.46	3.63	1.99	.1310	3.19	2.10	3.42	3.48	18.7	15.6	.09	5.9	16.6	.02	6.0	16.8
G-10392	.51	3.68	2.01	.1146	3.10	2.02	3.44	3.43	19.6	15.9	-.03	6.5	18.7	0.00	6.1	17.2
G-10431	.11	3.20	1.75	.2993	3.09	1.91	3.10	3.16	12.6	12.2	.90	3.2	3.9	.48	4.6	8.6
G-10432	.12	3.17	1.77	.2945	3.03	1.92	3.08	3.14	12.4	11.9	.84	2.9	4.0	.50	2.7	3.6
G-12409B	.27	4.00	2.16	.1454	3.49	2.19	3.65	3.66	23.1	17.4	.30	8.7	24.5	.07	10.2	28.2
G-12415	.22	3.36	1.89	.2435	3.27	2.09	3.27	3.37	14.2	13.7	.61	2.5	3.9	.25	4.2	9.1
G-12416	.12	3.55	1.94	.2531	3.41	2.13	3.37	3.46	16.6	14.7	.94	5.1	11.9	.32	6.6	16.5
G-12418	.37	3.76	2.11	.1430	3.23	2.12	3.51	3.49	19.8	15.9	.14	6.7	19.6	.01	9.3	26.7
G-12425	.44	3.84	2.15	.1089	3.41	2.23	3.62	3.66	21.3	17.8	.17	5.7	16.3	.03	5.7	16.5
G-10452	.41	3.97	2.19	.0937	3.32	2.21	3.67	3.67	23.2	18.0	-.05	7.6	22.7	0.00	8.8	25.8
G-12660H	.27	3.98	2.19	.1434	3.59	2.18	3.75	3.71	22.5	18.8	.37	6.0	16.4	.16	7.7	21.2
G-12670	.08	3.67	2.20	.2625	3.57	2.32	3.56	3.60	15.2	14.5	1.11	2.9	5.0	.76	3.5	7.1
G-12674	.06	3.61	2.09	.2679	3.52	2.24	3.48	3.54	16.2	15.0	1.08	3.7	7.6	.61	4.8	11.3
G-12676	.11	3.56	2.07	.2785	3.45	2.20	3.42	3.47	14.8	13.7	1.21	3.9	7.4	.69	4.4	9.4
G-12677	.07	3.50	1.99	.2655	3.41	2.15	3.39	3.45	15.1	14.3	.99	3.2	5.6	.41	3.6	7.1
G-12677B	.07	3.59	2.09	.2742	3.44	2.21	3.44	3.48	14.9	13.8	1.03	3.9	7.3	.52	5.2	11.5
G-14807	.11	3.88	2.23	.2021	3.71	2.33	3.73	3.76	19.2	17.4	.77	3.9	9.5	.28	5.7	15.1
G-15845	.21	4.25	2.48	.1089	3.86	2.47	4.04	4.01	24.3	20.8	.30	4.9	14.6	.03	7.8	23.5
G-15879	.06	4.61	2.73	.1508	4.35	2.73	4.38	4.34	27.1	23.0	.77	5.1	15.3	.34	8.1	24.3
G-158**	.23	4.42	2.61	.1021	3.99	2.60	4.17	4.14	25.8	21.2	.29	5.7	18.0	.05	8.5	26.2
G-15930	.24	4.60	2.77	.0586	3.65	2.51	4.31	4.09	28.8	22.5	.02	6.4	21.7	0.00	7.3	24.2
G-15949	.18	4.07	2.37	.1442	3.78	2.32	3.94	3.87	21.5	19.8	.46	3.2	8.0	.18	6.8	19.8

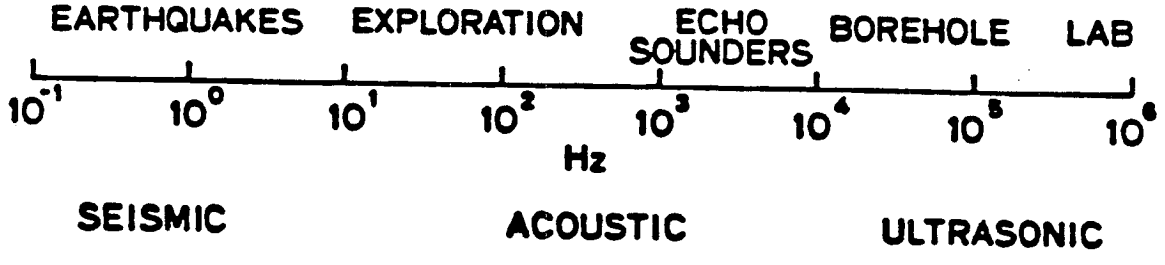
EARTHQUAKES
EXPLORATION
ECHO SOUNDERS
BOREHOLE
LAB
10^{-1}
10^{0}
10^{1}
10^{2}
10^{3}
10^{4}
10^{5}
10^{6}
Hz
SEISMIC
ACOUSTIC
ULTRASONIC

Fig. 1

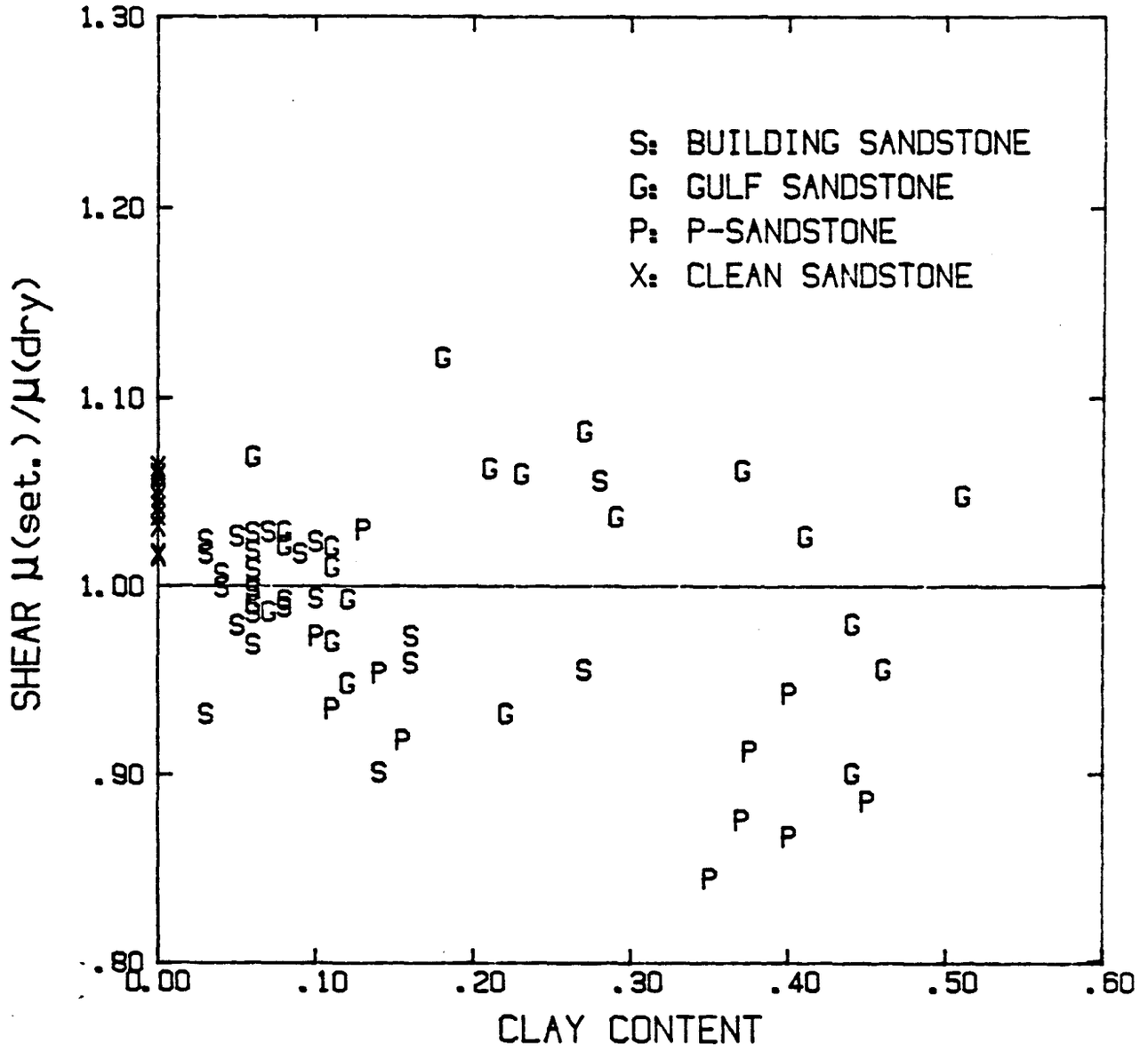
S: BUILDING SANDSTONE
G: GULF SANDSTONE
P: P-SANDSTONE
X: CLEAN SANDSTONE
SHEAR μ(set.)/μ(dry)
1.30
1.20
1.10
1.00
.90
.80
0.00
.10
.20
.30
.40
.50
.60
CLAY CONTENT

Fig. 2

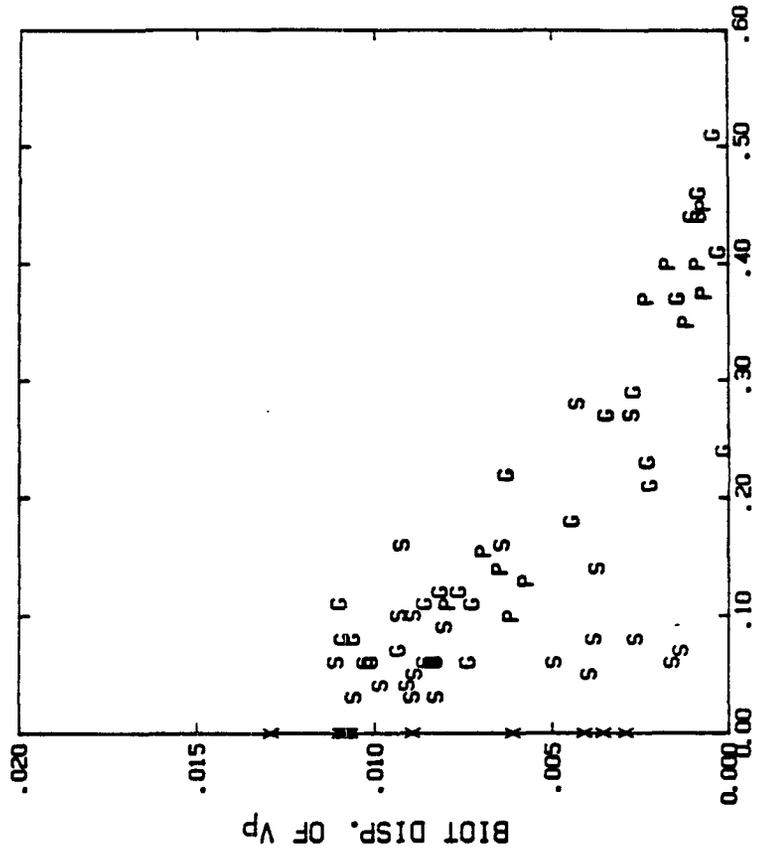
BIOT DISP. OF Vp
.020
.015
.010
.005
0.000
0.00
.10
.20
.30
.40
.50
.60
CLAY CONTENT

Fig. 3b

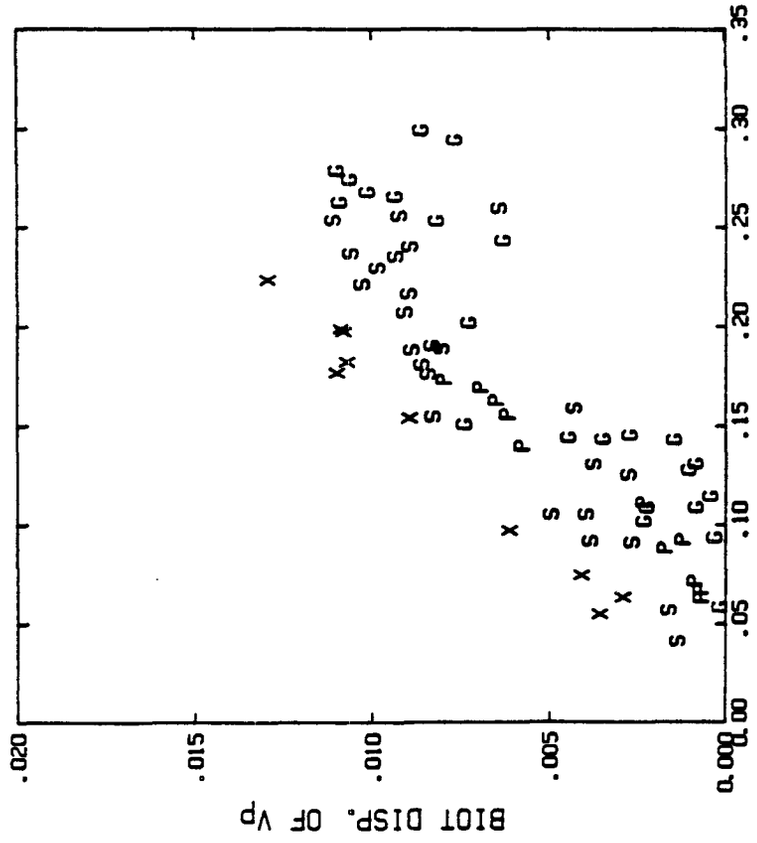
BIOT DISP. OF Vp
.020
.015
.010
.005
0.000
0.00
.05
.10
.15
.20
.25
.30
.35
POROSITY

Fig. 3a

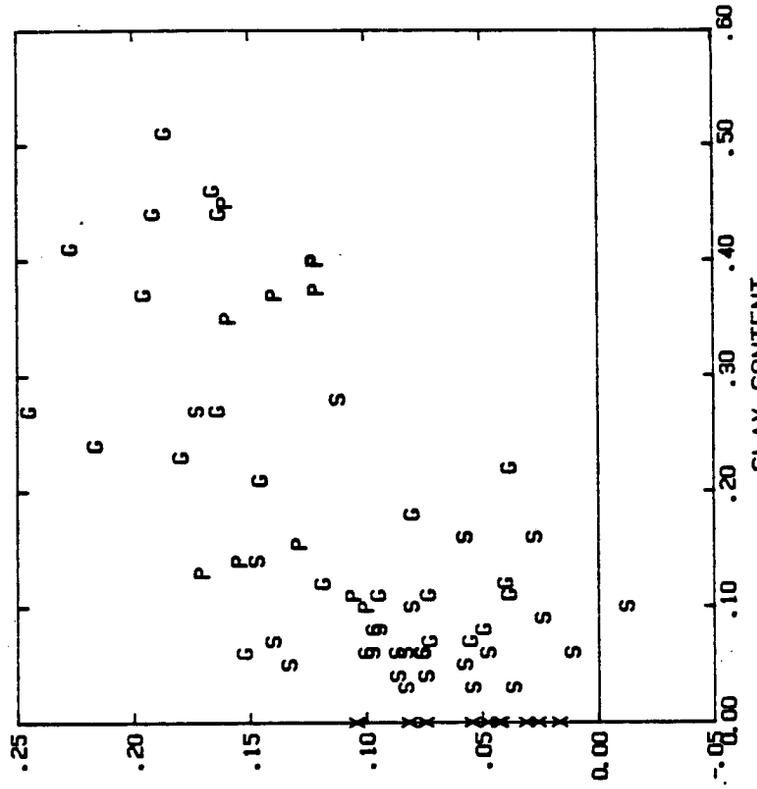
DISP. OF BULK K
.25
.20
.15
.10
.05
0.00
-.05
0.00
.10
.20
.30
.40
.50
.60
CLAY CONTENT

Fig. 4b

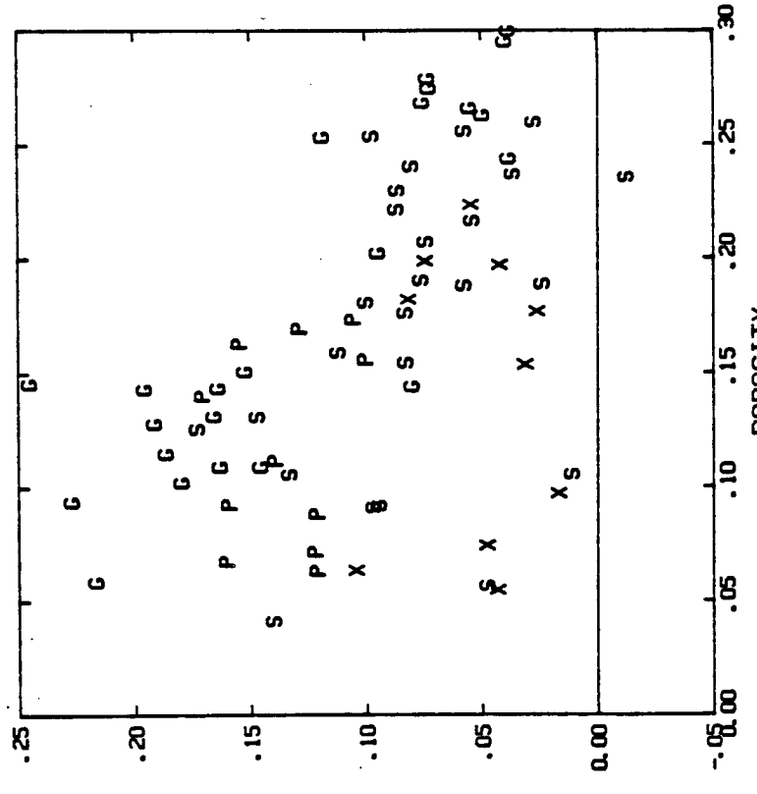
DISP. OF BULK K
.25
.20
.15
.10
.05
0.00
-.05
0.00
.05
.10
.15
.20
.25
.30
POROSITY

Fig. 4a

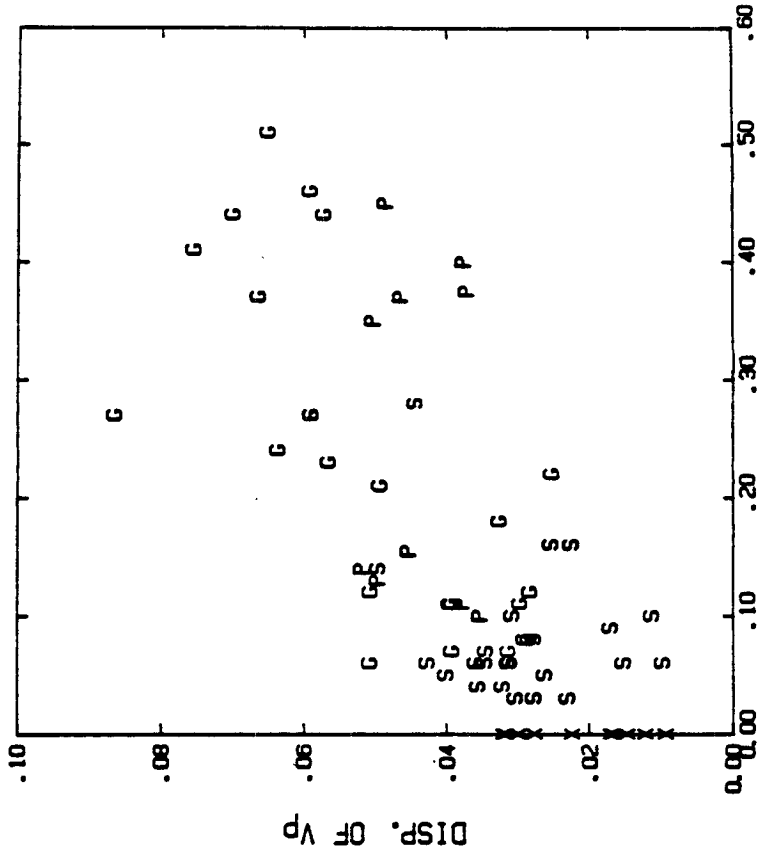
DISP. OF Vp
.10
.08
.06
.04
.02
0.00
.00
.05
.10
.15
.20
.25
.30
POROSITY

Fig. 5a

DISP. OF Vp
.10
.08
.06
.04
.02
0.00
.00
.10
.20
.30
.40
.50
.60
CLAY CONTENT

Fig. 5b

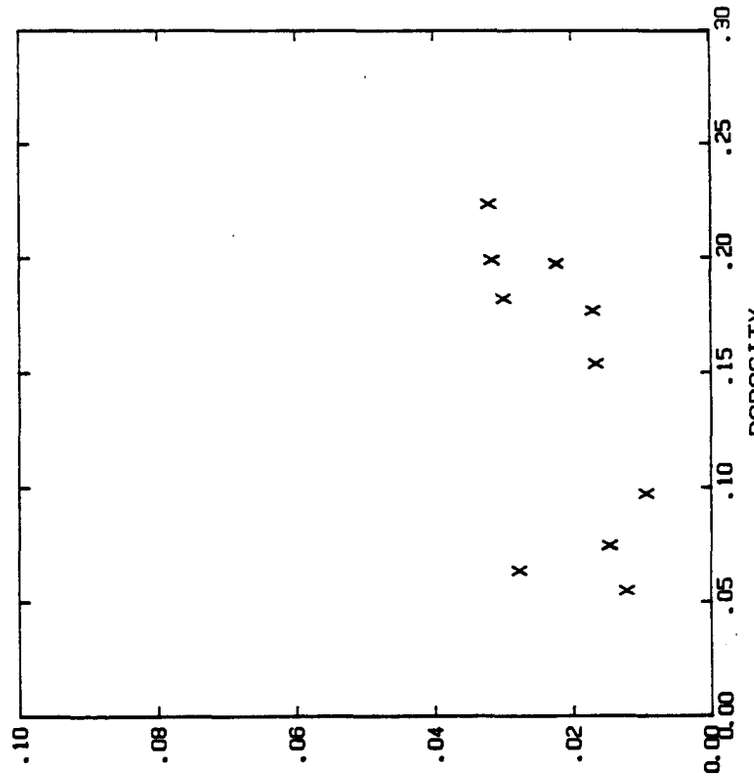
DISP. OF V_P
.10
.08
.06
.04
.02
0.00
0.00
.05
.10
.15
.20
.25
.30
POROSITY

Fig. 6b

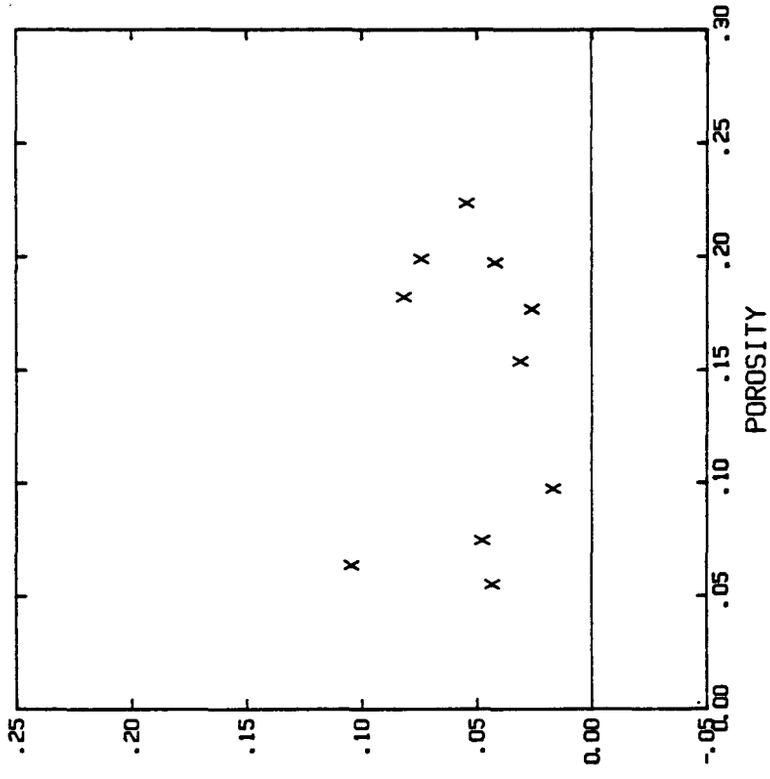
DISP. OF BULK K
.25
.20
.15
.10
.05
0.00
-.05
0.00
.05
.10
.15
.20
.25
.30
POROSITY

Fig. 6a

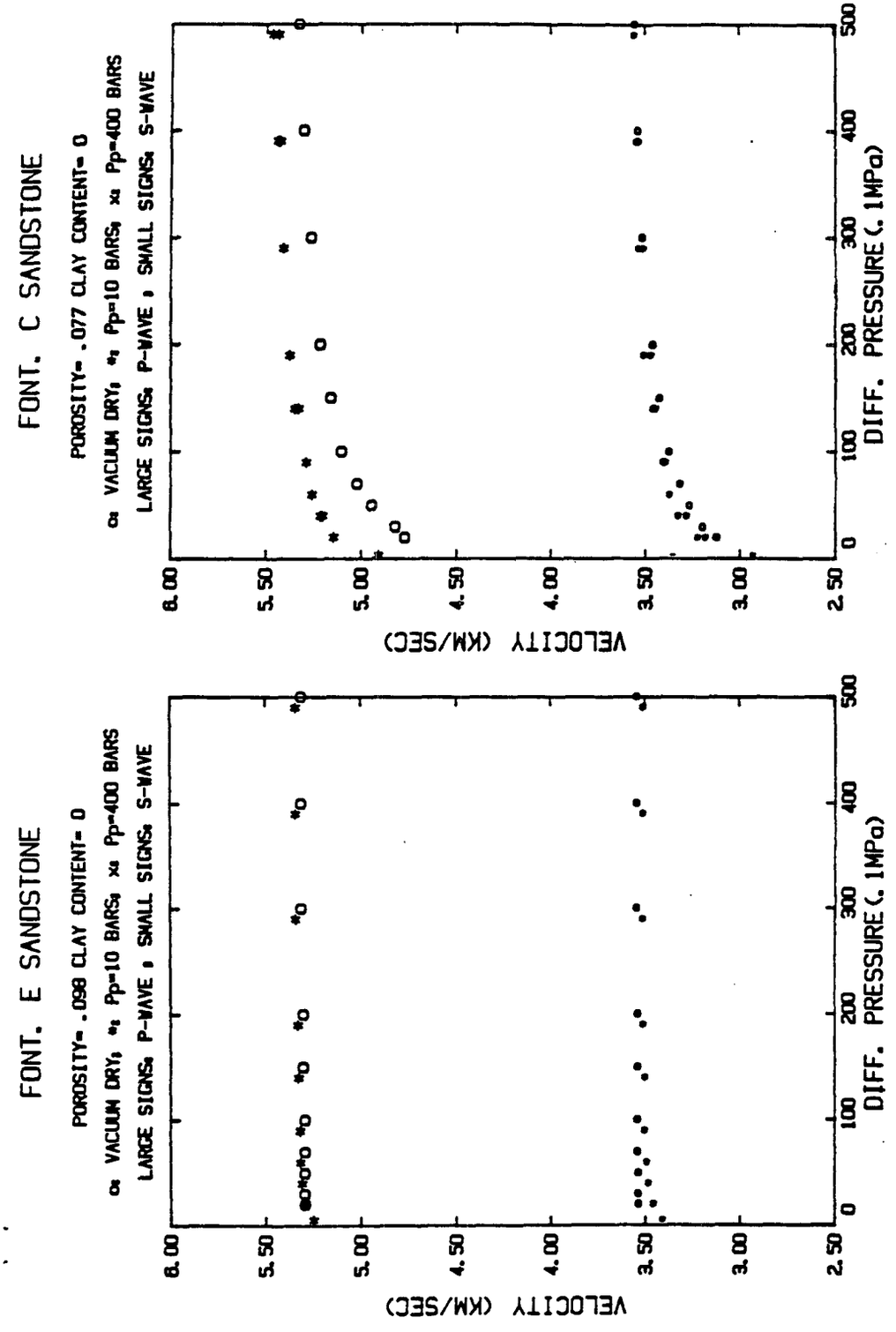
FONT. C SANDSTONE
POROSITY= .077 CLAY CONTENT= 0
o: VACUUM DRY; *: Pp=10 BARS; x: Pp=400 BARS
LARGE SIGNS: P-WAVE ; SMALL SIGNS: S-WAVE
VELOCITY (KM/SEC)
DIFF. PRESSURE(.1MPa)
FONT. E SANDSTONE
POROSITY= .098 CLAY CONTENT= 0
o: VACUUM DRY; *: Pp=10 BARS; x: Pp=400 BARS
LARGE SIGNS: P-WAVE ; SMALL SIGNS: S-WAVE
VELOCITY (KM/SEC)
DIFF. PRESSURE(.1MPa)

Fig. 7b

Fig. 7a

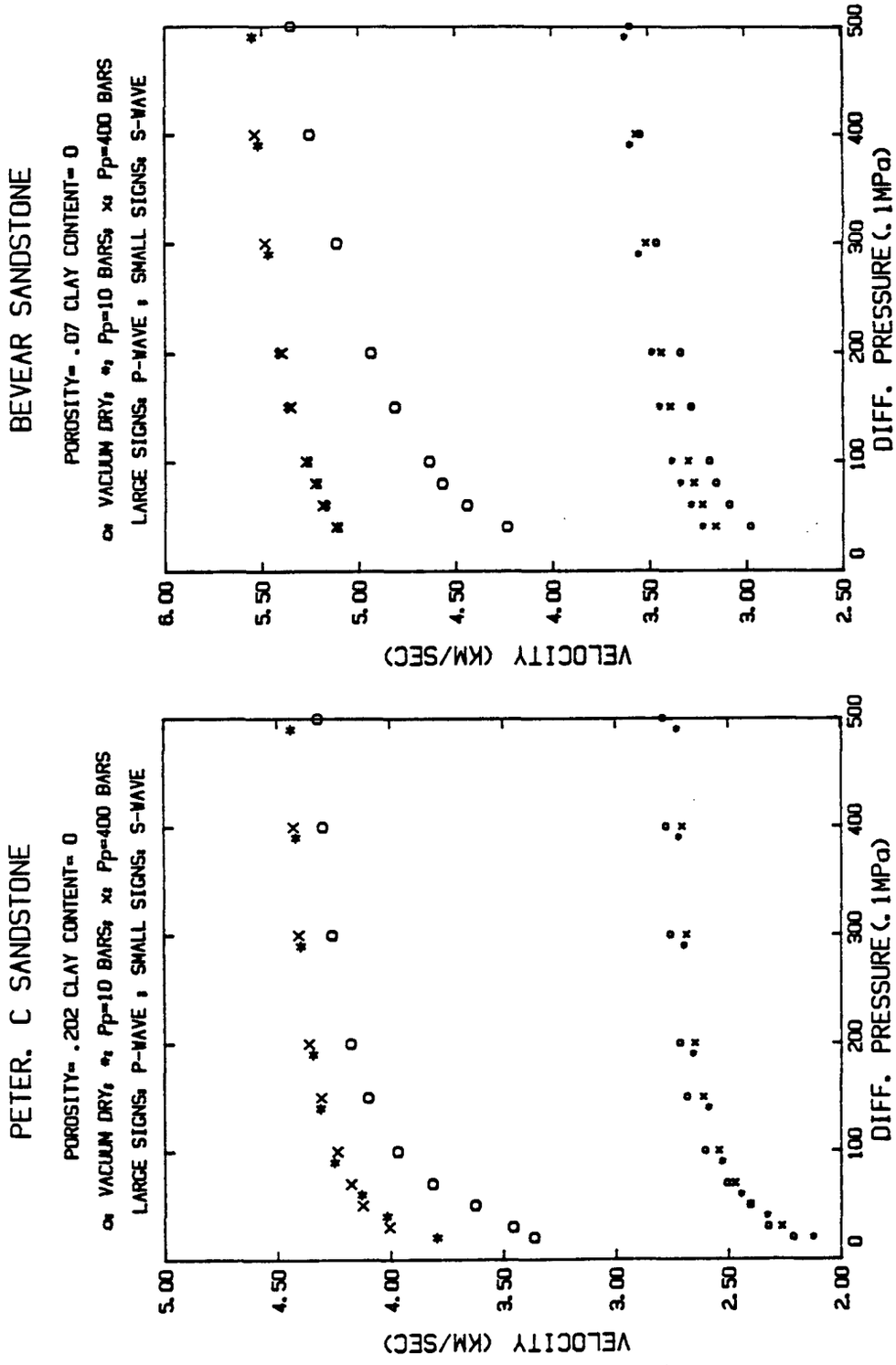
BEVEAR SANDSTONE
POROSITY= .07 CLAY CONTENT= 0
o= VACUUM DRY; *; Pp=10 BARS; x= Pp=400 BARS
LARGE SIGNS= P-WAVE ; SMALL SIGNS= S-WAVE
VELOCITY (KM/SEC)
DIFF. PRESSURE(.1MPa)
PETER. C SANDSTONE
POROSITY= .202 CLAY CONTENT= 0
o= VACUUM DRY; *; Pp=10 BARS; x= Pp=400 BARS
LARGE SIGNS= P-WAVE ; SMALL SIGNS= S-WAVE
VELOCITY (KM/SEC)
DIFF. PRESSURE(.1MPa)

Fig. 7d

Fig. 7c

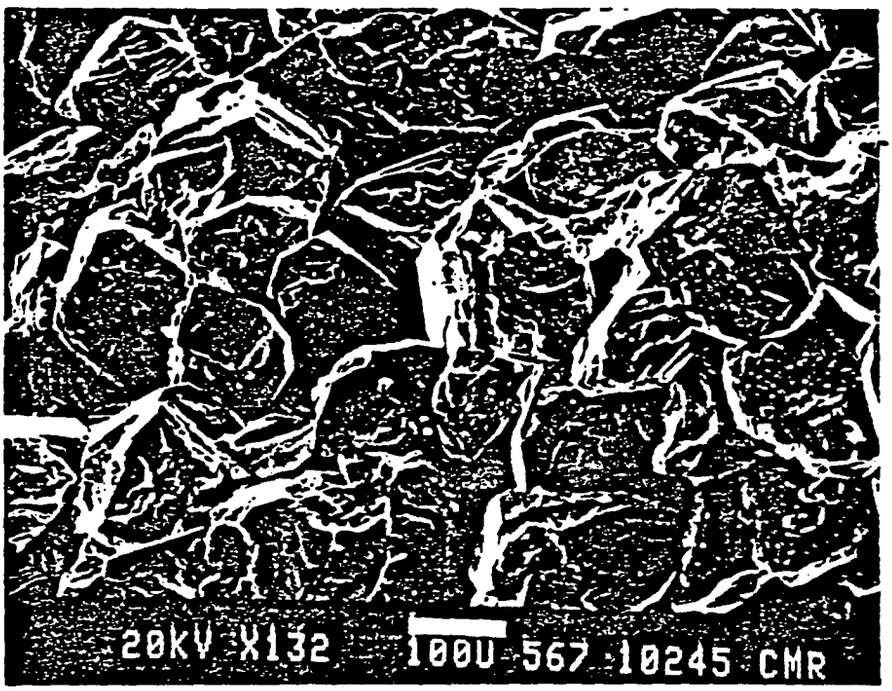

Fig. 8a

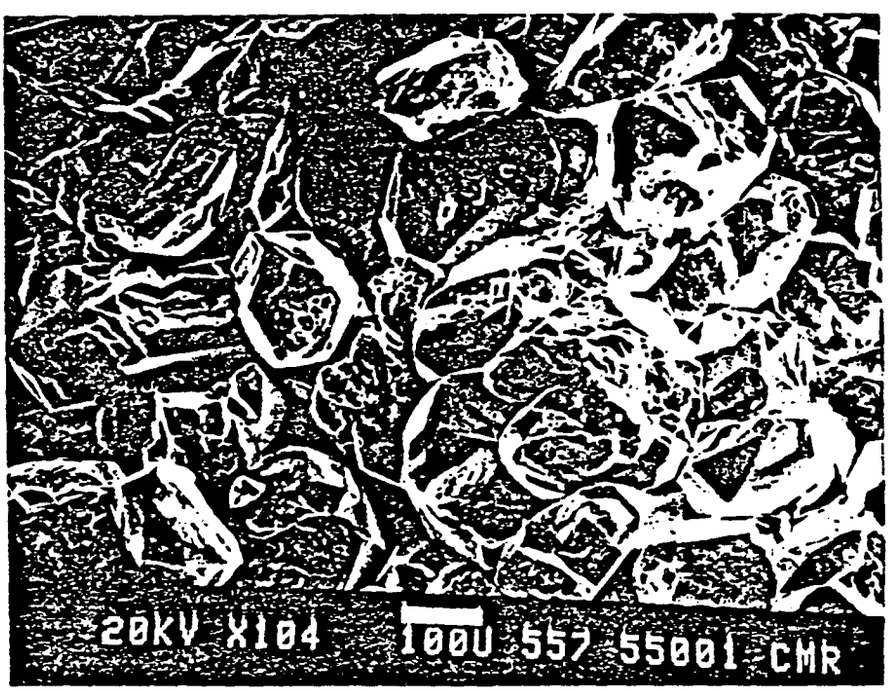

Fig. 8b

Fig. 8c

Fig. 8d

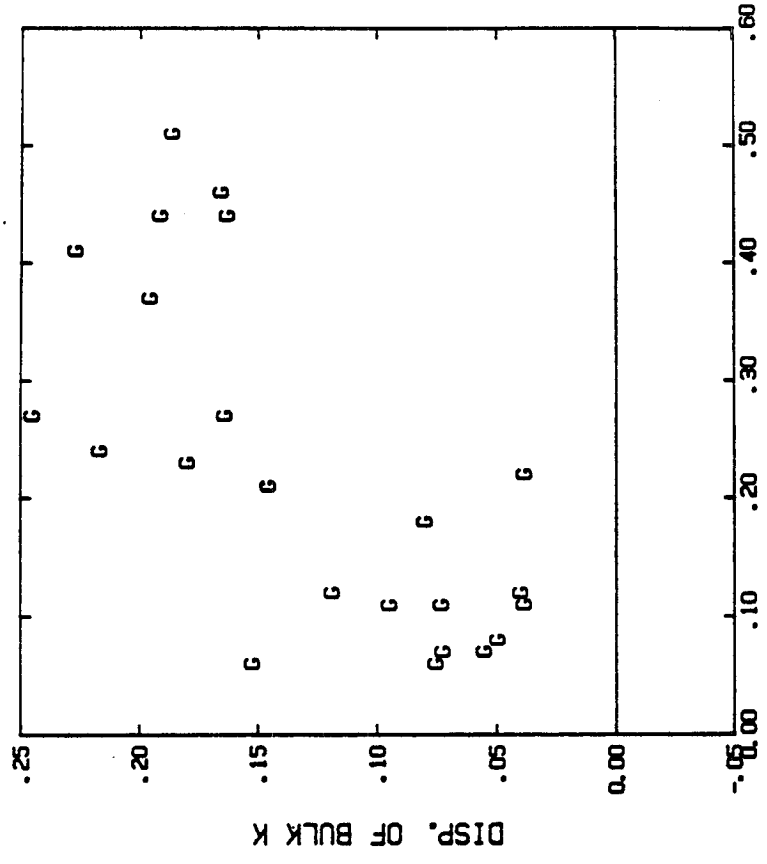
DISP. OF BULK K
.25
.20
.15
.10
.05
0.00
-.05
0.00
.05
.10
.15
.20
.25
.30
POROSITY

Fig. 9a

DISP. OF BULK K
.25
.20
.15
.10
.05
0.00
-.05
0.00
.10
.20
.30
.40
.50
.60
CLAY CONTENT

Fig. 9b

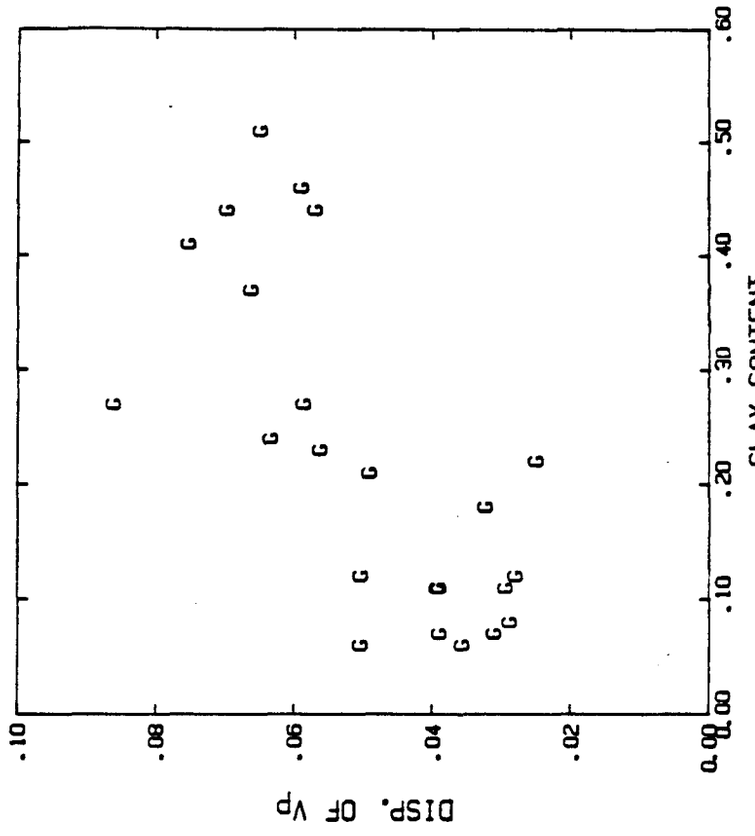
DISP. OF Vp
.10
.08
.06
.04
.02
0.00
.00
.10
.20
.30
.40
.50
.60
CLAY CONTENT

Fig. 9d

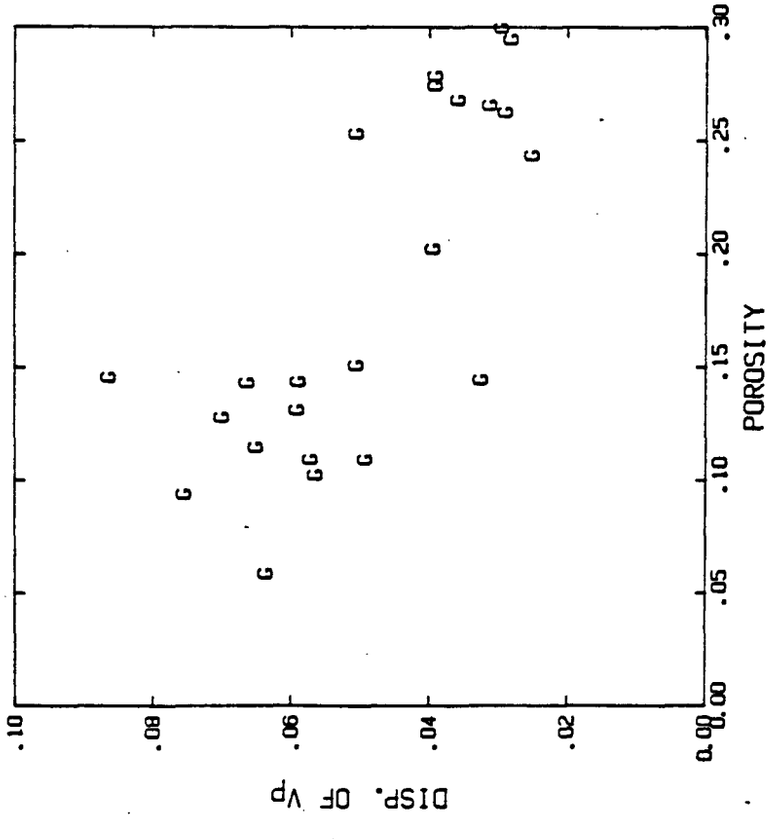
DISP. OF Vp
.10
.08
.06
.04
.02
0.00
.00
.05
.10
.15
.20
.25
.30
POROSITY

Fig. 9c

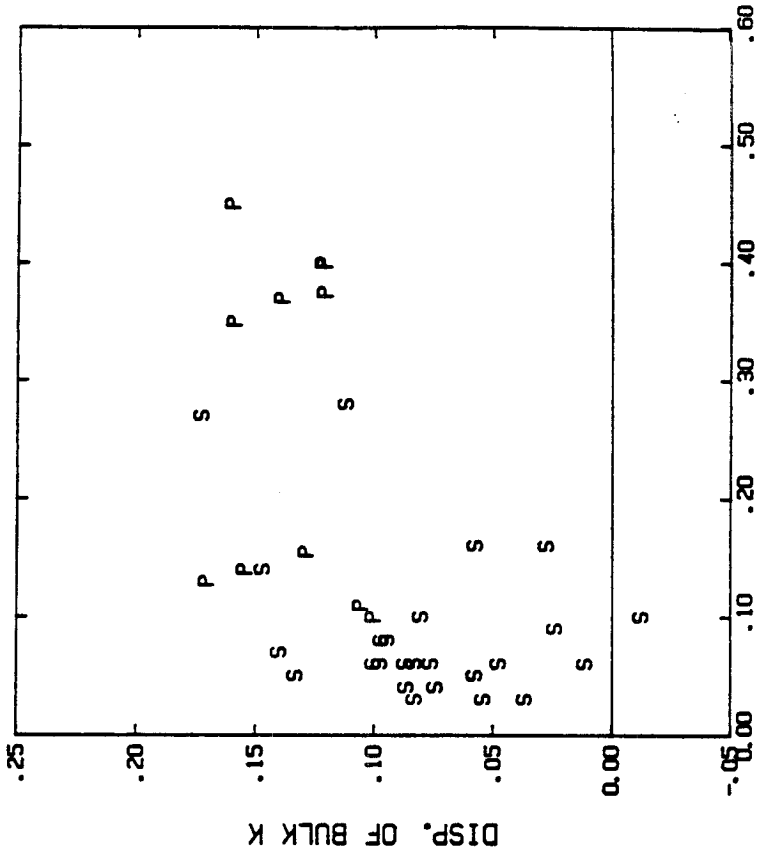

Fig. 10b

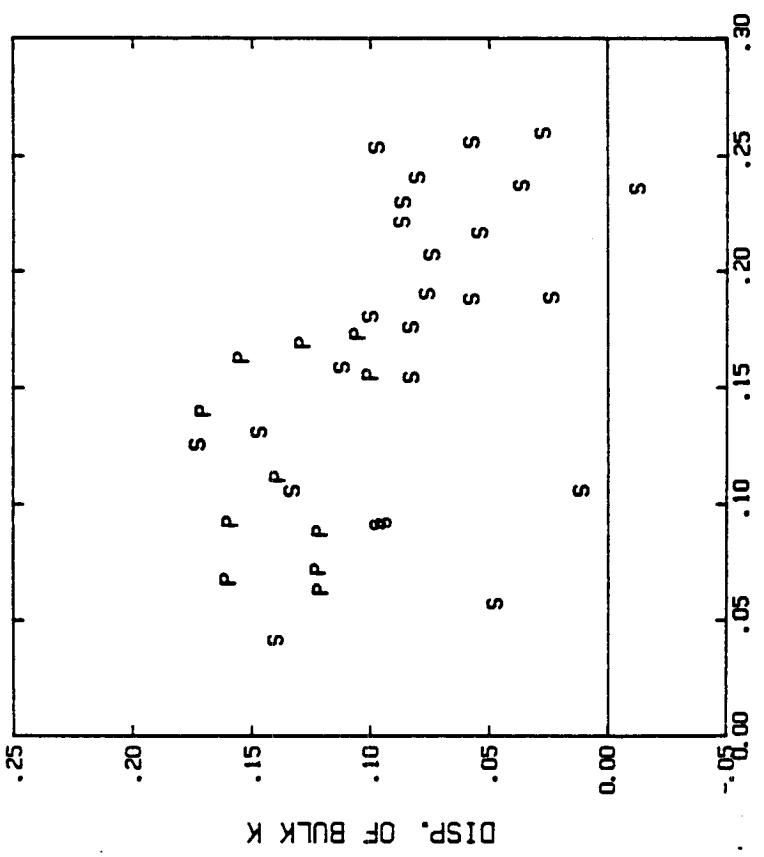

Fig. 10a

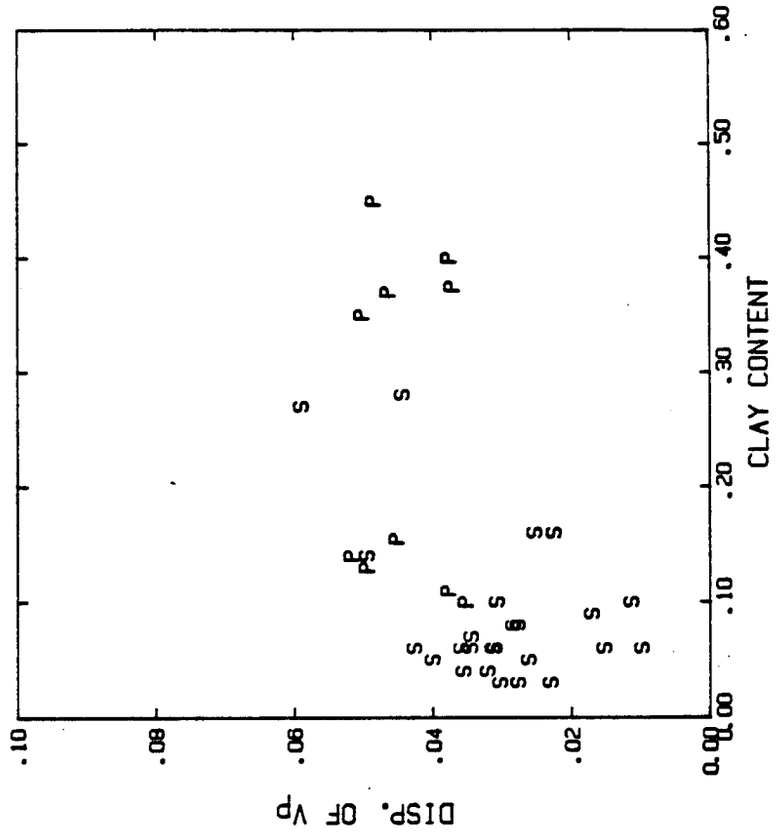

Fig. 10c

Fig. 10d

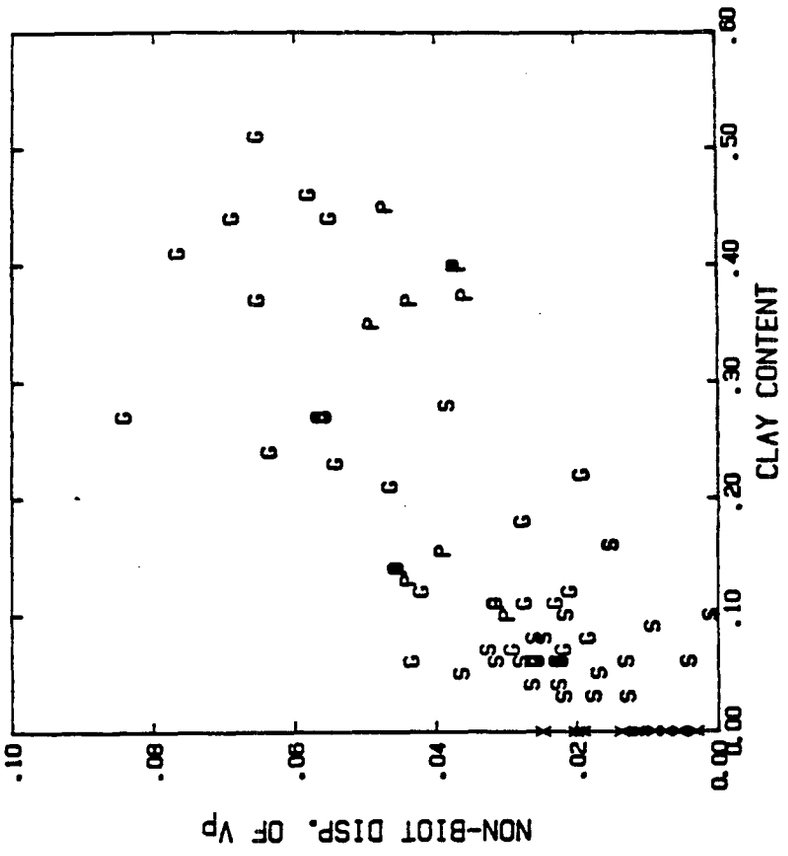

Fig. 11b

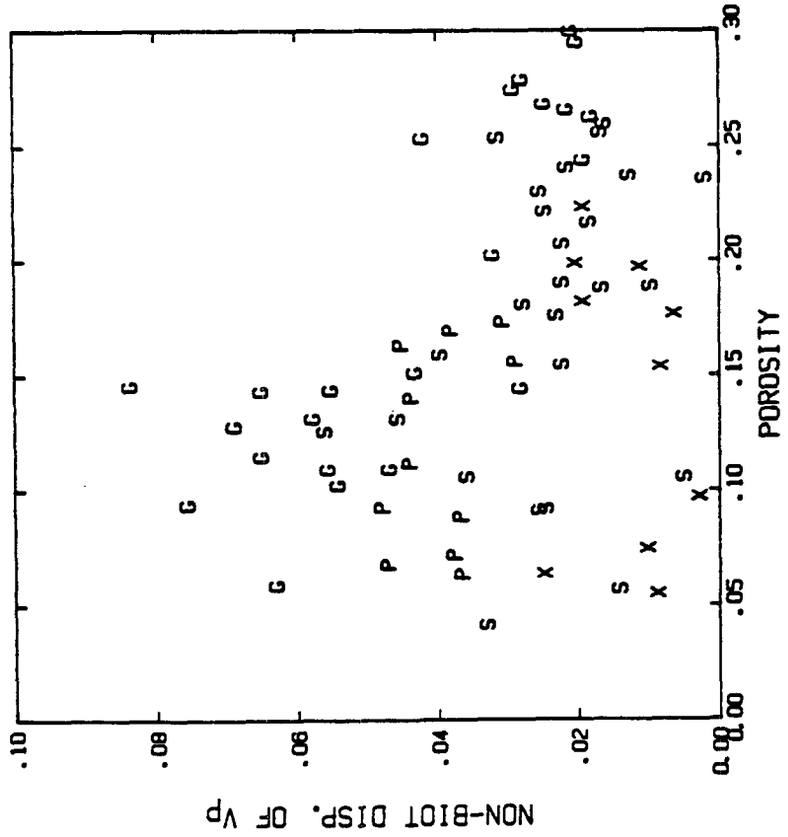

Fig. 11a

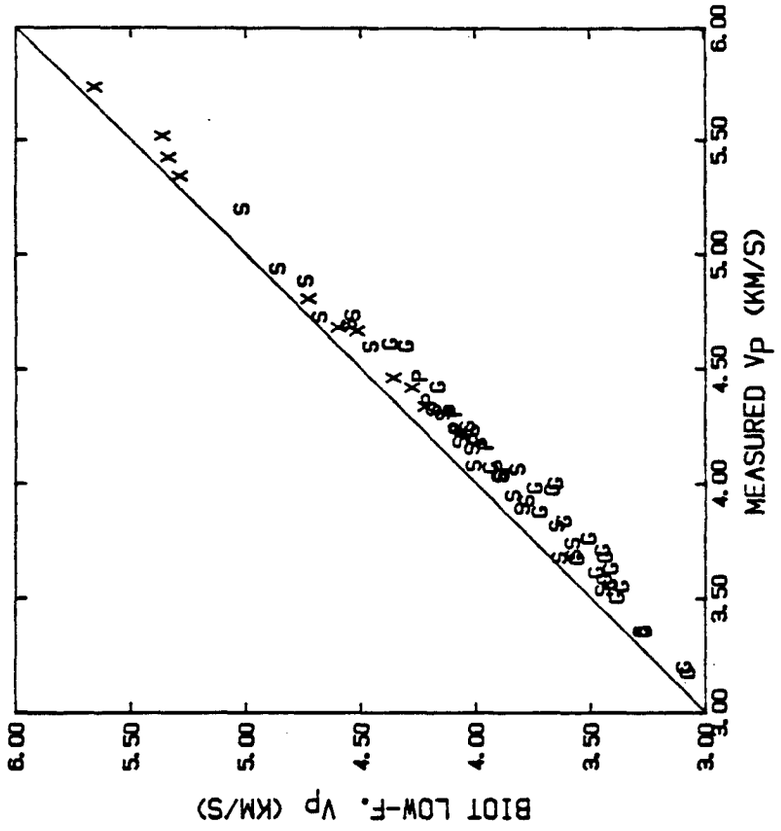

Fig. 12b

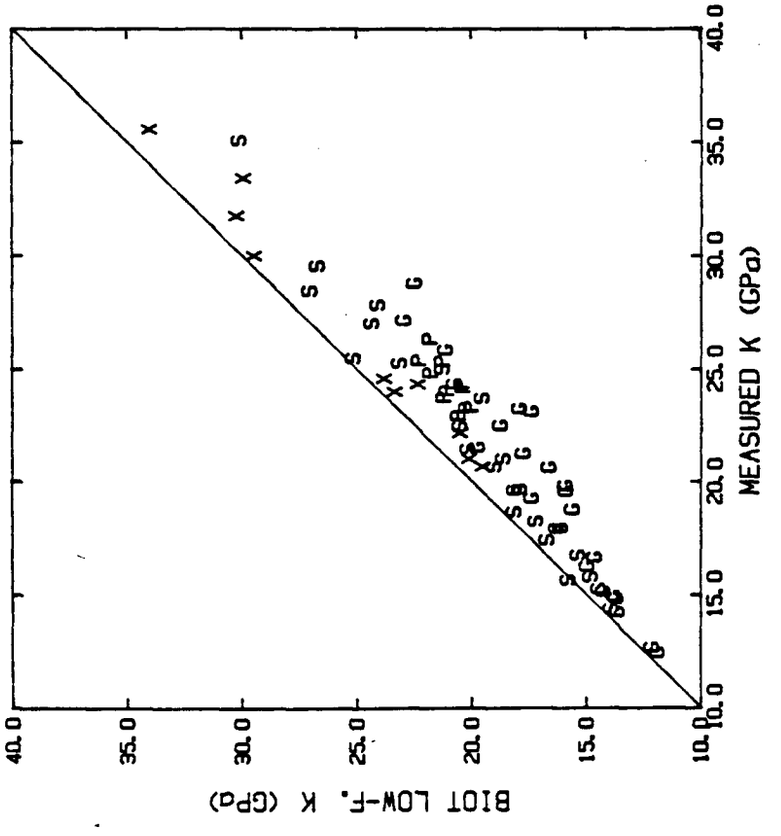

Fig. 12a

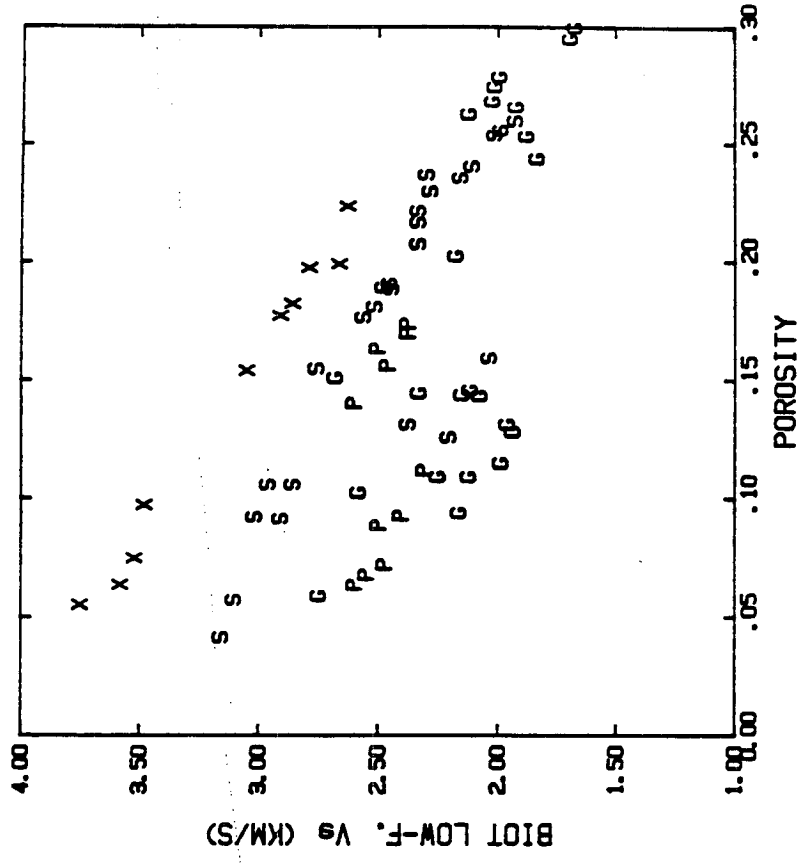

Fig. 13b

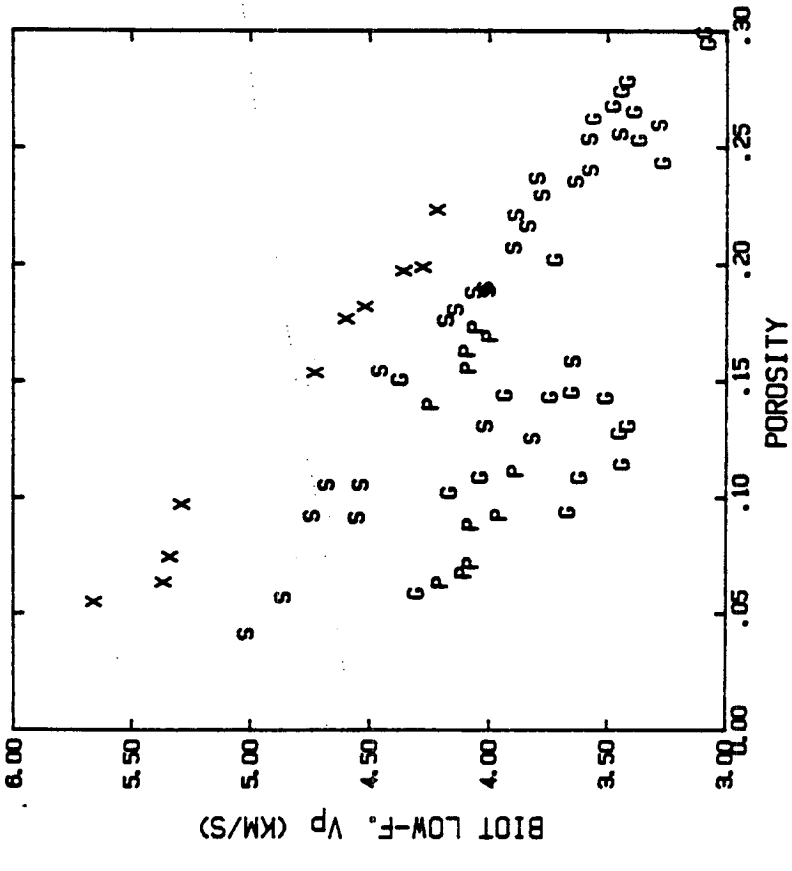

Fig. 13a

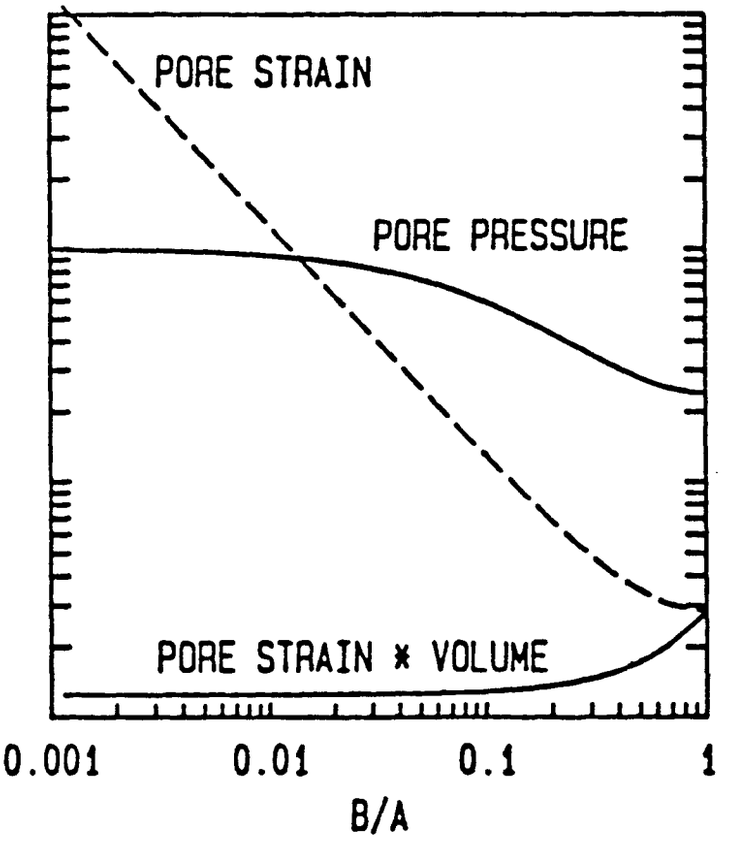
PORE STRAIN
PORE PRESSURE
PORE STRAIN * VOLUME
0.001
0.01
0.1
1
B/A

Fig. 14

CEMENT DEGREE

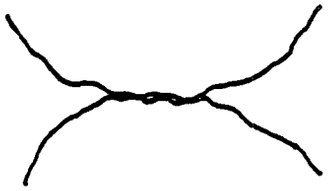

(1) a

POOR CEMENT

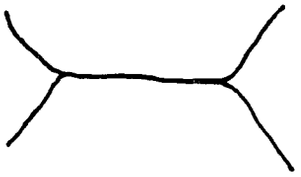

(1) b

GOOD CEMENT

CEMENT MATERIAL

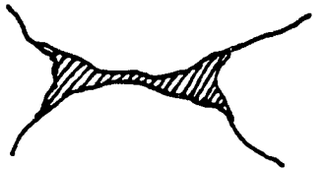

(2) a

HARD CEMENT

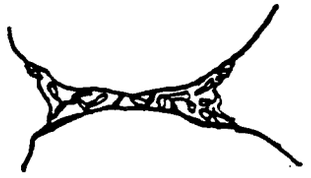

(2) b

SOFT CEMENT

ANGLE NEAR CONTACT (PORE SHAPE)

(3) a

SHARP ANGLE

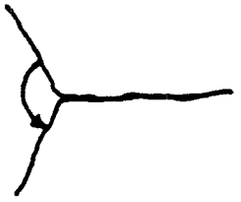

(3) b

WIDE ANGLE

Fig. 15(1)

POROSITY

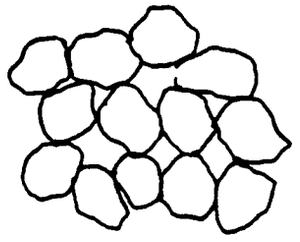

(4) a

HIGH POROSITY

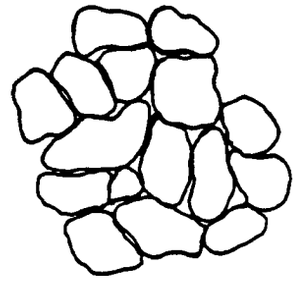

(4) b

LOW POROSITY

CONTACT AREA

(5) a

POOR CONTACTED

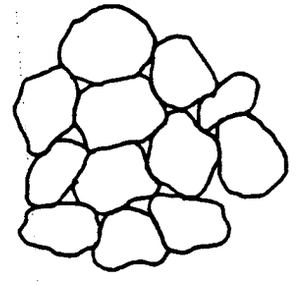

(5) b

WELL CONTACTED

COMPACTION

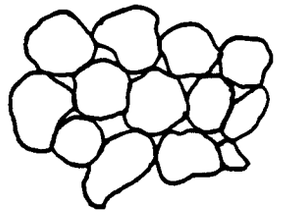

(6) a

WELL COMPACTED

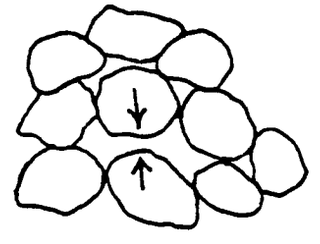

(6) b

POOR COMPACTED

Fig. 15(2)

CHAPTER VI

STUDY OF COMPACTION AND VELOCITIES OF SAND-CLAY MIXTURES

ABSTRACT

Laboratory studies of relationships among compaction, acoustic properties, and clay content in sand-clay mixtures were carried out. Both porosities and velocities for the Ottawa sand, clay powder (smectite), and their mixtures with clay weight fraction from 0 swept to 40 percent were measured as a function of confining pressure P_c up to 50 MPa and pore pressure P_p equal to 1 MPa. For pure sand under pressure, porosity and velocity show approximately an elastic behavior. Pure clay, however, can be permanently compacted. For sand-clay mixtures, porosity responses to up-loading pressure are dominated by clay content as well as velocities. Clays in mixtures are classified as bound, porous, or matrix, depending on their locations; the clay locations in sand frame relate to clay content. Permanent compactions of mixtures are dominated by the matrix clay.

Under a former terminal pressure, the sand-clay mixture exhibits elastic behaviors. Porosity-pressure and velocity-pressure relations are fairly independent of the clay content. Porosity decreases exponentially with increasing clay content, tending to a limit of the pure clay compaction. Moreover, compressional velocity V_p and bulk moduli increase with clay content from 0 to 3 percent; shear velocity V_s and moduli, however, remain fairly constant. For clay content increasing from 5 to 10 percent, bulk and shear moduli stay constant, while velocities tend to drop by increase of density with increasing porous clay. When the clay fraction is above 10 percent, the velocities and moduli again increase. They will likely reach a limit as clay fraction becomes matrix in which sand grains suspend.

Introduction

The compaction of unconsolidated materials is of considerable interest to sedimentologists and civil engineers. For nearly a hundred years, scientists (see, for example, Kelvin, 1887; Graton and Fraser, 1935; Coogan, 1970; Morror, 1971) have studied systems of heterogeneous and homogeneous, regular and irregular, packing as well as relationships between porosity and coordination numbers. Six regular geometric arrangements of spheres represent from loose to close

packing (Graton and Frazer, 1935). The coordination numbers shown in table 1 are from 6 to 12 (after Coogan and Manus, 1975). Murphy (1982) presented a curve to describe the mean total coordination numbers at a given porosity. Most of the models or experiments were carried out on the two-phase composite materials, consisting of granular solid and pore fluids. Allen and Chilingarian (1975) summaried laboratory results and chronology of sand compaction in detail. As they point out, certain aspects of sand compaction are not adequately studied; for example, quantitative evaluation of the effects of composition on compaction is needed. Colazas (1971) showed a relationship between void ratio and applied pressure for pure Ottawa sand and Ottawa sand mixed with clays (50 percent illite), revealing a significant clay effect on the compaction of the mixture. However, the effect of clay fraction on compaction was not emphasized. This phenomenon has been investigated in building foundation of geotechnics, but only for pressures up to a few MPa. Similarly, with respect to sea floor sediment, only the shallow part with porosity from 40 to 90 percent or above was carefully investigated.

Marine seismologists and exploratory engineers are also concerned with the acoustic properties of porous media. Velocities of unconsolidated sediments have been measured extensively in situ in studies of marine sediment and in well-logging (see, for example, Hamilton et al., 1970). However, only a few experimental studies for glass bead and unconsolidated sediments appear (Laughton, 1957; Domenico, 1977; Plona, 1980; Murphy, 1982;). Hardin et al. (1963, 1968) have measured velocities and moduli in soils and consolidated clay under low pressure. To our knowledge, there exist no published velocity measurements investigating effects of the clay content on both porosity and velocity in sand-clay mixtures. We therefore undertook an experiment to study systematically these effects under conditions in which confining and pore pressure are separately controlled.

Experimental Procedure

Sample

We used Ottawa sand and clay (smectite) to make samples. The Ottawa sand consisted of pure quartz grains with a round shape and middle range of grain size. The smectite consists of fine powders. The grain density of the sand was 2.64 g/cc measured by a helium porosimeter. The grain density of the smectite was 2.35 g/cc. A sample was obtained by mixing the sand and clay. The mixture was then placed into a tygon tube with two transducer end-plugs to form a cylinder. The tygon tube, 5 cm in diameter, was used as a jacket to seal the sample from hydromatic pressure medium. Samples contained clay fraction by weight from 0 to 40 percent. Each sample had a weight of 100 g and was around 3.0 cm long. The mixture of clay and sand was carefully shaken in a bottle. We compacted the samples by hand-shaking, tapping and pressuring the mixture in a consistent manner. The initial length of a sample was measured at the outside of the pressure vessel. Because of parallel unconformity of two interfaces between a sample and the two transducer end-plugs, the error of a measured sample length was about 0.5 mm.

Porosity measurement

The initial porosity of a sample was computed by

$$\phi_0 = \frac{V_0 - (W_s/\rho_s + W_c/\rho_c)}{V_0} \tag{1}$$

where ϕ_0 is the initial porosity, V_0 is the initial bulk volume computed from sample length and diameter, W_s and W_c are sand and clay weight in gram, and ρ_s and ρ_c are the density in g/cc for sand and clay. Porosities of dry sand and clay powder samples were measured by a helium-porosimeter at helium pressure equal to 0.7 MPa. Porosity of the pure sand was measured to equal 37.3 percent. From this porosity and sample weight, the grain density was calculated equal to 2.64 g/cc. Porosity of the clay frame was measured to equal 52 percent. Density of the clay powders is equal to 2.35 g/cc. On the basis of the above values, the initial porosity computed from equation (1) can be repeated within 1 percent of the bulk volume V_0.

We used deaerated solution with 0.5 mole concentration of sodium-chloride as pore fluid. It was assumed that grain volume keeps approximately constant in the pressure range used; thus the

change of the bulk volume was equal to the change of pore spaces only. This change can be measured by the volume change of pore fluid when the pore pressure keeps constant. In this manner, the porosity of a sample as a function of confining pressure can be carefully traced.

Acoustic measurement

The pulse transmission method (Birch, 1960) was used to measure compressional and shear velocities. The central frequencies of P and S transducers are 1.0 MHz. and 0.6 MHz respectively. It cannot be neglected that a sample length varies with pressure. The third transducer was mounted to monitor the ength change. As shown in Figure 1, the sender-transducer which could be freely moved along pillers emitted acoustic pulses. The pulse traveled through a sample to the receiver-transducer. The pulse was received by the monitor-transducer through hydromatic oil. Both receiver- and monitor-transducers were fixed on the pillers. The velocity of the hydromatic oil is calibrated as a function of confining pressure. Therefore, changes of sample length could be measured by the travel time change from the sender to the monitor transducer.

The experiments were carried out under confining pressure -- from 0 to 50 MPa -- and pore pressure 1 MPa controlled separately. Samples were vacuumed to 5 microns mercury high before injecting the pore fluid to ensure full saturation. Because there was a large permanent compaction in the first pressure cycle, velocities were measured during the up- and down-loading process. The first arrival of the P-wave was very clear. The relative error of V_p measurement was less than 2 percent, the main source of the error coming from the sample length measurement. The shear signal could not be distinguished from transit P-wave signals until the differential pressure was above 20 or 30 MPa. During down-loading, however, it could be traced even at differential pressure lower than 10 MPa. The relative error of V_s was less than 3 percent.

Compaction and Velocities of Ottawa Sand

Grain size distribution of Ottawa sand is shown in Figure 2 a. After initial hand-packing, the porosity of the sand is around 37.3 percent. This packing is disorder. Packing features are

grain contact and grain size heterogeneity, as shown in Figure 3. We measured velocities in two pressure cycles. The porosity and velocities as functions of confining pressure at pore pressure equal to 1 MPa are shown in Figures 4 a and 4 b.

In the first up-loading, there is a large porosity reduction as differential pressure increases from zero to 2 MPa (Figure 4 a). As the P_d increases, the porosity and velocity V_p do not behave smoothly. Sudden extra-compactions occur occasionally (Figure 4 a) and wave signal is disturbed, finally corresponding to an extra velocity increment (Figure 4 b), especially in differential pressure over 30 MPa. This phenomenon corresponds to crashing some grains under the pressure, leading to destruction of the original pore structure and grain contacts. The evidence is shown in Figure 2 b. After pressure loading, larger grains were fractured to grains with smaller sizes.

In the down-loading, the velocity V_p is higher than the corresponding velocity in the up-loading and decreases smoothly, following the power law $V_p \alpha P_d^{1/4}$. We did not observe the power transit from 1/4 to 1/6 with increasing differential pressure as Murphy did under uniaxial pressure (1982). At an identical pressure, the maximum of differences between the velocities during up- and down-loadings is 0.06 km/s, less than 3 percent of the original velocities. When the P_d is lower than 2 MPa, the velocity V_p falls back to the value for the up-loading pressure, shown a hysteresis behavior. The porosity, however, shows different features. At up-loading pressure, the permanent reduction of the porosity increases with increasing differential pressure. After the first pressure cycle, the porosity can not recover to the original value. At P_d equal to 10 bars, it decreases from 36.2 percent for up-loading to 34.2 percent for down loading as shown in Figure 4 a.

In the second pressure cycle, the velocities follow the former track in the first down-loading until P_d is over 30 MPa. At P_d equal to 50 MPa, however, the velocity increases from 2.47 to 2.51 km/s (Figure 4 b), corresponding to a porosity reduction from 32.0 to 31.4 percent (Figure 4 a).

It is important to note that the terminal pressure (Figures 4 a and b) in the up-loading can determine porosity and velocities in the down-loading. When the P_d increases from 50 to 60 MPa, then releases back to 50 MPa, the new porosity reduction is from 31.4 to 31.1 percent and the new velocity increment is from 2.51 to 2.53 km/s. Thus, porosity and velocity in the down-loading respond to the new permanent compaction. Moreover, in different down-loading, the porosity and velocity behaviors are similar, except that they are biased by the loading history. This similar response to the pressure suggests that the grain contact relaxation may dominate the porosity and velocity behaviors. As P_d decreases, grain contacts transit gradually from tight to loose and average coordination numbers decline following a similar process (Murphy, 1982). In addition, shear velocity shows a response similar to that of the compressional velocity.

Velocities for a vacuum dry sample were also measured (Figure 4 b). The sample was made of the same Ottawa sand. The data show a similar trend as reported by Domenico (1977) except for higher velocity and Poisson's ratio. A large reduction of shear velocity occurs (12 percent) after fluid saturation. The realistic physical mechanisms which responded to the compaction of the unconsolidated sand are very complicated and involve many processes such as adjustment, rotation, sliding, peeling, elastic deformation of grain contacts, fracture, and so on. These were discussed in detail by Allen et al. (1975).

Velocities of Clay (Smectite)

The compressional V_p and the shear velocity V_s of clay were measured. The sample was made of smectite powders. First, we measured a vacuum dry sample. A sharp shear signal could be observed even at P_c lower than 10 MPa. Then we saturated the sample in the pressure vessel. However, this was not possible because of locked pore connection on the surface of the sample. The mixture of clay powders with 33 percent water by weight was alternated to make a saturated sample.

The initial porosity of the clay frame at room pressure is over 52 percent. After first pressure cycle with a maximum confining pressure equal to 50 MPa, the porosity of both dry and saturated samples remained at about 12 percent. This permanent compaction suggests that

ductile deformation of clay powders should occur under 50 MPa, producing a much lower porosity than that of the clean sand. The compaction of clay also depends on time period. A longer time leads a close compaction. However, the compaction is limited by following factors: for the dry clay sample, the static friction among clay grains supports the external pressure to keep the pore space open somewhat; for the saturated sample, the clay grains with surface water will repel when they approach one another. These mechanisms suppress the clay compaction and keep pore spaces open.

Velocity data are shown in Figure 5. For the dry measurement, as P_c above 30 MPa, V_p increases drastically and V_s increases slightly. These behaviors may result in destruction of clay pore structures producing a lager compaction. Both V_p and V_s for the clay sample were lower than for the sand sample. The Poisson's ratio of dry clay (smectite) is 0.3 -- much larger than 0.18 of the dry sand. We measured the velocities for the saturated sample under drained condition. The pore pressure cannot be controlled because the permeability of the clay frame drastically decreases with the increasing P_d. Measured V_p is lower than that of the dry one, as opposed to the velocity feature of the sand (Figure 4 b). Moduli computed from velocity and density data reveal that the V_p reduction is caused by drastically decreasing shear modulus of clay by the water saturation. The shear V_s of saturated clay is about 0.4 km/s--much less than that of the dry sample. Both V_p and V_s show independent of the P_c in Figure 5. This may be caused by locking pore channels because of which differential pressure stays at a constant with increasing confining pressure. A low velocity zone with high pore pressure may be a case of a clay rich formation.

During this study, we find that longer loading and reloading period are favorable to compaction and increasing velocities for clay rich samples. These are cases which occurred in the field. Therefore, the above velocity results are low bounds for a clay formation.

The Compaction and Velocities in the Clay-Sand Mixture

In this section, we present data for the mixture of 20 percent clay (smectite) and 80 percent

sand, as compared with data for the Ottawa sand. The sand-clay mixture shows several important features.

1. The mixture of clay and sand has high permanent compaction under pressure (Figure 6 a). Porosity of the mixture is reduced from the initial 34.1 at zero pressure to 28.4 percent when P_d is equal to 3 MPa. The porosity decreases continuously to 19.0 percent with increasing pressure P_d equal to 50 MPa. The porosity reduction for the mixture is much larger than the corresponding reduction (37.9 to 32.0 percent) for the sand. The permanent reduction of porosity at P_d equal to 3 MPa is from 28.4 to 21.5 percent -- also much larger than the corresponding reduction from 35.9 to 34.0 percent for the sand. Obviously, these large differences are caused by clay effects. For down-loading, changes of porosity with pressure follow a different track than that for up-loading. These porosity differences are permanent compactions. Similar responses of the porosity to down-loading for the sand-clay mixture and for the clean sand suggest that these responses are dominated by a similar relaxation process.

In the second pressure cycle, the new permanent compaction happens again, but it is much smaller than for the first cycle. For comparison, porosity data for Ottawa sand are also plotted in Figure 6 a.

2. Both V_p and V_s of the mixture are larger than those of the sand, by 14 percent and 10 percent respectively at P_c equal to 50 MPa. For the mixture, there are large differences between velocities for up-loading and down-loading. These differences correspond to results of the permanent compactions. For up-loading, the V_p gradient for the mixture is larger than for the sand, because of larger compaction. For down-loading, the velocities of the mixture and the sand display a similar trend (Figure 6 b), since they are controlled by the the same mechanism. For comparison, the velocities as functions of the pressure for Ottawa sand are also plotted in Figure 6 b.

From the data shown in Figures 6 a and b, it can be confirmed that the clay fraction in the mixture plays an important role: it induces a large permanent reduction of the porosity leading to increase velocities. Compared with the clay mixture, clean sand can be considered a more or less

elastic material. It can therefore be expected that the increase of the clay fraction in the mixture will create more unelastic behaviors.

The Clay Effects on the Compaction and Velocities

The effects of the clay (smectite) in the clay sand mixture were systematically investigated. Fifteen samples are tested. The clay fractions were swept from 0 to 40 percent by weight. Some samples had the same clay fraction (e.g. 0, 1, and 10 percent) for testing reproducibility of the measurement. The two samples (3 and 8 percent of clay) were prepressured to P_d equal to 40 MPa and measured in the second pressure cycle. Therefore, data for them are stamped by pressure history and display different features from other samples.

Measurement for the samples with 30 and 40 percent clay was difficult because the permeability is so low that measurement takes a long time (several days to reach an equilibrium for each pressure condition). Figure 7 shows that time dependence. The porosity of the sample with 40 percent clay decreases exponentially from 15.4 to 14.1 percent during 8 days, and nearly reaches a termination (Figure 7 a). The V_p increases exponentially from 2.66 to 2.76 km/s during the same period (Figure 7 b). For this sample, the P_d increases to only 20 MPa because the pore pressure is not controllable. Usually the data point is taken at a condition near the equilibrium state to avoid false data.

It is noted that the clay fraction by weight is easily controlled for the purpose of making artificial samples. In order to be consistent with the porosity, the clay fraction by weight is converted by volume using the following formula:

$$C_v = \frac{C_w/\rho_c}{C_w/\rho_c + (1 - C_w)/\rho_s + \phi/\rho} \tag{2}$$

where C_w is clay weight fraction and ρ_c, ρ_s, and ρ are densities of clay, sand and mixture respectively. We note a sample by the clay weight fraction which is constant but we count the effects of clay by the clay volume fraction which varies with the pressure. Ten percent clay mixture, therefore, always means 10 percent clay by weight; the notation of the clay content for a coordinate axis always means clay volume fraction.

The measured porosities as functions of confining pressure for mixtures with clay content, 0, 1, 5, 10, 15, 20 and 30 percent are summaried in Figure 8 a. Similarly, the measured P-wave velocities as functions of confining pressure for the mixtures with clay content 0, 1, 5, 10, 15, 20, and 30 percent, and pure clay are summaried in Figure 8 b. Both of them show strong influences by the clay contents.

Effects of clay content on the compaction

As previously mentioned, the porosity responses to up- and down-loading are very different. For up-loading, the porosity vs. clay content is shown in Figure 9 a. There are five curves representing relations between porosity and clay content for the initial packing, and for conditions at confining pressure equal to 3, 10, 30 and 50 MPa with pore pressure equal to 1 MPa.

The initial porosity decreases with increasing the clay content. For clean sand the initial porosity is 38 percent. As the clay content reaches around 10 percent, the initial porosity falls to the lowest value 32.5 percent, then stays at this level until clay content reaches 15 percent. As the clay content increases continuously, the initial porosity increases moderately. For the 40 percent clay mixture, the initial porosity is 37 percent.

When differential pressure increases porosity reductions of the mixtures relate to clay content (Figure 9 a). As clay content increases from 0 to 5 percent, porosity reductions by pressure remain essentially constant, then it increases slightly with increasing the clay content from 5 to 10 percent. The porosity reductions drastically increase with the increasing clay content above 10 percent (Figure 9 a). For the 13 percent clay mixture, the porosity reduction is about 0.10 from 33.5 percent to 23.2 percent, 0.15 for the 20 percent clay mixture, and near 0.20 for the 30 percent one.

Two processes are involved in the clay effects on compaction of sand-clay mixtures. When assuming all the clay powders fill to pore spaces we obtain a dashed line (Figure 9 a) presenting a relation of porosity to clay content. In comparison with the dash line, one can see, as clay content increases from 1 to 5 percent clay powders fill mainly to pore spaces rather than grain

boundaries. When the clay content increases continuously, (above 5 percent) there is high possibility for more clay powders to become embedded into boundaries of sand grains. A thick layer of bound clay leads mainly to increase pore volume and porosity. These clay powders become matrix clay which dominates properties of rock matrix. At P_c equal to 50 MPa, if we assume that all the clay powders fill into pores, the porosity-clay content relation is shown as dotted line in Figure 9 a. Data suggest that these porosity reductions can be considered as most clay powders are in or pushed into pore spaces under pressure. At clay content above 10 percent, data show that some clay powders still remain among grain boundaries leading a relative increase of porosity.

The clay effect on the compaction occurs mainly during confining pressure increases from zero to 3 MPa. This effect is weaken and weaken as the pressure continuously increases. After the pressure above 30 MPa almost no effect of clay on compaction can be detected. Figure 9 a shows that at P_d 50 MPa, the porosity decreases linearly with increasing clay content from 0 to 10 percent. When the clay content increases continuously the porosity then falls into a mild exponential decay.

For down-loading, the relation between porosity and clay content established by the up-loading pressure remains (Figure 9 b). As the pressure decreases, for all samples porosity increases are similar. As pressure decreases from 50 to 30 MPa, porosity increases at about 0.07, and as pressure decreases from 10 to 3 MPa, prosity increases at about 0.12. No effect of the clay on the relation between the porosity and pressure remains. Pressure effect on the porosity is dominated by the grain contact relaxation.

We convert differential pressure to depth using porosities and densities of the mixture as functions of the pressure. The porosity versus depth for the mixture with 0, 10, 15, 20, 25, 30 percent clay content for the first down-loading is shown in Figure 10 a. The result shows that the effect of clay content on porosity reduction of sand-clay mixture extends to 3 km deep.

Effects of clay content on the velocities

Usually velocity of a porous medium under high differential pressure is dominated by its porosity. When the porosity decreases, the velocity will increase. For clay-sand mixtures, however, the velocity relates to both porosity and clay volume fraction.

Figure 11 a shows data of velocity vs. clay content for the down-loading pressure 50, 30, 10, 3 MPa. No matter how much clay a sample has, the velocity V_p as a function of the pressure displys similar behaviors. As confining pressure decreases from 50 to 3 MPa, for all the samples, velocities decrease about 0.50 km/s. The data suggest that the velocities as a function of pressure for the different samples shown in Figures 8 b and 11 a are dominated by relaxation of grain contacts. Clay does not show a special influence in the relaxation process.

The relation between velocity and clay content is almost independent of the pressure except that velocity decreases as pressure is released pressure (Figure 10 a). The relation between the velocity and clay content can be divided to three parts.

As clay content increases from zero to 3 percent, the velocity increases about 0.15 km/s. The increase of the velocity may be caused by a lubricant effect (Pilbeam, 1973). Small amounts of clay embedded in grain boundaries can induce a close packing and better grain contacts. Thus, the velocity of the mixture increases. However, the effect of bound clay on velocity is limited by its small amounts.

As clay content increases from 5 to 10 percent, velocity shows a slight tendency to decrease. As described in the last section, small amounts of clay (up tp 10 percent) are mainly porous clay. Elastic moduli of mixtures is essentially independent of the porous clay (as will be shown in the next section), while densities of mixtures will increase with increasing porous clay. A simple calculation shows that 10 percent porous clay can cause 2.5 percent velocity reduction by increasing the density of matrix. Because this density effect suppresses the bound clay effect, the velocity decreases.

When the clay content increases from 10 to 30 percent, velocity increases from 2.61 to 3.05 km/s at confining pressure equal to 50 MPa. The velocity increase relates to the effects of the matrix clay. Under pressure, the matrix clay can drastically change the packing pattern and

reduce the porosity, leading to an increase in the velocity. If clay weight fraction continuously increases, the sand will suspend in the clay matrix. Thus the velocity of the mixture is expected to decrease and tend to the velocity for the pure clay. For purpose of comparison, velocity vs. clay content in up-loading is shown in Figure 11 b.

The velocities V_p versus depth for the mixture with clay content 0, 10, 15, 20, 25, and 30 percent are shown in the Figure 10 b. The increase of the clay content from 0 to 30 percent may cause 0.5 km/s increment (20 to 25 percent increase) in velocity V_p for different depths. It must be noted that velocity data are based on the first down-loading with the maximum pressure P_c equal to 50 MPa. We can conclude that clay content is an important parameter in affecting the velocities in terms of their effects on the compaction of sand-clay mixture.

In down-loading, the shear velocity vs. clay content for pressure P_d equal to 50 and 30 MPa is shown in Figure 12. They exhibit a feature similar to the compressional velocities except for the V_s keeps fairly constant as clay fraction increases from 0 to 3 percent.

Effects of clay content on the moduli

We calculated dynamic bulk, shear, and Young's moduli from the velocity and density data at pressure 50 MPa as shown in Figure 13 a. The bulk modulus drastically increases, as clay content increases from 0 up to 3 percent, while the the shear modulus stays constant. This reveals that the bound clay can improve contacts among grains leading to an increase of the bulk modulus. However, bound clay with low shear modulus also causes a decrease of the shear modulus of the mixture. The shear modulus keeps constant as a result of these opposite effects.

When the clay fraction increases from 3 to 10 percent both bulk and shear modulus keep fairly constant. Again this fact certifies that the porous clay does not affect moduli of mixtures, while decreases of velocities in these mixtures are dominated by the density effect. As the clay continuously increases the bulk and shear modulus increase with a slow gradient (Figure 13 a). It can be assumed that a compaction of matrix clay causes a reduction of porosity. The porosity decrease dominates the increase of elastic moduli. While the Clay saturated with water has lower

moduli, especially lower shear modulus, than quartz grain. An increase of the clay fraction would cause a decrease of the moduli. However, the porosity effect is greater than the effect of clay content. Thus, through clay fraction increases, moduli of the mixture still increase.

The Poisson's ratios for the clay-sand mixtures (Figure 13 b) vary slightly. Differences of the Poisson's ratios are quite small, from 0.35 to 0.38, which suggests that the effect of the clay content on the Poisson's ratio can be neglected.

Discussion

Our data show that as the clay content increases the P-wave velocity appears to increase (Figures 8 b, 10 b and 11 a). In the mean time, the porosity decreases (Figures 8 a, 9 a, and 10 a). The P-wave velocities versus porosity for mixtures with clay content from 1 to 30 percent are summarized in Figure 14. In general, the data show that the P-wave velocity increases with decreasing porosity. However, the clay content also exhibits clear influences on the P-wave velocity as previously shown. The question is how to separate the clay effect on velocity from the porosity effect. For the purpose of comparison, we need to find how velocities of clean sand relate to its porosity. Unfortunately, no such relation for sand at high pressure has been presented in literature. Hamilton (1971) has given an empirical relation of bulk modulus to porosity for Ottawa sand.

$$\log K_b = 2.57664 - 4.27516\ \phi. \tag{3}$$

Here K_b is the bulk modulus in 10^9 dyn/cm^2, ϕ is the porosity. This equation is valid for depths 1 m or less of overburden pressure. We try to modify this equation for using at P_d equal to 50 MPa. For our sample, at P_d equal to 50 MPa the porosity is 0.32. For the dry sample, bulk and shear moduli are equal to 4.0 and 3.2 GPa; for the saturated sample bulk and shear moduli are equal to 9.0 and 3.0 GPa respectively. Using Gassmann's equation we calculated the grain bulk modulus of Ottawa sand from the above porosity and velocity data. The grain bulk modulus of Ottawa sand is equal to 41.7 GPa. We used a formula similar to equation (10) to fit both points: $\phi = 0$; $K = 41.7$ GPa and $\phi = 0.32$; $K = 9.0$ GPa. We obtained:

$$\log K_b = 1.6201 - 2.0808\ \phi \tag{4}$$

where K_b is the bulk modulus in GPa. Following Ogushwitz (1985), we assumed that Poisson's ratio is equal to 0.20 and obtain shear modulus equal to 31.3 GPa for Ottawa sand. A similar equation is obtained for the shear modulus:

$$\log \mu_b = 1.4955 - 3.1826\ \phi. \tag{5}$$

The V_p and the V_s of Ottawa sand can therefore be computed from moduli and density. The velocity-porosity relations are shown as dash lines in Figures 15 a and b. Numbers used to indicate date points in Figure 15 are clay weight fraction. Clay effects on velocities show complex situations because of different effects of the bound, porous and matrix clay. However, in comparison of data of mixtures with that of clean sand, as porosity keeps constant one can roughly see that both V_p and V_s decrease with increasing clay content. The clay effect on reducing velocity is much less than the porosity effect. A simple calculation shows that the clay effect is about 1/3.7 of the porosity effect on reducing V_p and about 1/2.6 of the porosity effect on reducing V_s. The clay effect on reducing shear velocity is relatively larger than that on reducing compressional velocity. These results are consistent with the clay effects on velocities of sandstones (Han, 1986), except for the lubrication effect of bound clay and the density effect of porous clay on velocities in unconsolidated mixtures. Actually, poorly consolidated sandstone such as Gulf sandstone with high clay content (Han, 1986) is more or less similar to a sand-clay mixture loaded by high pressure.

For clean sandstones, empirical relations of velocities to porosity at 40 MPa were obtained by Han (1986).

$$V_p = 6.08 - 8.06\ \phi \tag{6}$$

and

$$V_s = 4.06 - 6.27\ \phi. \tag{7}$$

These results are shown as solid line in figures 14 a and b. Differences between the solid line (for consolidated sandstones) and the dashed line (for unconsolidated sand) give a maximum effect of consolidation on velocities at different porosities. It can be concluded that except for porosity and

clay content effects, as one deals with velocity data of sandstones with different consolidations the effect of degree of consolidation degree should be taken into account.

Conclusion

Several important points can be concluded:

1. In comparison with sand-clay mixture, randomly packed Ottawa sand can be considered essentially as an elastic material. At pressures higher than 30 MPa, permanent compaction may occur because of grain fractures. Velocity hysteresis is very small compared with the sand-clay mixture.

2. The clay (smectite) can be permanently deformed. After loading pressure equal to 50 MPa, the clay porosity decreases from 52 percent to less than 12 percent. Clay compaction is constrained by friction (dry sample) and the surface water adsorbed (saturated sample). With increasing hydrostatic pressure, the clay properties change gradually from plastic to elastic. This process is reversible by releasing the pressure. The velocity V_p of saturated clay (33 percent water by weight) is less than that of dry clay. Shear velocity V_s is about 0.4 km/s -- much less than that of dry clay. These values give low bounds for clay formation in situ. For the up- and down-loading, velocities exhibit large differences because of permanent compaction during up-loading.

3. In sand-clay mixtures, clay content dominates the process of compaction. The more clay in the mixture, and under the higher pressure, the more is the permanent porosity reduction that occurs, especially with clay content above 10 percent. During compaction, the clay particles cause destruction of the old structure and bring about a new close packing in the mixture. Thus properties of the mixture change gradually from unelastic to elastic. The compaction of mixtures is restrained by the limitation of clay compaction. Permanent reductions of porosity occur mainly at low differential pressure. Long period loading and reloading which are natural processes in the crust, should bring more compaction in sand-clay mixtures.

Under a former terminal pressure, the sand-clay mixtures exhibit elastic behaviors. Porosity and velocity of compacted mixtures as functions of pressure appear to be slightly influenced by clay content. As P_c decreases from 50 to 3 MPa, porosities decrease about 0.02 - 0.03, and velocities decrease about 0.5 km/s for clay content swept from 0 to 30 percent. For compacted mixtures, porosities decrease exponentially with increasing clay content, tending to a limit of the pure clay compaction. Velocities of mixtures are dominated by their porosities. Clay effects on reducing velocities are smaller than the porosity effect. Small amounts of clay tend to increase velocity V_p and bulk modulus by their lubricating effects. Porous clay tends to decrease both V_p and V_s by its density effect. As clay content increases above 10 percent, porosity decreases, and velocities and moduli increase. They will likely reach a limit as clay fraction becomes matrix in which sand grains suspend.

The clay has lower moduli than quartz grains. As clay replaces sand grains, the moduli of the mixture should decrease, especially shear moduli. Data show that increase of velocities with increasing clay content is results from the reduction of porosity. The clay content has a smaller effect in decreasing velocity than the porosity does.

REFERENCES

Allen, D. R., and Chilingarian, G. V., 1975, Mechanics of sand compaction: In Development in sedimentology 18 A, Compaction of coarse-grained sediments, I. ed. Chilingarin, G. V. and Wolf, K. H., 4 -77.

Birch, F., 1960, The velocity of compressional waves in rocks to 10 kilobars, 1: J. Geophys. Res., **65**, 1083-1102.

Colazas, X. C., 1971, Subsidence, compaction of sediments and effects of water injection, Wilmigton and Long Beach offshore oil fields: Thesis, Univ. South. Calif.

Coogan, A. H., 1970, Measurements of compaction in oolitic grainstone: J. Sediment. Petrol., **40**, 921-929.

Coogan, A. H. and Manus R. W., 1975, Compaction and diagenesis of carbonate sands: in Development in sedimentology 18 A, Compaction of coarse-grained sediments, I. ed. Chilingarin, G. V. and Wolf, K. H., 78-165.

Domenico, S. N., 1977, Elastic properties of unconsolidated porous sand reservoirs: Geophysics **42**, 1339-1368.

Graton, L. C. and Fraser, H. J., 1935, Systematic packing of spheres with particular relation to porosity and permeability: J Geol., **35**, 785-909.

Hamilton, E. L., Bucker, H. P., Keir, D. L. and Whitney, J. A., 1970, Velocities of compressional and shear waves in marine sediments determined in situ from a research submersible: J. Geophys. Res., **75**, 4039-4049.

Hamilton, E. L., 1971, Elastic properties of marine sediments: J. Geophys. Res., **76**, 579-604.

Han, D., Effects of porosity and clay content on wave velocities of sandstones: in this volume Chapter 2, main body of which was published with coauthor Nur, A., and Morgan, F. D. in name, Effects of porosity and clay content on wave velocities of sandstones: Geophysics, 51, Nor., and in name, Velocity measurement and empirical modeling in sandstones: the Log Analyst.

Hardin, B. O. and Richart, F. E., 1963, Elastic wave velocities in granular soils: J. Soil Mech.

Found. Div.ASCE **89** (SM1), 33-35.

Hardin, B. O. and Black W. L., 1968, Vibration modulus of normally consolidated clay: J. Soil Mech. Found. Div. ASCE **94** (SM2), 353-369.

Kelvin, Lord, 1887, On the division of space with minimum partitional area: Phil. Mag., **24**, 503-514.

Laughton, A. S., 1957, Sound propagation in compacted ocean sediments: Geophysics, **22** 233-260.

Morror, N. R., 1971, Small-scale packing heterogeneities in porous sedimentary rocks: Bull. Am. Assoc. Pet. Geol., **55**, 514-522.

Murphy, W. F., 1982, Effects of microstructure and pore fluids on the acoustic properties of granular sedimentary materials: Thesis, Stanford Univ.

Ogushwitz, P. R., 1985, Applicability of the Biot theory. I. low-porosity materials: J. Acoust. Soc. Am. **77**, 429-440.

Pilbeam, C. C., and Vaisnys, J. R., 1973, Acoustic velocities and energy losses in granular aggregates: J. Geophys. Res., **78**, 810-824.

Plona T. J., 1980, Observation of a second bulk compressional wave in a porous medium at ultrasonic frequencies: Appl. Phys. Lett. **36**, 259-261.

TABLE CAPTION

Table 1. Six packing patterns relate to porosity and coordination number.

FIGURE CAPTIONS

Figure 1. Sketch of the set up of the experiment.

Figure 2. (a) Grain size distribution for the Ottawa sand used in this study (a) before the experiment, (b) after loading differential pressure 50 MPa.

Figure 3. (a) Sketch of packing heterogeneity, (b) Sketch of grain size heterogeneity for an unconsolidated granular aggregate.

Figure 4. The (a) porosity and (b) P-wave velocity vs. confining pressure at the pore pressure equal to 1 MPa in two pressure cycles for the dry and saturated Ottawa sand.

Figure 5. The velocity vs. confining pressure for the dry and saturated clay (33% water by weight mixed with smectite powders).

Figure 6. Comparison of the (a) porosity (b) P-wave velocity vs. confining pressure at the pore pressure equal to 1 MPa for the Ottawa sand and 80% sand mixed with 20% clay (smectite).

Figure 7. (a) The porosity decrease, (b) The velocity V_p increase with times at confining pressure equal to 20 MPa and pore pressure to 1 MPa for the mixture of 60% Ottawa sand with 40 clay (smectite) by weight.

Figure 8. (a) Porosity and (b) P-wave velocity versus confining pressure for mixture with clay content, 0, 1, 5, 10, 15, 20, and 30 percent, and pure clay (smectite mixed with 33 percent water by weight and for P-wave velocity only). The data show clear clay influences.

Figure 9. The porosity vs. clay content by volume fraction at the initial packing and the confining pressure 3, 10, 30 and 50 MPa, and the pore pressure 1 MPa in (a) the first up-loading, (b) the first down-loading. Dashed and dotted lines are calculated for the case in which clay totally fills into pore spaces at the initial packing and P_e equal to 50 MPa. The numbers plotted for date points are the clay weight fraction of the samples.

Figure 10. The (a) porosity and (b) P-wave velocity vs. the depth coverted from pressure and density data at the first down-loading for the mixtures with the clay content 0, 10, 15, 20, 25 and 30%. The numbers plotted for the data points are the clay weight fractions of the samples.

Figure 11. The P-wave velocity vs. the clay content by volume fraction at the confining pressure 50, 30, 10, 3 MPa, and the pore pressure 1 MPa in (a) the first down-loading, (b) the first up-loading.

Figure 12. The S-wave velocity vs. clay content by volume fraction at the confining pressure 50,

30 MPa, and the pore pressure 1 MPa in the first down-loading. The numbers plotted for the data points are the clay weight fractions of the samples.

Figure 13. The (a) bulk (K), Young's (E) and shear (μ) moduli vs. the clay content by volume fraction at the confining pressure equal to 50 MPa, and the pore pressure 1 MPa. The numbers plotted under date points are the clay weight fraction of the samples.

Figure 14. The P-wave velocity versus porosity for mixtures with clay content from zero to 30 percent. The data show an increase of the velocity with decreasing porosity.

Figure 15. The velocity (a) V_p, (b) V_s vs. the clay content by volume fraction at the confining pressure 50 MPa, and the pore pressure 1 MPa in the first down-loading. The numbers plotted for data points are the clay weight fraction of the samples. The dashed line is the velocity-porosity relation for clean sand. The dotted line is the velocity-porosity relation for clean sandstone.

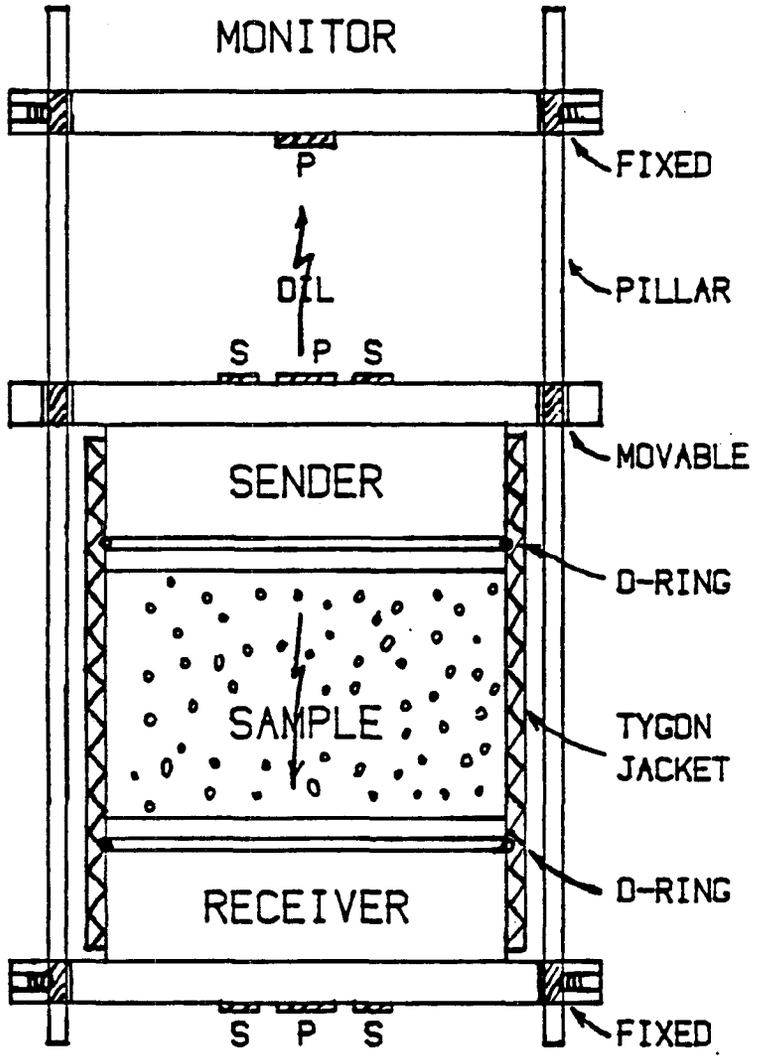
MONITOR
P
FIXED
OIL
PILLAR
S P S
MOVABLE
SENDER
O-RING
SAMPLE
TYGON
JACKET
O-RING
RECEIVER
S P S
FIXED
OIL

Fig. 1

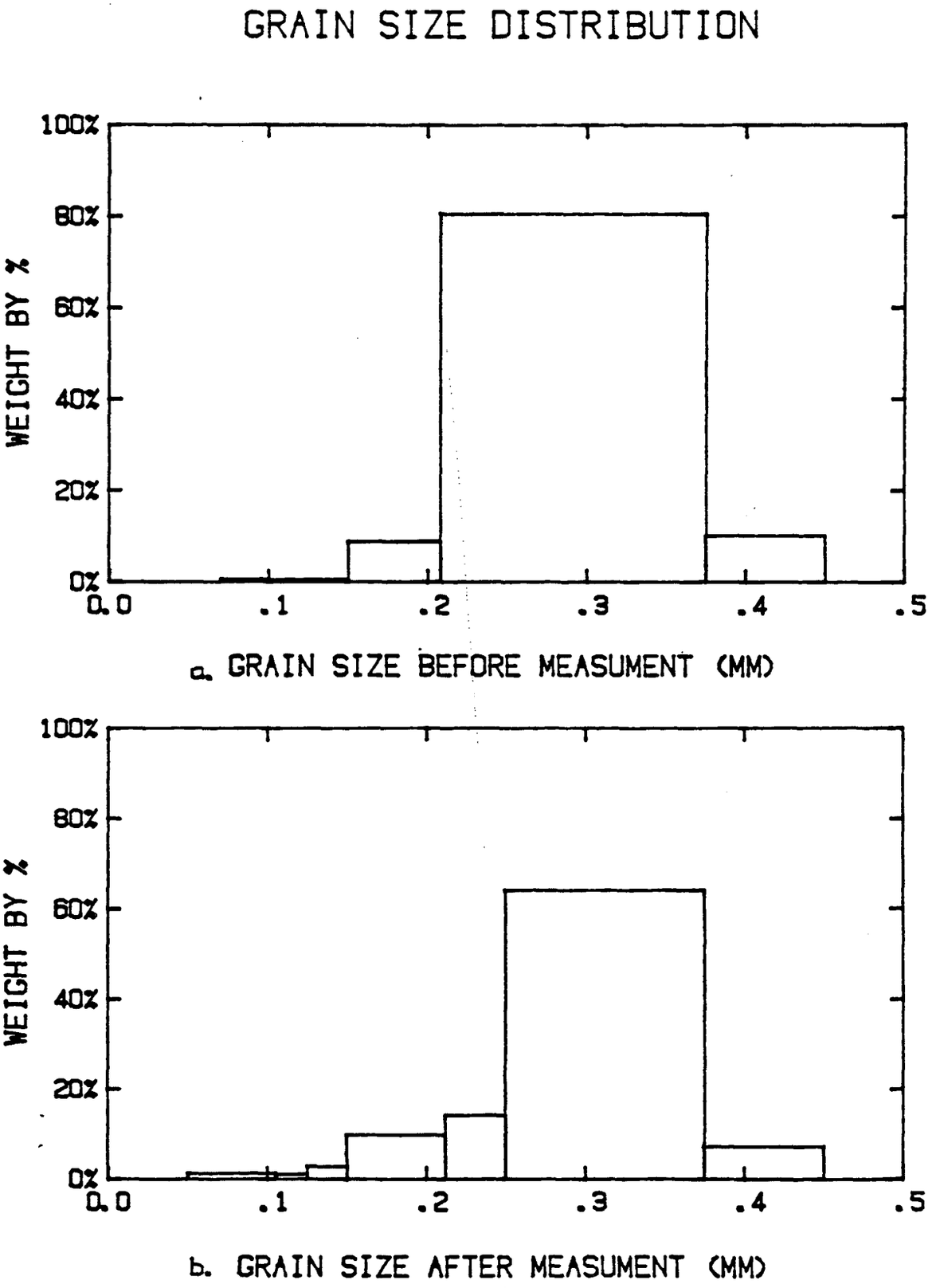
GRAIN SIZE DISTRIBUTION
100%
80%
60%
40%
20%
0%
WEIGHT BY %
0.0
.1
.2
.3
.4
.5
a. GRAIN SIZE BEFORE MEASUMENT (MM)
100%
80%
60%
40%
20%
0%
WEIGHT BY %
0.0
.1
.2
.3
.4
.5
b. GRAIN SIZE AFTER MEASUMENT (MM)

Fig. 2

Packing type	*Grain volume (%)*	*Pore volume (%)*	*Stability*	*Number of contacts by each grain*	
				below	*all sides*
Case 1, cubic	52.36	47.64	low	1	6
Case 2, orthorhombic	60.46	39.54	medium	2	8
Case 3, rhombohedral	74.05	25.95	high	4	12
Case 4, orthorhombic	60.46	39.54	low	1	8
Case 5, tetragonal	69.81	30.19	medium	2	10
Case 6, rhombohedral	74.05	25.95	high	4	12

TABEL 1

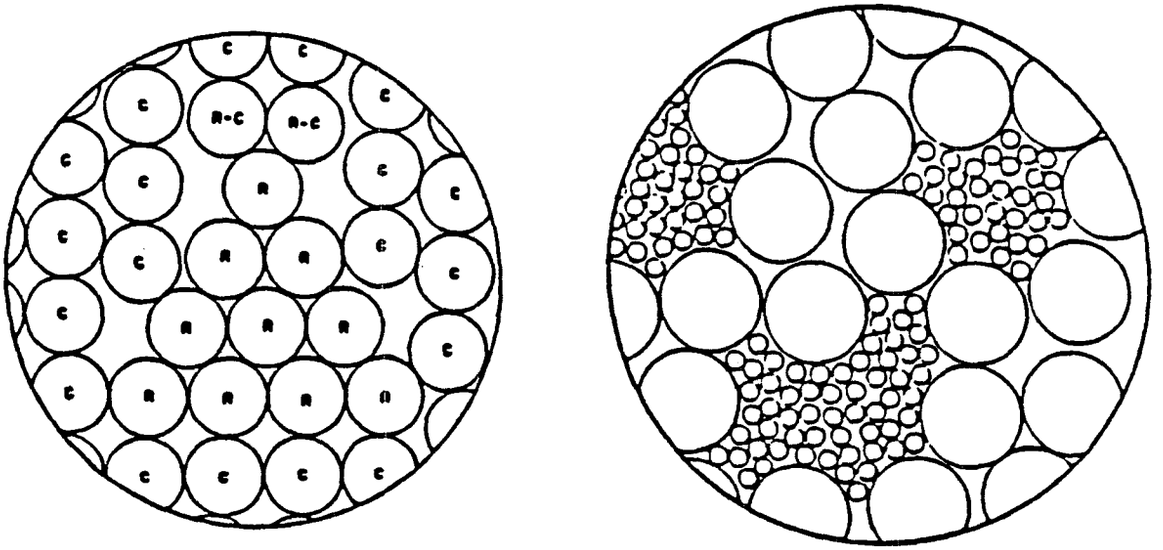

(a) (b)

Fig. 3

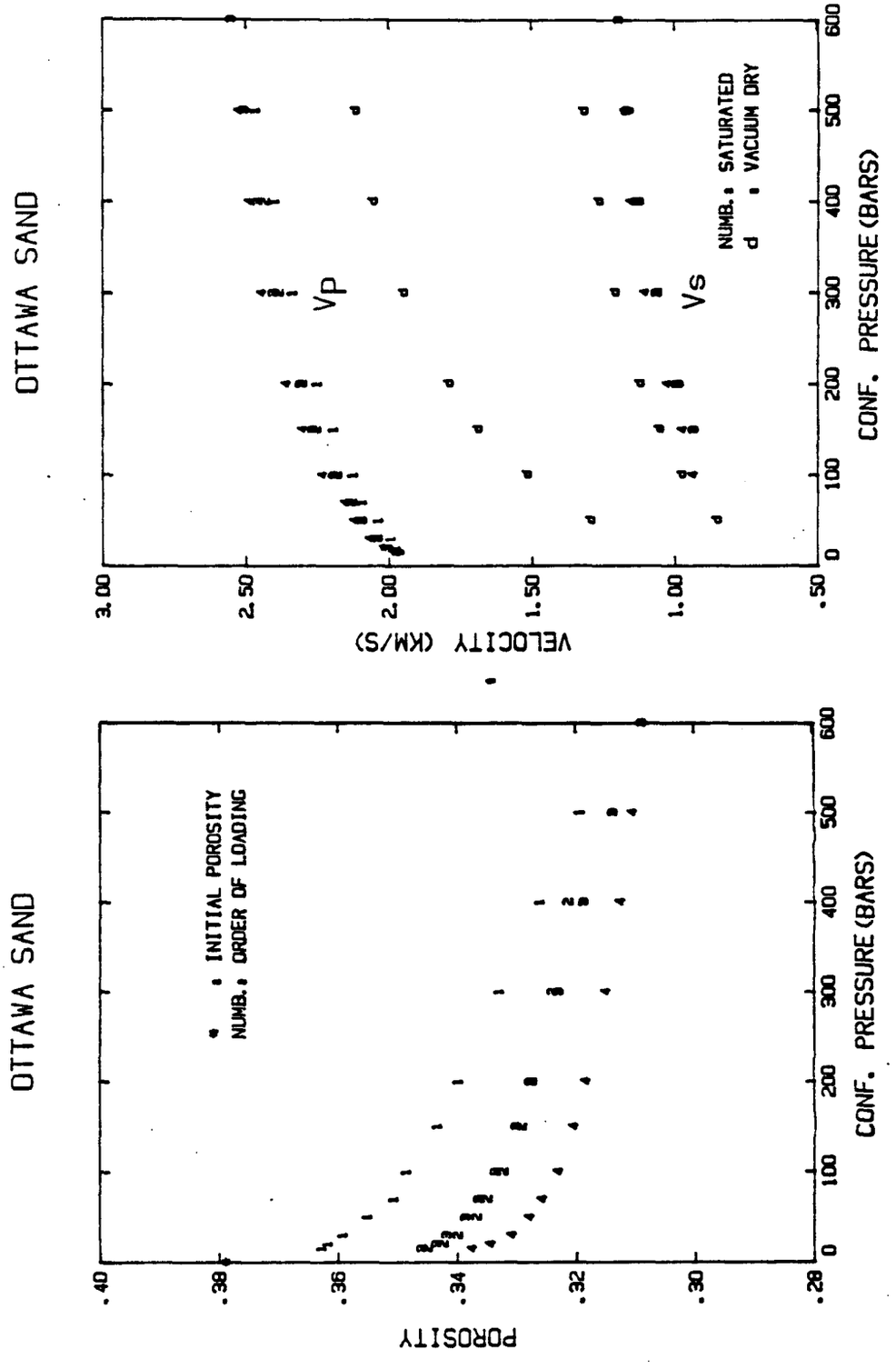
OTTAWA SAND
POROSITY
CONF. PRESSURE (BARS)
* : INITIAL POROSITY
NUMB.: ORDER OF LOADING
.40
.38
.36
.34
.32
.30
.28
0
100
200
300
400
500
600

Fig. 4a

OTTAWA SAND
VELOCITY (KM/S)
CONF. PRESSURE (BARS)
NUMB.: SATURATED
d : VACUUM DRY
Vp
Vs
3.00
2.50
2.00
1.50
1.00
.50
0
100
200
300
400
500
600

Fig. 4b

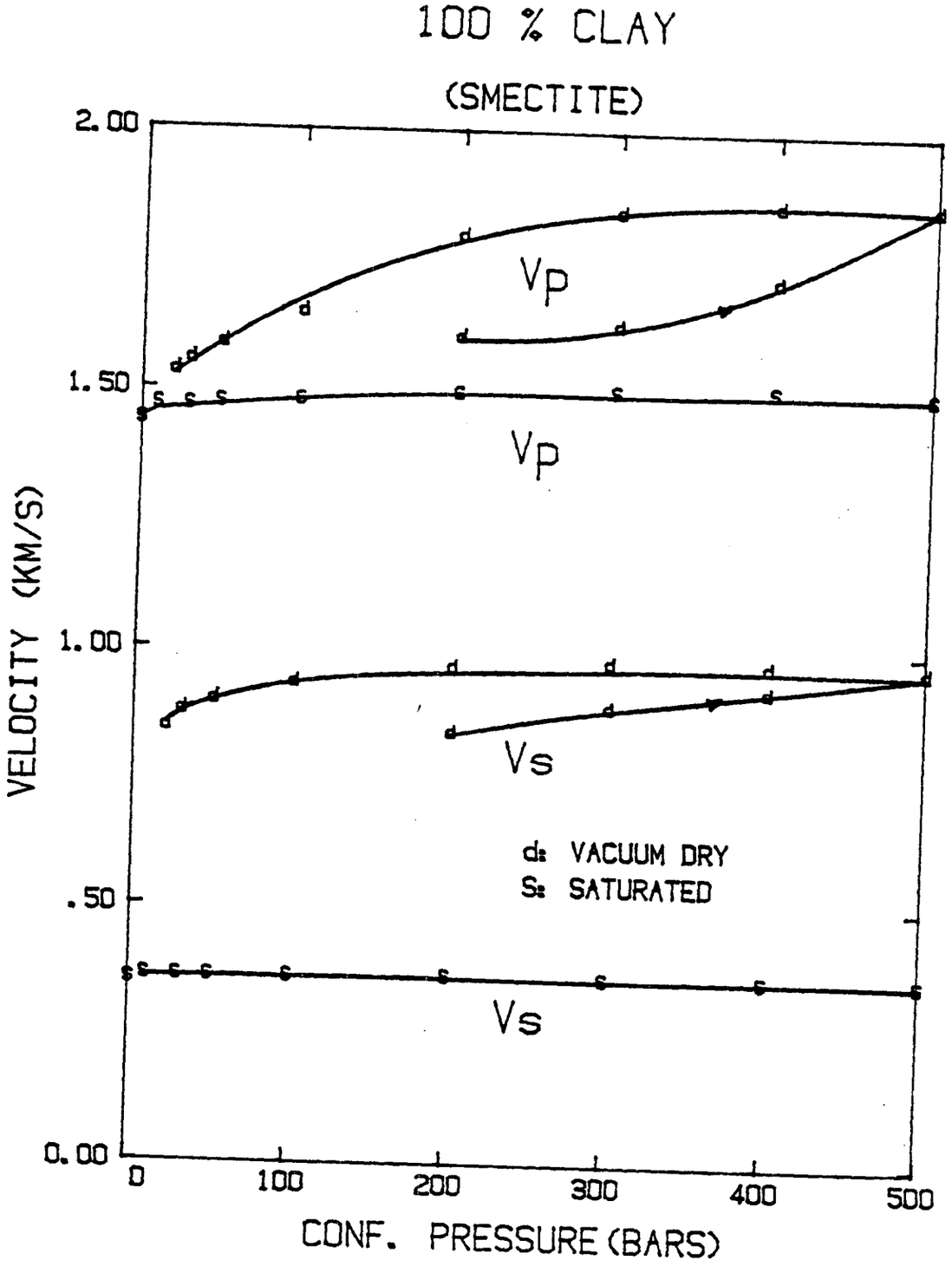
100 % CLAY
(SMECTITE)
2.00
1.50
1.00
.50
0.00
VELOCITY (KM/S)
Vp
Vp
Vs
Vs
d: VACUUM DRY
S: SATURATED
0
100
200
300
400
500
CONF. PRESSURE (BARS)

Fig. 5

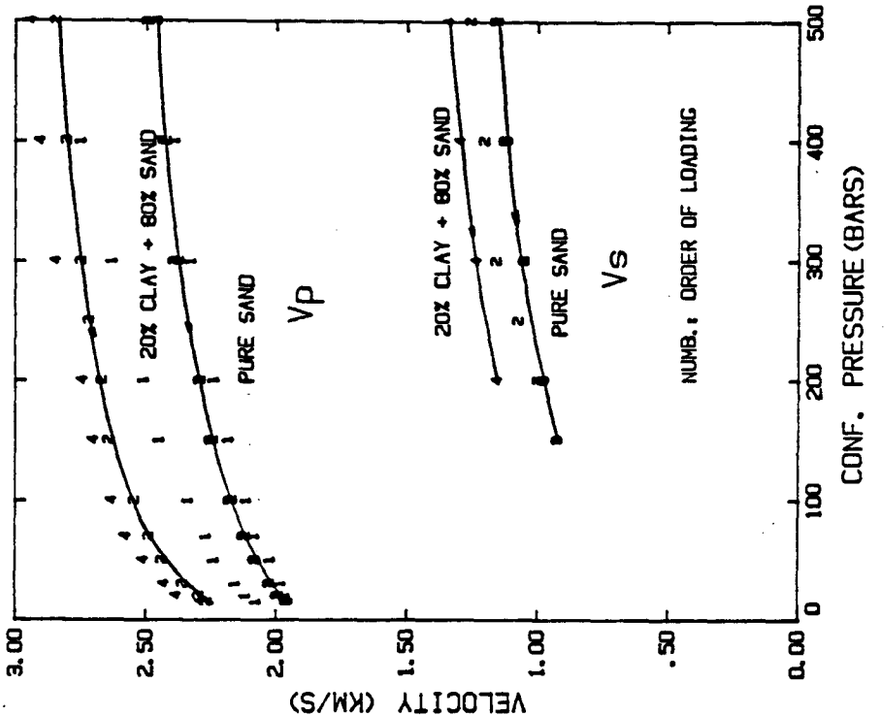
VELOCITY (KM/S)
3.00
2.50
2.00
1.50
1.00
.50
0.00
0
100
200
300
400
500
CONF. PRESSURE (BARS)
20% CLAY + 80% SAND
PURE SAND
Vp
Vs
NUMB.: ORDER OF LOADING

Fig. 6b

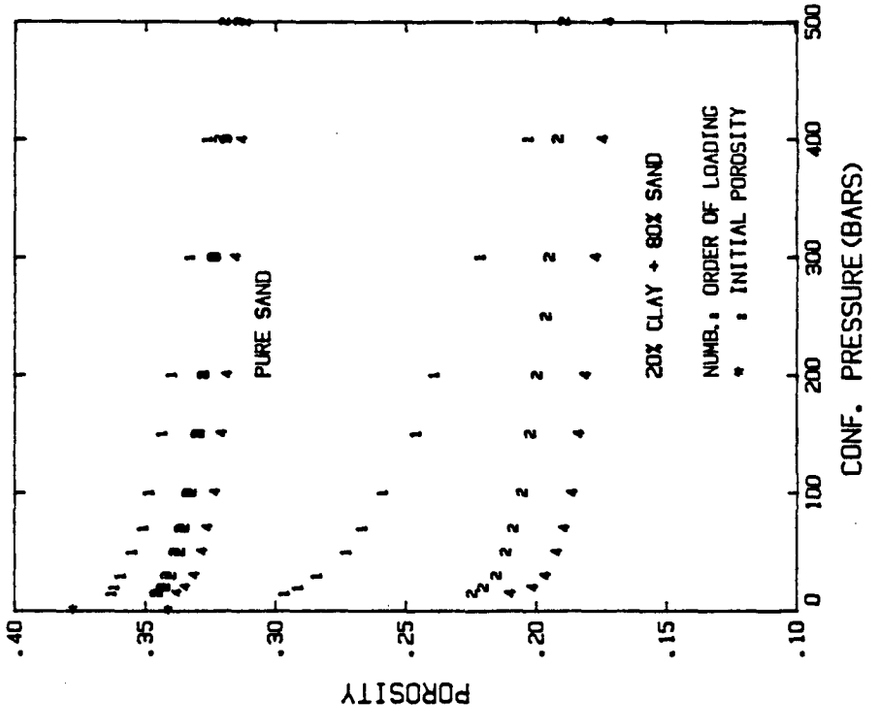
POROSITY
.40
.35
.30
.25
.20
.15
.10
0
100
200
300
400
500
CONF. PRESSURE (BARS)
PURE SAND
20% CLAY + 80% SAND
NUMB.: ORDER OF LOADING
* : INITIAL POROSITY

Fig. 6a

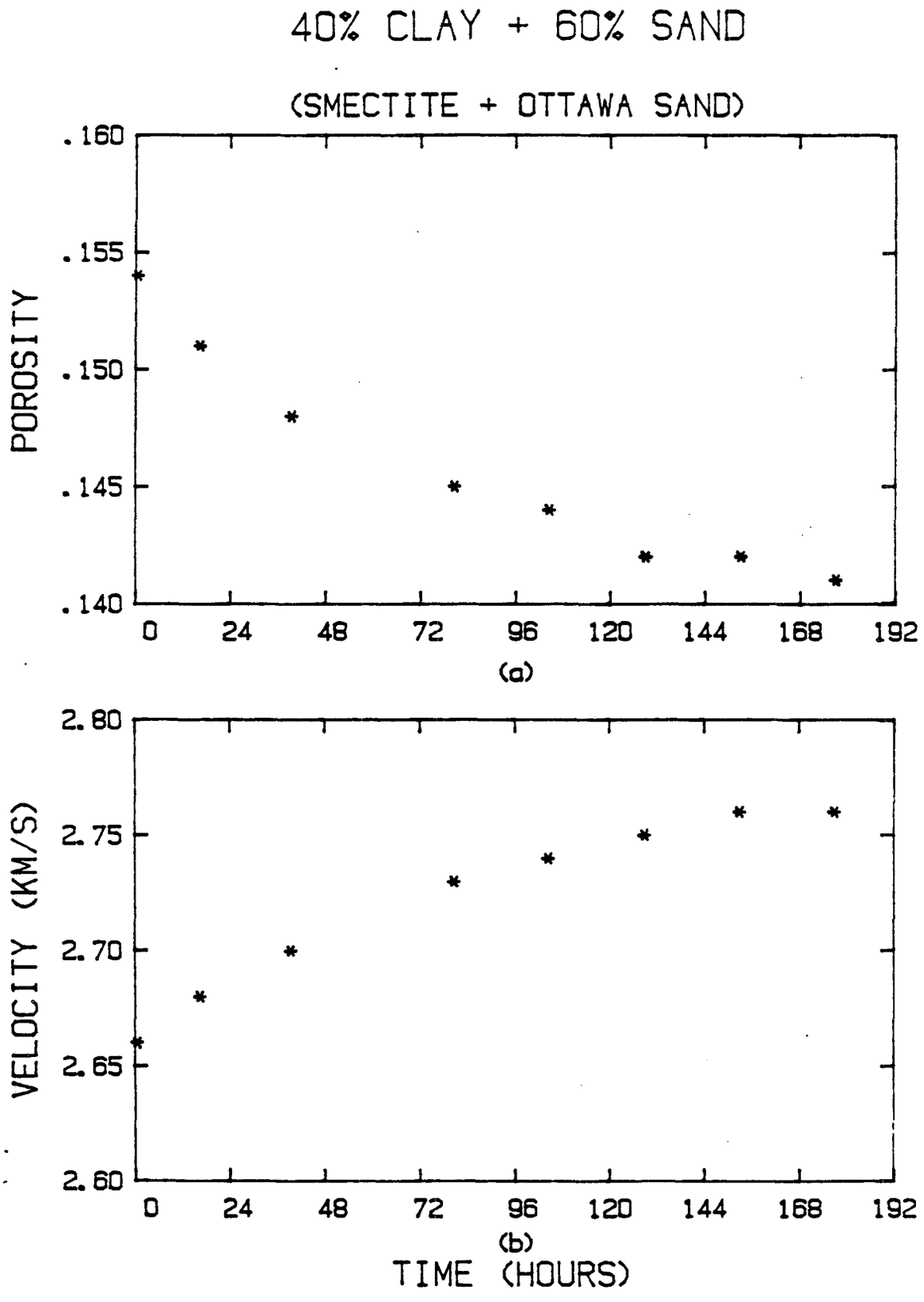
40% CLAY + 60% SAND
(SMECTITE + OTTAWA SAND)
POROSITY
.160
.155
.150
.145
.140
0
24
48
72
96
120
144
168
192
(a)
VELOCITY (KM/S)
2.80
2.75
2.70
2.65
2.60
0
24
48
72
96
120
144
168
192
(b)
TIME (HOURS)

Fig. 7

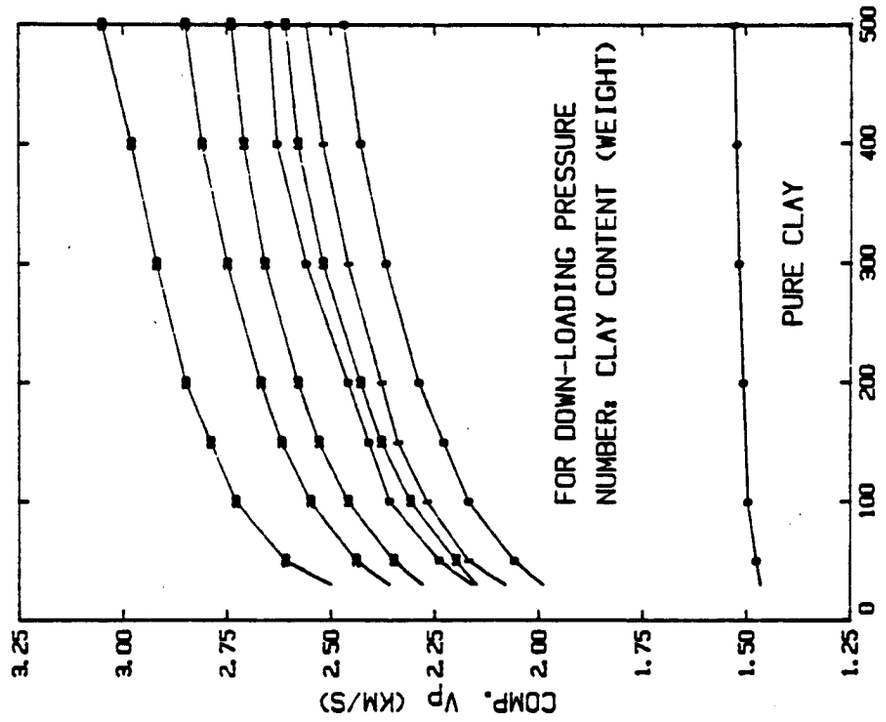
COMP. V_p (KM/S)
3.25
3.00
2.75
2.50
2.25
2.00
1.75
1.50
1.25
FOR DOWN-LOADING PRESSURE
NUMBER: CLAY CONTENT (WEIGHT)
PURE CLAY
0
100
200
300
400
500
CONF. PRESSURE (BAR)

Fig. 8b

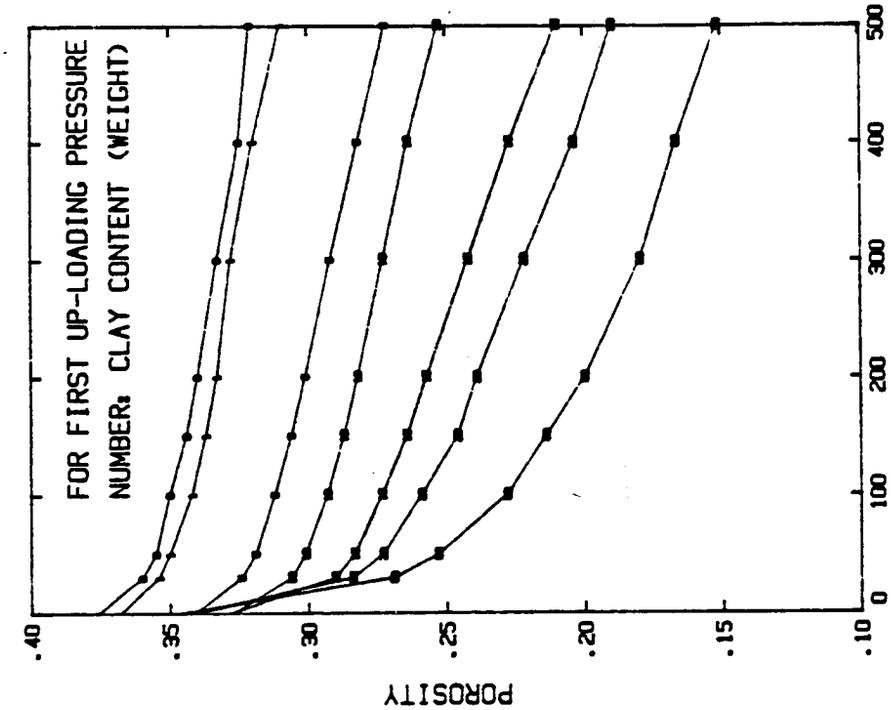
POROSITY
.40
.35
.30
.25
.20
.15
.10
FOR FIRST UP-LOADING PRESSURE
NUMBER: CLAY CONTENT (WEIGHT)
0
100
200
300
400
500
CONF. PRESSURE (BAR)

Fig. 8a

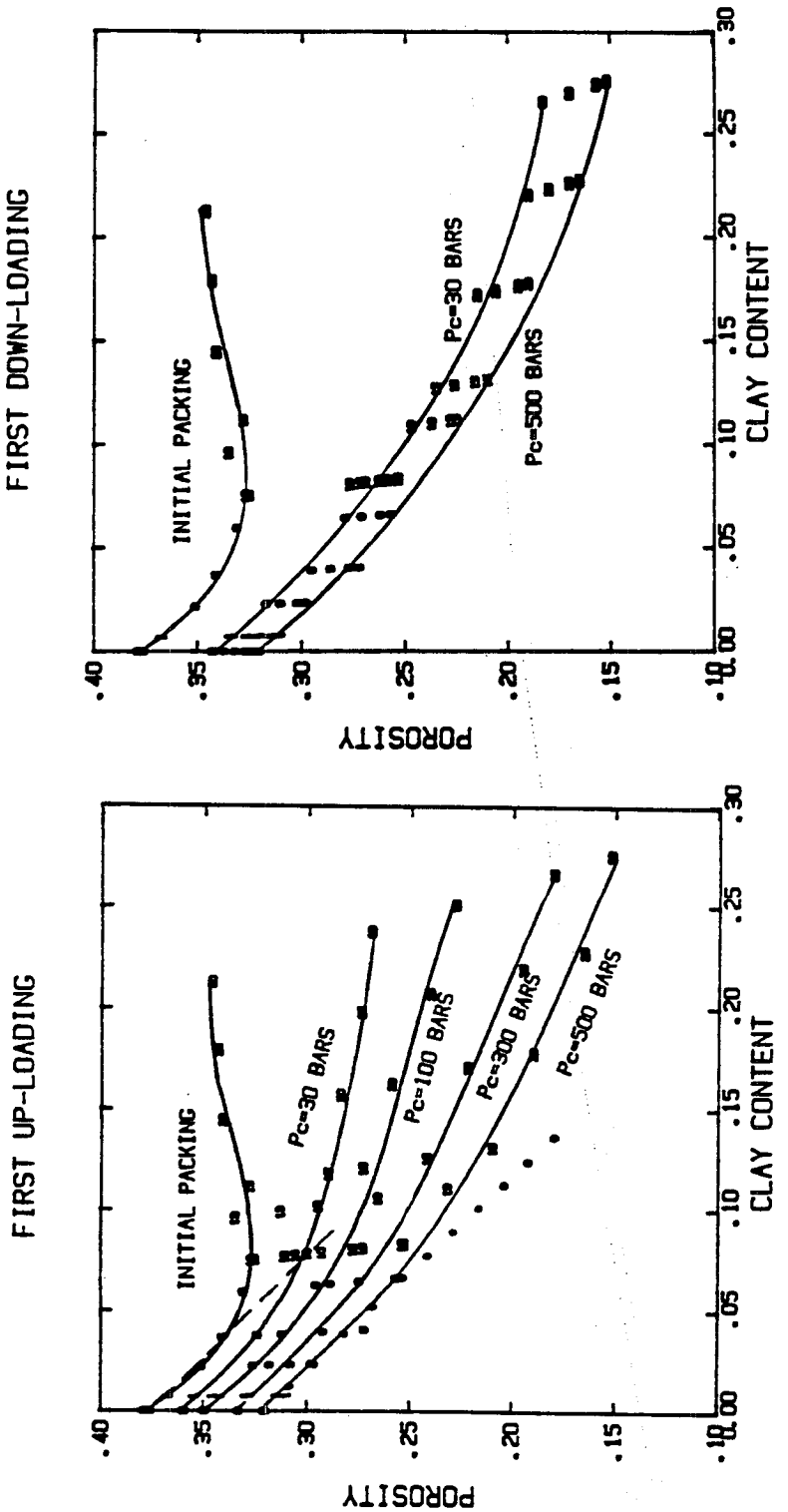
FIRST DOWN-LOADING
INITIAL PACKING
Pc=30 BARS
Pc=500 BARS
POROSITY
CLAY CONTENT
.40
.35
.30
.25
.20
.15
.10
.00
.05
.10
.15
.20
.25
.30

Fig. 9b

FIRST UP-LOADING
INITIAL PACKING
Pc=30 BARS
Pc=100 BARS
Pc=300 BARS
Pc=500 BARS
POROSITY
CLAY CONTENT
.40
.35
.30
.25
.20
.15
.10
.00
.05
.10
.15
.20
.25
.30

Fig. 9a

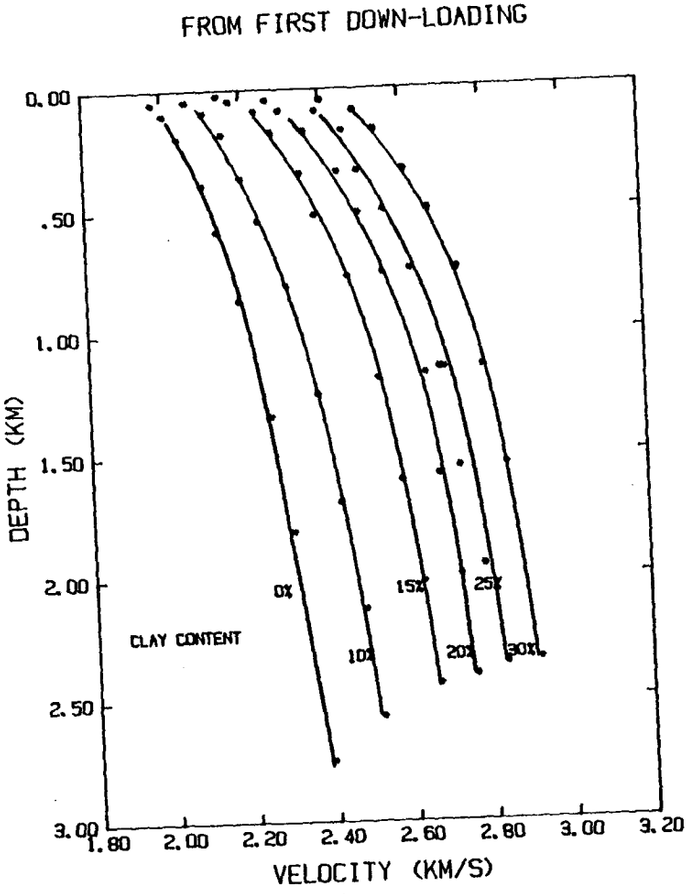

Fig. 10a

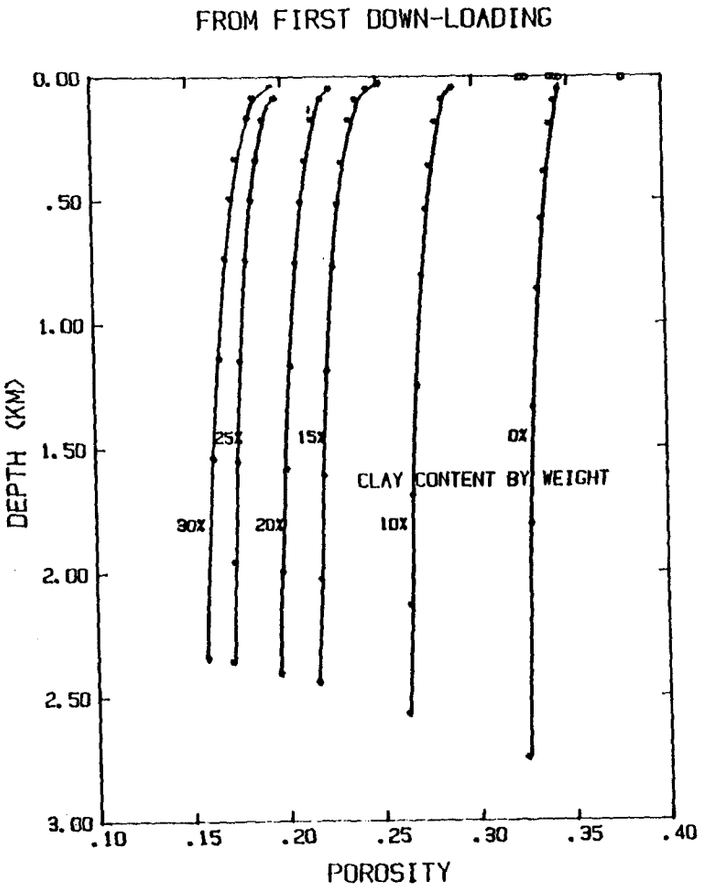

Fig. 10b

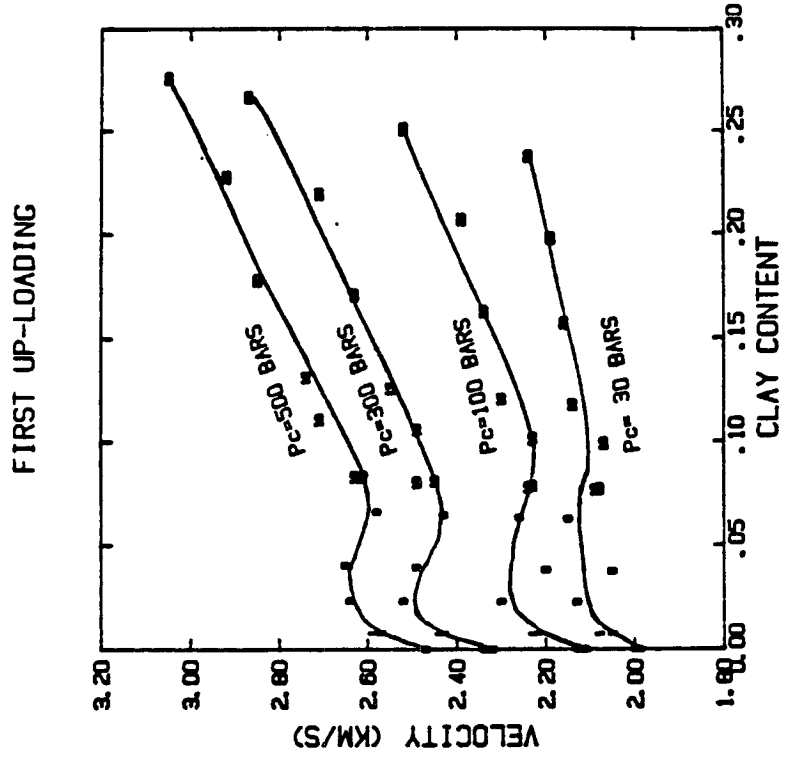

Fig. 11b

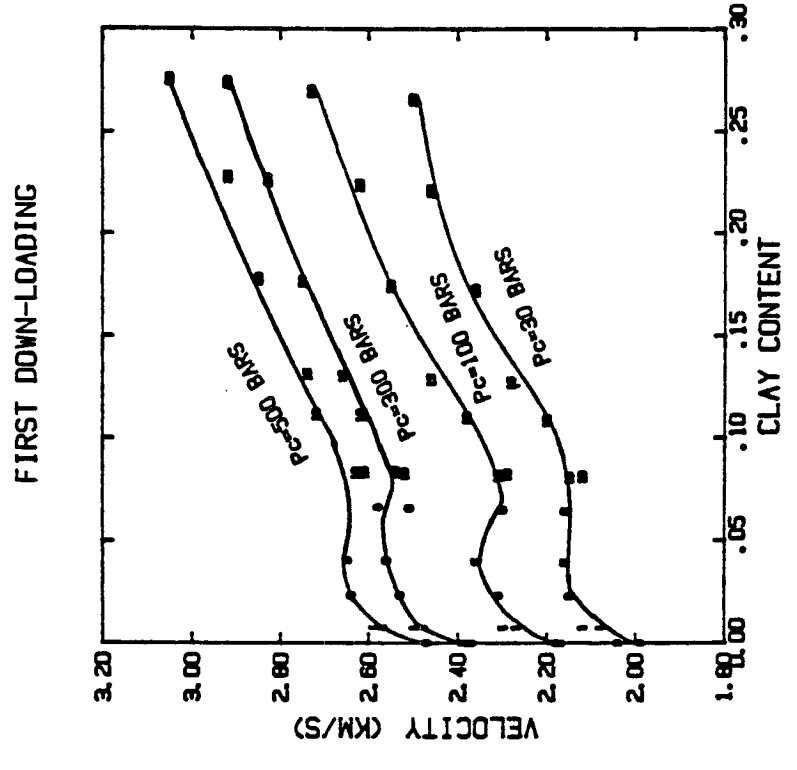

Fig. 11a

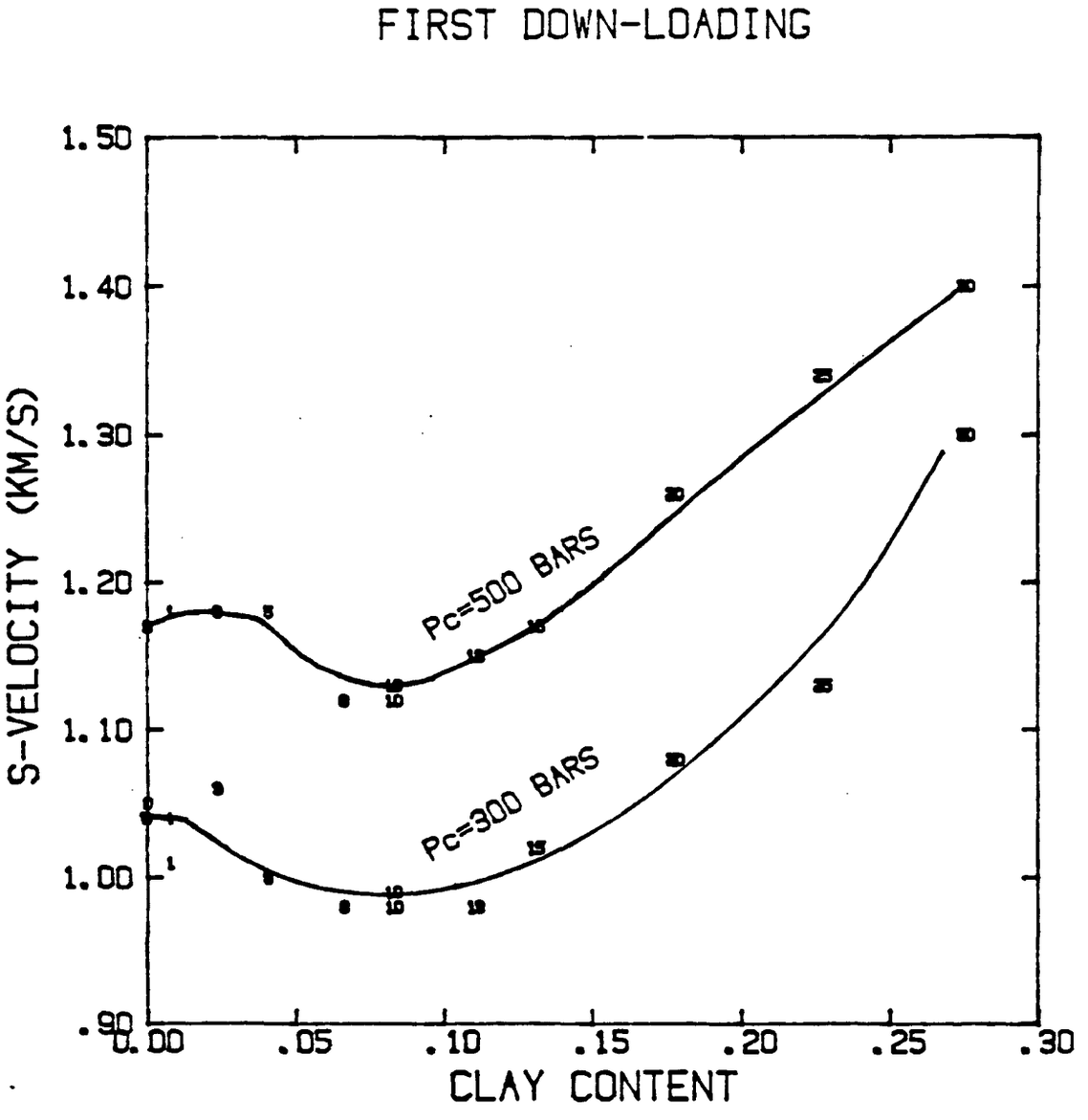
FIRST DOWN-LOADING
S-VELOCITY (KM/S)
1.50
1.40
1.30
1.20
1.10
1.00
.90
0.00
.05
.10
.15
.20
.25
.30
CLAY CONTENT
Pc=500 BARS
Pc=300 BARS

Fig. 12

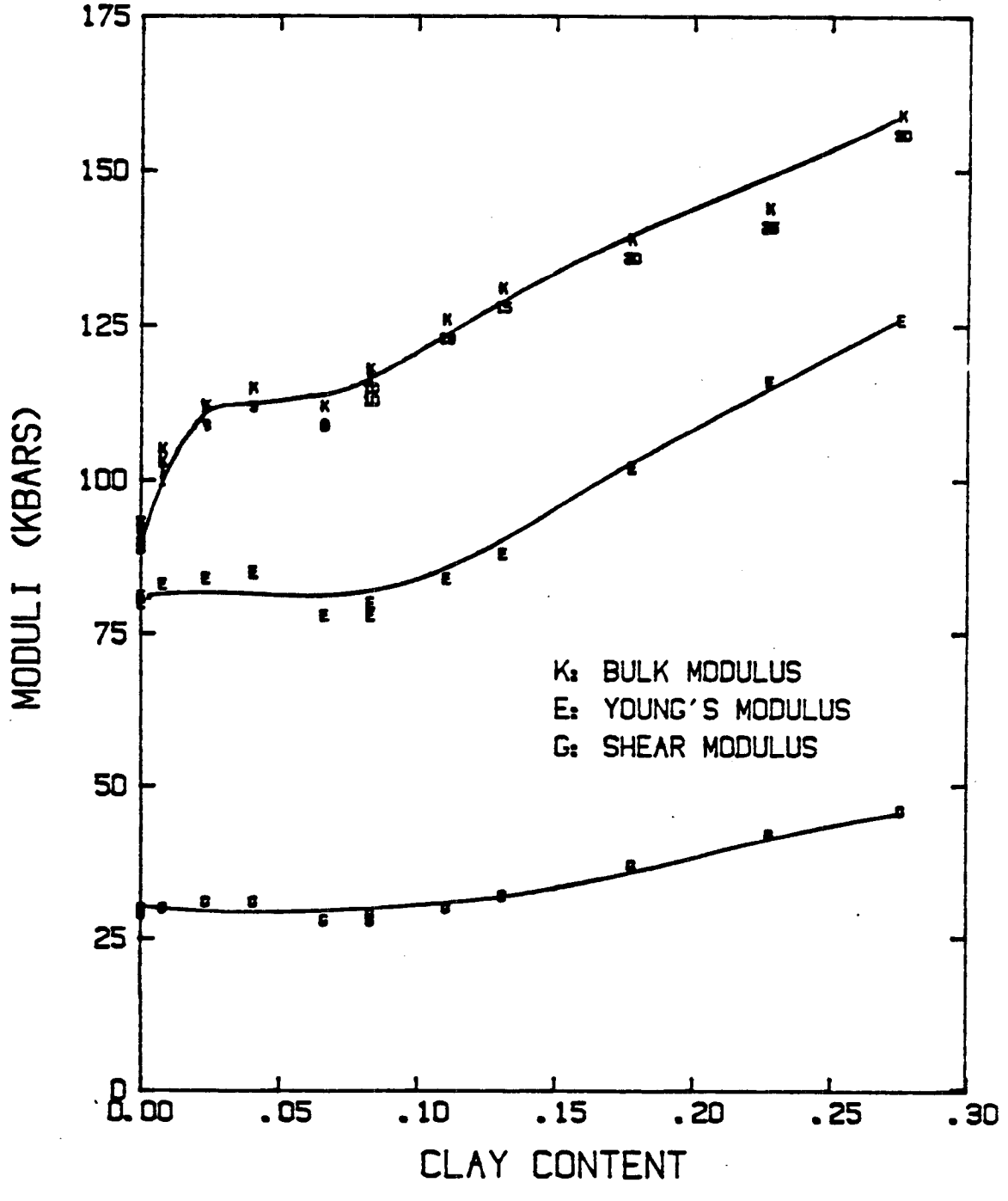
175
150
125
100
75
50
25
0
MODULI (KBARS)
0.00
.05
.10
.15
.20
.25
.30
CLAY CONTENT
K: BULK MODULUS
E: YOUNG'S MODULUS
G: SHEAR MODULUS

Fig. 13a

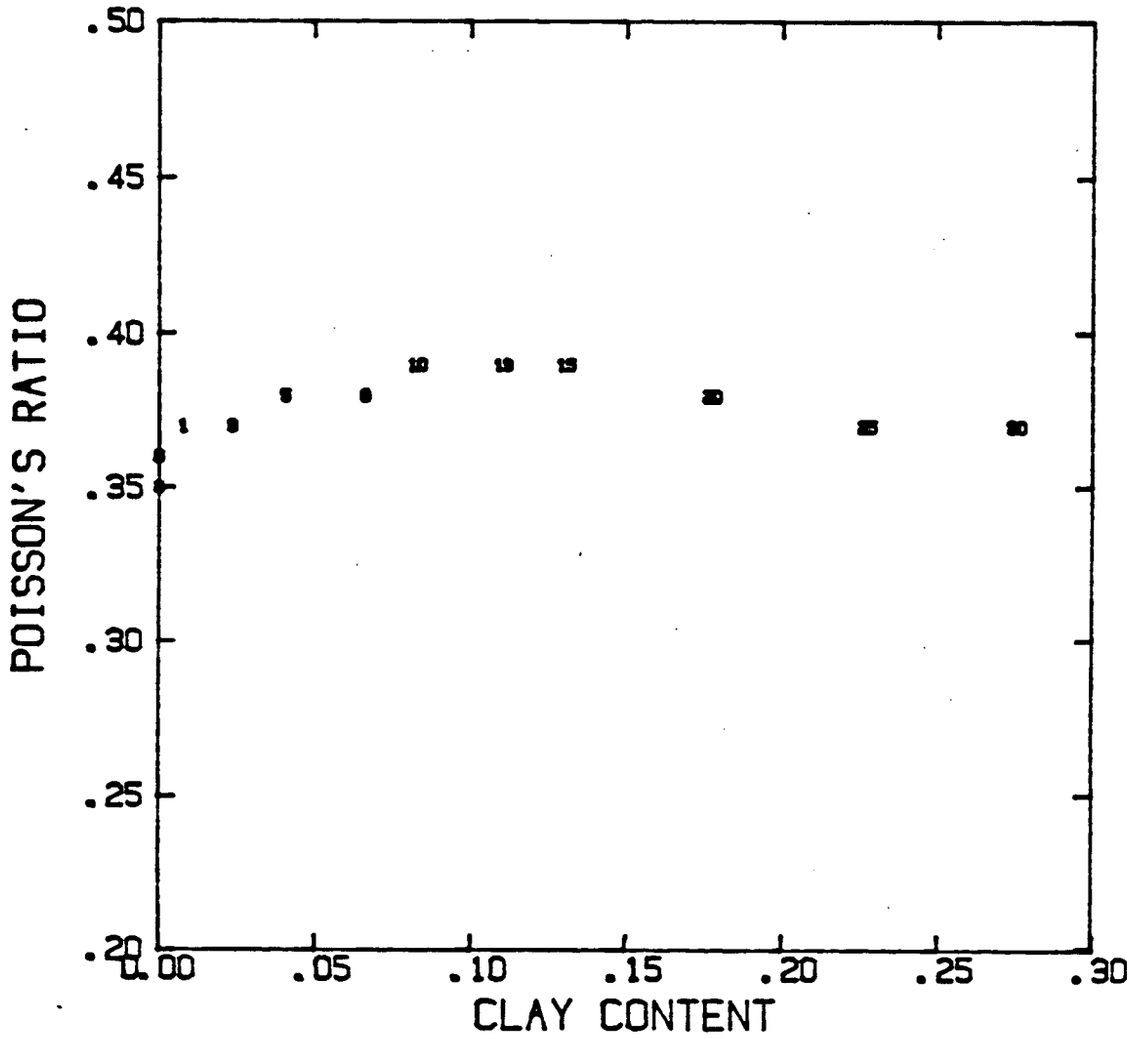
.50
.45
.40
.35
.30
.25
.20
POISSON'S RATIO
.00
.05
.10
.15
.20
.25
.30
CLAY CONTENT

Fig. 13b

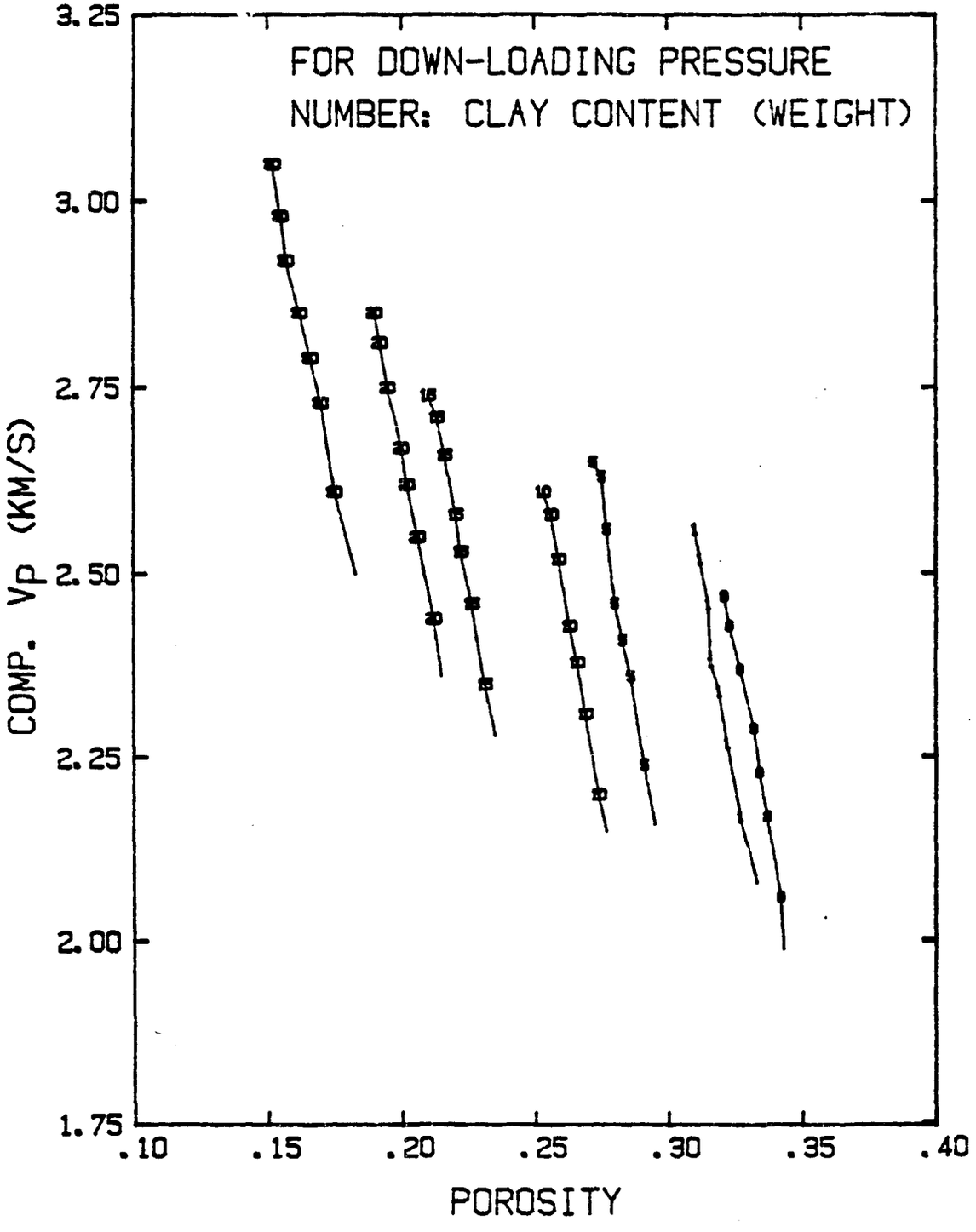
FOR DOWN-LOADING PRESSURE
NUMBER: CLAY CONTENT (WEIGHT)
COMP. Vp (KM/S)
3.25
3.00
2.75
2.50
2.25
2.00
1.75
.10
.15
.20
.25
.30
.35
.40
POROSITY

Fig. 14

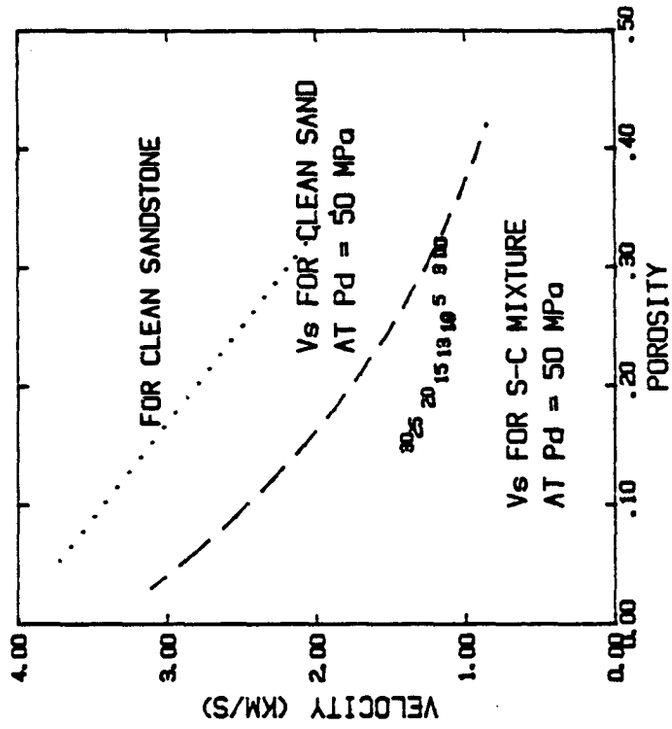

Fig. 15b

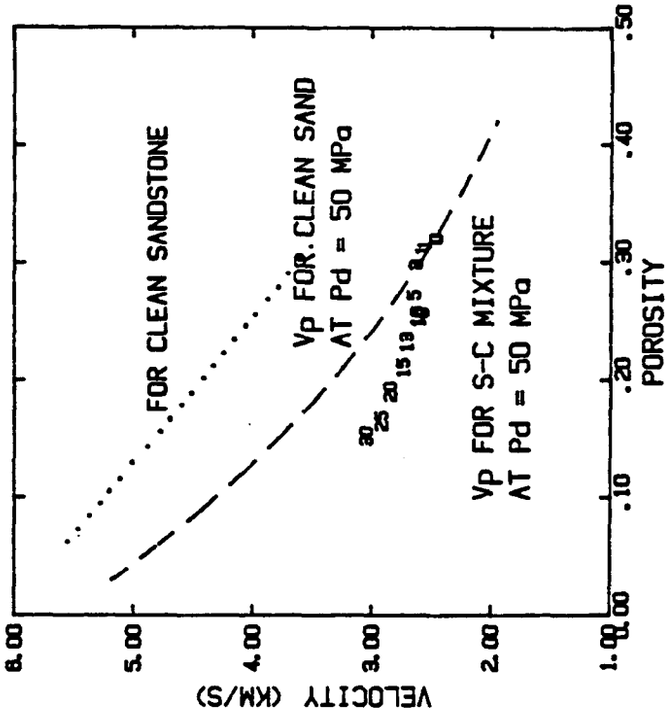

Fig. 15a